Institut für Nutzpflanzenwissenschaften und Ressourcenschutz (INRES)

Effects of elevated ozone on winter wheat and potential genetic and physiological mechanisms

Dissertation

zur Erlangung des Grades

Doktorin der Agrarwissenschaften (Dr. agr.)

der Landwirtschaftlichen Fakultät

der Rheinischen Friedrich-Wilhelms-Universität Bonn

von

Yanru Feng

aus

Shanxi, China

Bonn, 2024

Referent:	Prof. Dr. Michael Frei
Korreferent:	Prof. Dr. Gabriel Schaaf
Fachnahes Mitglied:	Prof. Dr. Eike Lüdeling
Vorsitzender:	Prof. Dr. Mathias Becker
Tag der mündlichen Prüfung:	19.04.2024

Angefertigt mit Genehmigung der Landwirtschaftlichen Fakultät der Universität Bonn

Contents

Abstract

Wheat is an ozone-sensitive crop with substantial global yield loss. It is necessary to make assessments of ozone impacts and to investigate the tolerance mechanisms and genetic factors conferring ozone tolerance in wheat. Contrasting wheat cultivars had been pre-selected from a larger wheat population with known ozone tolerance and exposed to season-long ozone fumigation in open-top chambers. Season-long ozone fumigation was conducted at an average ozone concentration of 70 ppb with three additional acute ozone episodes of around 150 ppb. This thesis is structured into three major parts:

(1) Based on the large variations of ozone responses in wheat, physiological traits contributing to yield losses or yield stability were identified under ozone stress in eighteen contrasting genotypes for modelling parameterization, that is, foliar chlorophyll content represented by normalized difference vegetation index and net CO_2 assimilation rate of young leaves during grain filling. LINTULCC2 crop model was further parametrized for two selected tolerant or sensitive varieties, respectively, with an ozone response routine. Parameters representing the distinct physiological responses of contrasting genotypes were specified to improve the accuracy of modelling simulation.

(2) Carbon (C) and nitrogen (N) allocation were analyzed in straw and grains under ozone stress. Elevated ozone exposure reduced the N absorption from soil and allocation from vegetative to reproductive organs, manifested as significantly reduced indicators of N use efficiency (NUE) with the exception of N utilization efficiency (NUtE). In addition, the relationship between harvest index (HI) and nitrogen harvest index (NHI) was changed by ozone stress, and the reduced regression slope between them indicated that ozone exposure significantly affected the relationship of N and biomass allocation into wheat grain.

(3) According to genetic backgrounds at ozone tolerant loci, tolerant and sensitive haplotypes represented by two genotypes, respectively, were used for gene expression, physiological and biochemical analyses. Tolerant and sensitive haplotypes showed consistently contrasting responses to ozone in terms of net photosynthetic rate, lipid peroxidation, apoplastic ascorbate, ascorbate peroxidase and peroxidase activity. Among candidate genes located within an ozone tolerant locus on chromosome 5A 592.04 - 593.33 Mb, the gene TraesCS5A01G400500 putatively involved in peroxidase activity was differently regulated in two haplotypes, with consistent sequence polymorphisms in the promoter region.

Taken together, this study improved the accuracy of modelling simulation for contrasting genotypes, assessed the C and N allocation and NUE among different genotypes and

investigated the potential genetic and physiological mechanisms. Further explorations were warranted to reveal the molecular mechanisms underlying ozone tolerance in wheat.

Kurzfassung

Weizen ist eine ozonempfindliche Kulturpflanze, die weltweit erhebliche Ertragseinbußen verursacht. Es ist notwendig, die Auswirkungen von Ozon zu bewerten und die Toleranzmechanismen und genetischen Faktoren zu untersuchen, die die Ozontoleranz bei Weizen vermitteln. Aus einer größeren Weizenpopulation mit bekannter Ozontoleranz wurden kontrastierende Weizensorten vorselektiert und einer saisonalen Ozonbegasung in offenen Kammern ausgesetzt. Die saisonale Ozonbegasung wurde bei einer durchschnittlichen Ozonkonzentration von 70 ppb durchgeführt, mit drei zusätzlichen akuten Ozonepisoden von etwa 150 ppb. Die vorliegende Arbeit gliedert sich in drei Hauptteile:

(1) Auf der Grundlage der großen Variationen der Ozonreaktionen bei Weizen wurden physiologische Merkmale, die zu Ertragseinbußen oder Ertragsstabilität unter Ozonstress beitragen, bei achtzehn kontrastierenden Genotypen für die Modellparametrisierung identifiziert, d.h. der Blattchlorophyllgehalt, dargestellt durch den normalisierten Differenzvegetationsindex, und die Netto-CO2-Assimilationsrate junger Blätter während der Kornfüllung. Das LINTULCC2-Pflanzenmodell wurde für zwei ausgewählte tolerante bzw. empfindliche Sorten mit einer Ozonreaktionsroutine weiter parametrisiert. Um die Genauigkeit der Simulation zu verbessern, wurden Parameter festgelegt, die die unterschiedlichen physiologischen Reaktionen der verschiedenen Genotypen repräsentieren.

(2) Die Verteilung von Kohlenstoff (C) und Stickstoff (N) wurde in Stroh und Körnern unter Ozonstress analysiert. Erhöhte Ozonbelastung reduzierte die N-Aufnahme aus dem Boden und die Allokation von vegetativen zu reproduktiven Organen, was sich in signifikant reduzierten Indikatoren der N-Nutzungseffizienz (NUE) mit Ausnahme der N-Verwertungseffizienz (NUtE) manifestierte. Darüber hinaus wurde die Beziehung zwischen dem Ernte-Index (HI) und dem Stickstoff-Ernte-Index (NHI) durch den Ozon-Stress verändert, und die reduzierte Regressions-Steigung zwischen ihnen deutete darauf hin, dass die Ozon-Exposition die Beziehung zwischen N und der Biomasse-Allokation in das Weizen-Korn signifikant beeinflusst.

(3) Entsprechend der genetischen Hintergründe an den ozontoleranten Loci wurden tolerante und sensible Haplotypen, die jeweils durch zwei Genotypen repräsentiert wurden, für Genexpressions- und biochemische Analysen verwendet. Tolerante und empfindliche Haplotypen zeigten durchweg unterschiedliche Reaktionen auf Ozon in Bezug auf die Netto-Photosyntheserate, die Lipidperoxidation und die apoplastische Ascorbat-, Ascorbatperoxidase- und Peroxidase-Aktivität. Unter den Kandidatengenen, die sich innerhalb

eines ozontoleranten Locus auf Chromosom 5A 592,04 - 593,33 Mb befinden, wurde das Gen TraesCS5A01G400500, das vermutlich an der Peroxidaseaktivität beteiligt ist, in zwei Haplotypen unterschiedlich reguliert, mit konsistenten Sequenzpolymorphismen im Promotorbereich.

Insgesamt verbesserte diese Studie die Genauigkeit der Modellsimulation für unterschiedliche Genotypen, bewertete die C- und N-Allokation und NUE zwischen verschiedenen Genotypen und untersuchte die potenziellen genetischen und physiologischen Mechanismen. Weitere Untersuchungen sind erforderlich, um die molekularen Mechanismen aufzudecken, die der Ozontoleranz bei Weizen zugrunde liegen.

Chapter 1: General Introduction

1.1 Tropospheric ozone and its impacts on plants

There are two phases of ozone (O_3) in the Earth's atmosphere, namely, the stratosphere and the troposphere. Unlike the former known as ozone layer protecting the earth's biota by absorbing harmful ultraviolet radiation, tropospheric ozone is a greenhouse gas responsible for direct radiative forcing of 0.35–0.37 W m^{-2} on the climate and pollutant detrimental to human health, crop and ecosystem productivity (Agathokleous et al., 2015; Chang et al., 2017; Gaudel et al., 2018; Monks et al., 2015). Tropospheric ozone is also termed as ground-level ozone lying between 0–10 km in the lower atmospheric region and a minor component comes from stratospheric influx, approximately 10% (Stevenson et al., 2006). The formation of the majority of tropospheric ozone is a complex series of photochemical reactions between primary air pollutants, such as volatile organic compounds (VOCs), nitrogen oxides (NOx = NO +NO_2), carbon monoxide (CO) and methane (CH_4) which are also known as ozone precursor gases (Ainsworth et al., 2012; Simpson et al., 2014).

Ozone concentrations have more than doubled since the Industrial Revolution and will increase further if precursor emissions rise as expected over this century. Ozone was first recognized as a detrimental air pollutant in North America during the 1950s, then gradually noticed in Europe and Japan in the 1970s, and eventually reported adverse effects of ozone in major urban and industrial regions throughout the world (Fowler et al., 2008; Haagen-Smit, 1952). The emissions of synthetic chlorofluorocarbon molecules are growing, which lead to ozone concentration depletion in the stratosphere. Control measures on emissions of NOx and VOCs, have been well established in North America and Western Europe, lead to reductions in peak ozone (Ainsworth, 2017). In contrast, despite decades of international policy efforts to mitigate global change, emissions of precursor gases of tropospheric ozone have been still rising in Asian countries and have outweighed trends in other regions (Ashmore, 2005). Rising ozone concentration is attributed to human activities, particularly increased global emission of nitrogen oxides, such as industrialization, urbanizations, deforestations, transportation, lack of legislation, rapid population and economic growth (Chang et al., 2017; Fowler et al., 2008)

Ozone is not uniformly distributed over the land surface and, in temperate regions with seasonality as ozone is a dynamic, short-lived air pollutant (Monks et al., 2015). For example, Ozone concentrations vary from approximately 20 ppb over parts of Australia and South America to 55–60 ppb in parts of Asia, the Middle East, Europe and North America (Ainsworth, 2017). Current ozone is considerably higher in the Northern Hemisphere than the Southern

Hemisphere. As high temperature and sunlight favor and accelerate ozone formation, high ozone concentrations occur in summer, with peak daily concentrations in late afternoon. Extreme high ozone concentrations reaching 200–400 ppb episodically occur in metropolitan areas or in more remote areas during heat waves, which have been far above the damage threshold level (40 ppb) had adverse effects on plants (Fowler et al., 2008). In Asia currently marked as ozone hotspot, the ozone pollution scenarios are rather severe in developing countries, which will be exacerbated in the 21st century (Mills et al., 2018b). Population-weighted mean concentrations of ozone increased globally by 8.9% from 1990 to 2013 with increases in most countries, except for modest decrease in North America, parts of Europe ,and several countries in Southeast Asia (Brauer et al., 2016). Rapid economic growth in China has yielded significant volumes of pollution emissions, the average values of the 90th percentile of daily maximum 8-hour average ozone concentration (MDA8), annual mean of the weekly average ozone concentration from 09:00 to 16:00 (M7), and cumulative exposure to hourly concentration exceeding 40 ppb (AOT40) for 31 capital cities showed an increasing trend between 2013 and 2017 (Zeng et al., 2019). Ozone dominated in air pollution of some Asian countries highlights that ozone will remain a major air pollutant threatening plants in the coming years.

As a powerful oxidant, ozone is absorbed into plant leaves via open stomatal pores (Mills et al., 2018b). Ozone induced crop damage can be categorized by chronic effects and acute effects. Responses of chronic ozone exposure differ from responses to acute ozone exposure since some of signaling and cellular responses depend on ozone concentration. Exposure of plants to an ozone concentration of typically more than 150 ppb for several hours to a few days leads to the acute effects, while chronic effects occur when plants experience a background ozone concentration less then 150 ppb for several weeks to months (Frei, 2015). Both result in ROS formation in the apoplast, including singlet oxygen ($^1O_2$), hydrogen peroxide (H_2O_2), superoxide radicals ($O_2^{\bullet-}$), hydroxyl radicals (•OH), and nitric oxide (NO) (Ainsworth, 2017). Then ozone and ozone-derived ROS cause direct oxidative damage, leading to subsequent programmed cell death (PCD) and ultimately appearing necrotic symptoms (Kangasjärvi et al., 2005). The presence and extent of leaf visible injury can be used as a surrogate of biological damage to the plants (Hayes et al., 2007). Leaf bronzing score (LBS) was used for evaluation of leaf symptoms (Alam et al., 2022; Frei et al., 2008; Ueda et al., 2015a). Ozone-induced oxidative stress also includes lipid peroxidation, chlorophyll bleaching, reduced photosynthesis, protein oxidation, cell membrane destruction, nucleic acids damage and eventually reduced

yield quantity associated with quality changes (Mills et al., 2018a).

It is generally admitted that, biochemical events occur before any development of visible symptoms of ozone damage. Peroxidation of membrane lipids is strongly affected by ROS and can be detected by increase in malondiadehyde (MDA) concentration that is considered an important indicator of oxidative lipid injury induced by ozone stress (Ashrafuzzaman et al., 2017; Ueda et al., 2013). Based on a meta-analysis of woody plants, elevated ozone between 90 and 101 ppb significantly increased foliar MDA content by 28% (Li et al., 2017). Compared with ambient plants, MDA in ozone-treated flag leaf was increased in two varieties of winter wheat under fully open-air field condition (Feng et al., 2011). Moreover, genotypic difference in MDA was found in 20 winter wheat cultivars which realsed at different time and MDA was increased by a greater magnitude in more recent than in older clutivars (Biswas et al., 2008).

Since ozone and ozone-derived ROS degrade photosynthetic pigments, especially chlorophyll and carotenoids, destruction of chlorophyll content was also considered an indicator of ozone-induced responses (Begum et al., 2020). A number of experiments using both chamber or Free Air Concentration Enrichment (FACE) setups found the significant reductions in pigment concentrations by biochemical measurements (Feng et al., 2008; Li et al., 2017; Yuan et al., 2016). For example, total chlorophyll content among nine soybean cultivars extracted with 95% ethanol were significantly reduced by more than a half at seed filling stage under elevated ozone (Zhang et al., 2014). In maize, compared to charcoal-filtered ambient air (CF), reductions of Chl *a*, Chl *b* and Chl *a*+*b* were significant by 53.3%, 51.4% and 52.7%, respectively, for ambient with a targeted ozone addition of 60 ppb (NF60) (Peng et al., 2020). Based on a non-destructive methods for spectral reflectance measurements, reduction in chlorophyll contents were also observed in wheat and rice, while tolerant genotypes showed less degradation of chlorophyll than sensitive ones (Ashrafuzzaman et al., 2017; Begum et al., 2020). Chorophyll degradation leads to reductions in light harvesting efficiency under elevated ozone, causing a series of photosynthtical responses including decreased photosynthesis and stomatal conductance, and increased rates of respiration. Photosynthesis has been the most broadly studied aspect of plant responses to ozone. Ozone exposure has adverse impacts on phtotsynthetic carbon assimilation due primarily to reduced carboxylation efficiency directly related to loss of ribulose 1,5-bisphophate carboxylase/oxygenase (Rubisco) activity (Fiscus et al., 2005). Detrimental effects of ozone stress on photosynthetic electron transport were reported, such as declines in F_v/F_m representing the efficiency of excitation energy capture by PSII in dark-adapted leaves (Calatayud and Barreno, 2001). In soybean, yield reduction induced by ozone exposure is mainly attributed to reduction of maximum rate of Rubisco

carboxylation (V_{cmax}) and maximum rates of electron transport (J_{max}) as well as ealier senescence (Sun et al., 2014). Moreover, stomata regulate the flux of ozone into leaves, and closure of stomata is one of the fastest physiological responses to elevated ozone, which is generally thought to occur as a response to inhibited photosynthetic carbon assimilation and increased substomatal CO_2 concentrations, rather than as a direct effect of ozone (Ainsworth et al., 2008; Paoletti and Grulke, 2005). In rice, reductions in stomatal conductance have been observed, which occur as soon as three hours after the exposure to ozone (Chen et al., 2011). In addition, age-related patterns of respiration were also being accelerated by ozone (Darrall, 1989; Dizengremel, 2001).

Potential global risk of increasing suface ozone exposure in year 2030 were examined accroding to two trajectories of ozone pollution: the Intergovernmental Panel on Climate Change Special Report on Emissions Scenarios (IPCC SRES) A2 and B1 storylines, and they represent upper- and lower-boundary projections, respectively. Under these two scenarios, total global agricultural losses woth $17–35 billion annually (an increase of +$6–17 billion from 2000) and $12–21 billion annually (an increase of +$1–3 billion in lossesd from 2000), respectively (Avnery et al., 2011). Moreover, crops showed different responses to ozone, and pervious studies declared that the sensivity to ozone declines in the order soybean > wheat > maize > rice, of which global yield were reduced annually by 12.4%, 7.1%, 4.4% and 6.1%, respectively, over 2010–2012 (Mills et al., 2018b). Ozone concentrations tend to be very heterogeneous across natural and agricutural regions as well as over seasons and years, resulting in different impacts on production. For example, wheat yield loss varied between the Northern and Sourthern Hemispheres, and reached by a mean of 9.9% and 6.2%, respectively (Mills et al., 2018a). Highest ozone-induced production losses for soybean are in North and South America whilst for wheat they are in India and China, for rice in parts of India, Bangladesh, China and Indonesia, and for maize in China and the United States (Mills et al., 2018b). East Asia is a hotspot of surface ozone pollution with annual crop production loss of US$ 63 billion (Figure 1.2), and China shows highest relative yield loss at 33%, 23% and 9% for wheat, rice and maize, respectively (Feng et al., 2022). These studies clearly illustrate that ozone-induced production losses pose a threat to the economy and food security.

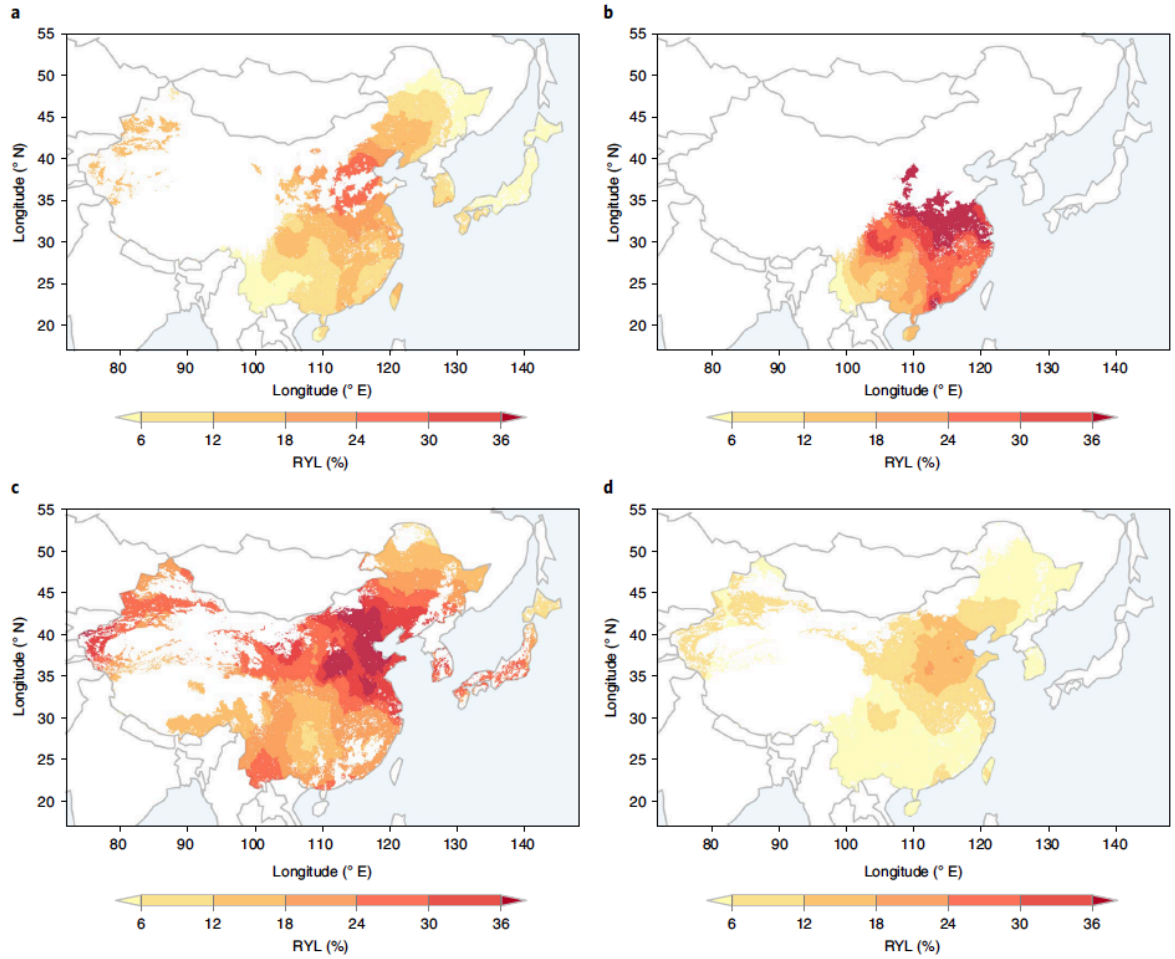

Figure 1.2 Relative yield losses (RYLs) for different crop calculated from Asian-specific exposure-RY relationships and the AOT40 values across China, Japan and South Korea. a-d, RYL(%) of inbred rice (a), hybrid rice (b), wheat (c) and maize (d) in Asia. Results was derived from AOT averaged across the latest availavle three years (China, 2017-2019; Japan, 2015-2017; and South Korea, 2016-2018). This figure was adapted from Feng et al. (2022).

In additon, the quality of grain and straw in cereal crops is also affects by ozone exposure. Grain quality changes induced by ozone stress is a cumulative process involving numerous physiochemical changes (Wang and Frei, 2011). For instance, higher protein concentration is often paralleled by an even more pronounced decrease in grain quantity under elevated ozone (Zheng et al., 2013). Numerous studies found that ozone exposure leads to an increase in the protein concentration while a reduction in the protein yield. Likewise, nutritionally important minerals concentration in wheat grain was also significantly increased by elevated ozone, including K, Mg, Ca, P, Zn, Mn and Cu (Broberg et al., 2015). It can be explained with a growth dilution effect, e.g. the negative effect of ozone on grain yield is the main factor related to protein concentration under ozone exposure, as it is much higher than the positive effect on grain N concentration (Fuhrer et al., 1990). However, starch concentration was reduced under

elevated ozone, which was attributed to ozone-induced accelerated senescence favoring the nitrogen remobilizaiton to the grain over photosynthetic processes required for the synthesis and loading of starch into the grain (Frei et al., 2012a; Wang and Frei, 2011). In rice, elevated ozone significantly increase grain chalkiness including chalkey grain percentage and chalkiness degree, indicating visual deterioration in grain and lower consumer acceptance (Wang et al., 2014). Lignin and phenolics are considered as anti-nutrients in ruminant diets based on the function of inhibiting the fermentation of cell wall material by rumen microbes (Frei, 2015). Exposure to elevated ozone during growth leads to higher lignin and phenolics concentration in the rice straw, affecting the feed resource for ruminant herbivores (Frei et al., 2011).

1.2 General tolerance mechanism to elevated ozone

Possible tolerance mechanisms to elevated ozone include stress avoidance and defense, which refer to controlling the entry of ozone into the leaf and improving detoxification of ozone in the plant tissue, respectively (Frei, 2015). Regarding the former mechanism, stomatal aperture is formed by two surrounding guard cells in the epidermis of plant leaves, controlling the entry of ozone influx, so stomatal closure is the first line of defense against ozone (Ainsworth, 2017). Short-term elevated ozone reduces stomatal conductance (g_s) in response to increased substomatal CO_2 concentration (Ci), and further exposure causes stomata to become sluggish in response to environmental stimuli (Paoletti and Grulke, 2005). Cultivars with faster stomatal dynamics benefit the control of gas exchanges even under ozone-induced stomatal sluggishness (Paoletti and Grulke, 2010). In the model plant *Arabidopsis thaliana*, stomatal conductance was considered the most critical factor determining ozone sensitivity under an acute ozone treatment (350 ppb for 7 h) (Brosché et al., 2010). The *SLOW ANION CHANNEL-ASSOCIATED 1* (*SLAC1*) preferentially expressed in guard cells is essential for stomatal closure in responses to ozone. The protein plasma membrane SLAC1 can mediate anion efflux and depolarization of the cell membranes, which subsequently controls potassium (K^+) efflux through K^+ channels (Vahisalu et al., 2008). In addition, SLAC1 is phosphorylated by the protein kinase OST1, and both of them were required for ROS-induced fast stomata closure under elevated ozone (Vahisalu et al., 2010). Based on functional analysis of nine *Arabidopsis thaliana ghr1* mutant alleles identified in two independent forward-genetic ozone-sensitivity screens, the leucine-rich repeat receptor-like kinase (LRR-RLK) GUARD CELL HYDROGEN PEROXIDE-RESISTANT1 (GHR1) is involved in stomatal responses to apoplastic ROS (Sierla et al., 2018). Moreover, stomatal movements regulate gas exchange, thus also directly

affecting the efficiency of photosynthesis and the sensitivity of plants to ozone. The GARP family transcription factors GOLDEN 2-LIKE1 (GLK1) or GLK2 affect the expression of genes related to stomatal movement, and plants expressing the chimeric repressors for them regulate chloroplast development and exhibit remarkable ozone tolerance with a closed-stomata phenotype (Nagatoshi et al., 2016). Since stomatal aperture changes in response to environmental conditions such as light intensity, temperature and air humidity, cumulative ozone flux or uptake through the stomata can explain a large portion of environmental variability in damaging effects of ozone including grain yield (Mills et al., 2011; Pleijel et al., 2000). However, mechanisms for ozone defense remain elusive and differ among species, even different experiments on the same species have conflicting results, thus requiring further exploration.

As a visible response to ozone exposure, leaf visible symptoms are characterized by pale green to yellowish color, and usually occur as unevenly distributed small spot-like lesions often along veins, which is similar to those caused by incompatible pathogen infection and leads to PCD (Wohlgemuth et al., 2002). ROS formation in the apoplast is a specific characteristic common to both ozone stress and pathogen infection (Rao et al., 2000a). A plausible hypothesis is that acute ozone mimics an elicitor of plant pathogen interactions at the whole-plant level and ozone-induced cell death exhibits several of the features associated with PCD, referred to as hypersensitive response (HR) (Rao and Davis, 2001). HR is dependent on a specific program of gene expression as demonstrated by the existence of various mutants that form the spontaneous lesions (Mcdowell and Dangl, 2000). Ambient ozone levels can induce pathogenesis-related proteins and may thereby alter the disposition of plants toward pathogen attack (Schraudner et al., 1992). In tobacco plants, two pathogenesis-related genes (PR genes), namely β-1,3-glucanase and chitinase, were induced under ozone stress. Moreover, the rapidity of the increase in β-1,3-glucanase mRNA demonstrates a very early response (Ernst et al., 1992). In tobacco, ozone induced biochemical responses similar to those induced by necrotizing pathogens, resulting in transient ninefold increase in salicylic acid (SA) compared to controls (Yalpani et al., 1994). In the salicylic acid pathway, phenylalanine ammonia-lyase (PAL) activity involved in plant responses to pathogen defense, and its mRNA level were also increased remarkably under ozone exposure (Ogawa et al., 2005). Leaf bronzing score (LBS) was used to quantify the visible ozone damage, ranging from zero (no visible damage) to nine (deaf leaf) based on the four topmost fully expanded leaves in rice (Wissuwa et al., 2006). Two QTLs associated with leaf bronzing were located on chromosome three and nine, and the former increased bronzing, while the latter is the opposite (Frei et al., 2008). Anthocyanins and proanthocyanidins (PAs) also play important roles in ozone resistance, and elevated ozone

caused up-regulation of *Malus crabapple* structural genes *McANS*, *McCHI*, *McANR* and *McF3H*, which promoted the accumulation of anthocyanins and proanthocyanidins (PAs). Moreover, WRKY transcription factor (TF) *McWRKY71* highly expressed in responses to ozone stress is involved in the regulations of anthocyanins and PAs biosynthesis (Zhang et al., 2022). Quantitative trait loci (QTL) analysis showed that loci were associated with distinct leaf developmental stages and were identified on multiple chromosomes for foliar injury in soybean (Burton et al., 2016). These studies provided clues to elucidate specific mechanisms for ozone tolerance for future crop breeding.

Enzymatic and non-enzymatic metabolism are highly important to scavenge ozone-derived ROS. Antioxidants are molecules reducing oxidative stress, and usually deprive ROS of excessive electrons to remove the toxicity and render more stable molecules. For instance, ascorbic acid (AsA), one of the most important antioxidants, has two hydroxyl groups (-OH) and is capable of donating two electrons, producing two keton groups (=O). The *vtc1,* a semi-dominant ozone-sensitive mutant accumulating only 30% of wild-type levels, was isolated and showed that ascorbate concentration affects foliar resistance to ozone. It was putatively the result of a biosynthetic defect: less $_{L}$-[^{14}C]ascorbic acid as a percentage of total soluble ^{14}C accumulates in vtc1 than in wild type (Conklin et al., 1997; Conklin et al., 1996). In the subsequent analyses, other three *vtc* mutants were also isolated and have differing ozone sensitivities, in which *vtc2-1* and *vtc-2-2* had less than a half of AsA in the leaf tissue of mature plants compared with wild-type (Conklin et al., 2000). Moreover, AsA is commonly known to induce senescence, playing an important role in conjunction with various plant hormones in regulating gene expression during senescence (Barth et al., 2006). Transcript of eight senescence-associated genes (*SAGs*) is characterized induction by ozone in Arabidopsis, for example, *SAG13* (senescence-associated gene), *SAG21*, *ERD1* (early responsive to dehydration), and *BCB* (blue copper-binding protein) were induced within 2 to 4 d of ozone treatment; *SAG18*, *SAG20*, and *ACS6* (ACC synthase) were induced within 4 to 6 d; and *CCH* (copper chaperone) was induced within 6 to 8 d (Miller et al., 1999). AsA also can scavenge ROS via the enzymatic network of the ascorbate-glutathione cycle (Noctor and Foyer, 1998). A rice TOS17 insertion mutant (ND6172) for a GDP-$_{D}$-mannose-3',5'-epimerase gene involved in AsA biosynthesis, had around 20–30% lower AsA level than the wild-type (Nipponbare) companied with more severe visible leaf symptoms under ozone exposure (Frei et al., 2012b). Besides, the apoplast is the extraprotoplastic matrix of plant cells and consists of all compartments beyond the plasmalemma, including the cell wall (Dietz, 1997; Pignocchi

and Foyer, 2003). Apoplastic ascorbate contributes to the differential ozone sensitivity in two varieties of winter wheat under fully open-air field conditions (Feng et al., 2010). Compared with the charcoal-filtered treatment, apoplastic reduced AsA were significantly increased by elevated ozone in tobacco, soybean, poplar and peach (Dai et al., 2019; Dai et al., 2020). After ozone exposure, reduced AsA doubled in resistant genotypes, whereas the most sensitive genotype seemed unable to regenerate AsA from oxidized ascorbate (DHA) (Dumont et al., 2014). In sap bean, leaf apoplast AsA was significantly higher in tolerant genotypes compared with sensitive genotypes, indicating that apoplastic AsA contributes the detoxification of ozone (Burkey and Eason, 2002; Cheng et al., 2007). The apoplastic enzyme ascorbate oxidase (AO) also regulates the redox state of the apoplastic ascorbate pool (Pignocchi and Foyer, 2003). Transgenic tobacco with over-expression of AO in the apoplast had reduced redox stare of ascorbate, while accompanied with a substantial increase in foliar injury (Sanmartin et al., 2003). These studies provided evidence that AsA in the leaf tissue and apoplast have the function of ozone detoxification, may determine the ozone sensitivity in plant.

A novel gene, *OZONE-RESPONSIVE APOPLASTIC PROTEIN 1* (*OsORAP1*), was suggested as a candidate gene underlying *OzT9* in rice, and the knockout line enhances cell death in ozone stress (Ueda et al., 2015b). Plant hormones are major factors participating in the responses to ozone and are also involved in determining the extent of ozone-induced cell death, such as SA, ethylene (ET) and jasmonic acid (JA) (Kangasjärvi et al., 2005). QTL were identified linking detrimental effects of ozone with leaf and biomass traits, and a co-located genes encoding S-adenosyl methionine synthetase (*SAMS*), involved in the production of ET, showed divergent responses between tolerant and sensitive genotypes in poplar (Street et al., 2011). Components of one signaling pathway can affect signaling through other pathways, and the interaction of different dependent signaling pathways is indispensable for ozone-induced plant defense responses. For instance, JA signaling pathways reduced cell death by attenuating the ozone-induced oxidative burst and SA-mediated HR cell death (Rao et al., 2000b). In addition to the mechanisms of ozone-induced cell death, explanation for reduced biomass and grain yield induced by ozone have been investigated to some extent. A single locus on chromosome 6A was identified associated with the ozone-induced yield loss in rice based on the Sasanishiki/Habataki chromosome segment substitution lines, and the *ABERRANT PANICLE ORGANIZATION 1* (*APO1*) was suggested a potential candidate gene (Tsukahara et al., 2015; Tsukahara et al., 2013). The response of 23 varieties to ozone was assessed based on different phenotypes including dry weight loss, and a dry weight-associated QTL was located on

chromosome eight, namely *OzT8* (Frei et al., 2008). Further research confirmed that *OzT8* locus confers ozone tolerance via biochemical acclimation, such as photosynthetic capacity, not avoidance, making it a potentially valuable target for breeding of ozone tolerance into future rice lines (Chen et al., 2011).

1.3 Wheat: an important but ozone-sensitive cereal

Wheat is one of the most important food crops, widely grown and consumed across different regions, providing 19% of the daily calories and 21% of protein requirements for human (Shiferaw et al., 2013). As the human population continues to grow, wheat production must increase by more than 50% over current levels by 2050 to meet demand (Tadesse et al., 2019). Based on ploidy levels, cultivated wheats could be diploids einkorns (2n = 2x = 14, AA), tetraploids emmers (2n = 4x = 28, BBAA) and hexaploid common wheat *T. aestivum* (2n = 6x = 42, BBAADD) (Shewry, 2009). The hexaploid common wheat is considered a spontaneous hybridization between the tetraploid wheat species *T.tuigidum* (2n = 2x = 28, BBAA) and the diploid species *Aegilops tauchii* var. *strangulate* (2n = 2x = 14, DD) (Dvorak et al., 1998). The hexaploid bread wheat and the tetraploid durum wheat are currently main types, accounting for about 95% and 5%, respectively, of the world wheat production (Tadesse et al., 2016). The former is used for making bread and noodles, and the latter is used to make couscous and pasta (Walkowiak et al., 2020).

However, wheat is one of the most sensitive crops to ozone stress, with global yield reducing annually by 7.1% (Mills et al., 2018a). Moreover, compared to the older varieties, recently released high-yielding wheat varieties tend to be more sensitive to ozone, which partly explained by their higher stomatal conductance (Biswas et al., 2009). Ozone reduced wheat yields by a mean 9.9% in the northern hemisphere and 6.2% in the southern hemisphere over 2010–2012, corresponding to some 85 Tg (million tonnes) of lost grain (Mills et al., 2018a). These global losses would increase to 25.8% by 2030, with 44.4% and 25.7% losses in South and East Asia, respectively (Avnery et al., 2011). Asia produces large portions of the world cereals, and on average, 44% of wheat came from the region between 2014 and 2018. In China, the highest relative yield loss reached 33% for wheat, which is much greater than for rice and maize from 2017 to 2019 (Feng et al., 2022). A recent study estimated that the annual average losses of wheat yield reached 26.5 Mt, accounting for 17% of the total yield without ozone impact from 2010 to 2021, indicating the heavy ozone-induce damages on wheat in China (Wang et al., 2023). Nevertheless, ozone exposure also affects wheat grain quality, for example, strong negative effects on thousand kernel weight and starch concentration were observed in a

meta-analysis based on 42 experiments performed in Asia, Europe and North America (Broberg et al., 2015).

During the growth season, tropospheric ozone also causes multiple types of damage to wheat, such as foliar necrotic symptoms (Figure 1.2) (Begum et al., 2020), limited carbon dioxide uptake by inducing partial stomatal closure or less efficient stomatal control (Feng et al., 2008), reduced net photosynthetic rate (Akhtar et al., 2010), loss of the activity of Calvin cycle enzymes such as Rubisco (Inada et al., 2012) as well as premature leaf senescence (Ojanpera et al., 1998). Large variation in ozone tolerance of wheat was observed in different phenotypic responses (Biswas et al., 2008; Feng et al., 2008; Singh et al., 2018). The sensitivity of plants to ozone has been linked to ozone flux controlled by stomata and antioxidant capacity determined by antioxidant pools and enzymes. Unlike it, ozone-induced reduction in photosynthetic rates of wheat would be largely attributed to non-stomatal factors (Biswas et al., 2008). Many studies have clarified the mechanism of plant defense to ozone damage in relation to detoxification of ROS through enzymatic and non-enzymatic antioxidant metabolism in wheat (Feng et al., 2016). For instance, superoxide dismutase (SOD), peroxidase (POX) and guaiacol peroxidase were associated with varying levels of sensitivity against elevated ozone in different wheat cultivars (Fatima et al., 2018). Recently, a genome-wide association study (GWAS) was conducted based on a diversity panel of 150 wheat genotypes, and genetic variation regarding physiological and yield responses to elevated ozone was explored throughout the growing season. Significant marker-trait associations were identified for LBS on chromosome 5A and for vegetation indices including normalized difference vegetation index (NDVI) and Lichtenthaler index 2 (Lic2) on chromosomes 6B and 6D (Begum et al., 2020). The variable responses to ozone in different physiological traits and yield lay the foundation for ozone tolerance breeding in wheat to secure food supply.

Figure 1.2 Quantification of foliar ozone damage symptoms in wheat as leaf bronzing score ranging from 1 to 10. This figure was adapted from Begum et al. (2020).

1.4 Research objectives

In this thesis, I will focus on three main objectives in the following three chapters regarding the ozone effects on wheat and the potential tolerance mechanism.

(I) There are large genotypic variations of ozone tolerance in wheat due to distinct physiological traits, which are insufficiently reflected in current crop models simulating ozone responses.

The main objectives of this study were therefore: (1) estimating the impacts of elevated ozone on contrasting wheat cultivars and ranking them in terms of ozone tolerance; (2) identifying physiological traits underlying the ability to maintain high grain yield under ozone stress; (3) calibrating a crop growth model to simulate tolerant and sensitive cultivar responses to ozone, and establishing specific model parameters that represent ozone tolerant and sensitive wheat ideotypes. Thereby, this study will improve the accuracy of ozone impact assessment and help to project and upscale the effects of ozone tolerance breeding.

(II) Carbon (C) and nitrogen (N) are important basic elements for plant growth. The responses to ozone might be cultivar-specific and the dynamics of N uptake and translocation under ozone stress are poorly understood. Moreover, the role of the C:N ratio and its contribution to yield-related traits, as well as the relationship with NUE indicators remains elusive in wheat.

The specific aims of this investigation were to (1) estimate the impacts of elevated ozone concentration on straw C and N in different growth stages and their allocation to grain, (2) explore the effects of ozone on different NUE indicators in different cultivars, and (3)

determine the relationships between the straw C:N ratio and productivity among different cultivars.

(III) Differential responses to ozone were observed for foliar symptom formation quantified as LBS, which showed the highest heritability. Significant marker-trait associated with LBS under ozone stress were used to form haplotypes representing groups of genotypes within the population that differed significantly in ozone tolerance. Eleven candidate genes were identified to be involved in the redox biology of plants and could underline symptom formation at elevated ozone (Begum et al., 2020). The effective use of such candidate genes in the breeding of ozone-tolerant wheat requires further characterization of sequence polymorphisms, transcriptional or translational regulation, and their physiological role in ozone tolerance.

This study represents an in-depth investigation aimed at understanding the molecular and physiological mechanisms based on the different responses to elevated ozone in contrasting haplotypes for gene markers associated with LBS (two ozone-sensitive genotypes and two ozone-tolerant genotypes). In this study, two specific hypotheses were investigated: (1) Different genotypes representing either tolerant or sensitive haplotypes of wheat will show consistent physiological responses to ozone that are linked to their genetic constitution. (2) Among the candidate genes located within a previously identified locus on chromosome 5A, genes showing consistent differential expression and/or sequence polymorphisms between tolerant and sensitive haplotypes may confer ozone tolerance in wheat.

References

Agathokleous, E., Saitanis, C.J., Koike, T., 2015. Tropospheric O_3, the nightmare of wild plants: a review study. J. Agric.Meteorol. 71, 142-152.

Ainsworth, E.A., 2017. Understanding and improving global crop response to ozone pollution. Plant J 90, 886-897.

Ainsworth, E.A., Rogers, A., Leakey, A.D., 2008. Targets for crop biotechnology in a future high-CO_2 and high-O_3 world. Plant Physiol. 147, 13-19.

Ainsworth, E.A., Yendrek, C.R., Sitch, S., Collins, W.J., Emberson, L.D., 2012. The Effects of Tropospheric Ozone on Net Primary Productivity and Implications for Climate Change. Annu. Rev. Plant Biol. 63, 637-661.

Akhtar, N., Yamaguchi, M., Inada, H., Hoshino, D., Kondo, T., Izuta, T., 2010. Effects of ozone on growth, yield and leaf gas exchange rates of two Bangladeshi cultivars of wheat (Triticum aestivum L.). Environ. Pollut. 158, 1763-1767.

Alam, M.S., Maina, A.W., Feng, Y., Wu, L.-B., Frei, M., 2022. Interactive effects of tropospheric ozone and blast disease (Magnaporthe oryzae) on different rice genotypes. Environ. Sci. Pollut. Res. 29, 48893-48907.

Ashmore, M.R., 2005. Assessing the future global impacts of ozone on vegetation. Plant Cell Environ. 28, 949-964.

Ashrafuzzaman, M., Lubna, F.A., Holtkamp, F., Manning, W.J., Kraska, T., Frei, M., 2017. Diagnosing ozone stress and differential tolerance in rice (Oryza sativa L.) with ethylenediurea (EDU). Environ. Pollut. 230, 339-350.

Avnery, S., Mauzerall, D.L., Liu, J., Horowitz, L.W., 2011. Global crop yield reductions due to surface ozone exposure: 2. Year 2030 potential crop production losses and economic damage under two scenarios of O_3 pollution. Atmos. Environ. 45, 2297-2309.

Barth, C., De Tullio, M., Conklin, P.L., 2006. The role of ascorbic acid in the control of flowering time and the onset of senescence. J. Exp. Bot. 57, 1657-1665.

Begum, H., Alam, M.S., Feng, Y., Koua, P., Ashrafuzzaman, M., Shrestha, A., Kamruzzaman, M., Dadshani, S., Ballvora, A., Naz, A.A., Frei, M., 2020. Genetic dissection of bread wheat diversity and identification of adaptive loci in response to elevated tropospheric ozone. Plant Cell Environ. 43, 2650-2665.

Biswas, D.K., Xu, H., Li, Y.G., Sun, J.Z., Wang, X.Z., Han, X.G., Jiang, G.M., 2008. Genotypic differences in leaf biochemical, physiological and growth responses to ozone in 20 winter wheat cultivars released over the past 60 years. Glob. Chang. Biol. 14, 46-59.

Biswas, D.K., Xu, H., Yang, J.C., Li, Y.G., Chen, S.B., Jiang, C.D., Li, W.D., Ma, K.P., Adhikary, S.K., Wang, X.Z., Jiang, G.M., 2009. Impacts of methods and sites of plant breeding on ozone sensitivity in winter wheat cultivars. Agric. Ecosyst. Environ. 134, 168-177.

Brauer, M., Freedman, G., Frostad, J., van Donkelaar, A., Martin, R.V., Dentener, F., van Dingenen, R., Estep, K., Amini, H., Apte, J.S., Balakrishnan, K., Barregard, L., Broday, D., Feigin, V., Ghosh, S., Hopke, P.K., Knibbs, L.D., Kokubo, Y., Liu, Y., Ma, S., Morawska, L., Sangrador, J.L., Shaddick, G., Anderson, H.R., Vos, T., Forouzanfar, M.H., Burnett, R.T., Cohen, A., 2016. Ambient Air Pollution Exposure Estimation for the Global Burden of Disease 2013. Environ. Sci. Technol. 50, 79-88.

Broberg, M.C., Feng, Z., Xin, Y., Pleijel, H., 2015. Ozone effects on wheat grain quality - a summary. Environ. Pollut. 197, 203-213.

Brosché, M., Merilo, E., Mayer, F., Pechter, P., Puzõrjova, I., Brader, G., Kangasjärvi, J.,

Kollist, H., 2010. Natural variation in ozone sensitivity among Arabidopsis thaliana accessions and its relation to stomatal conductance. Plant Cell Environ. 33, 914-925.

Burkey, K.O., Eason, G., 2002. Ozone tolerance in snap bean is associated with elevated ascorbic acid in the leaf apoplast. Physiol. Plant. 114, 387-394.

Burton, A.L., Burkey, K.O., Carter, T.E., Orf, J., Cregan, P.B., 2016. Phenotypic variation and identification of quantitative trait loci for ozone tolerance in a Fiskeby III × Mandarin (Ottawa) soybean population. Theor. Appl. Genet. 129, 1113-1125.

Calatayud, A., Barreno, E., 2001. Chlorophyll a fluorescence, antioxidant enzymes and lipid peroxidation in tomato in response to ozone and benomyl. Environ. pollut. 115, 283-289.

Chang, K.-L., Petropavlovskikh, I., Cooper, O.R., Schultz, M.G., Wang, T., 2017. Regional trend analysis of surface ozone observations from monitoring networks in eastern North America, Europe and East Asia. Elem. Sci. Anth. 5.

Chen, C.P., Frei, M., Wissuwa, M., 2011. The *OzT8* locus in rice protects leaf carbon assimilation rate and photosynthetic capacity under ozone stress. Plant Cell Environ. 34, 1141-1149.

Cheng, F.Y., Burkey, K.O., Robinson, J.M., Booker, F.L., 2007. Leaf extracellular ascorbate in relation to O_3 tolerance of two soybean cultivars. Environ. Pollut. 150, 355-362.

Conklin, P.L., Pallanca, J.E., Last, R.L., Smirnoff, N., 1997. L-ascorbic acid metabolism in the ascorbate-deficient Arabidopsis mutant vtc1. Plant Physiol. 115, 1277-1285.

Conklin, P.L., Saracco, S.A., Norris, S.R., Last, R.L., 2000. Identification of ascorbic acid-deficient Arabidopsis thaliana mutants. Genetics 154, 847-856.

Conklin, P.L., Williams, E.H., Last, R.L., 1996. Environmental stress sensitivity of an ascorbic acid-deficient Arabidopsis mutant. Proc. Natl. Acad. Sci. 93, 9970-9974.

Dai, L., Feng, Z., Pan, X., Xu, Y., Li, P., Lefohn, A.S., Harmens, H., Kobayashi, K., 2019. Increase of apoplastic ascorbate induced by ozone is insufficient to remove the negative effects in tobacco, soybean and poplar. Environ. Pollut. 245, 380-388.

Dai, L., Kobayashi, K., Nouchi, I., Masutomi, Y., Feng, Z., 2020. Quantifying determinants of ozone detoxification by apoplastic ascorbate in peach (Prunus persica) leaves using a model of ozone transport and reaction. Glob. Chang. Biol. 26, 3147-3162.

Darrall, N.M., 1989. The effect of air pollutants on physiological processes in plants. Plant Cell Environ. 12, 1-30.

Dietz, K.-J., 1997. Functions and responses of the leaf apoplast under stress. Progress in Botany: Structural Botany Physiology Genetics Taxonomy Geobotany/Fortschritte der

Botanik Struktur Physiologie Genetik Systematik Geobotanik, 221-254.

Dizengremel, P., 2001. Effects of ozone on the carbon metabolism of forest trees. Plant Physiol. Biochem. 39, 729-742.

Dumont, J., Keski-Saari, S., Keinanen, M., Cohen, D., Ningre, N., Kontunen-Soppela, S., Baldet, P., Gibon, Y., Dizengremel, P., Vaultier, M.N., Jolivet, Y., Oksanen, E., Le Thiec, D., 2014. Ozone affects ascorbate and glutathione biosynthesis as well as amino acid contents in three Euramerican poplar genotypes. Tree Physiol. 34, 253-266.

Dvorak, J., Luo, M.-C., Yang, Z.-L., Zhang, H.-B., 1998. The structure of the Aegilops tauschii genepool and the evolution of hexaploid wheat. Theor. Appl. Genetics 97, 657-670.

Ernst, D., Schraudner, M., Langebartels, C., Sandermann, H., 1992. Ozone-induced changes of mRNA levels of β-1,3-glucanase, chitinase and 'pathogenesis-related' protein 1b in tobacco plants. Plant Mol. Biol. 20, 673-682.

Fatima, A., Singh, A.A., Mukherjee, A., Agrawal, M., Agrawal, S.B., 2018. Variability in defence mechanism operating in three wheat cultivars having different levels of sensitivity against elevated ozone. Environ. Exp. Bot. 155, 66-78.

Feng, Z., Kobayashi, K., Ainsworth, E.A., 2008. Impact of elevated ozone concentration on growth, physiology, and yield of wheat (Triticum aestivum L.): a meta-analysis. Glob. Chang. Biol. 14, 2696-2708.

Feng, Z., Pang, J., Kobayashi, K., Zhu, J., Ort, D.R., 2011. Differential responses in two varieties of winter wheat to elevated ozone concentration under fully open-air field conditions. Glob. Chang. Biol. 17, 580-591.

Feng, Z., Pang, J., Nouchi, I., Kobayashi, K., Yamakawa, T., Zhu, J., 2010. Apoplastic ascorbate contributes to the differential ozone sensitivity in two varieties of winter wheat under fully open-air field conditions. Environ. Pollut. 158, 3539-3545.

Feng, Z., Wang, L., Pleijel, H., Zhu, J., Kobayashi, K., 2016. Differential effects of ozone on photosynthesis of winter wheat among cultivars depend on antioxidative enzymes rather than stomatal conductance. Sci. Total Environ. 572, 404-411.

Feng, Z., Xu, Y., Kobayashi, K., Dai, L., Zhang, T., Agathokleous, E., Calatayud, V., Paoletti, E., Mukherjee, A., Agrawal, M., Park, R.J., Oak, Y.J., Yue, X., 2022. Ozone pollution threatens the production of major staple crops in East Asia. Nat. Food 3, 47-56.

Fiscus, E.L., Booker, F.L., Burkey, K.O., 2005. Crop responses to ozone: uptake, modes of action, carbon assimilation and partitioning. Plant Cell Environ. 28, 997-1011.

Fowler, D., Amann, M., Anderson, R., Ashmore, M., Cox, P., Depledge, M., Derwent, D., Grennfelt, P., Hewitt, N., Hov, O., 2008. Ground-level ozone in the 21st century: future

trends, impacts and policy implications.

Frei, M., 2015. Breeding of ozone resistant rice: relevance, approaches and challenges. Environ. Pollut. 197, 144-155.

Frei, M., Kohno, Y., Tietze, S., Jekle, M., Hussein, M.A., Becker, T., Becker, K., 2012a. The response of rice grain quality to ozone exposure during growth depends on ozone level and genotype. Environ. Pollut. 163, 199-206.

Frei, M., Kohno, Y., Wissuwa, M., Makkar, H.P.S., Becker, K., 2011. Negative effects of tropospheric ozone on the feed value of rice straw are mitigated by an ozone tolerance QTL. Glob. Chang. Biol. 17, 2319-2329.

Frei, M., Tanaka, J.P., Wissuwa, M., 2008. Genotypic variation in tolerance to elevated ozone in rice: dissection of distinct genetic factors linked to tolerance mechanisms. J. Exp. Bot. 59, 3741-3752.

Frei, M., Wissuwa, M., Pariasca-Tanaka, J., Chen, C.P., Sudekum, K.H., Kohno, Y., 2012b. Leaf ascorbic acid level--is it really important for ozone tolerance in rice? Plant Physiol. Biochem. 59, 63-70.

Fuhrer, J., Lehnherr, B., Moeri, P., Tschannen, W., Shariat-Madari, H., 1990. Effects of ozone on the grain composition of spring wheat grown in open-top field chambers. Environ. pollut. 65, 181-192.

Gaudel, A., Cooper, O.R., Ancellet, G., Barret, B., Boynard, A., Burrows, J.P., Clerbaux, C., Coheur, P.-F., Cuesta, J., Cuevas, E., 2018. Tropospheric Ozone Assessment Report: Present-day distribution and trends of tropospheric ozone relevant to climate and global atmospheric chemistry model evaluation. Elem. Sci. Anth. 6, 39.

Haagen-Smit, A.J., 1952. Chemistry and Physiology of Los Angeles Smog. Industrial & Engineering Chemistry 44, 1342-1346.

Hayes, F., Mills, G., Harmens, H., Norris, D., 2007. Evidence of widespread ozone damage to vegetation in Europe (1990-2006). ICP Vegetation Programme Coordination Centre, CEH Bangor, UK.

Inada, H., Kondo, T., Akhtar, N., Hoshino, D., Yamaguchi, M., Izuta, T., 2012. Relationship between cultivar difference in the sensitivity of net photosynthesis to ozone and reactive oxygen species scavenging system in Japanese winter wheat (Triticum aestivum). Physiol. Plant 146, 217-227.

Kangasjärvi, J., Jaspers, P., Kollist, H., 2005. Signalling and cell death in ozone-exposed plants. Plant Cell Environ. 28, 1021-1036.

Li, P., Feng, Z., Catalayud, V., Yuan, X., Xu, Y., Paoletti, E., 2017. A meta-analysis on growth,

physiological, and biochemical responses of woody species to ground-level ozone highlights the role of plant functional types. Plant Cell Environ. 40, 2369-2380.

Mcdowell, J.M., Dangl, J.L., 2000. Signal transduction in the plant immune response. Trends Biochem. Sci. 25, 79-82.

Miller, J.D., Arteca, R.N., Pell, E.J., 1999. Senescence-associated gene expression during ozone-induced leaf senescence in Arabidopsis. Plant Physiol. 120, 1015-1023.

Mills, G., Pleijel, H., Braun, S., Büker, P., Bermejo, V., Calvo, E., Danielsson, H., Emberson, L., Fernández, I.G., Grünhage, L., Harmens, H., Hayes, F., Karlsson, P.-E., Simpson, D., 2011. New stomatal flux-based critical levels for ozone effects on vegetation. Atmos. Environ. 45, 5064-5068.

Mills, G., Sharps, K., Simpson, D., Pleijel, H., Broberg, M., Uddling, J., Jaramillo, F., Davies, W.J., Dentener, F., Van den Berg, M., Agrawal, M., Agrawal, S.B., Ainsworth, E.A., Buker, P., Emberson, L., Feng, Z., Harmens, H., Hayes, F., Kobayashi, K., Paoletti, E., Van Dingenen, R., 2018a. Ozone pollution will compromise efforts to increase global wheat production. Glob. Chang. Biol. 24, 3560-3574.

Mills, G., Sharps, K., Simpson, D., Pleijel, H., Frei, M., Burkey, K., Emberson, L., Uddling, J., Broberg, M., Feng, Z., Kobayashi, K., Agrawal, M., 2018b. Closing the global ozone yield gap: Quantification and cobenefits for multistress tolerance. Glob. Chang. Biol. 24, 4869-4893.

Monks, P.S., Archibald, A.T., Colette, A., Cooper, O., Coyle, M., Derwent, R., Fowler, D., Granier, C., Law, K.S., Mills, G.E., Stevenson, D.S., Tarasova, O., Thouret, V., von Schneidemesser, E., Sommariva, R., Wild, O., Williams, M.L., 2015. Tropospheric ozone and its precursors from the urban to the global scale from air quality to short-lived climate forcer. Atmos. Chem. Phys. 15, 8889-8973.

Nagatoshi, Y., Mitsuda, N., Hayashi, M., Inoue, S.-I., Okuma, E., Kubo, A., Murata, Y., Seo, M., Saji, H., Kinoshita, T., Ohme-Takagi, M., 2016. GOLDEN 2-LIKE transcription factors for chloroplast development affect ozone tolerance through the regulation of stomatal movement. Proc. Natl. Acad. Sci. 113, 4218-4223.

Noctor, G., Foyer, C.H., 1998. Ascorbate and glutathione: Keeping active oxygen under control. Annual Review of Plant Physiology and Plant Molecular Biology 49, 249-279.

Ogawa, D., Nakajima, N., Sano, T., Tamaoki, M., Aono, M., Kubo, A., 2005. Regulation of salicylic acid synthesis in ozone-exposed tobacco and Arabidopsis.

Ojanpera, K., Patsikka, E., Ylaranta, T., 1998. Effects of low ozone exposure of spring wheat on net CO_2 uptake, Rubisco, leaf senescence and grain filling. New Phytol. 138, 451-

460.

Paoletti, E., Grulke, N.E., 2005. Does living in elevated CO_2 ameliorate tree response to ozone? A review on stomatal responses. Environ. pollut. 137, 483-493.

Paoletti, E., Grulke, N.E., 2010. Ozone exposure and stomatal sluggishness in different plant physiognomic classes. Environ. Pollut. 158, 2664-2671.

Peng, J., Shang, B., Xu, Y., Feng, Z., Calatayud, V., 2020. Effects of ozone on maize (Zea mays L.) photosynthetic physiology, biomass and yield components based on exposure- and flux-response relationships. Environ. Pollut. 256, 113466.

Pignocchi, C., Foyer, C.H., 2003. Apoplastic ascorbate metabolism and its role in the regulation of cell signalling. Curr. Opin. Plant. Biol. 6, 379-389.

Pleijel, H., Danielsson, H., Karlsson, G.P., Gelang, J., Karlsson, P., Selldén, G., 2000. An ozone flux–response relationship for wheat. Environ. pollut. 109, 453-462.

Rao, M.V., Davis, K.R., 2001. The physiology of ozone induced cell death. Planta 213, 682-690.

Rao, M.V., Koch, J.R., Davis, K.R., 2000a. Ozone: a tool for probing programmed cell death in plants. Programmed Cell Death in Higher Plants, 101-114.

Rao, M.V., Lee, H.-i., Creelman, R.A., Mullet, J.E., Davis, K.R., 2000b. Jasmonic acid signaling modulates ozone-induced hypersensitive cell death. Plant Cell 12, 1633-1646.

Sanmartin, M., Drogoudi, P.D., Lyons, T., Pateraki, I., Barnes, J., Kanellis, A.K., 2003. Over-expression of ascorbate oxidase in the apoplast of transgenic tobacco results in altered ascorbate and glutathione redox states and increased sensitivity to ozone. Planta 216, 918-928.

Schraudner, M., Ernst, D., Langebartels, C., Sandermann Jr, H., 1992. Biochemical plant responses to ozone: III. Activation of the defense-related proteins β-1, 3-glucanase and chitinase in tobacco leaves. Plant Physiol. 99, 1321-1328.

Shewry, P.R., 2009. Wheat. J. Exp. Bot. 60, 1537-1553.

Shiferaw, B., Smale, M., Braun, H.-J., Duveiller, E., Reynolds, M., Muricho, G., 2013. Crops that feed the world 10. Past successes and future challenges to the role played by wheat in global food security. Food Secur. 5, 291-317.

Sierla, M., Horak, H., Overmyer, K., Waszczak, C., Yarmolinsky, D., Maierhofer, T., Vainonen, J.P., Salojarvi, J., Denessiouk, K., Laanemets, K., Toldsepp, K., Vahisalu, T., Gauthier, A., Puukko, T., Paulin, L., Auvinen, P., Geiger, D., Hedrich, R., Kollist, H., Kangasjarvi, J., 2018. The Receptor-like Pseudokinase GHR1 Is Required for Stomatal Closure. Plant Cell 30, 2813-2837.

Simpson, D., Arneth, A., Mills, G., Solberg, S., Uddling, J., 2014. Ozone — the persistent menace: interactions with the N cycle and climate change. Curr. Opin. Environ. Sustain. 9-10, 9-19.

Singh, A.A., Fatima, A., Mishra, A.K., Chaudhary, N., Mukherjee, A., Agrawal, M., Agrawal, S.B., 2018. Assessment of ozone toxicity among 14 Indian wheat cultivars under field conditions: growth and productivity. Environ. Monit. Assess. 190, 190.

Stevenson, D.S., Dentener, F.J., Schultz, M.G., Ellingsen, K., Van Noije, T.P.C., Wild, O., Zeng, G., Amann, M., Atherton, C.S., Bell, N., Bergmann, D.J., Bey, I., Butler, T., Cofala, J., Collins, W.J., Derwent, R.G., Doherty, R.M., Drevet, J., Eskes, H.J., Fiore, A.M., Gauss, M., Hauglustaine, D.A., Horowitz, L.W., Isaksen, I.S.A., Krol, M.C., Lamarque, J.-F., Lawrence, M.G., Montanaro, V., Müller, J.-F., Pitari, G., Prather, M.J., Pyle, J.A., Rast, S., Rodriguez, J.M., Sanderson, M.G., Savage, N.H., Shindell, D.T., Strahan, S.E., Sudo, K., Szopa, S., 2006. Multimodel ensemble simulations of present-day and near-future tropospheric ozone. J. Geophys. Res. 111.

Street, N.R., James, T.M., James, T., Mikael, B., Jaakko, K., Mark, B., Taylor, G., 2011. The physiological, transcriptional and genetic responses of an ozone-sensitive and an ozone tolerant poplar and selected extremes of their F2 progeny. Environ. Pollut. 159, 45-54.

Sun, J., Feng, Z., Ort, D.R., 2014. Impacts of rising tropospheric ozone on photosynthesis and metabolite levels on field grown soybean. Plant Sci. 226, 147-161.

Tadesse, W., Amri, A., Ogbonnaya, F.C., Sanchez-Garcia, M., Sohail, Q., Baum, M., 2016. Wheat, Genetic and Genomic Resources for Grain Cereals Improvement, pp. 81-124.

Tadesse, W., Sanchez-Garcia, M., Assefa, S.G., Amri, A., Bishaw, Z., Ogbonnaya, F.C., Baum, M., 2019. Genetic gains in wheat breeding and its role in feeding the world. Crop Breeding, Genetics and Genomics 1.

Tsukahara, K., Sawada, H., Kohno, Y., Matsuura, T., Mori, I.C., Terao, T., Ioki, M., Tamaoki, M., 2015. Ozone-Induced Rice Grain Yield Loss Is Triggered via a Change in Panicle Morphology That Is Controlled by *ABERRANT PANICLE ORGANIZATION 1* Gene. PLoS One 10, e0123308.

Tsukahara, K., Sawada, H., Matsumura, H., Kohno, Y., Tamaoki, M., 2013. Quantitative trait locus analyses of ozone-induced grain yield reduction in rice. Environ. Exp. Bot. 88, 100-106.

Ueda, Y., Frimpong, F., Qi, Y., Matthus, E., Wu, L., Holler, S., Kraska, T., Frei, M., 2015a. Genetic dissection of ozone tolerance in rice (Oryza sativa L.) by a genome-wide association study. J. Exp. Bot. 66, 293-306.

Ueda, Y., Siddique, S., Frei, M., 2015b. A Novel Gene, *OZONE-RESPONSIVE APOPLASTIC PROTEIN1*, Enhances Cell Death in Ozone Stress in Rice. Plant Physiol. 169, 873-889.

Ueda, Y., Uehara, N., Sasaki, H., Kobayashi, K., Yamakawa, T., 2013. Impacts of acute ozone stress on superoxide dismutase (SOD) expression and reactive oxygen species (ROS) formation in rice leaves. Plant Physiol. Biochem. 70, 396-402.

Vahisalu, T., Kollist, H., Wang, Y.-F., Nishimura, N., Chan, W.-Y., Valerio, G., Lamminmäki, A., Brosché, M., Moldau, H., Desikan, R., Schroeder, J.I., Kangasjärvi, J., 2008. SLAC1 is required for plant guard cell S-type anion channel function in stomatal signalling. Nature 452, 487-491.

Vahisalu, T., Puzõrjova, I., Brosché, M., Valk, E., Lepiku, M., Moldau, H., Pechter, P., Wang, Y.-S., Lindgren, O., Salojärvi, J., Loog, M., Kangasjärvi, J., Kollist, H., 2010. Ozone-triggered rapid stomatal response involves the production of reactive oxygen species, and is controlled by SLAC1 and OST1. Plant J. 62, 442-453.

Walkowiak, S., Gao, L., Monat, C., Haberer, G., Kassa, M.T., Brinton, J., Ramirez-Gonzalez, R.H., Kolodziej, M.C., Delorean, E., Thambugala, D., Klymiuk, V., Byrns, B., Gundlach, H., Bandi, V., Siri, J.N., Nilsen, K., Aquino, C., Himmelbach, A., Copetti, D., Ban, T., Venturini, L., Bevan, M., Clavijo, B., Koo, D.-H., Ens, J., Wiebe, K., N'Diaye, A., Fritz, A.K., Gutwin, C., Fiebig, A., Fosker, C., Fu, B.X., Accinelli, G.G., Gardner, K.A., Fradgley, N., Gutierrez-Gonzalez, J., Halstead-Nussloch, G., Hatakeyama, M., Koh, C.S., Deek, J., Costamagna, A.C., Fobert, P., Heavens, D., Kanamori, H., Kawaura, K., Kobayashi, F., Krasileva, K., Kuo, T., Mckenzie, N., Murata, K., Nabeka, Y., Paape, T., Padmarasu, S., Percival-Alwyn, L., Kagale, S., Scholz, U., Sese, J., Juliana, P., Singh, R., Shimizu-Inatsugi, R., Swarbreck, D., Cockram, J., Budak, H., Tameshige, T., Tanaka, T., Tsuji, H., Wright, J., Wu, J., Steuernagel, B., Small, I., Cloutier, S., Keeble-Gagnère, G., Muehlbauer, G., Tibbets, J., Nasuda, S., Melonek, J., Hucl, P.J., Sharpe, A.G., Clark, M., Legg, E., Bharti, A., Langridge, P., Hall, A., Uauy, C., Mascher, M., Krattinger, S.G., Handa, H., Shimizu, K.K., Distelfeld, A., Chalmers, K., Keller, B., Mayer, K.F.X., Poland, J., Stein, N., Mccartney, C.A., Spannagl, M., Wicker, T., Pozniak, C.J., 2020. Multiple wheat genomes reveal global variation in modern breeding. Nature 588, 277-283.

Wang, Y., Frei, M., 2011. Stressed food – The impact of abiotic environmental stresses on crop quality. Agric. Ecosyst. Environ. 141, 271-286.

Wang, Y., Song, Q., Frei, M., Shao, Z., Yang, L., 2014. Effects of elevated ozone, carbon dioxide, and the combination of both on the grain quality of Chinese hybrid rice.

Environ. Pollut. 189, 9-17.

Wang, Y., Wang, Y., Feng, Z., Yuan, X., Zhao, Y., 2023. The impacts of ambient ozone pollution on China's wheat yield and forest production from 2010 to 2021. Environ. Pollut. 330, 121726.

Wissuwa, M., Ismail, A.M., Yanagihara, S., 2006. Effects of zinc deficiency on rice growth and genetic factors contributing to tolerance. Plant Physiol. 142, 731-741.

Wohlgemuth, H., Mittelstrass, K., Kschieschan, S., Bender, J., Weigel, H.-J., Overmyer, K., Kangasjärvi, J., Sandermann, H., Langebartels, C., 2002. Activation of an oxidative burst is a general feature of sensitive plants exposed to the air pollutant ozone. Plant Cell Environ. 25, 717-726.

Yalpani, N., Enyedi, A., Le□N, J., Raskin, I., 1994. Ultraviolet light and ozone stimulate accumulation of salicylic acid, pathogenesis-related proteins and virus resistance in tobacco. Planta 193.

Yuan, X., Calatayud, V., Gao, F., Fares, S., Paoletti, E., Tian, Y., Feng, Z., 2016. Interaction of drought and ozone exposure on isoprene emission from extensively cultivated poplar. Plant Cell Environ. 39, 2276-2287.

Zeng, Y., Cao, Y., Qiao, X., Seyler, B.C., Tang, Y., 2019. Air pollution reduction in China: Recent success but great challenge for the future. Sci. Total Environ. 663, 329-337.

Zhang, J., Wang, Y., Mao, Z., Liu, W., Ding, L., Zhang, X., Yang, Y., Wu, S., Chen, X., Wang, Y., 2022. Transcription factor McWRKY71 induced by ozone stress regulates anthocyanin and proanthocyanidin biosynthesis in Malus crabapple. Ecotoxicol. Environ. Saf. 232, 113274.

Zhang, W., Wang, G., Liu, X., Feng, Z., 2014. Effects of elevated O_3 exposure on seed yield, N concentration and photosynthesis of nine soybean cultivars (Glycine max (L.) Merr.) in Northeast China. Plant Sci. 226, 172-181.

Zheng, F., Wang, X., Zhang, W., Hou, P., Lu, F., Du, K., Sun, Z., 2013. Effects of elevated O_3 exposure on nutrient elements and quality of winter wheat and rice grain in Yangtze River Delta, China. Environ. Pollut. 179, 19-26.

Chapter 2: Identifying and modelling key physiological traits that confer tolerance or sensitivity to ozone in winter wheat

Manuscript published in Environment Pollution 2022 Vol 304, 119251

Environmental Pollution 304 (2022) 119251

Contents lists available at ScienceDirect

Environmental Pollution

journal homepage: www.elsevier.com/locate/envpol

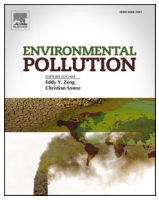

Identifying and modelling key physiological traits that confer tolerance or sensitivity to ozone in winter wheat☆

Yanru Feng [a,b,1], Thuy Huu Nguyen [b,1], Muhammad Shahedul Alam [a], Lisa Emberson [d], Thomas Gaiser [b], Frank Ewert [b,c], Michael Frei [a,*]

[a] Department of Agronomy and Crop Physiology, Institute of Agronomy and Plant Breeding, Justus Liebig University Giessen, 35390, Giessen, Germany
[b] Institute of Crop Science and Resource Conservation (INRES), Crop Science, University of Bonn, 53115, Bonn, Germany
[c] Leibniz Centre for Agricultural Landscape Research (ZALF), Institute of Landscape Systems Analysis, 15374, Muencheberg, Germany
[d] Environment and Geography Department, University of York, YO10 5NG, UK

ARTICLE INFO

Keywords:
Air pollution
Breeding
Cereals
Food security
Global change
Crop modelling

ABSTRACT

Tropospheric ozone threatens crop production in many parts of the world, especially in highly populated countries in economic transition. Crop models suggest substantial global yield losses for wheat, but typically such models fail to address differences in ozone responses between tolerant and sensitive genotypes. Therefore, the purpose of this study was to identify physiological traits contributing to yield losses or yield stability under ozone stress in 18 contrasting wheat cultivars that had been pre-selected from a larger wheat population with known ozone tolerance. Plants were exposed to season-long ozone fumigation in open-top chambers at an average ozone concentration of 70 ppb with three additional acute ozone episodes of around 150 ppb. Compared to control conditions, average yield loss was 18.7 percent, but large genotypic variation was observed ranging from 2.7 to 44.6 percent. Foliar chlorophyll content represented by normalized difference vegetation index and net CO_2 assimilation rate of young leaves during grain filling were the physiological traits most strongly correlated with grain yield losses or stability. Accumulative effects of chronic ozone exposure on photosynthesis were more detrimental for grain yield than instantaneous effects of acute ozone shocks, or accelerated senescence of older leaves represented by changes in the ratio of brown leaf area/green leaf area index. We used experimental data of two selected tolerant or sensitive varieties, respectively, to parametrize the LINTULCC2 crop model expanded with an ozone response routine. By specifying parameters representing the distinct physiological responses of contrasting genotypes, we simulated yield losses of 7 percent (tolerant) or 33 percent (sensitive). By considering genotypic differences in ozone response models, this study helps to improve the accuracy of simulation studies, estimate the effects of adaptive breeding, and identify physiological traits for the breeding of ozone tolerant wheat varieties that could deliver stable yields despite ozone exposure.

1. Introduction

Tropospheric ozone (O_3) has become one of the key environmental issues in many areas of the world. It is a major air pollutant with oxidant nature produced from precursor pollutants in photochemical reactions, including nitrous oxides (NOx), carbon monoxide (CO), methane (CH_4) and volatile organic compounds (VOCs) (Mills et al., 2018b; Simpson et al., 2014; The Royal Society, 2008). Since mitigation of tropospheric ozone pollution was identified as one important strategy to safeguard food production (Avnery et al., 2013), international policy efforts were made for reducing precursor emissions. However, a variety of human activities, such as the burning of fossil fuels for transport, thermal power plants and home heating systems, continue to contribute to ozone formation, resulting in continuous increases in tropospheric ozone (Sicard,

Abbreviations: LBS, leaf bronzing score; OTC, open top chamber; SD, standard deviation; DAT, day after transplanting; NDVI, normalized difference vegetation index; LAI, total leaf area index; GLAI, green leaf area index; BLAI, brown leaf area index; SLA, specific leaf area; Y, instantaneous ozone flux threshold; A_{sat}, maximum saturated photosynthesis rate; V_{cmax}, maximum carboxylation rate of Rubisco.

☆ This paper has been recommended for acceptance by Pavlos Kassomenos.

* Corresponding author.
E-mail address: michael.frei@agrar.uni-giessen.de (M. Frei).

[1] These authors should be considered as joint first authors.

https://doi.org/10.1016/j.envpol.2022.119251
Received 19 January 2022; Received in revised form 10 March 2022; Accepted 30 March 2022
Available online 4 April 2022

Anav, De Marco, & Paoletti, 2017; Yeung et al., 2019). For instance, the ozone concentration is rising in China reaching 70 ppb in some regions, thus exceeding the threshold of 40 ppb considered to affect crop yields significantly (Zeng et al., 2019).

Ozone diffuses into the leaves primarily through the stomatal pores during photosynthetic gas exchange, and forms into reactive oxygen species (ROS). Ozone and ozone-derived ROS can cause direct oxidative damage, including peroxidation of lipids, chlorophyll bleaching, protein oxidation, damage to nucleic acids, and destruction of cell membranes (Ainsworth, 2017). This results in visible foliar injury (Ueda et al., 2015), reduction of photosynthetic capacity (Wilkinson et al., 2012), alterations of carbon allocation (Peng et al., 2021), and finally adverse impacts on yield (Feng et al. 2008; Ren et al., 2020) and grain quality (Broberg et al., 2015; Frei et al., 2012). Global economic losses were estimated at $17-$35 billion annually due to crop yield reductions induced by ozone (Avnery et al., 2011).

Wheat is one of the most ozone-sensitive crops (Mills et al., 2007). Elevated ozone can accelerate leaf senescence and leads to leaf symptoms, consisting of chlorotic spots, often degenerating into necrotic lesions (Begum et al., 2020; Picchi et al., 2017). Lower photosynthetic rates lead to biomass reduction and yield losses (Feng et al., 2008; Feng et al., 2011). A meta-analysis indicated that wheat yield was reduced by 34% under elevated ozone ranging from 7 to 12 h day^{-1} (60–89 ppb) compared with charcoal-filtered air (Feng et al., 2008). According to a recent ozone risk assessment, wheat yields were reduced by 9.9% and 6.2% in the northern and southern hemispheres over 2010–2012, respectively (Mills et al., 2018a). With the continuous rise of ozone concentration in some parts of the world, the global loss of wheat production was predicted to range between 5.4% and 25.8% by 2030, with the highest losses (11.2%–44.4%) occurring in South Asia (Avnery et al., 2011). Similar results were obtained by Teixeira et al. (2011) for wheat, which were larger than for other crops and could partly be mitigated by crop management. However, the effects of breeding were not considered in these studies, although cultivar-specific and variable responses to ozone were observed for different physiological traits and yield (Begum et al., 2020; Singh et al., 2018; Feng et al., 2008; Wang et al., 2015). Such genetic variation lays the foundation for ozone tolerance breeding in wheat to reduce yield losses as an effective strategy to secure food supply.

Crop models can be important tools for the estimation and projection of ozone effects on crop yields. Although experimental evidence of the negative effects of ozone on wheat production is abundant, only a few crop models have considered the impacts of ozone stress on wheat growth and development (Ewert et al., 1999; Guarin et al., 2019; Lobell & Asseng, 2017; van Oijen and Ewert, 1999). Over the past few decades, different metrics were developed to relate ozone concentrations to grain yield, such as AOT40 and SUM06 (accumulated ozone exposure over threshold of 40 ppb and 60 ppb, respectively) and M7 and M12 (seasonal 7 h and 12 h mean ozone concentration during daylight, respectively) as the most commonly used indexes in Europe (Emberson et al., 2018; Musselman et al., 2006). These metrics can be used directly in risk assessment studies that use a dose-response relationship to relate ozone concentrations or flux to relative yield losses (Mills et al., 2018a). Such concentration-based ozone metrics was also used in process-based ecosystem modelling frameworks to incorporate an ozone effect (Emberson et al., 2018). However, certain crop characteristics and environmental conditions could modulate the ozone flux from stomatal ozone uptake. To allow for this, a flux-based metric was developed to assess the relationship between stomatal ozone flux and crop yield (Emberson, Ashmore, Cambridge, Simpson, & Tuovinen, 2000). By simulating the stomatal limitations regulating ozone uptake, those flux-based models gave a better estimation of ozone damage on crop productivity and yield than concentration-based models (Pleijel et al., 2007). The flux-based approach was developed as combined stomatal-photosynthesis model, for instance AFRCWHEAT2-O3 (Ewert & Porter, 2000). This model simulates the effects of ozone exposure on leaf photosynthesis and leaf duration based on the assumptions that ozone taken up via the stomata has a short-term and a long-term effect on the Rubisco-limited rate of photosynthesis (Ewert & Porter, 2000). The approach can also be applied within land-ecosystem models for instance the crop model LPJmL, which estimated historical global yield losses from ozone pollution for wheat (Schauberger et al., 2019). Recently, a new model GLAM-ROC was introduced that incorporates ozone flux via the modelling of transpiration, while the new GLAM-Parti module simulates ozone damage by assuming that transpiration use efficiency and harvest index decreased linearly above 10 ppb ozone (Droutsas et al., 2020). These various crop models provide different approaches to estimate the stomatal ozone uptake effects, which are used to capture the interactions of ozone and climatic variables for yield prediction on the field (Droutsas et al., 2020; Guarin et al., 2019), regional (Tao et al., 2017), and global scales (Schauberger et al., 2019) in wheat. To our best knowledge, very few crop models address the genetic variability of wheat responses to ozone. Guarin et al. (2019) simulated different responses of wheat cultivars (tolerant, intermediate, and sensitive) in their crop model by relating 7 h/day ozone concentration metrics with grain yield. More detailed responses of physiological traits like photosynthesis capacity (i.e. maximum carboxylation rate or net photosynthesis) or leaf area growth (green and brown leaf and chlorophyll content) to ozone flux through stomata from different cultivars have rarely been considered in modelling studies. This limitation adversely affects the accuracy of specific wheat yield loss estimates. Ideally, models could be parameterised for different genotypes to ensure accurate model predictions for different wheat cultivars (Makowski et al. 2002). Such genotypic parameterization can provide important insight for future ozone-tolerance breeding schemes. Moreover, while field-based evidences of ozone induced yield losses are still rare, crop models could be useful to advance our understanding of diverse responses of wheat to ozone.

In the current study, different physiological traits of 18 contrasting wheat genotypes were monitored during a season-long ozone fumigation, including spectral reflectance of leaf surfaces, photosynthetic capacity, biomass and leaf area index (LAI), as well as yield components at harvest. We hypothesized that there is large genotypic variation in ozone tolerance in wheat due to distinct physiological traits, which are insufficiently reflected in current crop models simulating ozone responses. The main objectives of this study were therefore: (1) estimating the impacts of elevated ozone on contrasting wheat cultivars and ranking them in terms of ozone tolerance; (2) identifying physiological traits underlying the ability to maintain high grain yield under ozone stress; (3) calibrating a crop growth model to simulate tolerant and sensitive cultivar responses to ozone, and establishing specific model parameters that represent ozone tolerant and sensitive wheat ideotypes. Thereby, this study will improve the accuracy of ozone impact assessment and help to project and upscale the effects of ozone tolerance breeding.

2. Materials and methods

2.1. Plant materials and growth condition

The experiment was conducted in a greenhouse at the University of Bonn (Germany) from December 2019 to July 2020. Eighteen wheat genotypes with contrasting responses to ozone (Table A. 1 in Appendix) were pre-selected based on leaf bronzing score (LBS) and grain yield from a larger population of 150 genotypes that had been screened for ozone adaptive breeding in a previous study (Begum et al., 2020). The seeds were sown in trays inside a greenhouse and all cultivars germinated within one week. Then all trays were transferred to a climate chamber at 4 °C for vernalisation. Nine weeks after sowing, seedlings were transplanted into 288 pots (Dimensions 25 cm × 25 cm × 25 cm) filled with Terrasoil in the greenhouse. Each cultivar had 16 pots containing 5 seedlings, respectively. Eight open-top chambers (OTCs)

(length 2.6 m, width 2.1 m, height 1.7 m) were built up around the pots with transparent plastic sheets, and randomly assigned to two treatments (control and ozone) with four replicates each. Two pots for each cultivar in each chamber were randomly arranged in subplots. An automated irrigation system was set up for all pots to maintain a rate of 80 mL/pot/day in the vegetative stage and 100 mL/pot/day in the reproductive stage, until the end of June. To control aphids, "Morpilan" 0.05% and "Confidor" 0.04% were sprayed in the greenhouse for three times during the growth season. A dispenser of sulfur (Hotbox Sulfume, Hotbox International Ltd., Brough, England) was placed in the middle of the greenhouse for preventing powdery mildew infection. High-pressure sodium lamps were installed around 2 m above the plant canopy to ensure a minimum photosynthetically active radiation (PAR) of 400 μmol m^{-2} s^{-1} for 12 h daytime from 8.00 h to 20.00 h. The temperature was controlled automatically by heating and opening the roof and side windows of the greenhouse. Temperature and relative humidity were measured continuously at 2-min intervals using sensor type 224.401 (RAM GmbH Mess-und Regeltechnik, Herrsching, Germany). PAR was measured by a silicon sensor PAR 5.3 (version 7.1418.00.04, spectral range 380–700 nm, Thies Clima, Göttingen, Germany). Wind speed was detected by small wind transmitter (version 4.3515.5.61, Thies Clima, Göttingen, Germany). Both PAR and wind speed were logged at 10min interval by the DL16 data logger (Thies Clima, Göttingen, Germany). From transplanting to harvest, the average daytime (8.00 h–20.00 h) and nighttime (20.00 h–8.00 h) temperatures were 23.7 °C and 17.0 °C, average relative humidity were 35.8% and 57.5%, respectively. The average, minimum, and maximum PAR during daylight hours (8.00 h–20.00 h) were 739.8, 400, and 1535.3 μmol m^{-2} s^{-1}, respectively. Since we focused on effects of different ozone levels, the CO_2 concentration was not measured. We assumed a constant CO_2 concentration of 410 ppm for the whole day in all simulations by the crop model.

2.2. Ozone treatment and monitoring

When plants entered the stem elongation phase at four weeks after transplanting, ozone fumigation was started at a target level of 70 ppb for 7 h every day (9.00 h–16.00 h) to induce chronic stress. Custom-made ozone generators (UB 01; Gemke Technik GmbH, Ennepetal, Germany) were used to generate ozone with dried air passing through silica gels as input. The ozone output was controlled by an ozone monitor (K 100 W; Dr. A. Kuntze GmbH, Meerbusch, Germany) and continuously detected inside the fumigation chambers with a calibrated amperometric ozone sensor (GE 760 O3; Dr. A. Kuntze GmbH) that was frequently exchanged as such sensors loose sentitivity over time. The generated ozone was percolated through water to remove nitrogen oxides and blown into a central pipe above the ozone chambers, from which it was distributed into the chambers via three parallel perforated pipes that branched off at a distance of 0.5 m from each other. An additional handheld ozone monitor (series 500; Aeroqual Ltd, Auckland, New Zealand) was used to ensure even ozone distribution in the ozone chambers and monitor ozone concentrations independently. The average ozone concentration recorded was 70.3 ppb ± 21.0 SD (standard deviation) in ozone treatment, and the average concentration in control conditions was 27.8 ppb ± 6.1 SD. During the growth season, acute fumigation was applied three times at week 8, 10 and 13 after transplanting to simulate peak ozone episodes, and most plants were in the booting/ear emergence stage, flowering and ripening stage, respectively. The average concentration of acute stress was 151.4 ppb ± 27.4 SD and it also lasted 7 h (9:00 h - 16:00 h). Ozone fumigation was stopped at one week before harvest (week 20 after transplanting) when the plants were in the ripening stage.

Visible leaf symptoms were evaluated on DAT 99 (99 days after transplanting). A leaf bronzing score (LBS) was assigned to four fully expanded leaves of each plant from 0 (no ozone-induced symptoms) to 10 (the whole leaf severely damaged) (Begum et al., 2020).

2.3. Spectral reflectance

A spectroradiometer Polypen RP410 (Photon Systems Instruments, Drasov, Czech Republic) with an internal light source (Xenon incandescent lamp 380–1050 nm) and a UVIS detector (380–790 nm) was used to monitor the spectral reflectance of leaves in week 5, 8, 11, 13, 15 and 17 after transplanting. The measurements were performed on three points at 20 cm distance from the tip of the second youngest fully expanded leaves, which were randomly selected from each plant without distinguishing main tiller or secondary tiller, and the average of three points was calculated. Calibration with white reference was made prior to measurements every time, and also performed repeatedly when promted by the device. Vegetation indices were selected based on significant responses to ozone in a previous study (Begum et al., 2020) including normalized difference vegetation index (NDVI), simple ratio index (SR), modified chlorophyll absorption and reflectance index (MCARI), simple ratio pigment index (SRPI), Carter index 1 (Ctr1), Lichtenthaler index 2 (Lic2), Gitelson and Merzlyzak index 2 (GM2), anthocyanin reflectance index 1 (ARI1) and carotenoid reflectance index 2 (CRI2).

2.4. Gas exchange and A/Ci curve

Ten contrasting wheat cultivars were further selected based on LBS and grain yield for in-depth gas exchange measurements. The youngest fully expanded leaves of one randomly selected plant from each pot were measured regardless of main or secondary tiller in week 6, 11 and 16 after transplanting. A portable photosynthetic gas exchange system (LI-6400XT, LI-COR, Inc., Lincoln, Nebraska, USA) was used to determine net carbon assimilation rate/photosynthesis, stomatal conductance, intercellular CO_2 concentration, and transpiration. *A/Ci* curves were measured on the same plants with the following intercellular CO_2 concentrations: 400, 300, 200, 100, 50, 400, 600, 800, 1000, 1200, 1600 and 2000 ppm CO_2 under a constant PPFD of 1500 μmol photons m^{-2} s^{-1}, block temperature of 20 °C, flow rate at 300 μmol/s and relative humidity at 40%–70%. All measurements were conducted on sunny days between 9:00 h and 16:00 h (Ashrafuzzaman et al., 2018). Based on the measured *A/Ci* curves, the maximum carboxylation rate of ribulose 1,5-bisphosphate (RuBP) carboxylase/oxygenase (Rubisco;V_{cmax}) and the maximum electron transport rate (J_{max}) were estimated by package "plantecophys" (Duursma, 2015) in program R (R Core Team, 2018).

2.5. Growth traits and yield

During the growing season, repeated destructive biomass analyses were carried out, by collecting one aboveground plant randomly selected from each chamber for each cultivar in week 5, 9, 12, 15 and 18 after transplanting. Tiller number and spike number were measured during collection. Then, these subsamples were separated into stem, spike (ripe and un-ripe), green leaf and brown leaf. Leaf area of fresh leaves was immediately determined with a LI-3100 area meter (LI-COR, Inc., Lincoln, Nebraska, USA). We acknowledge the potential effects of sequential harvesting on the remaining plants which could alternate growth and the ozone dynamics within canopy. We assumed soil surface area for each plant as 25 cm × 25 cm/5 = 125 cm^2. The canopy LAI was converted to m^2 of leaf area per m^2 of soil surface area. Based on that, the total leaf area index (LAI), green leaf area index (GLAI) and brown leaf area index (BLAI) were determined. The ratio of BLAI by LAI (BLAI/LAI) was also calculated (Carretero et al., 2010). The different organs of each plant were weighted, and oven-dried at 105 °C for 72 h until constant weight for dry biomass measurement. Specific leaf area (SLA) was calculated as leaf area per unit dry matter. Days to flowering and maturity time for each genotype under ozone and control conditions were also recorded. Days to flowering was recorded based on the criterion that 70% of flowering was visible for each genotype. The date of maturity was recorded when the peduncles of 75% plants for each

genotype were no longer green during the ripening stage. All plants were harvested at week 21 after transplanting (DAT144).

After harvesting, besides the measurements of biomass and leaf area as before, plant height was also measured. After drying harvested plants in the oven at 65 °C for 72 h, yield components were determined, including spike length, grain yield, thousand kernel weight, filled grain number, straw biomass, and harvest index. Moreover, dry matter content was also assessed as the ratio between dry mass and fresh mass for spike and straw, respectively.

2.6. Statistical analysis

Mixed model three-way ANOVA using the packages "nlme" and "emmeans" in program R (R Core Team, 2018) was run to identify the effects of treatment, genotype, DAT and their interactions as fixed effects, while chamber was set as a random effect. Responses of individual genotypes to ozone stress were then evaluated by pairwise comparison. Relative values (ratio of value for plants grown under ozone treatment relative to control condition) were calculated for all phenotypic traits for all genotypes. Based on relative values of yield components and physiological parameters from the last measuring date, correlations were analysed by pair-wise Pearson's correlation coefficients, followed by principal component analysis (PCA) after standardization. R package "factoextra" and "FactoMineR" were used to plot the factor loadings of the first and second principal components (R Core Team, 2018).

2.7. Crop modelling

2.7.1. Description of crop model

We used the crop model LINTULCC2, which calculates phenology, leaf growth, assimilate partitioning, water balance, and root growth following the procedure outlined in Rodriguez et al. (2001). The assimilation rate of the sunlit and shaded leaf was calculated using the C_3 photosynthesis biochemical model of Farquhar and von Caemmerer (1982) (Table A. 2 and Supplemental methods A. 1 in Appendix). Stomatal conductance (g_s) was calculated according to the model of Leuning (1995) for sunlit and shaded leaves separately (Supplemental methods A. 1 in Appendix). The model requires hourly air temperature, actual vapor pressure, rainfall, wind speed, and photosynthetically active radiation (PAR). LINTULCC2 executes at daily time steps (phenology, leaf growth, assimilate partitioning, water balance, and root growth), while assimilation is calculated at hourly time step (Nguyen et al., 2020). To simulate the ozone effects on crop growth processes, we introduced an additional routine to simulate hourly ozone uptake through leaf stomata into the original LINTULCC2 model (Supplemental methods A. 2 in Appendix).

2.7.2. Ozone stress functions

Following the approach by Ewert and Porter (2000), we distinguished between instantaneous and accumulative effects of ozone exposure. To consider the instantaneous effects on photosynthesis, we assumed that ozone becomes toxic if the ozone flux into the stomata is above a certain threshold. The instantaneous damage factor on photosynthesis (f_{O3t}, [-]) was calculated hourly for sunlit leaves. The f_{O3t} was set to 1 if ozone uptake is low and decreased linearly with increasing instantaneous ozone flux $OZIF_t$ based on two instantaneous ozone damage coefficients γ_1 [-] and γ_2 [(nmol O_3 m^{-2} $s^{-1})^{-1}$] (Equation (D1.1), D1.2 and D1.3; Table 1). The γ_1/γ_2 [nmol O_3 m^{-2} s^{-1}] allows for low ozone concentrations to be detoxified without direct effects on the photosynthetic system.

$$f_{O3t} = 1 \quad for\ OZIF_t \leq \gamma_1/\gamma_2 \tag{D1.1}$$

$$f_{O3t} = 1 + \gamma_1 - \gamma_1 * OZIF_t \quad for\ \gamma_1/\gamma_2 < OZIF_t \leq (1+\gamma_1)/\gamma_2 \tag{D1.2}$$

$$f_{O3t} = 0 \quad for\ OZIF_t \geq (1+\gamma_1)/\gamma_2 \tag{D1.3}$$

In our modelling work, we assumed that the onset of leaf senescence was characterized via a cumulative ozone flux threshold (C_{LAO3}, [mmol m^{-2}]). Above this C_{LA03}, the rate of green leaf area loss increases linearly (brown leaf is increased while green leaf is decreased). The leaf area loss per soil area unit due to ozone ($DLAI_{O3}$, [-]) was estimated based on the daily rate of leaf area loss $dDLAI_{O3}/dt$ (Equation D2).

$$\frac{dDLAI_{O3}}{dt} = f_{LA} * \mathrm{MaxO3Se} * LAI \tag{D2}$$

where LAI [-] is leaf area index. MaxO3Se [d^{-1}] is the maximum rate of the leaf area loss due to ozone. f_{LA} is a factor accounting for the effects of ozone on the rate of leaf area loss. f_{LA} increases linearly with the increase of the cumulative ozone flux (C_{O3}) towards the completion of leaf senescence with the coefficient (γ_4, [(mmol $m^{-2})^{-1}$]):

$$f_{LA} = \max(\min(\gamma_4 * (C_{O3} - C_{LAO3}), 1), 0) \tag{D3}$$

where cumulative ozone flux (C_{O3}, [mmol m^{-2}]) was calculated as in Equation (D4):

Table 1
List of parameter variables, ranges and optimized values after calibration.

Symbols	Explanation and units	Range	References	Tolerant parameters (TP)	Sensitive parameters (SP)
PHY	Phyllochron [°Cd]	70–160	Hay and Porter (2006)	104	
MinTTAN	Minimum thermal time from sowing to anthesis [°Cd]	900–1200	This study	1100	
GFDUR	Thermal time in grain filling period [°Cd]	900–1200	This study	810	
V_{cmax}	Maximum carboxylation rate of Rubisco [μmol m^{-2} s^{-1}]	30-120*; mean of 64.5, range 40.6–89.2 under control treatment**	*von Caemmerer (2000); **this study	62.1	
maxSLA	Maximum specific leaf area [m^2 g^{-1}]	0.01–0.048	Amanullah et al. (2007)	0.032	
γ_1	Ozone instantaneous damage coefficients (intercept) [-]	[-]	Ewert and Porter (2000)	0.027	
γ_2	Ozone instantaneous damage coefficients (slope) [(nmol m^{-2} $s^{-1})^{-1}$]	[-]	Ewert and Porter (2000)	0.0045	
C_{LSO3}	Minimal threshold of cumulative ozone for photosynthesis [mmol m^{-2}]	[-]	Osborne et al. (2019)	22	
C_{LAO3}	Minimal threshold of cumulative ozone for leaf senescence [mmol m^{-2}]	[-]	Osborne et al. (2019)	20.5	
MaxO3Se	Maximum rate of leaf area loss due to ozone [d^{-1}]	[-]	This study	0.045	
γ_3	Ozone accumulative damage coefficient on photosynthesis [(nmol $m^{-2})^{-1}$]	[-]	This study	0.005 * 10^{-6}	0.034 * 10^{-6}
γ_4	Ozone accumulative damage coefficient on leaf senescence [(nmol $m^{-2})^{-1}$]	[-]	This study	0.007 * 10^{-6}	0.025 * 10^{-6}

$$C_{O3} = \int_{t_1}^{t_2} OZIF_t * dt \quad \text{(D4)}$$

where t_1 and t_2 are the time start and end of ozone fumigation, respectively. The green leaf area (*GLAI*) was calculated by subtracting the leaf area loss due to ozone by equation (D5):

$$\frac{dGLAI}{dt} = \frac{dLAI_{gl}}{dt} - \frac{dDLAI_{O3}}{dt} \quad \text{(D5)}$$

where $dLAI_{gl}/dt$ is daily green leaf area change rate after considering effects of shading, aging, and water stress on leaf growth after anthesis. Finally, in our model, we considered the effect of leaf senescence on photosynthesis via the factor (f_{LS}, [-]). This factor was based on a coefficient (γ_3, [(mmol m^{-2})$^{-1}$]) which characterizes the slope of a linear relationship between photosynthesis and a cumulative ozone flux threshold (C_{LS03}, [mmol m^{-2}]) (Equation D6).

$$f_{LS} = 1 - \max\left(\min(1, (\gamma_3 * (C_{O3} - C_{LSO3})), 0\right) \quad \text{(D6)}$$

For parameterization of instantaneous and accumulative effects on photosynthesis, we employed the function min (f_{O3t}, f_{LS}), which was used in Equation (B3) (Supplemental methods A. 1 in Appendix). The instantaneous effects might become significant in the case of acute and high ozone concentration exposure ($f_{O3t} < f_{LS}$). When wheat plants are exposed to low ozone for prolonged periods, ozone induced leaf senescence resulted in a considerable reduction of photosynthetic capacity (Feng et al., 2011). The f_{LS} comes into operation ($f_{LS} < f_{O3t}$) when $C_{O3} > C_{LSO3}$.

2.7.3. Optimization and estimates of ozone modelling parameters for different cultivar groups

Data from four cultivars (two tolerant and two sensitive ones, selection criteria in results section) were used to parametrize the model. We performed model simulations for all cultivars and treatments from transplanting date (DAT0), anthesis date (DAT70), through to maturity date (DAT130). The model was first calibrated for phenological growth of all cultivars considering parameters of phyllochron (PHY), minimum thermal time from transplanting to anthesis (minTTAN), and thermal time from anthesis to maturity (GFDUR) (Table 1; Fig. 1). Secondly, the model was calibrated based on total aboveground dry biomass and GLAI of five measured dates of all cultivars under the control treatment (Fig. 1). Maximum carboxylation rate of Rubisco (V_{cmax}) and maximum specific LAI (maxSLA) were equidistantly changed by 2 μmol m^{-2} s^{-1} from 30 to 120 μmol m^{-2} s^{-1} for V_{cmax} and by 0.001 m^2 g^{-1} from 0.01 to 0.048 m^2 g^{-1} for maxSLA (Table 1). This resulted in 49 × 36 = 1794 simulations. The root mean square errors (RMSE) and correlation coefficient (r) of simulated and observed dry biomass and GLAI and absolute bias error of simulated and observed grain yield were estimated for each simulation. We firstly selected the simulations with the high r (higher than 0.75 and 0.65 for biomass and GLAI, respectively) and low RMSE (lower than 1 kg m^{-2} and 1.75 [-] for biomass and GLAI, respectively) based on the scripts which are implemented in the R statistical software (R Core Team, 2018). Then, amongst chosen simulations, a simulation with the lowest absolute bias error (for grain yield) was determined that allows to find the "best" suitable set of V_{cmax} and maxLAI.

Ozone flux threshold (Y) was commonly employed in the ozone-flux models for different winter wheat cultivars in Europe (González-Fernández et al., 2013; Emberson et al., 2003). An instantaneous ozone flux threshold reflects the species or cultivar-specific detoxification capacity. Using the model from Pleijel et al. (2007), single values of Y could not represent the yield variability responses of cultivars and geographical conditions to ozone in winter wheat (González-Fernández et al., 2013; Feng et al., 2012, Zhu et al., 2015; Wu et al., 2016). More specific Y for specific genotypes or certain regions (González-Fernández et al., 2013; Feng et al., 2012) or even different values of Y in one growing season (Wu et al., 2016) have been suggested for that model in wheat. In fact, the ozone flux threshold Y was specified differently among models and cultivars, ranging from 0 or 6 nmol m^{-2} s^{-1} for spring wheat (Emberson et al., 2000), or 13.5 nmol m^{-2} s^{-1} (Ewert and Porter, 2000), or 2 nmol m^{-2} s^{-1} (Lombardozzi et al., 2012), from 12 to 16 nmol m^{-2} s^{-1} in winter wheat in China (Feng et al., 2012) or 10–12 nmol m^{-2} s^{-1} (Dai et al., 2020). The Y threshold (= 6 nmol m^{-2} s^{-1}) was often used in European studies for wheat (Emberson et al.,

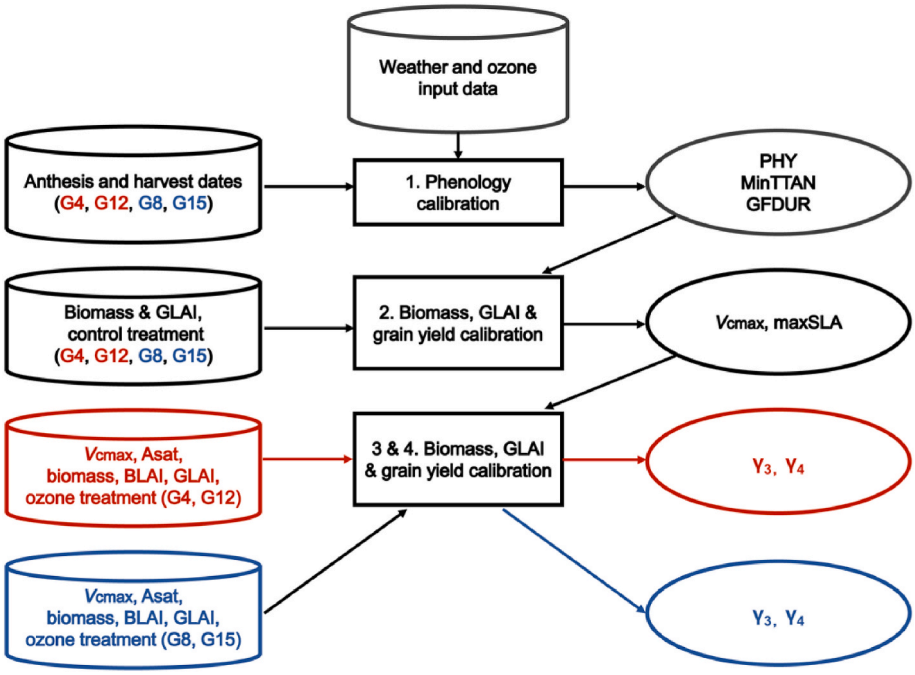

Fig. 1. Description of the modelling workflow with reference to the cultivars, observed data, and ozone treatments as well as the modelling parameters used at each stage of the model calibration (see also Table 1). The red colour indicates sensitive cultivars (G4 and G12), while the blue colour indicates tolerant cultivars (G8 and G15). (For interpretation of the references to colour in this figure legend, the reader is referred to the Web version of this article.)

2000; Pleijel et al., 2007). This threshold influences the estimates of cumulative ozone flux, which determines the points when ozone-induced senescence begins (Osborne et al., 2019). For the sake of simplification, we set the $\gamma_1 = 0.027$ [-] and $\gamma_2 = 0.0045$ [(nmol m^{-2} s^{-1})$^{-1}$] for all later simulations with ozone treatment so that the Y threshold is also equal to $\gamma_1/\gamma_2 = 6$ nmol m^{-2} s^{-1} (Table 1). When exposed to elevated ozone, the flag leaf of a sensitive winter wheat genotype has a larger reduction in photosynthesis capacity as compared to those in a tolerant wheat genotype (Feng et al., 2011). In our experiment, we did not observe varietal differences in terms of the onset of leaf senescence among cultivars. The cumulative ozone flux threshold from which the onset of leaf senescence starts and brown leaf area increases was set at $C_{LA03} = 20.5$ mmol m^{-2}. The cumulative ozone flux threshold at which f_{LS} becomes more pronounced (below 1) and suppresses photosynthetic activity was set at $C_{LSO3} = 22$ mmol m^{-2} (Table 1) (Osborne et al., 2019). The magnitude of f_{LS} and f_{LA} were estimated through changing the slope γ_3 and γ_4, respectively, which differentiated between tolerant and sensitive genotypes. In the third step, the model was further calibrated for the sensitive cultivars (cultivar 4 and 12) to determine the ozone–related parameters γ_3 and γ_4 relying on the measured data of V_{cmax}, light saturated photosynthesis rate (A_{sat}), total aboveground dry biomass, brown and green leaf area, and NDVI. Finally, the third step was repeated for the tolerant cultivars by using observed data from cultivar 8 and 15 to determine γ_3 and γ_4 parameters (Table 1; Fig. 1).

3. Results

3.1. Phenotypic responses indicate large variation in ozone tolerance

3.1.1. Leaf spectral reflectance indices

As stress indicators, leaf spectral reflectance indices were monitored repeatedly during growth. Although for all genotypes and sampling dates, there was no significant treatment effect, significant interactions between genotype and treatment were detected for all traits. For individual sampling days, most vegetation indices only significantly responded to ozone stress at DAT120, except for MCARI and CRI2 (Table A. 3 in Appendix). Among them, NDVI (representing chlorophyll content) and Lic2 (representing chlorophyll/carotenoid ratio) were considered suitable for the non-invasive diagnosing of ozone stress in wheat (Begum et al., 2020), and decreased by 20.4% and 12.5%, respectively (Table A. 3 in Appendix). The relative values of different genotypes ranged from 0.53 to 1.08 for NDVI, and from 0.63 to 1.10 for Lic2, which indicated substantial genotypic differences in ozone tolerance. Based on relative values, all genotypes were ranked from most tolerant to most sensitive. Some genotypes showed significant differences for both NDVI and Lic2 at DAT120 (Fig. 2).

3.1.2. Gas exchange and photosynthetic capacity

In order to investigate the effects of ozone fumigation on photosynthesis, gas exchange of the youngest fully expanded leaves was measured three times during different growth stages in selected genotypes. Averaged over all genotypes and all sampling days, net CO_2 assimilation and transpiration showed significant effects of the treatment, genotype and interaction level, whereby net CO_2 assimilation was reduced by 34.0% at DAT111 (Table A. 4 in Appendix). Although stomatal conductance and intercellular CO_2 did not significantly respond to the treatment averaged across all sampling days, we observed significant reduction of stomatal conductance by 20.8% at DAT111 (Table A. 4 in Appendix). Generally, significant treatment main effects for all genotypes were seen only on the last measuring day. In addition, V_{cmax} and J_{max} were both significantly affected under ozone treatments compared with the control and showed a significant treatment response on DAT111 (Table A. 4 in Appendix). Some genotypes significantly responded to ozone in terms of net CO_2 assimilation and stomatal conductance, but not in terms of V_{cmax} and J_{max}, although negative trends were seen. Genotypes were also ranked as tolerant or sensitive according to their relative response in photosynthesis (Fig. 3).

3.1.3. Biomass, leaf area index, and yield

Different phenotypical traits were measured repeatedly during the growth season in order to obtain continuous data representing ozone damage. Tiller number significantly responded to the treatment and was reduced by 6.2% due to ozone (Table A. 5 in Appendix). Ozone had a highly significant treatment effect on total dry biomass, which led to average final reduction by 14.5% (Table A. 5 in Appendix). Generally, the weight of different fractions showed significant treatment effects towards the late growth stages. Spike dry weight was significantly decreased by 17.9%, when averaged across all genotypes and all sampling dates (Table A. 5 in Appendix).

As a key vegetation parameter for crop modelling, LAI was significantly affected after prolonged fumigation, although there was no significant treatment effect on most measuring days. Especially, highly significant differences were seen in BLAI/LAI, and the average ratio due to ozone significantly increased by 87.9% compared to control condition at DAT126 (Table A. 5 in Appendix). SLA also showed a significant difference between control and ozone treatment across all genotypes at DAT126. LBS was also recorded as a visible foliar symptom due to ozone exposure, and showed a highly significant response to the treatment (Table A. 5 in Appendix).

At the end of the experiment, different yield components were determined. Grain yield, filled grain number and thousand kernel

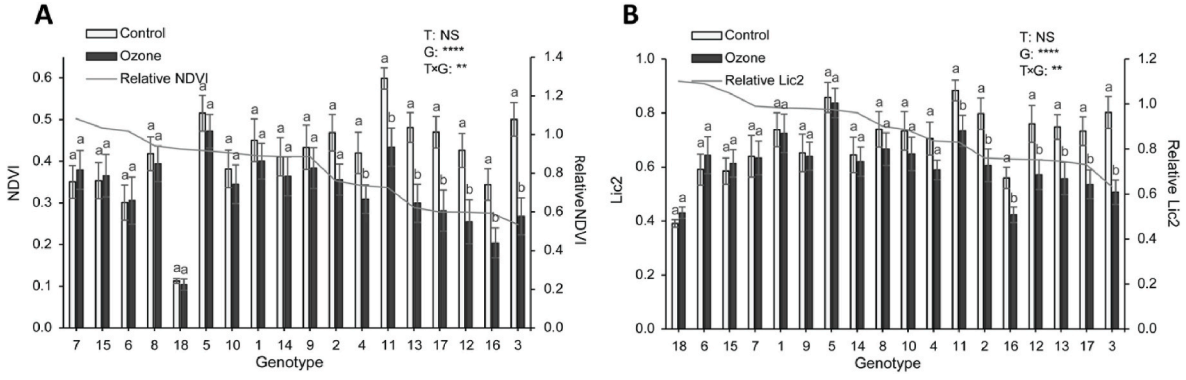

Fig. 2. Selected vegetation indices at 120 days after transplanting of eighteen wheat genotypes in control and ozone conditions. A, Normalized difference vegetation index; B, Lichtenthaler index 2. Bars indicate mean values and standard errors (n = 20). Genotypes were arranged from tolerant to sensitive based on relative value. Bars not sharing the same superscript letters are significantly different at $P < 0.05$ within the genotypes. T: treatment; G: genotype; T × G: treatment by genotype interaction; $^{**}P < 0.01$; $^{****}P < 0.0001$; NS: not significant.

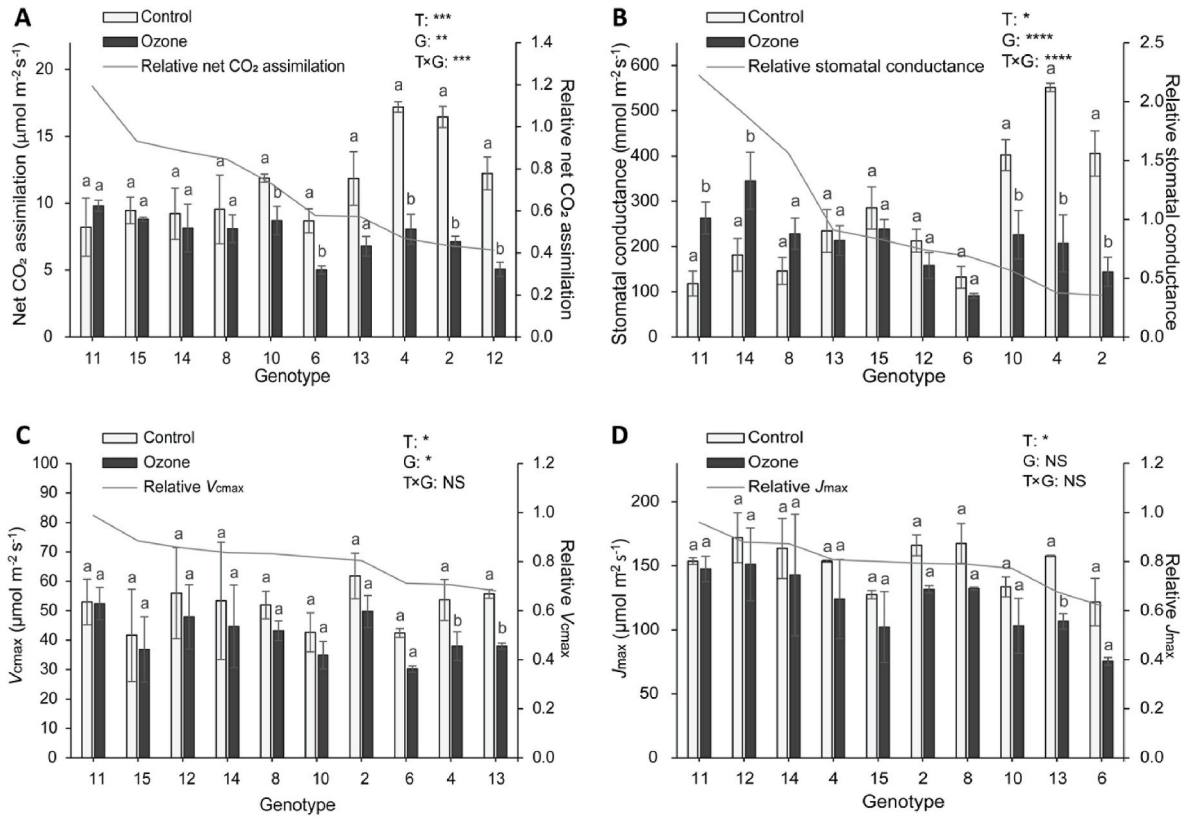

Fig. 3. Photosynthetic parameters of ten selected wheat genotypes at 111 days after transplanting in control and ozone conditions. Bars indicate mean values and standard errors (n = 4). A, Net CO_2 assimilation; B, Stomatal conductance; C, V_{cmax}; D, J_{max}. Genotypes were arranged from tolerant to sensitive based on relative value. Bars not sharing the same superscript letters are significantly different at $P < 0.05$ within the genotypes. T: treatment; G: genotype; T × G: treatment by genotype interaction; $^{*}P < 0.05$; $^{**}P < 0.01$; $^{***}P < 0.001$, $^{****}P < 0.0001$; NS: not significant.

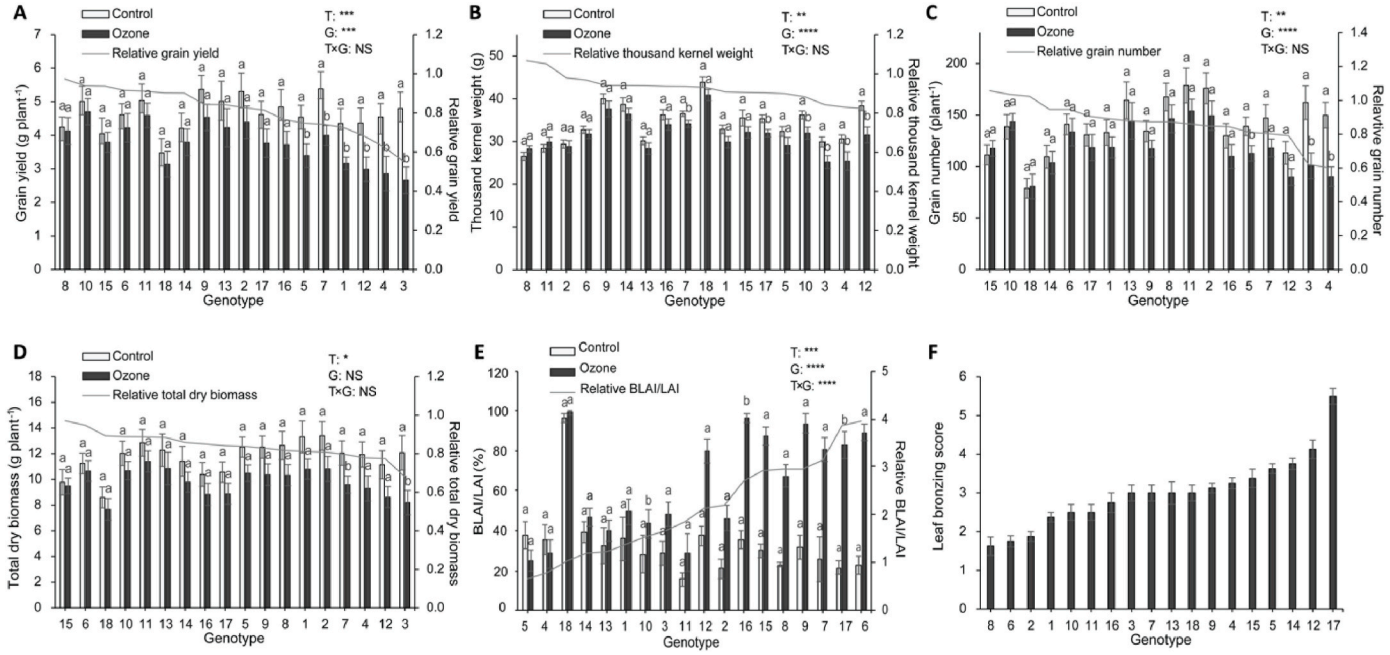

Fig. 4. Growth parameters and yield components of eighteen wheat genotypes in control and ozone conditions. A, Grain yield; B, Thousand kernel weight; C, Grain number; D, Total dry biomass; E, BLAI/LAI at 126 days after transplanting; F, Leaf bronzing score at 99 days after translating. Genotypes were arranged from tolerant to sensitive based on relative value. Bars indicate mean values and standard errors (n = 4). Bars not sharing the same superscript letters are significantly different at $P < 0.05$ within the genotypes. T: treatment; G: genotype; T × G: treatment by genotype interaction; $^{*}P < 0.05$; $^{**}P < 0.01$; $^{***}P < 0.001$, $^{****}P < 0.0001$; NS: not significant.

weight showed significant treatment effects due to declines in the ozone treatment compared to control conditions (Table A. 5 in Appendix). Average yield reduction among all genotypes was 18.7%. Harvest index showed highly significant interaction between genotype and treatment and decreased by 4.8% (Table A. 5 in Appendix). Although no statistical significance for other yield-related traits occurred, the average values due to ozone across all genotypes were also reduced to varying degrees (Table A. 5 in Appendix). All those traits showed genotypic variation of wheat responses to ozone. Although treatment by genotype interaction for grain yield was not significant (presumably due to the variation occurring in the large dataset with many genotypes), large variation occurred with yield losses ranging from 2.7% to 44.6%. Also, pair-wise comparison within genotypes indicated that some genotypes showed significant yield reductions, while others did not. As with other traits, genotypes were ranked as tolerant and sensitive according to their relative values (Fig. 4). In summary, plant growth traits were negatively affected only after prolonged ozone fumigation.

Based on the relative values of important physiological parameters and yield components under both conditions, we analysed correlations followed by principal component analysis for selected traits in order to explore how different traits were interrelated. Grain yield was positively correlated with different traits, including NDVI, net CO_2 assimilation, total dry biomass, grain number, thousand kernel weight and harvest index (Fig. 5). The factor loadings of principal components 1 and 2 explained 24.7% and 34.0% of total variances, respectively (Figure A. 1 in Appendix). The grain yield clustered with NDVI, net CO_2 assimilation, further confirming the positive correlations between them.

3.2. Modelling and parameter optimization

Based on our experimental results, contrasting genotypes were selected for modelling by the following criteria: (1) Genotypes showed contrasting grain yield responses as indicated by differential pairwise comparisons between control and ozone treatment, which was significant for the sensitive but non-significant for the tolerant genotypes (Fig. 4). (2) Genotypes showed consistent tolerant/sensitive responses in this current and a previous experiment (Begum et al., 2020). This is illustrated by highly significant treatment by genotype interaction for the selected set of genotypes when combining data from both experiments (Figure A. 2 in Appendix); (3) We selected genotypes for which CO_2 assimilation data were available from the current experiment. Following these criteria, we selected 8 and 15 as the tolerant group, and 4 and 12 as the sensitive group for model fitting.

In our study, we did not observe significant differences in anthesis and maturity dates between the two treatments when considering four selected cultivars (4, 12, 8, and 15). The anthesis dates of control and ozone treatments were at DAT71 ± 12 and 69 ± 11, respectively, while the maturity dates of control and ozone treatments were at DAT132 ± 5

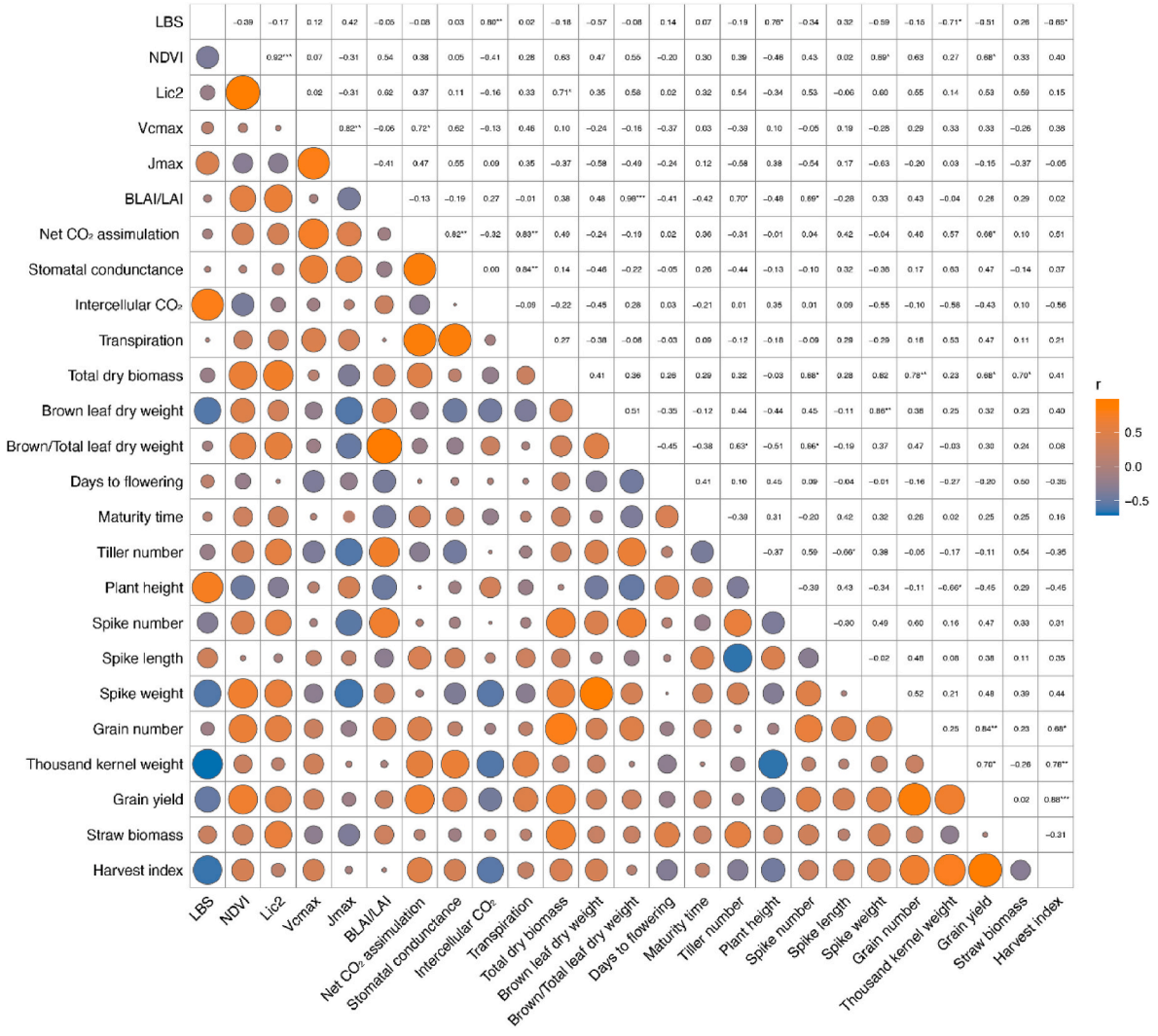

Fig. 5. Pearson correlation matrix for relative values (ozone/control) of phenotypic traits of ten different wheat genotypes exposed to ozone. Number represents correlation coefficient; $*P < 0.05$; $**P < 0.01$; $***P < 0.001$; n = 20.

and 128 ± 6, respectively. There was also no significant difference in anthesis and maturity date between the two groups of cultivars within the same treatment. The anthesis dates of sensitive and tolerant groups were at DAT71 ± 7 and 69 ± 14, respectively, while the maturity dates were DAT133 ± 6 and 127 ± 3, respectively. By comparisons with corresponding observed data, the simulated biomass and LAI matched relatively well before DAT126 in the control treatment. Overall, the r and RMSE of dry biomass under control were 0.95 and 0.46 kg m^{-2}, respectively, while r and RMSE of GLAI were 0.85 and 1.35, respectively. The model was able to simulate the reduction of biomass and green leaf area in the ozone treatment as compared to the control, especially after DAT84 for the sensitive cultivars (Figure A. 3 in Appendix). The greater reduction in simulated biomass growth and GLAI in the ozone treatments for the sensitive cultivars were explained by the larger decrease of measured V_{cmax} and A_{sat}, increase of brown leaves, and reduction of NDVI at the grain filling period as compared to the tolerant group (Fig. 6).

The mean of observed yield reductions for sensitive and tolerant groups were 34.4% and 4.5%, respectively (Fig. 7). With the γ_3 and γ_4 parameters derived from sensitive cultivars (Fig. 1), the model simulated the yield reduction for these cultivars relatively well (33%, Fig. 7). In contrast, γ_3 and γ_4 parameters derived from the tolerant cultivars simulated 7% yield reduction (Fig. 7), which was 2.5% higher than the mean of observed yield reduction in these cultivars (4.5%). The difference of observed grain yield reduction between the two groups of cultivars was 34.4%–4.5% = 29.9%, while the difference of simulated grain yield reduction was 33%–7% = 26%.

4. Discussion

4.1. Effects of elevated ozone on grain yield in wheat

We conducted chronic ozone fumigation at a mean concentration of 70 ppb and three episodes of acute ozone exposure at a concentration of 151 ppb in OTCs to simulate current pollution scenarios observed in some Asian countries such as Bangladesh or India (Alexandratos & Bruinsma, 2012). After season-long fumigation, there was significant yield loss (18.7%) induced by elevated ozone, but this was less than the yield reduction (24.4%) at an average ozone concentration of 69 ppb in a previous meta-analysis based on 53 reported studies by Feng et al. (2008). The observed differences in yield loss may be due to different experimental systems and perhaps the fact that many published experiments tend to employ rather sensitive genotypes in order to be able to monitor explicit ozone responses. The effects of ozone on wheat are cultivar-specific (Feng et al., 2018a; Feng et al., 2016), which means that the selection of genotype affects the research outcome. In this study we deliberately selected both tolerant and sensitive genotypes. Higher sensitivity to ozone was previousely found in newly released wheat cultivars due to higher stomatal conductance and lower antioxidative capacity (Biswas et al., 2008; Pleijel et al., 2006), which was not confirmed in this study, perhaps due to cultivar selection and different experimental systems.

4.2. Physiological traits related to wheat yield under ozone stress

We aimed to elucidate physiological traits that affect grain yield under ozone stress. Ozone enters the plants through the stomata and produces ROS, negatively affects photosynthesis, and ultimately leads to cell death and thus a loss of photosynthetic area (Ueda et al., 2015).

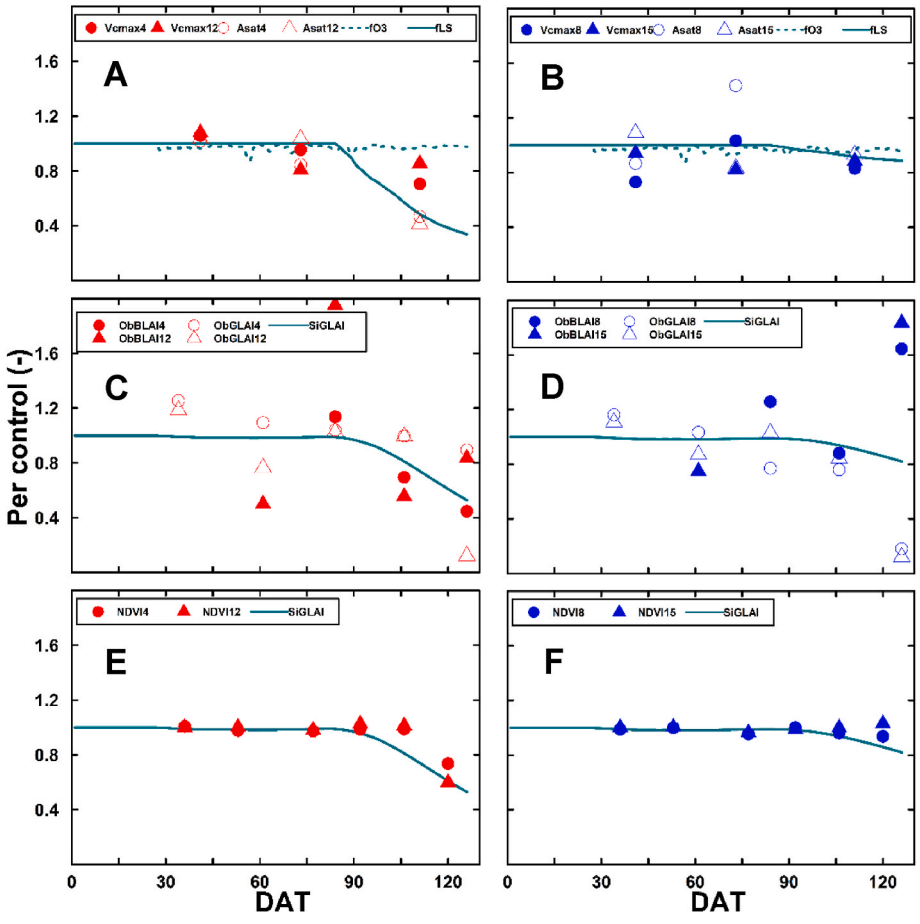

Fig. 6. Observed and simulated effects of ozone exposure on sensitive cultivars (left panel, cultivar 4 and 12) and tolerant cultivars (right panel, cultivar 8 and 15) on (A & B) the maximum carboxylation rate of Rubisco (V_{cmax}) and saturated leaf photosynthesis rate (A_{sat}); (C & D) brown leaf area (BLAI) and green leaf area (GLAI); (E & F) normalized difference vegetation index (NDVI). Different points indicate the different measured values throughout growing season. The cyan lines indicate the simulated values. The f_{O3} is the daily mean of eight hourly f_{O3t} values. The f_{O3t} is the factor considering the instantaneous effects of elevated ozone on instantaneous photosynthesis (Supplemental Methods A. 1 in Appendix; Equation (D1.1), D1.2, and D1.3). The f_{LS} is the factor considering the decline in the Rubisco-limited rate of photosynthesis in senescing leaves (Supplemental Methods A. 1 in Appendix and Equation D3). The SiGLAI is a ratio of simulated green leaf area under ozone over simulated green leaf area under control. (For interpretation of the references to colour in this figure legend, the reader is referred to the Web version of this article.)

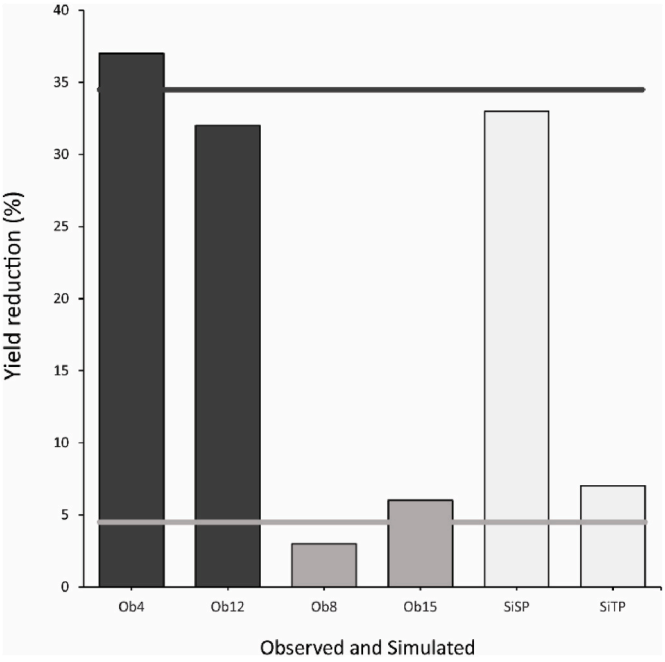

Fig. 7. Comparison of observed yield reduction of sensitive and tolerant cultivars (black bars) with simulated yield reduction (grey bars). The SiSP indicates the simulated result using ozone parameters derived from sensitive cultivars (SP), while SiTP indicates the simulated result using ozone parameters derived from tolerant cultivars (TP) (Table 1). The horizontal black line represents the mean of yield reduction from two sensitive cultivars (4 & 12). The horizontal grey line shows the mean of yield reduction from two tolerant cultivars (8 & 15).

Accelerated leaf senescence affects leaf lifespan and thus synthesis of carbohydrates for seed loading (Gebbing & Schnyder, 1999), thereby affecting grain yield (Osborne et al., 2019). Our results confirmed that leaf senescence is induced by elevated ozone in wheat, as indicated by different physiological traits, such as LBS, LAI, chlorophyll content (represented by NDVI), as well as photosynthesis. Notably leaf cohorts used for measurements of leaf spectral reflectance indices, gas exchange and photosynthetic capacity were changed due to the frequent emergence of new leaves. After plants entered into the heading stage, the exposure time to ozone of youngest and second youngest leaves selected for measurements became progressively longer. Relative differences between the two treatments and between genotypes were analysed to avoid artefacts that may derive from changing of leaf cohorts. Based on that, we ranked genotypes from tolerant to sensitive for each trait (Figs. 2–4). Although sensitivity rankings of genotypes for different traits were inconsistent, key physiological traits associated with yield under elevated ozone were identified by correlation analyses and principal component analysis, i.e. NDVI and net CO_2 assimilation (Fig. 5; Figure A. 1 in Appendix).

Most vegetation indices measured in this study were significantly changed when plants were exposed to prolonged periods of ozone fumigation (Table A. 3 in Appendix), indicating that elevated ozone strongly affected the pigment composition in leaves towards the end of the growth season. Among them, NDVI is one of the most frequently used vegetation indices associated primarily with chlorophyll content (Miloš et al., & Alica, 2018), which can characterize photosynthetic potential and responses to biotic and abiotic stresses (Shah et al., 2017). NDVI was previously employed to detect diverse stress responses, including salinity (Shah et al., 2017), mineral toxicity (Wu et al., 2019), ozone stress (Ashrafuzzaman et al., 2017; Begum et al., 2020) and others. In our study NDVI showed significant decline due to ozone exposure by 20.4% at DAT120 (Table A. 3 in Appendix). Moreover, NDVI was positively correlated with spike weight and grain yield indicates that ozone-induced loss of chlorophyll contributes to the final yield reduction in wheat, as seen in previous reports (Hassan et al., 2019; Naser et al., 2020; Sid'ko et al., 2017).

In addition, most of the photosynthetic parameters that we measured were significantly reduced by elevated ozone, including net CO_2 assimilation, stomatal conductance, V_{cmax} and J_{max} (Table A. 4 in Appendix). The observed decrease in V_{cmax} and J_{max} points towards ozone effects on Rubisco carboxylation capacity and the Calvin cycle, which is in agreement with previous reports (Chen et al., 2011; Goumenaki et al., 2010). However, only net CO_2 assimilation was strongly positively associated with grain yield in our research. Stomatal regulation was suggested as a possible tolerance mechanism, but no significant correlation was found between stomatal conductance and grain yield in this study. This indicates that ozone tolerance in wheat is related to maintaining carbon assimilation rate while under ozone stress, rather than reducing ozone uptake through stomatal closure. In C_3 plants, net assimilation rate is mostly considered as the balance between gross photosynthesis by Rubisco carboxylation and respiration. A report found that carbon and nitrogen utilization pathways and rapid signalling events can also influence the observed rate of net photosynthesis (Tcherkez & Limami, 2019), implying that net CO_2 assimilation is the result of complex underlying mechanisms. However, even small increases in the net assimilation can result in large increases in biomass, and hence yield, over the entire growing season (Parry et al., 2011). Futhermore, antioxidative capacity determined by different antioxidative pools and enzymes, was reported to be responsible for the differential ozone-induced effects on photosynthesis in winter wheat among cultivars (Feng et al., 2016). The apoplast forms the first line of defense against ozone damage, in which apoplastic ascorbic acid acts as an important factor determining ozone tolerance in wheat (Baier et al., 2005; Feng et al., 2010). Although across all genotypes, plants in the ozone treatment matured faster than those under control condition, no correlation of maturity time with ozone tolerance or final grain yield was observed (Table A. 5 in Appendix; Fig. 5).

As an indicator of above-ground biomass, LAI was directly measured by destructive sampling. While LAI was significantly reduced by ozone treatment as in previous studies (Yadav et al., 2019), we also introduced the novel ozone response trait BLAI/LAI as a measure of leaf senescence. Although BLAI/LAI was significantly affected by ozone on DAT126, it was not significantly correlated with grain yield (Fig. 5) and was thus not critical for ozone tolerance. LBS was not significantly correlated with BLAI/LAI, net CO_2 assimilation or spectral reflectance indices, as they represent the leaf status in distinct positions within the plants. LAI was determined for the whole plant, while LBS was determined on the four youngest fully expanded leaves, and net CO_2 assimilation and spectral reflectance indices such as NDVI were detected on the first and second youngest fully expanded leaves, respectively. Crop photosynthesis is directly associated with light interception by the canopy (Sarlikioti et al., 2011). The uppermost leaves intercept a lot of radiation compared to the leaves in the lower canopy layers (Caldwell et al., 1986; Spitters et al., 1986), and therefore contribute more to the final yield (Reynolds et al., 2012). Therefore, the BLAI/LAI index, which was dominated by brown leaves in the lower canopy layer, may have been less decisive in determining grain yields. This suggests that measurements of flag leaf physiological traits would be an interesting topic that should be focused on in future studies.

4.3. Calibration for tolerant and sensitive cultivars in the crop model LINTULCC2-Ozone

Based on yield and yield-correlated physiological traits, two groups of cultivars with distinct sensitivity to ozone were selected for parameterizing the LINTULCC2 crop model. Previously, this model was validated and compared with different crop models for spring wheat (Rodriguez et al., 2001) and used to simulate the effects of elevated CO_2 and drought conditions (Ewert et al., 2002), or for winter wheat growing

under different soil types and water treatments (Nguyen et al., 2020). In this study, an additional routine to simulate hourly ozone uptake through leaf stomata was introduced to the original LINTULCC2 following a well-tested approach for spring wheat by Ewert and Porter (2000).

Modelling methods aiming to accurately simulate ozone damage to crops must be able to capture naturally occurring variation in ozone sensitivity or tolerance. Previous studies employing O_3 flux-yield relationship models, which do not explicitly simulate crop growth and yield (Emberson et al., 2000; Pleijel et al., 2007), strongly suggest a requirement of more specific ozone parameters (i.e. ozone flux threshold) for distinct wheat genotypes or for certain wheat growing regions (Osborne et al., 2019; Feng et al., 2012; González-Fernández et al., 2013). This is exemplified in a study, which found that different ozone flux thresholds were required in a single growing season to represent the variation of ozone detoxification caused by time of day and growth stages for winter wheat growing in China (Wu et al., 2016). For the dynamic crop growth models with the inclusion of ozone stress, very few studies directly simulate the physiological processes and the variation of responses of different wheat genotypes as presented in this study.

In our study, the modelling parameterization for simulating the performance of contrasting wheat genotypes was carried out using detailed information of different physiological traits of a wide range of wheat cultivars. To our best knowledge, this data was unique for model fine-tuning aiming at capturing sensitivity or tolerance of wheat to ozone. We optimized the LINTULCC2-Ozone model step by step based on dynamic aboveground biomass, leaf area, and grain yield under controlled levels of elevated ozone for two groups of cultivars (sensitive and tolerant) (Table 1; Fig. 1) along with various physiological traits (Fig. 6). Comparison of observed and simulated yield reduction (Fig. 7) demonstrated that the model was able to capture the contrasting responses of yield from two groups. The two parameter γ3 and γ4 (Table 1; Figure A. 4 in Appendix) derived from the measurement of V_{cmax}, A_{sat}, BLAI, GLAI, and NDVI (Fig. 6) accounted for $-26\%/-29.9\% \approx 87\%$ of yield differences between the two cultivar groups. For the LINTULCC2-Ozone, these are two key and specific parameters that represented the differences between distinct genotypes (Figure A. 5 in Appendix). Our measured data and modelling results emphasize the importance of ozone damages on chlorophyll content (as seen in the reduction of NDVI), A_{sat}, and V_{cmax} at the late period of the growing season (i.e. after anthesis). These findings are in line with the experimental evidences in Feng et al. (2011) and Osborne et al. (2019), and with modelling studies (Guarin et al., 2019; Osborne et al., 2019).

Experimental studies have revealed that ozone is most damaging under high chlorophyll contents and light saturated photosynthetic conditions that tend to occur during the later part of the growing season (i.e. grain-filling) (Feng et al., 2011; Osborne et al., 2019). These studies suggest that ozone induced accelerated senescence is more pronounced and important than direct effects on instantaneous photosynthesis. The instantaneous reduction of carboxylation capacity due to ozone is thought to occur during acute ozone episodes (Farage et al., 1991). These instantaneous effects were considered in some crop models (Ewert and Porter, 2000; Tao et al., 2017; Cappelli et al., 2016; Schauberger et al., 2019). In our work, the instantaneous effect on photosynthesis rate (f_{O3t}) was also considered, because we included three episodes of high fumigated ozone (around 151 ppb). However, based on the experimental results, our model was parameterised to emphasize the importance of the Rubisco-limited rate of photosynthesis in senescing leaves (f_{LS}) and accumulative effects on leaf senescence (f_{LA}), especially from the onset of leaf senescence to harvest (i.e. minimum function in Equation (B3), Supplemental methods A. 1 in Appendix), which was consistent with the recent work by Osborne et al. (2019). In fact, the f_{O3t} (representing the instantaneous effects) was much higher (less negative effects) than f_{LS} (representing the accumulative effects) from the start of leaf senescence (Fig. 6). Nevertheless, given the highly varying ozone concentration within growing season under field conditions in some regions (i.e. India, Bangladesh or east China), the acute effects of ozone on photosynthesis should not be ruled out when the model is employed for these areas.

A recent trend in crop modelling aims at assisting breeders to understand genotype × environment interaction to improve varieties (Martre et al., 2017; Chenu et al., 2017). Crop modelling or subroutines in crop models were used to characterize breeding and production environments based on different traits and data collected under controlled conditions, e.g. leaf growth under drought (Chenu et al., 2008), phenology (He et al., 2012; Gouache et al., 2017; Messina et al., 2009), or grain yield (van Oosterom et al., 2021). Our experimental and modelling study is in line with these efforts of understanding responses of various wheat genotypes at different ozone levels. We measured different physiological traits including leaf gas exchange and agronomical indices for 18 winter wheat genotypes (selected from 150 genotypes, Begum et al., 2020) growing in pots using open-top chambers to simulate specific ozone concentrations. This experimental setup allowed us to quantify many physiological traits in a controlled environment for a large number of cultivars as an input for modelling parametrization. The limited size of the pots did not allow for an extensive sampling of aboveground dry matter, which in some instances caused high standard deviations. However, these shortcomings inherent to controlled environment experiments may not have affected the relative differences between the treatments and between genotypes, and the final relative yield loss shown in the experiment can be reproduced by the model simulations. However, considering the differences that have been observed between controlled open-top chamber and field-based FACE-experiments (Feng et al., 2018b), further experimental studies under field conditions will be helpful to validate and fine-tune the current model. Additionally, instantaneous and continuous measurements of gas exchange (i.e. CO_2 and H_2O) at both leaf and canopy levels under ozone condition are often lacking, which might require further experimental studies to confirm the instantaneous effects of ozone.

5. Conclusions

In conclusion, we identified NDVI and CO_2 assimilation rate of young leaves as critical physiological parameters for maintaining high wheat grain yield under ozone stress. Based on our experimental data we parameterised a crop model that simulates distinct responses of tolerant and sensitive wheat cultivars to ozone. This will improve global impact assessment of ozone adaptation options such as cultivar selection, and helps to identify physiological traits to be targeted in adaptive breeding.

Author contributions statement

M.F., T.H.N., Y.F. and M.S.A planned and designed the research; Y.F. performed the experiment and analysed the data. T.H.N. performed the crop modelling. F.E., T.G., and L.E. provided advice and guidance in crop modelling; Y.F, and T.H.N wrote the first manuscript. M.F. supervised and completed the writing with contributions from all the authors.

Declaration of competing interest

The authors declare that they have no known competing financial interests or personal relationships that could have appeared to influence the work reported in this paper.

Acknowledgements

We thank Gunther Krauss (University of Bonn) for meaningful discussions regarding the crop model and Josef Bauer and his team for the support in the experimental work. The authors would like to thank China Scholarship Council for providing a PhD fellowship to Yanru Feng (No. CSC201906300077) and the SUSCROP project for providing Post-Doc funding to Thuy Huu Nguyen (No. 031 B0170 B).

Appendix A. Supplementary data

Supplementary data to this article can be found online at https://doi.org/10.1016/j.envpol.2022.119251.

References

Ainsworth, E.A., 2017. Understanding and improving global crop response to ozone pollution. Plant J. 90, 886–897. https://doi.org/10.1111/tpj.13298.

Alexandratos, N., Bruinsma, J., 2012. World Agriculture towards 2030/2050: the 2012 Revision.

Amanullah, Hassan, M.J., Nawab, K., Ali, A., 2007. Response of specific leaf area (SLA), leaf area index (LAI) and leaf area ratio (LAR) of maize (Zea mays L.) to plant density, rate and timing of nitrogen application. World Appl. Sci. J. 2, 235–243.

Ashrafuzzaman, M., Haque, Z., Ali, B., Mathew, B., Yu, P., Hochholdinger, F., de Abreu Neto, J.B., McGillen, M.R., Ensikat, H.J., Manning, W.J., Frei, M., 2018. Ethylenediurea (EDU) mitigates the negative effects of ozone in rice: insights into its mode of action. Plant Cell Environ. 41, 2882–2898. https://doi.org/10.1111/pce.13423.

Ashrafuzzaman, M., Lubna, F.A., Holtkamp, F., Manning, W.J., Kraska, T., Frei, M., 2017. Diagnosing ozone stress and differential tolerance in rice (Oryza sativa L.) with ethylenediurea (EDU). Environ. Pollut. 230, 339–350. https://doi.org/10.1016/j.envpol.2017.06.055.

Avnery, S., Mauzerall, D.L., Fiore, A.M., 2013. Increasing global agricultural production by reducing ozone damages via methane emission controls and ozone-resistant cultivar selection. Global Change Biol. 19, 1285–1299. https://doi.org/10.1111/gcb.12118.

Avnery, S., Mauzerall, D.L., Liu, J., Horowitz, L.W., 2011. Global crop yield reductions due to surface ozone exposure: 2. Year 2030 potential crop production losses and economic damage under two scenarios of O3 pollution. Atmos. Environ. 45, 2297–2309. https://doi.org/10.1016/j.atmosenv.2011.01.002.

Baier, M., Kandlbinder, A., Golldack, D., Dietz, K.J., 2005. Oxidative stress and ozone: Perception, signalling and response. Plant, Cell Environ 28, 1012–1020. https://doi.org/10.1111/j.1365-3040.2005.01326.x.

Begum, H., Alam, M.S., Feng, Y., Koua, P., Ashrafuzzama, M., Shrestha, A., Kamruzzaman, M., Dadshani, S., Ballvora, A., Naz, A.A., Frei, M., 2020. Genetic dissection of bread wheat diversity and identification of adaptive loci in response to elevated tropospheric ozone. Plant Cell Environ. 43, 2650–2665. https://doi.org/10.1111/pce.13864.

Biswas, D.K., Xu, H., Li, Y.G., Sun, J.Z., Wang, X.Z., Han, X.G., Jiang, G.M., 2008. Genotypic differences in leaf biochemical, physiological and growth responses to ozone in 20 winter wheat cultivars released over the past 60 years. Global Change Biol. 14, 46–59. https://doi.org/10.1111/j.1365-2486.2007.01477.x.

Broberg, M.C., Feng, Z., Xin, Y., Pleijel, H., 2015. Ozone effects on wheat grain quality - a summary. Environ. Pollut. 197, 203–213. https://doi.org/10.1016/j.envpol.2014.12.009.

Caldwell, M.M., Meister, H.P., Tenhunen, J.D., Lange, O.L., 1986. Canopy structure, light microclimate and leaf gas exchange of Quercus coccifera L. in a Portuguese macchia: measurements in different canopy layers and simulations with a canopy model. Trees (Berl.) 1, 25–41.

Cappelli, G, Confalonieri, R, Dentener, F, Van Den Berg, M., 2016. Modelling inclusion, testing and benchmarking of the impacts of ozone pollution on crop yields at regional level Module development and testing and benchmarking with the WOFOST generic crop model. In: EUR, 28395. EN. Luxembourg (Luxembourg): Publications Office of the European Union; JRC103907.

Carretero, R., Serrago, R.A., Bancal, M.O., Perelló, A.E., Miralles, D.J., 2010. Absorbed radiation and radiation use efficiency as affected by foliar diseases in relation to their vertical position into the canopy in wheat. Field Crop. Res. 116, 184–195. https://doi.org/10.1016/j.fcr.2009.12.009.

Chen, C.P., Frei, M., Wissuwa, M., 2011. The OzT8 locus in rice protects leaf carbon assimilation rate and photosynthetic capacity under ozone stress. Plant Cell Environ. 34, 1141–1149. https://doi.org/10.1111/j.1365-3040.2011.02312.x.

Chenu, K., Chapman, S.C., Hammer, G.L., MClean, G., Salah, H.B.H., Tardieu, F., 2008. Short-term responses of leaf growth rate to water deficit scale up to whole-plant and crop levels: an integrated modelling approach in maize. Plant Cell Environ. 31, 378–391. https://doi.org/10.1111/j.1365-3040.2007.01772.x.

Chenu, K., Porter, J.R., Martre, P., Basso, B., Chapman, S.C., Ewert, F., Bindi, M., Asseng, S., 2017. Contribution of crop models to adaptation in wheat. Trends Plant Sci. 22, 472–490. https://doi.org/10.1016/j.tplants.2017.02.003.

Dai, L., Kobayashi, K., Nouchi, I., Masutomi, Y., Feng, Z., 2020. Quantifying determinants of ozone detoxification by apoplastic ascorbate in peach (Prunus persica) leaves using a model of ozone transport and reaction. Glob. Chang. Biol. 26, 3147–3162. https://doi.org/10.1111/gcb.15049.

Droutsas, I., Challinor, A.J., Arnold, S.R., Mikkelsen, T.N., Hansen, E.M.Ø., 2020. A new model of ozone stress in wheat including grain yield loss and plant acclimation to the pollutant. Eur. J. Agron. 120, 126125. https://doi.org/10.1016/j.eja.2020.126125.

Duursma, R.A., 2015. Plantecophys–An R package for analysing and modelling leaf gas exchange data. PLoS One 10, e0143346. https://doi.org/10.1371/journal.pone.0143346.

Emberson, L.D., Ashmore, M.R., Cambridge, H.M., Simpson, D., Tuovinen, J.P., 2000. Modelling stomatal ozone flux across Europe. Environ. Pollut. 109, 403–413. https://doi.org/10.1016/S0269-7491(00)00043-9.

Emberson, L.D., Ashmore, M.R., Murray, F., 2003. Air Pollution Impacts on Crops and Forests – a Global Assessment. Imperial College Press, London, UK.

Emberson, L.D., Pleijel, H., Ainsworth, E.A., van den Berg, M., Ren, W., Osborne, S., Mills, G., Pandey, D., Dentener, F., Büker, P., Ewert, F., Koeble, R., Van Dingenen, R., 2018. Ozone effects on crops and consideration in crop models. Eur. J. Agron. 100, 19–34. https://doi.org/10.1016/j.eja.2018.06.002.

Ewert, F., Porter, J.R., 2000. Ozone effects on wheat in relation to CO_2: modelling short-term and long-term responses of leaf photosynthesis and leaf duration. Global Change Biol. 6, 735–750. https://doi.org/10.1046/j.1365-2486.2000.00351.x.

Ewert, F., Rodriguez, D., Jamieson, P., Semenov, M.A., Mitchell, R.A.C., Goudriaan, J., Porter, J.R., Kimball, B.A., Pinter Jr., P.J., Manderscheid, R., Weigel, H.J., Fangmeier, A., Fereres, E., Villalobos, F., 2002. Effects of elevated CO_2 and drought on wheat: testing crop simulation models for different experimental and climatic conditions. Agric. Ecosyst. Environ. 93, 249–266. https://doi.org/10.1016/S0167-8809(01)00352-8.

Ewert, F., van Oijen, M., Porter, J.R., 1999. Simulation of growth and development processes of spring wheat in response to CO_2 and ozone for different sites and years in Europe using mechanistic crop simulation models. Eur. J. Agron. 10, 231–247. https://doi.org/10.1016/S1161-0301(99)00013-1.

Farage, P.K., Long, S.P., Lechner, E.G., Baker, N.R., 1991. The sequence of change within the photosynthetic apparatus of wheat following short-term exposure to ozone. Plant Physiol. 95, 529–535. https://doi.org/10.1104/pp.95.2.529.

Farquhar, G.D., von Caemmerer, S., 1982. Modelling of photosynthetic response to environmental conditions. In: Physiological Plant Ecology II: Water Relations and Carbon Assimilation. Springer Berlin Heidelberg, pp. 549–587.

Feng, Z., Jiang, L., Calatayud, V., Dai, L., Paoletti, E., 2018a. Intraspecific variation in sensitivity of winter wheat (Triticum aestivum L.) to ambient ozone in northern China as assessed by ethylenediurea (EDU). Environ. Sci. Pollut. Res. Int. 25, 29208–29218. https://doi.org/10.1007/s11356-018-2782-8.

Feng, Z., Kobayashi, K., Ainsworth, E.A., 2008. Impact of elevated ozone concentration on growth, physiology, and yield of wheat (Triticum aestivum L.): a meta-analysis. Global Change Biol. 14, 2696–2708. https://doi.org/10.1111/j.1365-2486.2008.01673.x.

Feng, Z., Pang, J., Kobayashi, K., Zhu, J., Ort, D.R., 2011. Differential responses in two varieties of winter wheat to elevated ozone concentration under fully open-air field conditions. Global Change Biol. 17, 580–591. https://doi.org/10.1111/j.1365-2486.2010.02184.x.

Feng, Z., Pang, J., Nouchi, I., Kobayashi, K., Yamakawa, T., Zhu, J., 2010. Apoplastic ascorbate contributes to the differential ozone sensitivity in two varieties of winter wheat under fully open-air field conditions. Environ. Pollut. 158, 3539–3545. https://doi.org/10.1016/j.envpol.2010.08.019.

Feng, Z., Tang, H., Uddling, J., Pleijel, H., Kobayashi, K., Zhu, J., Oue, H., Guo, W., 2012. A stomatal ozone flux-response relationship to assess ozone-induced yield loss of winter wheat in subtropical China. Environ. Pollut. 164, 16–23. https://doi.org/10.1016/j.envpol.2012.01.014.

Feng, Z., Uddling, J., Tang, H., Zhu, Z., Kobayashi, K., 2018b. Comparison of crop yield sensitivity to ozone between open-top chamber aand free-air experiments. Global Change Biol. 24, 2231–2238. https://doi.org/10.1111/gcb.14077.

Feng, Z., Wang, L., Pleijel, H., Zhu, J., Kobayashi, K., 2016. Differential effects of ozone on photosynthesis of winter wheat among cultivars depend on antioxidative enzymes rather than stomatal conductance. Sci. Total Environ. 572, 404–411. https://doi.org/10.1016/j.scitotenv.2016.08.083.

Frei, M., Kohno, Y., Tietze, S., Jekle, M., Hussein, M.A., Becker, T., Becker, K., 2012. The response of rice grain quality to ozone exposure during growth depends on ozone level and genotype. Environ. Pollut. 163, 199–206. https://doi.org/10.1016/j.envpol.2011.12.039.

Gebbing, T., Schnyder, H., 1999. Pre-anthesis reserve utilization for protein and carbohydrate synthesis and grains of wheat. Plant Physiol. 121, 871–878. https://doi.org/10.1104/pp.121.3.871.

González-Fernández, I., Bermejo, V., Elvira, S., de la Torre, D., González, A., Navarrete, L., Sanz, J., Calvete, H., Lafarga, A., Armesto, A.P., Calvo, A., 2013. Modelling ozone stomatal flux of wheat under mediterranean conditions. Atmos. Environ. 67, 149–160. https://doi.org/10.1016/j.atmosenv.2012.10.043.

Gouache, D., Bogard, M., Pegard, M., Thepot, S., Garcia, C., Hourcade, D., Paux, E., Rousset, M., Deswarte, J., Le, X., 2017. Field Crops Research Bridging the gap between ideotype and genotype: challenges and prospects for modelling as exemplified by the case of adapting wheat (Triticum aestivum L.) phenology to climate change in France. Field Crop. Res. 202, 108–121. https://doi.org/10.1016/j.fcr.2015.12.012.

Goumenaki, E., Taybi, T., Borland, A., Barnes, J., 2010. Mechanisms underlying the impacts of ozone on photosynthetic performance. Environ. Exp. Bot. 69, 259–266. https://doi.org/10.1016/j.envexpbot.2010.04.011.

Guarin, J.R., Kassie, B., Mashaheet, A.M., Burkey, K., Asseng, S., 2019. Modelling the effects of tropospheric ozone on wheat growth and yield. Eur. J. Agron. 105, 13–23. https://doi.org/10.1016/j.eja.2019.02.004.

Hassan, M.A., Yang, M., Rasheed, A., Yang, G., Reynolds, M., Xia, X., Xiao, Y., He, Z., 2019. A rapid monitoring of NDVI across the wheat growth cycle for grain yield prediction using a multi-spectral UAV platform. Plant Sci. 282, 95–103. https://doi.org/10.1016/j.plantsci.2018.10.022.

Hay, R.K., Porter, J.R., 2006. The Physiology of Crop Yield. Blackwell publishing.

He, J., Le Gouis, J., Stratonovitch, P., Allard, V., Gaju, O., Heumez, E., Orford, S., Griffiths, S., Snape, J.W., Foulkes, M.J., Semenov, M.A., Martre, P., 2012. Simulation of environmental and genotypic variations of final leaf number and anthesis date for wheat. Eur. J. Agron. 42, 22–33. https://doi.org/10.1016/j.eja.2011.11.002.

Leuning, R., 1995. A critical appraisal of a combined stomatal-photosynthesis model for C3 plants. Plant Cell Environ. 18, 339–355. https://doi.org/10.1111/j.1365-3040.1995.tb00370.x.

Lobell, D.B., Asseng, S., 2017. Comparing estimates of climate change impacts from process-based and statistical crop models. Environ. Res. Lett. 12, 015001.
Lombardozzi, D., Levis, S., Bonan, G., Sparks, J.P., 2012. Predicting photosynthesis and transpiration responses to ozone: Decoupling modeled photosynthesis and stomatal conductance. Biogeosciences 9, 3113–3130. https://doi.org/10.5194/bg-9-3113-2012.
Makowski, D., Wallach, D., Tremblay, M., 2002. Using a Bayesian approach to parameter estimation; comparison of the GLUE and MCMC methods. Agronomie 22, 191–203.
Martre, P., Yin, X., Ewert, F., 2017. Field Crops Research Modeling crops from genotype to phenotype in a changing climate. Field 202, 1–4. https://doi.org/10.1016/j.fcr.2017.01.002.
Messina, C., Hammer, G., Dong, Z., Podlich, D., Cooper, M., 2009. Modelling crop improvement in a G x E x M framework via gene – trait – phenotype relationships. In: Sadras, V.O., Miralles, D.J. (Eds.), Crop Physiology. Applications for Genetic Improvement and Agronomy. Elservier Inc. https://doi.org/10.1016/B978-0-12-374431-9.00010-4.
Mills, G., Buse, A., Gimeno, B., Bermejo, V., Holland, M., Emberson, L., Pleijel, H., 2007. A synthesis of AOT40-based response functions and critical levels of ozone for agricultural and horticultural crops. Atmos. Environ. 41, 2630–2643. https://doi.org/10.1016/j.atmosenv.2006.11.016.
Mills, G., Sharps, K., Simpson, D., Pleijel, H., Broberg, M., Uddling, J., Jaramillo, F., Davies, W.J., Dentener, F., Van den Berg, M., Agrawal, M., Agrawal, S.B., Ainsworth, E.A., Buker, P., Emberson, L., Feng, Z., Harmens, H., Hayes, F., Kobayashi, K., Paoletti, E., Van Dingenen, R., 2018a. Ozone pollution will compromise efforts to increase global wheat production. Global Change Biol. 24, 3560–3574. https://doi.org/10.1111/gcb.14157.
Mills, G., Sharps, K., Simpson, D., Pleijel, H., Frei, M., Burkey, K., Emberson, L., Uddling, J., Broberg, M., Feng, Z., Kobayashi, K., Agrawal, M., 2018b. Closing the global ozone yield gap: quantification and cobenefits for multistress tolerance. Global Change Biol. 24, 4869–4893. https://doi.org/10.1111/gcb.14381.
Miloš, B., Josef, H., Jana, M., Kateřina, S., Alica, K., 2018. Dehydration-induced changes in spectral reflectance indices and chlorophyll fluorescence of Antarctic lichens with different thallus color, and intrathalline photobiont. Acta Physiol. Plant. 40, 1–19. https://doi.org/10.1007/s11738-018-2751-3.
Musselman, R., Lefohn, A., Massman, W., Heath, R., 2006. A critical review and analysis of the use of exposure- and flux-based ozone indices for predicting vegetation effects. Atmos. Environ. 40, 1869–1888. https://doi.org/10.1016/j.atmosenv.2005.10.064.
Naser, M., Khosla, R., Longchamps, L., Dahal, S., 2020. Using NDVI to differentiate wheat genotypes productivity under dryland and irrigated conditions. Sensors 12, 824. https://doi.org/10.3390/rs12050824.
Nguyen, T.H., Langensiepen, M., Vanderborght, J., Hüging, H., Mboh, C.M., Ewert, F., 2020. Comparison of root water uptake models in simulating CO_2 and H_2O fluxes and growth of wheat. Hydrol. Earth Syst. Sci. 24, 4943–4969. https://doi.org/10.5194/hess-24-4943-2020.
Osborne, S., Pandey, D., Mills, G., Hayes, F., Harmens, H., Gillies, D., Buker, P., Emberson, L., 2019. New insights into leaf physiological responses to ozone for use in crop modelling. Plants 8, 84. https://doi.org/10.3390/plants8040084.
Parry, M.A., Reynolds, M., Salvucci, M.E., Raines, C., Andralojc, P.J., Zhu, X.G., Price, G. D., Condon, A.G., Furbank, R.T., 2011. Raising yield potential of wheat. II. Increasing photosynthetic capacity and efficiency. J. Exp. Bot. 62, 453–467. https://doi.org/10.1093/jxb/erq304.
Peng, J., Xu, Y., Shang, B., Agathokleous, E., Feng, Z., 2021. Effects of elevated ozone on maize under varying soil nitrogen levels: biomass, nitrogen and carbon, and their allocation to kernel. Sci. Total Environ. 765, 144332. https://doi.org/10.1016/j.scitotenv.2020.144332.
Picchi, V., Monga, R., Marzuoli, R., Gerosa, G., Faoro, F., 2017. The ozone-like syndrome in durum wheat (Triticum durum Desf.): mechanisms underlying the different symptomatic responses of two sensitive cultivars. Plant Physiol. Biochem. 112, 261–269. https://doi.org/10.1016/j.plaphy.2017.01.011.
Pleijel, H., Danielsson, H., Emberson, L., Ashmore, M.R., Mills, G., 2007. Ozone risk assessment for agricultural crops in Europe: further development of stomatal flux and flux–response relationships for European wheat and potato. Atmos. Environ. 41, 3022–3040. https://doi.org/10.1016/j.atmosenv.2006.12.002.
Pleijel, H., Eriksen, A.B., Danielsson, H., Bondesson, N., Selldén, G., 2006. Differential ozone sensitivity in an old and a modern Swedish wheat cultivar—grain yield and quality, leaf chlorophyll and stomatal conductance. Environ. Exp. Bot. 56, 63–71. https://doi.org/10.1016/j.envexpbot.2005.01.004.
R Core Team, 2018. R: A Language and Environment for Statistical Computing. R Foundation for Statistical Computing, Vienna. https://www.R-project.org.
Ren, X., Shang, B., Feng, Z., Calatayud, V., 2020. Yield and economic losses of winter wheat and rice due to ozone in the Yangtze River Delta during 2014-2019. Sci. Total Environ. 745, 140847. https://doi.org/10.1016/j.scitotenv.2020.140847.
Reynolds, M., Foulkes, J., Furbank, R., Griffiths, S., King, J., Murchie, E., Parry, M., Slafer, G., 2012. Achieving yield gains in wheat. Plant Cell Environ. 35, 1799–1823. https://doi.org/10.1111/j.1365-3040.2012.02588.x.
Rodriguez, D., Ewert, F., Goudriaan, J., Manderscheid, R., Burkart, S., Weigel, H.J., 2001. Modelling the response of wheat canopy assimilation to atmospheric CO_2 concentrations. New Phytol. 150, 337–346. https://doi.org/10.1046/j.1469-8137.2001.00106.x.
Sarlikioti, V., de Visser, P.H., Marcelis, L.F., 2011. Exploring the spatial distribution of light interception and photosynthesis of canopies by means of a functional-structural plant model. Ann. Bot. 107, 875–883. https://doi.org/10.1093/aob/mcr006.
Schauberger, B., Rolinski, S., Schaphoff, S., Müller, C., 2019. Global historical soybean and wheat yield loss estimates from ozone pollution considering water and temperature as modifying effects. Agric. For. Meteorol. 265, 1–15. https://doi.org/10.1016/j.agrformet.2018.11.004.
Shah, S.H., Houborg, R., McCabe, M.F., 2017. Response of chlorophyll, carotenoid and SPAD-502 measurement to salinity and nutrient stress in wheat (Triticum aestivum L.). Agronomy 7, 61. https://doi.org/10.3390/agronomy7030061.
Sicard, P., Anav, A., De Marco, A., Paoletti, E., 2017. Projected global ground-level ozone impacts on vegetation under different emission and climate scenarios. Atmos. Chem. Phys. 17, 12177–12196. https://doi.org/10.5194/acp-17-12177-201.
Sid'ko, A.F., Botvich, I.Y., Pisman, T.I., Shevyrnogov, A.P., 2017. Estimation of chlorophyll content and yield of wheat crops from reflectance spectra obtained by ground-based remote measurements. Field Crop. Res. 207, 24–29. https://doi.org/10.1016/j.fcr.2016.10.023.
Simpson, D., Arneth, A., Mills, G., Solberg, S., Uddling, J., 2014. Ozone — the persistent menace: interactions with the N cycle and climate change. Curr. Opin. Environ. Sustain. 9, 9–19. https://doi.org/10.1016/j.cosust.2014.07.008.
Singh, A.A., Fatima, A., Mishra, A.K., Chaudhary, N., Mukherjee, A., Agrawal, M., Agrawal, S.B., 2018. Assessment of ozone toxicity among 14 Indian wheat cultivars under field conditions: growth and productivity. Environ. Monit. Assess. 190, 1–4. https://doi.org/10.1007/s10661-018-6563-0.
Spitters, Cjt, Toussaint, Hajm, Goudriaan, J., 1986. Separating the diffuse and direct component of global radiation and it's implications for modeling canopy photothesis Part I. Components of incoming radiation. Agric. For. Meteorol. 38, 217–229. https://doi.org/10.1016/0168-1923(86)90060-2.
Tao, F., Feng, Z., Tang, H., Chen, Y., Kobayashi, K., 2017. Effects of climate change, CO2 and O3 on wheat productivity in Eastern China, singly and in combination. Atmos. Environ. 153, 182–193. https://doi.org/10.1016/j.atmosenv.2017.01.032.
Tcherkez, G., Limami, A.M., 2019. Net photosynthetic CO2 assimilaiton: more than just CO_2 and O_2 reduction cycles. New Phytol. 223, 520–529. https://doi.org/10.1111/nph.15828.
Teixeira, E., Fischer, G., van Velthuizen, H., van Dingenen, R., Dentener, F., Mills, G., Walter, C., Ewert, F., 2011. Limited potential of crop management for mitigating surface ozone impacts on global food supply. Atmos. Environ. 45, 2569–2576. https://doi.org/10.1016/j.atmosenv.2011.02.002.
The Royal Society, 2008. Ground-level Ozone in the 21st Century: Future Trends, Impacts and Policy Implications.
Ueda, Y., Frimpong, F., Qi, Y., Matthus, E., Wu, L., Holler, S., Kraska, T., Frei, M., 2015. Genetic dissection of ozone tolerance in rice (Oryza sativa L.) by a genome-wide association study. J. Exp. Bot. 66, 293–306. https://doi.org/10.1093/jxb/eru419.
van Oijen, M., Ewert, F., 1999. The effects of climatic variation in Europe on the yield response of spring wheat cv. Minaret to elevated CO2 and O3: an analysis of open-top chamber experiments by means of two crop growth simulation models. Eur. J. Agron. 10, 249–264. https://doi.org/10.1016/S1161-0301(99)00014-3.
van Oosterom, EJ Van, Kulathunga, M.R.D.L., Deifel, K.S., Mclean, G.B., Barrasso, C., Wu, A., Messina, C., Hammer, G.L., 2021. Dissecting and modelling the comparative adaptation to water limitation of sorghum and maize: role of transpiration efficiency , transpiration rate and height. silico Plants 3, 1–12. https://doi.org/10.1093/insilicoplants/diaa012.
von Caemmerer, S., 2000. Biochemical Models of Leaf Photosynthesis. CSIRO Publishing, Collingwood.
Wang, L., Pang, J., Feng, Z., Zhu, J., Kobayashi, K., 2015. Diurnal variation of apoplastic ascorbate in winter wheat leaves in relation to ozone detoxification. Environ. Pollut. 207, 413–419. https://doi.org/10.1016/j.envpol.2015.09.040.
Wilkinson, S., Mills, G., Illidge, R., Davies, W.J., 2012. How is ozone pollution reducing our food supply? J. Exp. Bot. 63, 527–536. https://doi.org/10.1093/jxb/err317.
Wu, L.B., Holtkamp, F., Wairich, A., Frei, M., 2019. Potassium ion channel gene OsAKT1 affects iron translocation in rice plants exposed to iron toxicity. Front. Plant Sci. 10, 579. https://doi.org/10.3389/fpls.2019.00579.
Wu, R., Zheng, Y., Hu, C., 2016. Evaluation of the chronic effects of ozone on biomass loss of winter wheat based on ozone flux-response relationship with dynamical flux thresholds. Atmos. Environ. 142, 93–103. https://doi.org/10.1016/j.atmosenv.2016.07.025.
Yadav, A., Bhatia, A., Yadav, S., Kumar, V., Singh, B., 2019. The effects of elevated CO2 and elevated O3 exposure on plant growth, yield and quality of grains of two wheat cultivars grown in north India. Heliyon 5, e02317. https://doi.org/10.1016/j.heliyon.2019.e02317.
Yeung, L.Y., Murray, L.T., Martinerie, P., Witrant, E., Hu, H., Banerjee, A., Orsi, A., Chappellaz, J., 2019. Isotopic constraint on the twentieth-century increase in tropospheric ozone. Nature 570, 224–227. https://doi.org/10.1038/s41586-019-1277-1.
Zeng, Y., Cao, Y., Qiao, X., Seyler, B.C., Tang, Y., 2019. Air pollution reduction in China: recent success but great challenge for the future. Sci. Total Environ. 663, 329–337. https://doi.org/10.1016/j.scitotenv.2019.01.262.
Zhu, Z., Sun, X., Zhao, F., Meixner, F.X., 2015. Ozone concentrations, flux and potential effect on yield during wheat growth in the Northwest-Shandong Plain of China. J. Environ. Sci. (China) 34, 1–9. https://doi.org/10.1016/j.jes.2014.12.022.

Chapter 3: Alteration of carbon and nitrogen allocation in winter wheat under elevated ozone

Manuscript published in Plant Science 2024 Vol 338, 111924

Plant Science 338 (2024) 111924

Contents lists available at ScienceDirect

Plant Science

journal homepage: www.elsevier.com/locate/plantsci

Alteration of carbon and nitrogen allocation in winter wheat under elevated ozone

Yanru Feng [a,b], Muhammad Shahedul Alam [a], Feng Yan [a], Michael Frei [a,*]

[a] Department of Agronomy and Crop Physiology, Institute of Agronomy and Plant Breeding, Justus Liebig University Giessen, 35390 Giessen, Germany
[b] Institute of Crop Science and Resource Conservation (INRES), Crop Science, University of Bonn, 53115 Bonn, Germany

ARTICLE INFO

Keywords:
Air pollution
Ozone
Cereals
Nitrogen allocation
Grain quality

ABSTRACT

Tropospheric ozone accelerates senescence and shortens grain filling, consequently affecting the remobilization and allocation efficiency of aboveground biomass and nutrients into grains in cereal crops. This study investigated carbon (C) and nitrogen (N) concentrations repeatedly in shoot biomass during the growth period and in grain after the harvest in eighteen wheat genotypes under control and ozone treatments in open-top chambers. Season-long ozone fumigation was conducted at an average ozone concentration of 70 ppb with three additional acute ozone episodes of around 150 ppb. Although there were no significant differences in straw C and N concentrations between the two treatments, the straw C:N ratio was significantly increased after long-term ozone fumigation, and the grain C:N ratio decreased under elevated ozone without significance. Grain N concentrations increased significantly under ozone stress, whereas N yield declined significantly due to grain yield losses induced by ozone. Moreover, different indicators of N use efficiency were significantly reduced with the exception of N utilization efficiency (NUtE), indicating that elevated ozone exposure reduced the N absorption from soil and allocation from vegetative to reproductive organs. The linear regression between straw C:N ratio and productivity indicated that straw C:N was not a suitable trait for predicting wheat productivity due to the low coefficient of determination (R^2). Nitrogen harvest index (NHI) was not significantly affected by ozone stress among all genotypes. However, elevated ozone concentration changed the relationship between harvest index (HI) and NHI, and the reduced regression slope between them indicated that ozone exposure significantly affected the relationship of N and biomass allocation into wheat grains. The cultivar "Jenga" showed optimal ozone tolerance due to less yield reduction and higher NUE after ozone exposure. The genotypes with higher nutrient use efficiencies are promising to cope with ozone-induced changes in nitrogen partitioning.

1. Introduction

Tropospheric ozone (O_3) is a phytotoxic air pollutant, which is produced in photochemical reactions of precursor gases such as nitrogen oxides (NOx) and volatile organic components (VOCs) (Monks et al., 2015; Simpson et al., 2014). Anthropogenic gas emissions arising from rapid urbanization and industrialization, have contributed to high surface ozone concentrations over the past decades, especially in East and South Asian countries (Cooper et al., 2014; Sicard et al., 2017). For example, despite stringent emission control measures, including the Air Pollution Prevention and Control Action Plan, there was still an increasing trend of ozone pollution in China. The summertime surface ozone in eastern China from 2013 to 2018 is among the highest in the world, and the maximum 8-h average (MDA8) in summertime was regionally 58.5 ppb (Han et al., 2020). Many metropolitan areas in China have experienced severe regional ozone pollution in recent years, such as Beijing-Tianjin-Hebei (BTH), the Yangtze River Delta (YRD) and the Pearl River Delta (PRD) (Lu et al., 2018). Especially, ozone pollution in urban areas of China was severe due to high anthropogenic emission, and the daily MDA8 ozone concentrations often exceed the air quality standard of 80 ppb (Wang et al., 2022; Wei et al., 2022). Frequent and persistent ozone pollution with concentrations typically over 40 ppb, would result in adverse effects on vegetation, leading to substantial yield reductions and posing a serious threat to global food security (Avnery et al., 2013; Sicard et al., 2017). It has been estimated that ozone reduces global yield annually by 7.1%, 4.4% and 6.1% for wheat, maize and rice, respectively (Mills et al., 2018). In China, the highest relative yield losses for these three crops reached 33%, 23% and 9%, respectively

* Corresponding author.
E-mail address: michael.frei@agrar.uni-giessen.de (M. Frei).

https://doi.org/10.1016/j.plantsci.2023.111924
Received 11 September 2023; Received in revised form 17 October 2023; Accepted 14 November 2023
Available online 20 November 2023

(Feng et al., 2022b). The severity of ozone effects on crop production has been a cause for concern and urges us to take actions against rising ozone.

As a powerful oxidant, ozone enters leaves mainly via open stomatal pores and then forms reactive oxygen species (ROS), thereby triggering metabolic disorders, reducing photosynthetic capacity and accelerating senescence, altering nutrient accumulation and allocation, and eventually resulting in yield losses and quality changes (Ainsworth, 2017; Wilkinson et al., 2012). The effects of ozone on crops and their physiological mechanisms have been studied extensively and are well understood (Feng et al., 2022b). For example, the observed effects of elevated ozone on leaf nitrogen (N) content and the effects on the light saturated photosynthetic rate (A_{sat}) suggested that losses in leaf N contributed to ozone-induced declines in photosynthesis of soybean (Zhang et al., 2014). Photosynthesis is considered a sensitive trait to ozone and is associated with ozone-induced yield reductions in crops (Feng et al., 2018a; Flowers et al., 2007; Pleijel et al., 1998), partly due to reduction in carbon (C) assimilation capacity induced by changes of photosynthetic apparatus under ozone stress in soybean (Morgan et al., 2003). In maize, ozone also affected the uptake and accumulation of nutrients, including a reduction in N content, thus reducing N uptake efficiency (NUE) (Peng et al., 2020). Based on the basic elements C and N forming plant biomass, ecological stoichiometry provides an integrative approach for the relative elemental composition of plants, by employing the C:N ratio, and is essential for predicting plant productivity (Elser et al., 2000). For instance, a negative correlation between the C:N ratio and yield in maize has been reported (Peng et al., 2021). Moreover, the coordinated response and shift in the elemental stoichiometry under abiotic stress plays an important role in stress acclimation (Rivas-Ubach et al., 2012). Therefore, understanding C and N allocation and their ecological stoichiometric responses under ozone stress is essential for estimating the effects of ozone on crops.

Wheat is one of the main staple crops on a global scale and has been classified as highly sensitive to ozone, with the critical level (AOT40) for 5% yield reduction at 3.3 ppm h (Feng et al., 2008; Mills et al., 2007). Ozone-induced reductions in wheat yield were also accompanied by changes in grain quality (Broberg et al., 2015; Pleijel et al., 2018; Pleijel et al., 1997). Elevated ozone accelerates leaf senescence and shortens grain development in wheat, which leads to N remobilization from vegetative tissues to grain (Wang and Frei, 2011). Previous studies found that ozone reduced the translocation of accumulated N from straw and leaves to grains under ozone stress, leading to a significantly lower nitrogen harvest index (NHI) and N efficiency (Broberg et al., 2021). Reduced NUE induced by ozone stress indicates nutrient leaching from agroecosystems, causing environmental pollution and economic losses (Broberg et al., 2017). According to a meta-analysis of grain quality in wheat, the average protein yield was significantly reduced by more than 15% under ozone stress compared to charcoal-filtered air, although the protein concentration was positively influenced by ozone (Broberg et al., 2015). Nevertheless, the C:N ratio of grain was reduced under ozone exposure, which was considered an indirect effect of reduced carbohydrate accumulation (Zheng et al., 2013).

Although a number of studies have investigated the impacts of elevated ozone concentration on nutrient elements and N uptake in wheat, the responses to ozone might be cultivar-specific and the dynamics of C and N allocation in straw during growth stages and in grain at harvest under ozone stress are poorly understood. Moreover, the role of the straw C:N ratio and its contribution to yield-related traits, as well as the relationship with NUE indicators remains elusive in wheat. In order to address these knowledge gaps, this study evaluated the effect of ozone exposure on C and N concentrations in straw repeatedly during the growth season and in grain after harvest, as well as different NUE indicators and their regression relationships among eighteen wheat genotypes under control and elevated ozone concentration. We hypothesized that there are large genotypic variations of C and N accumulation under elevated ozone concentration in wheat, and long-term ozone fumigation could alter the relationships of different physiological parameters related to C and N allocation. The specific aims of this investigation were to (1) estimate the impacts of elevated ozone concentration on straw C and N in different growth stages and their allocation to grain, (2) explore the effects of ozone on different NUE indicators in different cultivars, and (3) determine the relationships between the straw C:N ratio and productivity among different cultivars.

2. Materials and methods

2.1. Plant materials and ozone exposure

The experiment was carried out in open-top chambers (OTCs, length 2.6 m, width 2.1 m, height 1.7 m) at the University of Bonn, Germany, from December 2019 to July 2020 (Feng et al., 2022a). Based on leaf bronzing score and grain yield, eighteen wheat cultivars (Table A1) were selected with contrasting tolerance to ozone from a larger population of 150 genotypes that had previously been screened for ozone adaptive breeding in a genome-wide association study (Begum et al., 2020). After germination in quickpots, seedlings were vernalized in a climate chamber at 4 °C for eight weeks and then transplanted into a total of 288 pots (dimensions 25 cm × 25 cm × 25 cm), filled with Terrasoil (total N concentration < 0.05%). In each chamber, there were two pots for each genotype, and each pot contained 5 plants. At the beginning, 5 g "NovaTec classic 12–8–16″ (12% N, 8% P_2O_5, 16% K_2O) was applied to each pot. During the growing period, all pots were automatically irrigated with 0.15% "KristalonGrünmarke 18–18–18″ (18% N, 18% P_2O_5, 18% K_2O) at a rate of 80 mL/pot/day in the vegetative stage for 60 days, 100 mL/pot/day in the reproductive stage for 70 days and 60 mL/pot/day for 10 days after stopping ozone fumigation on DAT132 (132 days after transplanting).

Eight OTCs were built up in the greenhouse, including four replicates for the control and ozone treatments. The ozone fumigation lasted for 107 days by custom-made ozone generators (UB 01; Gemke Technik GmbH, Ennepetal, Germany) with a target of 70 ppb for 7 h (09:00–16:00 h) in ozone chambers. The ozone output was automatically controlled by an ozone monitor (K 100 W; Dr. A. Kuntze GmbH, Meerbusch, Germany) and monitored by additional handheld ozone monitors (series 500; Aeroqual Ltd, Auckland, New Zealand) at the level of plant canopy. Throughout the fumigation season, the actual average ozone concentration was 70.3 ppb ± 21.0 SD (standard deviation) in the ozone treatment and 27.8 ppb ± 6.1 SD in the control conditions. To simulate peak ozone episodes, acute fumigation was applied three times at weeks 8, 10 and 13 after transplanting with an average ozone concentration of 151.4 ppb ± 27.4 SD. Temperature and relative humidity inside the greenhouse were recorded by a sensor type 224.401 (RAM GmbH Mess-und Regeltechnik, Herrsching, Germany). From transplanting to harvest, the average temperatures during daytime (8:00–20:00 h) and nighttime (20.00–8.00 h) were 23.7 °C and 17.0 °C, and for relative humidity, 35.8% and 57.5%, respectively. A detailed description of the OTC system can be found in Feng et al. (2022a).

2.2. Plant sampling and measurement

A total of six timepoints were sampled for all cultivars. At weeks 5, 9, 12, 15 and 18 after transplanting, one above-ground plant for each cultivar was randomly collected from the pots for interval sampling in each chamber. At week 21 after transplanting (DAT144), the remaining five plants for each cultivar were harvested at ground level and separated into straw and grain for yield-related measurements. Those samples were weighed and ground using a ball mill after oven-drying at 105 °C for 72 h to a steady weight for measurements. The C and N concentrations, i.e., the proportion of C or N in the corresponding subsample, were determined using an elemental analyzer with two replicates for each subsample (Elementar UNICUBE, Elementar

Analysysteme GmbH, Langenselbold, Germany). C:N ratio was defined by the ratio of C concentration (or content) to N concentration (or content) in different subsamples. Yield attributes (total dry biomass, grain yield, grain number, thousand kernel weight and HI), in which HI was derived by dividing grain yield by total aboveground biomass, were analyzed at the final harvest stage (Feng et al., 2022a).

2.3. Calculation

N yield (grain N uptake) and grain C uptake were calculated as the product of yield and grain N concentration, and grain C concentration, respectively. Plant N uptake (NUP) or plant C uptake, determined as total aboveground N (C) in whole plants, was calculated as the sum of straw N (C) uptake and grain N (C) uptake. The N harvest index (NHI) or C harvest index (CHI) was defined as the proportion of grain N (C) uptake in plant N (C) uptake at maturity (final harvest) and was computed following Eqs. (1) - (2) (Congreves et al., 2021; Peng et al., 2020).

$$NHI = \frac{Grain\quad N\quad uptake}{Plant\quad N\quad uptake} \tag{1}$$

$$CHI = \frac{Grain\quad C\quad uptake}{Plant\quad C\quad uptake} \tag{2}$$

C internal efficiency (IE_c) is the ratio of kernel yield to total C accumulation in the aboveground plant, indicating the C conversion efficiency of aboveground plant uptake C to kernel yield (Eq. (3)). N utilization efficiency (NUtE) is the ability to produce yield relative to aboveground plant tissue N (Eq. (4)) (Peng et al., 2020).

$$IE_c = \frac{Grain\quad yield}{Plant\quad C\quad uptake} \tag{3}$$

$$NUtE = \frac{Grain\quad yield}{Plant\quad N\quad uptake} \tag{4}$$

The amount of fertilizer in the pots was same, and fertilizer N was calculated as the cumulative N inputs throughout whole growth season for each plant. N balance intensity (NBI) was calculated from the sum of fertilizer N inputs and removals for yield N (Eq. (5)). N use efficiency (NUEcrop) was defined as the proportion of fertilizer N that was utilized and allocated to grain (Eq. (6)). Partial-factor productivity (PFP) and partial N balance (PNB) represent the conversion efficiency of input N to grain yield and plant N uptake, respectively (Eqs. (7) - (8)) (Congreves et al., 2021; Duan et al., 2014).

$$NBI = Grain\quad N\quad uptake - Fertilizer\quad N \tag{5}$$

$$NUEcrop = \frac{Grain\quad N\quad uptake}{Fertilizer\quad N} \times 100 \tag{6}$$

$$PFP = \frac{Grain\quad yield}{Fertilizer\quad N} \tag{7}$$

$$PNB = \frac{Plant\quad N\quad uptake}{Fertilizer\quad N} \tag{8}$$

2.4. Statistical analysis

Straw C and N concentrations and the C:N ratio were subjected to three-way analysis of variance (ANOVA) with a mixed linear model, in which treatment, genotype, DAT and their interactions were considered fixed effects, while chamber was considered a random effect. Yield-related parameters and NUE indicators were subjected to two-way ANOVA to test the effects of treatment, genotypes and their interactions. Relative values (ratio of value for plants grown under ozone treatment relative to control condition) were calculated for all parameters from the last sampling date for all genotypes, followed by correlation analyses using pairwise Pearson's correlation coefficients. Two-way analysis of covariance (ANCOVA) was applied to estimate the significance of differences among slopes of linear regressions between different production-related parameters under control and ozone conditions. R packages "nlme" and "emmeans" were used for ANOVA and ANCOVA (R Core Team, 2018).

3. Results

3.1. Straw C and N

To investigate the effects of ozone on straw C and N concentrations during the growth stage, plants were collected and measured repeatedly for six timepoints to obtain continuous data. Across all sampling dates, straw C and N concentrations were not significantly affected by ozone exposure. However, significant effects occurred between genotypes, DAT and for their interaction (Table 1). Compared to the control condition, ozone tended to decrease straw N concentration, but few individual genotypes were significantly affected by ozone in terms of straw C and N concentrations at different growth stages (Fig. A1 and A2). A significant reduction of N concentration due to ozone treatment occurred late in the growing season at DAT106 and DAT126. Moreover, straw C:N ratios increased after anthesis and were significantly affected by treatment, genotype and DAT among all sampling dates. Especially after prolonged fumigation, ozone significantly increased the straw C:N ratio by 12.2% at harvest compared to control condition (Fig. 1; Table 1).

3.2. Grain C and N

The responses of grain N content to elevated ozone differed among cultivars. Averaged over all genotypes, grain C and N concentrations were increased by 2.1% and 4.8%, respectively, and showed significant effects at the ozone and genotype levels (Table 2). Compared to control condition, the grain C:N ratio decreased by 2.6% in the ozone treatment among all genotypes, but it was not significant. There were no significant treatment responses of CHI and NHI, but large variations occurred in NHI among all genotypes ranging from relative values 0.8 to 1.5 (Table 2, Fig. 3A). In addition, the N yield after ozone treatment was significantly decreased by 15.0% compared to the control condition (Table 2). Sensitive cultivars 1 and 17 showed significant differences between the control and ozone treatment in the grain C:N ratio and the former decreased in NHI by 24.7% after ozone exposure (Fig. 2C, Fig. 3A). Among all genotypes, cultivar 8 had highest relative N yield with increased NHI without significance (Fig. 2D). Combined with the N content from straw and grain, the NUP showed a highly significant difference at the treatment and genotype levels and decreased by 19.5% after long-term ozone fumigation among all genotypes (Table 2).

3.3. C internal efficiency and NUE indicators

Relative to the control condition, ozone treatment did not significantly change IE_c and NUtE, but there was large variation in NUtE, with relative values ranging from 0.7 to 1.5 (Table 2, Fig. 3B). Moreover, ozone treatment resulted in significant decreases of 15.0% and 3.4% for NUEcrop and NBI, respectively, compared to control condition, and large variation occurred in NUEcrop, with relative values ranging from 0.6 to 1.0 (Table 2, Fig. 3C-D). In comparison with the control condition, the significant reductions in PFP and PNB after ozone fumigation were 19.1% and 19.5%, respectively, among all genotypes (Table 2). Both PFP and PNB varied greatly across different genotypes, with wide ranges of relative values (Fig. 3E-F). Elevated ozone had less impacts on NUE responses of cultivars 8, 10 and 15 according to NUEcrop, NBI and PFP.

3.4. Relationship between production-related parameters

The C:N ratio, which represents the coordination of C and N

Table 1
Descriptive statistics and ANOVA results of straw carbon and nitrogen concentrations and their ratios in wheat under control and ozone conditions. Mean values per individual plant of all genotypes are shown. Different superscript letters following mean values within one row indicate significant differences at $P < 0.05$ (n = 72) by Tukey's HSD test.

Trait	Date	Control		Ozone		ANOVA						
		Mean	SD	Mean	SD	T	G	DAT	G×T	DAT×T	DAT×G	DAT×G×T
Straw C concentration (%)	DAT34	41.50a	0.62	41.62a	0.59	0.3224	< .0001	< .0001	0.2196	0.0090	< .0001	0.2780
	DAT61	42.40a	1.18	42.74a	0.89							
	DAT84	42.75a	1.00	42.70a	1.04							
	DAT106	39.45a	1.61	39.22a	2.11							
	DAT126	36.89a	1.72	36.97a	1.84							
	Harvest	35.75a	2.93	36.39a	1.97							
Straw N concentration (%)	DAT34	3.65a	0.81	3.42a	0.80	0.2296	< .0001	< .0001	0.2231	0.0053	0.0008	0.8966
	DAT61	4.71a	0.45	4.82a	0.42							
	DAT84	4.52a	0.43	4.48a	0.42							
	DAT106	3.90a	0.41	3.62b	0.55							
	DAT126	2.40a	0.48	2.16b	0.49							
	Harvest	1.78a	0.46	1.64a	0.47							
Straw C:N ratio	DAT34	11.96a	2.89	12.89a	3.20	0.0359	< .0001	< .0001	0.0553	0.0002	< .0001	0.8820
	DAT61	9.09a	1.06	8.94a	0.83							
	DAT84	9.55a	0.97	9.62a	0.92							
	DAT106	10.22a	1.68	11.05b	1.34							
	DAT126	15.95a	3.25	18.00b	4.21							
	Harvest	21.28a	5.18	23.87b	6.44							

Abbreviations: DAT, days after transplanting; G, genotype; SD, standard deviation; T, treatment.

metabolism might be an important indicator of productivity (Peng et al., 2021). Based on the correlation analyses, the straw C:N ratio was significantly correlated with NUP, NHI, NUtE and PNB (Fig. A3). ANCOVA was further applied to estimate the significance of slopes of linear regressions between the straw C:N ratio and its associated traits and yield-related parameters. The regressions between the straw C:N ratio and grain number and thousand kernel weight were all significant but with low R^2. In both treatments, the straw C:N ratio had a significant positive relationship with grain number and a significant negative relationship with thousand kernel weight (Fig. 4B-C). The straw C:N ratio was significantly correlated with total dry biomass and their linear regression was extremely inferred by ozone stress. Elevated ozone exposure tended to weaken the relationship between the straw C:N ratio and NUP, N yield, grain yield, NHI, NUtE and PNB. There were significant regression slopes between the straw C:N ratio and NHI and NUtE, but both regressions in the ozone treatment had P values > 0.05, implying insignificant relationships (Fig. 4G-H). The R^2 values of regressions between straw C:N and different traits were lower than those between harvest index (HI) and CHI and NHI. The regressions between them were analyzed and found to be significant with high R^2. Elevated ozone did not affect the positive relationship between HI and CHI, but the regression slope between HI and NHI was significantly decreased by 37.8% in the ozone treatment relative to the control condition (Fig. 5A-B).

4. Discussion

In this study, eighteen wheat genotypes were analyzed for C and N allocation and their ecological stoichiometry under ozone stress. To investigate the ozone effects during all developmental stages, straw C and N concentrations were analyzed repeatedly during the growth season, and only the straw C:N ratio was significantly affected by ozone exposure. The differences in average straw C:N between the two treatments were greater with increasing ozone fumigation duration (Table 1, Fig. 1). The significant increase in the straw C:N ratio under ozone exposure and a reduction without significance in the grain C:N ratio at harvest compared to control condition, imply that ozone affects nutrient partitioning in different parts of the plant (Table 2). This could be related to premature senescence, which is a general ozone-induced response in wheat and a key factor behind the yield reduction, because ozone shortens the grain filling period with less time for nutrient translocation (Gelang et al., 2000; Grandjean and Fuhrer, 1989). During senescence, degradation of chlorophyll is accompanied by N remobilization from vegetative to reproductive organs (Maillard et al., 2015). Compared to the control condition, a higher grain N concentration was observed in the ozone treatment among all genotypes in our study, while a significant reduction in N yield indicated lower protein deposition in the grain. Generally, protein deposition in cereal grains tends to be favored over starch accumulation during accelerated senescence induced by elevated ozone, and the production and translocation of carbohydrates to the grain is more sensitive to environmental stresses than protein accumulation (Wang and Frei, 2011). Ozone can also increase soluble sugar concentration and carbohydrate retention in leaves to provide respiratory energy for the protection, maintenance and repair of plant structures (Grantz, Farrar, 2000; Rai and Agrawal, 2012). However, carbohydrate accumulation in leaves might also cause a feedback inhibition of photosynthetic capacity and induce premature senescence (Ghosh et al., 2020). In addition, ozone-induced membrane damage also affected photosynthate transfer via the phloem (Meyer et al., 1997). As a result, the reduction in photosynthate and inhibition of C translocation from the source to sink lead to reduction of concurrent carbon fixation during grain filling. In contrast to that, protein synthesis is less affected by ozone stress, because amino acids derived from protein degradation are released during accelerated leaf senescence to compensate for the shortened grain filling period and the nitrogen shortage due to reduction in N uptake from soil (Triboi and Triboi-Blondel, 2002). The growth dilution effect was considered to be a main factor related to higher protein concentrations but reduction in N yield, i.e., the negative effect on grain yield was much higher than the positive ozone effect on grain N concentration (Fuhrer et al., 1990; Pleijel and Uddling, 2012).

Ozone-induced yield loss attributes to a combination of different yield components. A meta-analysis found that individual grain weight was the most responsible trait for yield reduction with the elevated ozone ranging from 31 to 200 ppb (Feng et al., 2008). However, perhaps due to the cultivar selection and different experimental systems, reduced grain number per plant was the most important contributor to the yield reduction induced by ozone exposure in this study (Fig. 4B), followed by thousand kernel weight, which was based on significance of correlation between different yield-related traits (Feng et al., 2022a). Elevated ozone exposure affected the development of the reproductive organs, thereby reducing the grain number and thousand kernel weight, eventually leading to the lower grain yield.

The HI is an important indicator of the convension efficiency of

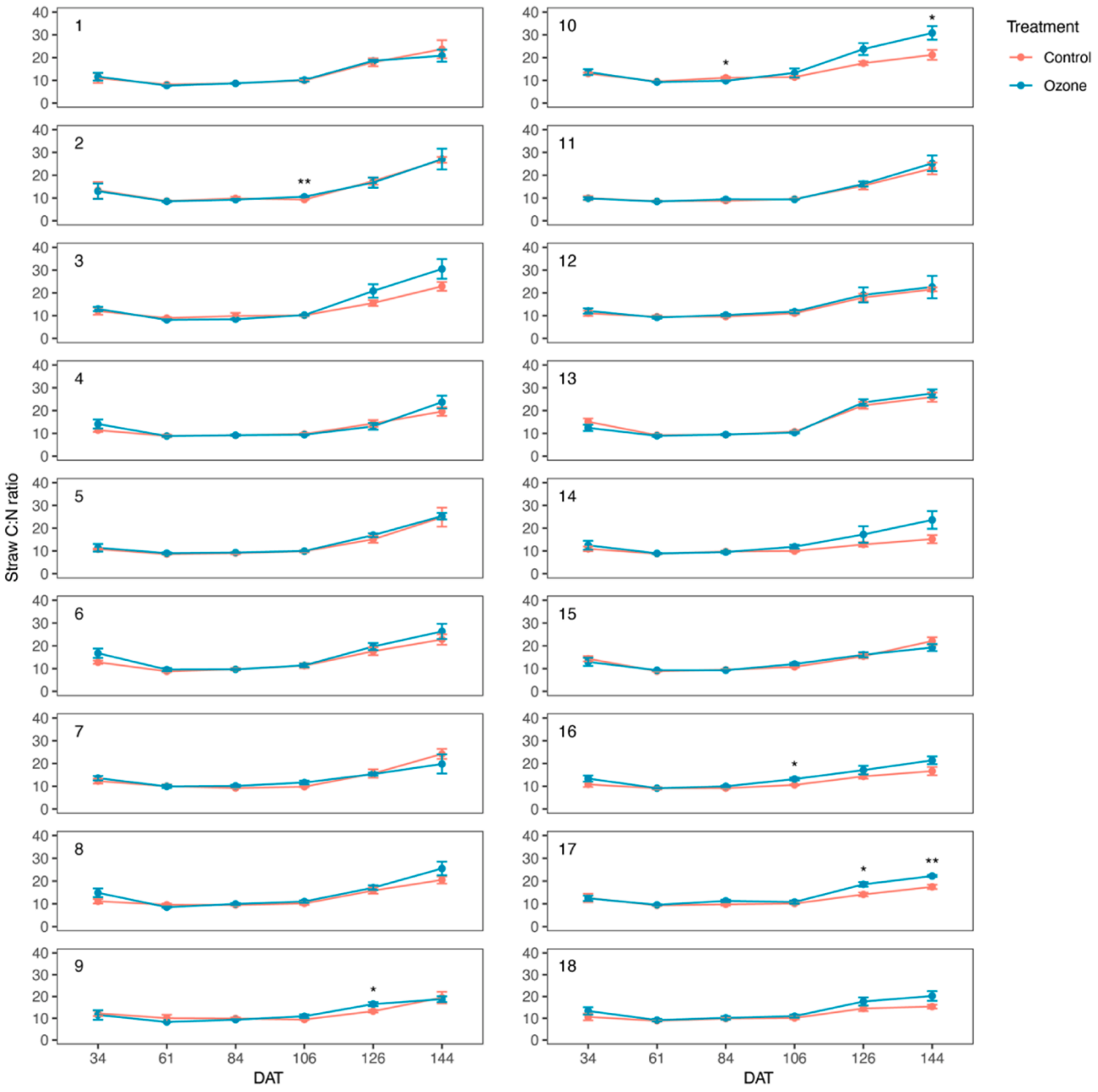

Fig. 1. Straw C:N ratio of different wheat genotypes during the growth season under control and ozone conditions. Within the growth stage, an asterisk (*) indicates a significant treatment difference at $P < 0.05$, and a double asterisk (**) indicates a significant treatment difference at $P < 0.01$ (n = 4) by Student's *t* test.

aboveground biomass to grain and was reduced by elevated ozone in wheat, contributing significantly to the reduction in grain yield (Luo et al., 2015; Pleijel et al., 2014). Element HI indicates the efficiency of nutrient remobilization and transport from vegetative to reproductive tissues during grain filling, as well as post-anthesis nutrient uptake with transport directly from root to grain (Lv et al., 2020). NHI represents the proportion of N contained in the grain to the total aboveground N content and is one of the highest among 13 element HI, including nutrients and nonessential elements in wheat, indicating the importance of N in plant growth (Broberg et al., 2021). Although without significance, NHI increased after ozone fumigation among all genotypes, which was consistent with the higher N concentration in grain. Large variations in N partitioning were previously observed among 30 Indian wheat cultivars under different N supplies (Nehe et al., 2020). In this study, there was also a pronounced variation in NHI with respect to relative values ranging from approximately 0.8 to 1.5, indicating that the effect of ozone on NHI differs largely between wheat genotypes. In addition, NHI is related to the growing environment, including fertilizer application of N and abiotic stress, such as ozone stress (Baresel et al., 2008; Broberg et al., 2021). In addition, both treatments had strong positive correlations between HI and NHI and CHI, while the regression slope between HI and NHI was significantly decreased by ozone stress compared to control condition, indicating that ozone treatment significantly affects the coupling relationship of the N-related nutrition allocation and biomass allocation to grain in wheat.

This study applied equal amounts of fertilizer to each plant and calculated the amount of N applied to the soil throughout the growing season. With the exception of NUtE representing the yield produced per unit of N acquired by the plant shoot, other NUE indictors were significantly decreased by elevated ozone concentration compared to control condition (Table 2). Among them, NBI and PFP focus on the economically valuable portion of plants especially crop yield. NUEcrop and PNB

Table 2
Descriptive statistics and ANOVA results of grain carbon and nitrogen concentrations and NUE indicators in wheat under control and ozone conditions. Mean values per individual plant of all genotypes are shown.

Trait	Control		Ozone		ANOVA		
	Mean	SD	Mean	SD	T	G	G×T
Grain C concentration (%)	42.35	0.61	43.25	0.67	0.0357	0.0058	0.1858
Grain N concentration (%)	3.13	0.23	3.28	0.22	0.0240	< .0001	0.5005
Grain C:N ratio	13.60	0.87	13.25	0.83	0.0561	< .0001	0.7601
NUP (g/plant)	0.27	0.06	0.22	0.06	00018	0.1017	0.1574
N yield (g/plant)	0.15	0.03	0.12	0.03	0.0029	0.0011	0.6311
CHI	0.46	0.13	0.46	0.15	0.9832	0.0973	0.5425
NHI	0.56	0.13	0.59	0.15	0.3429	0.0365	0.2947
IE_C	1.10	0.30	1.07	0.34	0.7119	0.0972	0.5412
NUtE	18.00	4.39	17.99	4.61	0.9985	0.0219	0.3060
NUEcrop (%)	18.38	3.37	15.62	4.07	0.0029	0.0011	0.6311
NBI	-0.64	0.03	-0.67	0.03	0.0029	0.0011	0.6311
PFP	5.90	1.09	4.77	1.25	0.0008	0.0014	0.5947
PNB	0.34	0.08	0.27	0.08	0.0018	0.1017	0.1574

Abbreviations: CHI, C harvest index; G, genotype; NBI, N balance intensity; NHI, N harvest index; NUP, total plant N uptake; NUEcrop, crop N use efficiency; NUtE, N utilization efficiency; PFP, partial-factor productivity; PNB, partial N balance; SD, standard deviation; T, treatment.

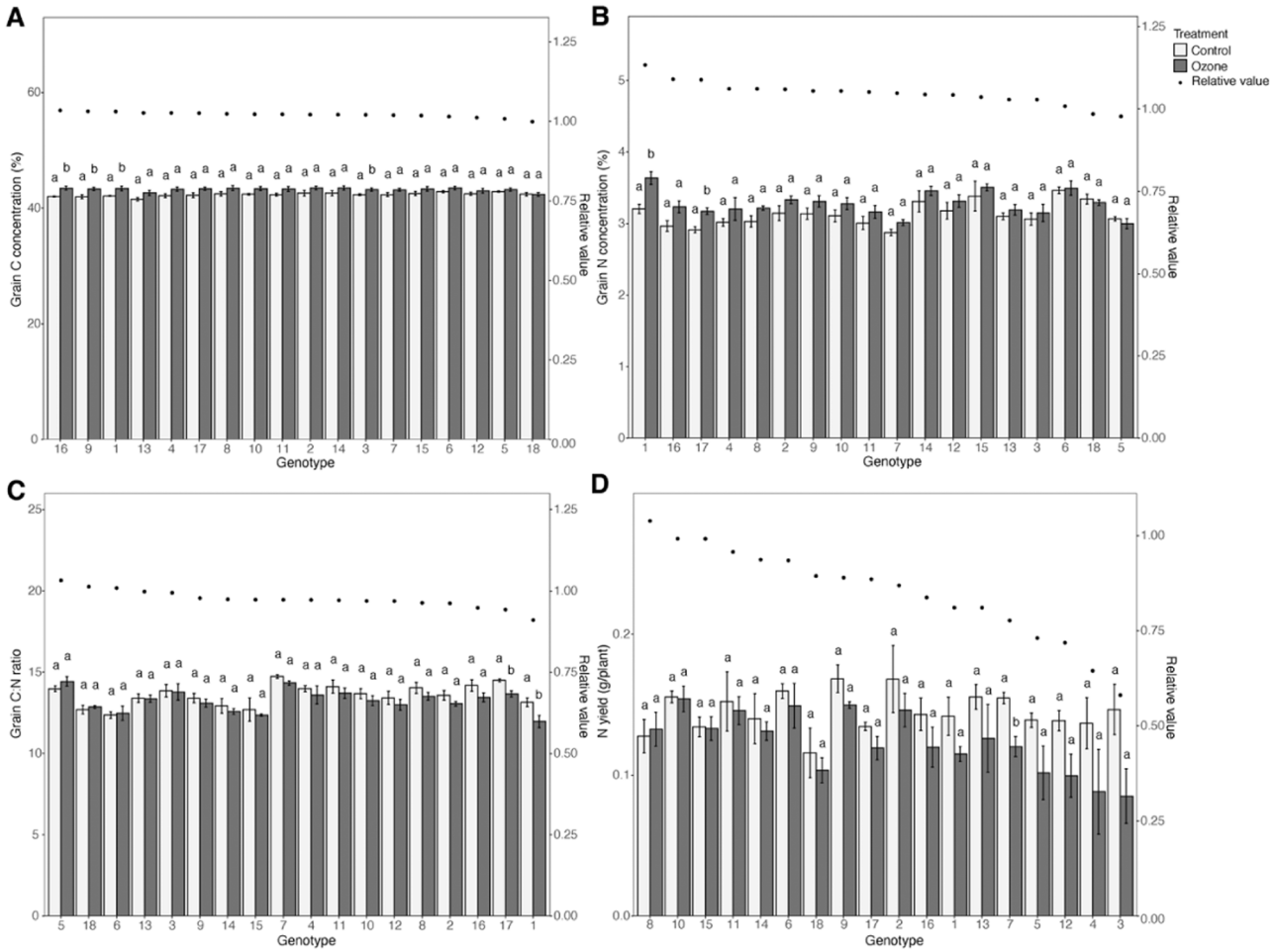

Fig. 2. Grain C and N concentrations and N yield of different wheat genotypes under control and ozone treatments. Bars indicate mean values and standard errors (n = 4). A, Grain C concentration; B, Grain N concentration; C, Grain C:N ratio; D, N yield. Bars not sharing the same superscript letters are significantly different at $P < 0.05$ within the genotypes by Student's *t* test.

represent the proportion of N yield and plant N content, respectively, relative to fertilizer N applied. The latter was less than 1 in all genotypes, suggesting sufficient N application and a net surplus of N supply in this cropping system (Congreves et al., 2021; Martinez-Feria et al., 2018). NBI and NUEcrop are analogous calculations between N yield and N fertilizer, and our results indicate that N accumulated in soil during the growth period. Deficient N in soil decreases the production of cytokinin, which has the function of retarding senescence, leading to leaf protein degradation (Barneix, 2007; Gan and Amasino, 1995). However, in this study, the availability of N was abundant to satisfy the N demand of plants, and the large variation of different NUE indicators revealed substantial genotypic differences at this N fertilizer application rate

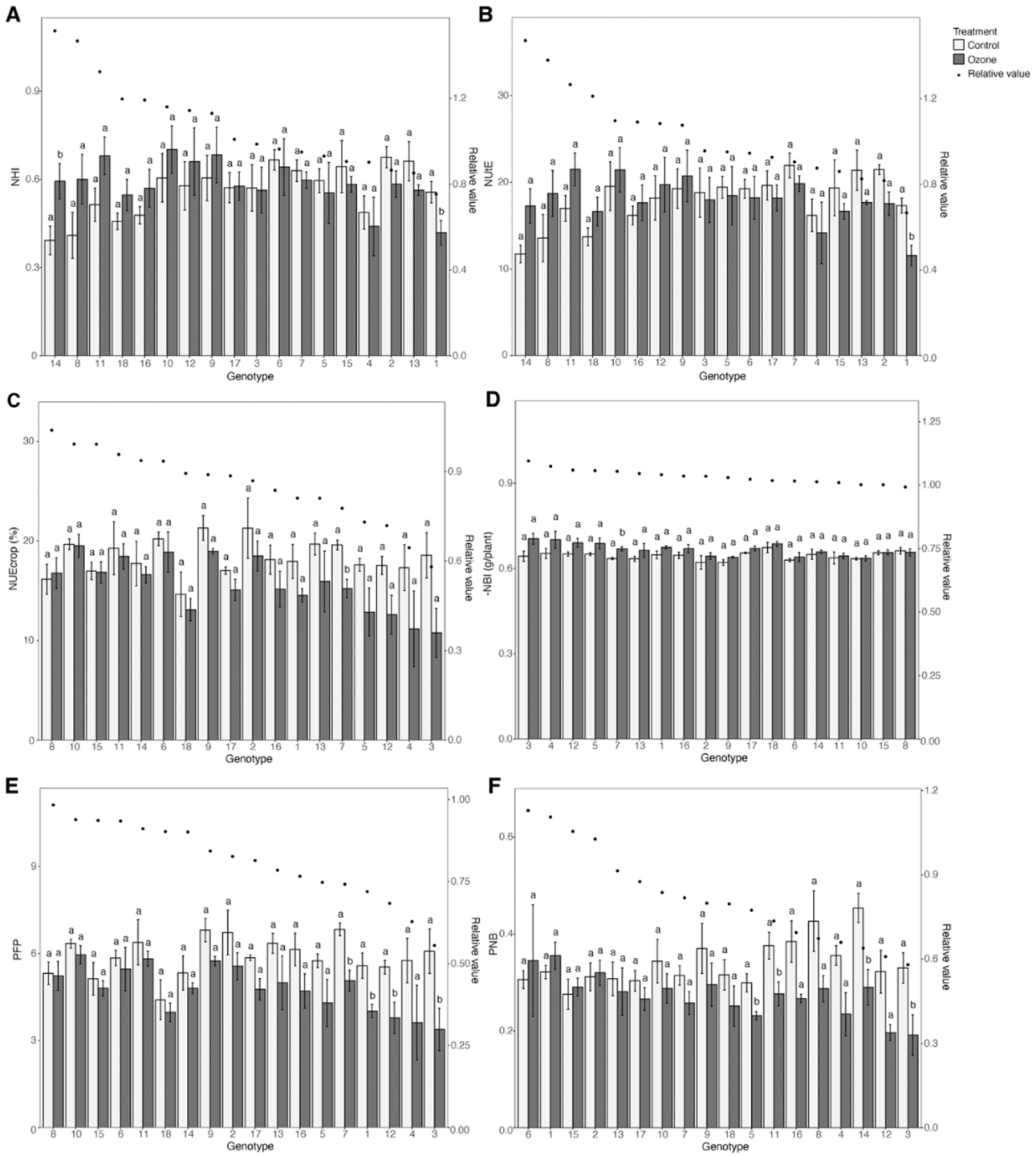

Fig. 3. N harvest index and different NUE indicators of different wheat genotypes under control and ozone treatments. Bars indicate mean values and standard errors (n = 4). A, N harvest index; B, N utilization efficiency; C, Crop N use efficiency; D, N balance intensity; E, Partial-factor productivity; F, Partial N balance. Bars not sharing the same superscript letters are significantly different at $P < 0.05$ within the genotypes by Student's *t* test.

under ozone exposure. To investigate the effects of ozone on NUE, relative differences between two treatments were analyzed for all NUE indicators to eliminate the potential effects of N inputs. Improving the economic part of crop production is an urgent issue for agricultural sustainability, while reduced NUE indicates that elevated ozone concentration significantly reduced the N uptake from soil by plant roots, increasing the risk of N leaching and its associated environmental impacts, such as eutrophication and nitrous oxide emissions (Salim and Raza, 2019).

Plants tend to maintain a balance of chemical elements in each organ for optimal growth and reproduction (Sterner and Elser, 2003; Yuan and Chen, 2015). Among these elements, C and N act as limiting elements in plant growth and are strongly coupled in their biochemical functions (Ågren, 2008). In this study, we attempted to understand the relationships between straw C:N and its associated traits and productivity. Significant regressions were observed between the straw C:N ratio and grain number and thousand kernel weight, although with a low R^2. Significant positive relationships between straw C:N ratio and total dry

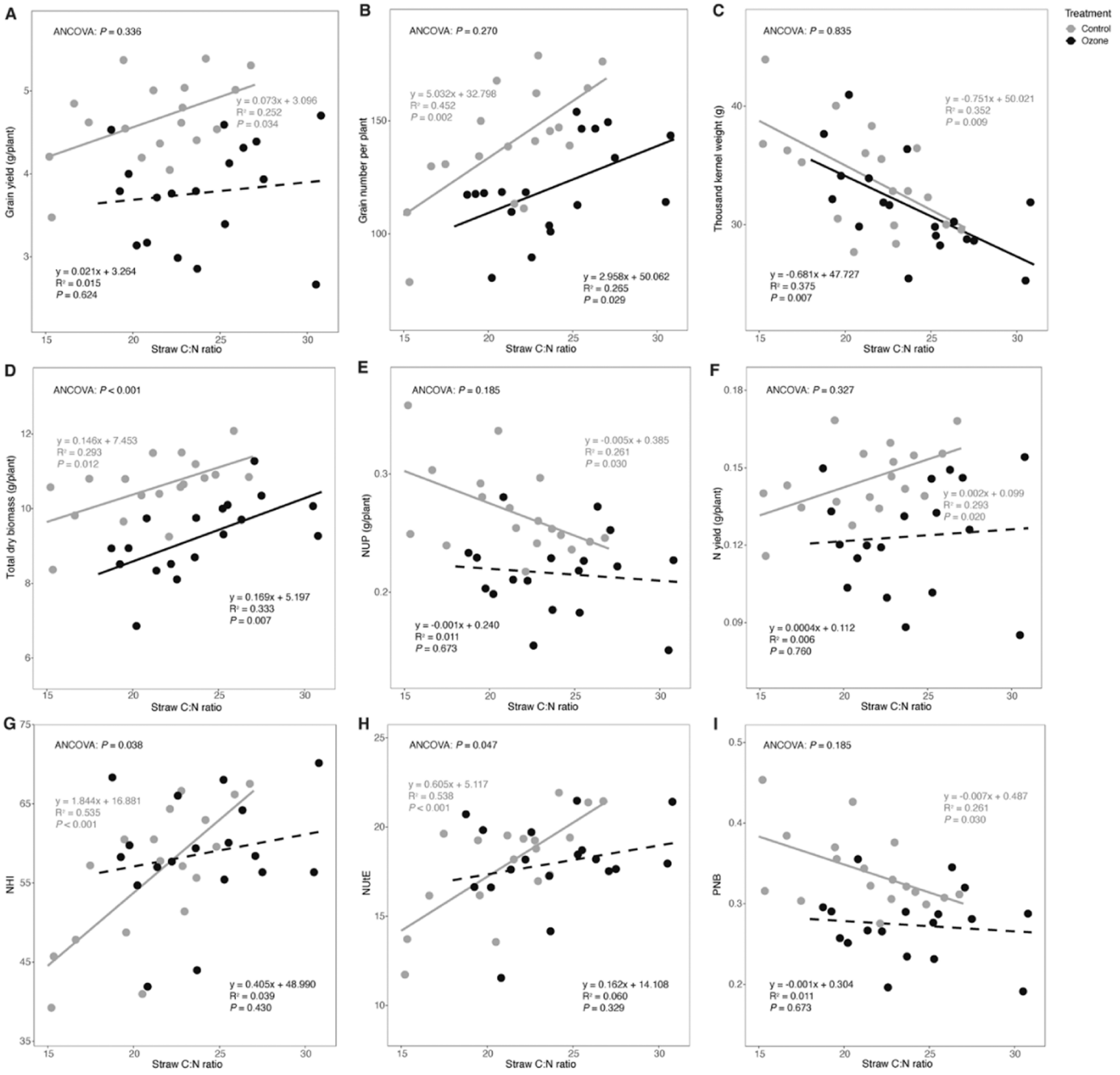

Fig. 4. Linear responses of the straw C:N ratio against different yield-related components and N uptake at harvest under control and ozone conditions. Solid and dashed lines represent significant and insignificant relationships, respectively. $P < 0.05$ in ANCOVA indicates a significant difference between regression slopes in control and ozone treatments (n = 18). The biomass and yield-related components were reported in our previous study (Feng et al., 2022a).

biomass were observed under control and ozone treatments, and the extreme significant differences of regressions between treatments indicated ozone effects on biomass and nutrient proportion in wheat. Elevated ozone concentration weakened the relationship between the straw C:N ratio and NUP, N yield, grain yield, NHI, NUtE and PNB, indicating that wheat stoichiometric coupling of C and N concentration in aboveground plants was fragile in the face of elevated ozone concentration. As shown by regression slopes with low R^2, straw C:N was not suitable for predicting yield-related parameters and N uptake at a certain fertilizer level in wheat. In maize, by comparing the nutrient allocation to different organs, significant regressions occurred between the root C:N ratio and kernel yield under ambient air and elevated ozone, suggesting that root C:N ratio close relates to maize productivity (Peng et al., 2021). The nutrient allocation pattern between above and belowground biomass is an important indicator of the whole plant responses to ozone exposure. Ozone stress inhibits root growth and biomass formation. If ozone-induced reductions in root biomass are greater than those in shoot in some species, the absorption and utilization of nutrients is reduced (Shang et al., 2017; Gu et al., 2023). Indeed, a close association between root growth and carbon transport to roots has been reported under elevated ozone (Topa et al., 2004). Further experiments are warranted to unravel the nutrient allocation and stoichiometry in different organs of wheat under ozone exposure.

Eighteen distinct genotypes performed differently in terms of N efficiency with a large range after long-term ozone fumigation. Among those, cultivar 8 “Jenga” exhibited optimal ozone tolerance with the

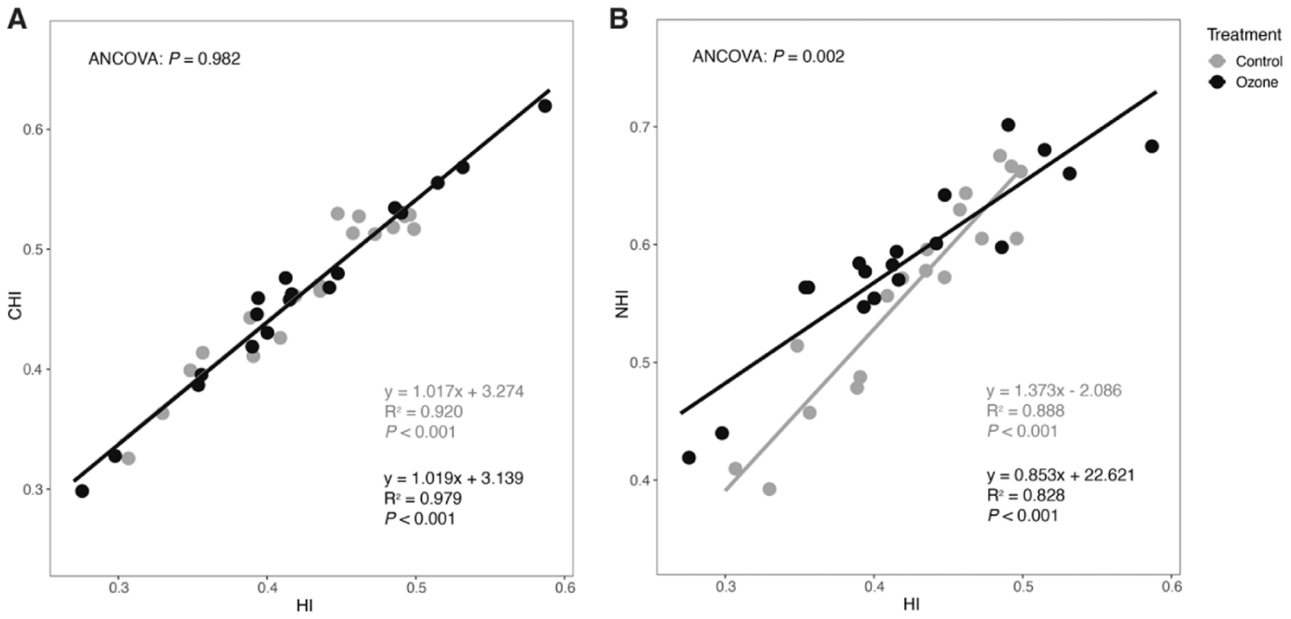

Fig. 5. Linear responses of the harvest index against the C harvest index (A) and N harvest index (B). Solid and dashed lines represent significant and insignificant relationships, respectively. $P < 0.05$ in ANCOVA indicates significantly different regression slopes between the control and ozone treatments (n = 18).

highest relative values of grain yield (Feng et al., 2022a) and different NUE indicators, including NUEcrop, NBI and PFP (Figs. 2 and 3). Previous studies found that ozone exposure not only resulted in reduction in the accumulation of carbohydrate in the shoot, but also the inhibition of photosynthate translocation from source to sink, such as roots and reproductive organs (Rai and Agrawal, 2012). The ozone effects on phloem transport out of leaves is possibly attributed to oxidative damage of the plasmalemma or plasmodesmata in mesophyll or phloem companion cell (Grantz and Farrar, 1999), which is in line with the physiological traits of this cultivar. Season-long ozone fumigation did not significantly affect the photosynthesis and membrane lipids of this cultivar (Feng et al., 2023), which might partly explain the effective production and translocation of carbohydrates and amino acids to grain. In addition, cultivars 10 and 15 could also be potential ozone tolerant cultivars due to high relative NUE.

In the interpretation of these results, we should consider that Free Air Concentration Enrichment (FACE) experiments are more realistic, but OTC system have the advantage of effective control of N fertilizer application to each plant. Considering that wheat had higher ozone sensitivity in field-based FACE-experiments than in OTCs (Feng et al., 2018b), experimental studies under field conditions are required for further validation of ozone-tolerant cultivar and exploration of tolerance mechanism in wheat.

5. Conclusions

Taken together, the straw C:N ratios, and C and N concentrations in grain were significantly influenced by ozone, and the N yield was also significantly decreased after long-term ozone fumigation compared to control condition. The weak relationships between the straw C:N ratio and productivity, especially under ozone treatment, suggest that straw C:N is not a suitable trait to indicate wheat productivity or N uptake. Furthermore, a significant reduction in the regression slope between HI and NHI was observed among all genotypes under ozone exposure in wheat. Consistent with this, NUE indicators indicating the N convention efficiency from vegetative to reproductive organs were significantly decreased by ozone in wheat apart from NUtE. The large variations in ozone responses of different genotypes provided a basis for selecting genotypes with higher NUE, with cultivar 8 “Jenga” showing optimal ozone tolerance that can help to mitigate the negative impacts of ozone-induced reduction in grain filling.

CRediT authorship contribution statement

Yanru Feng: Conceptualization, Investigation, Data curation, Writing – original draft. **Muhammad Shahedul Alam:** Methodology, Writing – review & editing. **Feng Yan:** Methodology, Software, Writing – review & editing. **Michael Frei:** Supervision, Conceptualization, Methodology, Writing – review & editing.

Declaration of Competing Interest

The authors declare that they have no known competing financial interests or personal relationships that could have appeared to influence the work reported in this paper.

Data Availability

Data will be made available on request.

Acknowledgments

The authors wish to thank the China Scholarship Council for providing a PhD fellowship to Yanru Feng (No. CSC201906300077).

Appendix A. Supporting information

Supplementary data associated with this article can be found in the online version at doi:10.1016/j.plantsci.2023.111924.

References

G.I. Ågren, Stoichiometry and nutrition of plant growth in natural communities, Annu. Rev. Ecol. Evol. Syst. 39 (2008) 153–170, https://doi.org/10.1146/annurev.ecolsys.39.110707.173515.

E.A. Ainsworth, Understanding and improving global crop response to ozone pollution, Plant J. 90 (2017) 886–897, https://doi.org/10.1111/tpj.13298.

S. Avnery, D.L. Mauzerall, A.M. Fiore, Increasing global agricultural production by reducing ozone damages via methane emission controls and ozone-resistant cultivar selection, Glob. Chang. Biol. 19 (2013) 1285–1299, https://doi.org/10.1111/gcb.12118.

J.P. Baresel, G. Zimmermann, H.J. Reents, Effects of genotype and environment on N uptake and N partition in organically grown winter wheat (Triticum aestivum L.) in Germany, Euphytica 163 (2008) 347–354, https://doi.org/10.1007/s10681-008-9718-1.

A.J. Barneix, Physiology and biochemistry of source-regulated protein accumulation in the wheat grain, J. Plant Physiol. 164 (2007) 581–590, https://doi.org/10.1016/j.jplph.2006.03.009.

H. Begum, M.S. Alam, Y. Feng, P. Koua, M. Ashrafuzzaman, A. Shrestha, M. Kamruzzaman, S. Dadshani, A. Ballvora, A.A. Naz, M. Frei, Genetic dissection of bread wheat diversity and identification of adaptive loci in response to elevated tropospheric ozone, Plant Cell Environ. 43 (2020) 2650–2665, https://doi.org/10.1111/pce.13864.

M.C. Broberg, Z. Feng, Y. Xin, H. Pleijel, Ozone effects on wheat grain quality - a summary, Environ. Pollut. 197 (2015) 203–213, https://doi.org/10.1016/j.envpol.2014.12.009.

M.C. Broberg, J. Uddling, G. Mills, H. Pleijel, Fertilizer efficiency in wheat is reduced by ozone pollution, Sci. Total Environ. 607–608 (2017) 876–880, https://doi.org/10.1016/j.scitotenv.2017.07.069.

M.C. Broberg, Y. Xu, Z. Feng, H. Pleijel, Harvest index and remobilization of 13 elements during wheat grain filling: experiences from ozone experiments in China and Sweden, Field Crops Res 271 (2021), 108259, https://doi.org/10.1016/j.fcr.2021.108259.

K.A. Congreves, O. Otchere, D. Ferland, S. Farzadfar, S. Williams, M.M. Arcand, Nitrogen use efficiency definitions of today and tomorrow, Front. Plant Sci. 12 (2021), 637108, https://doi.org/10.3389/fpls.2021.637108.

O.R. Cooper, D.D. Parrish, J. Ziemke, N.V. Balashov, M. Cupeiro, I.E. Galbally, S. Gilge, L. Horowitz, N.R. Jensen, J.F. Lamarque, V. Naik, S.J. Oltmans, J. Schwab, D. T. Shindell, A.M. Thompson, V. Thouret, Y. Wang, R.M. Zbinden, D. Helmig, P. Palmer, Global distribution and trends of tropospheric ozone: an observation-based review, Elem. Sci. Anth. 2 (2014), 000029, https://doi.org/10.12952/journal.elementa.000029.

Y. Duan, M. Xu, S. Gao, X. Yang, S. Huang, H. Liu, B. Wang, Nitrogen use efficiency in a wheat–corn cropping system from 15 years of manure and fertilizer applications, Field Crops Res 157 (2014) 47–56, https://doi.org/10.1016/j.fcr.2013.12.012.

J.J. Elser, W.F. Fagan, R.F. Denno, D.R. Dobberfuhl, A. Folarin, A. Huberty, S. Interlandi, S.S. Kilham, E. McCauley, K.L. Schulz, Nutritional constraints in terrestrial and freshwater food webs, Nature 408 (2000) 578–580, https://doi.org/10.1038/35046058.

Y. Feng, T.H. Nguyen, M.S. Alam, L. Emberson, T. Gaiser, F. Ewert, M. Frei, Identifying and modelling key physiological traits that confer tolerance or sensitivity to ozone in winter wheat, Environ. Pollut. 304 (2022a), 119251, https://doi.org/10.1016/j.envpol.2022.119251.

Y. Feng, L.-B. Wu, S. Autarmat, M.S. Alam, M. Frei, Characterization of candidate genes for ozone tolerance in winter wheat (Triticum aestivum L.) and associated physiological mechanisms, Environ. Exp. Bot. 211 (2023), https://doi.org/10.1016/j.envexpbot.2023.105368.

Z. Feng, V. Calatayud, J. Zhu, K. Kobayashi, Ozone exposure- and flux-based response relationships with photosynthesis of winter wheat under fully open air condition, Sci. Total Environ. 619–620 (2018a) 1538–1544, https://doi.org/10.1016/j.scitotenv.2017.10.089.

Z. Feng, K. Kobayashi, E.A. Ainsworth, Impact of elevated ozone concentration on growth, physiology, and yield of wheat (Triticum aestivum L.): a meta-analysis, Glob. Chang. Biol. 14 (2008) 2696–2708, https://doi.org/10.1111/j.1365-2486.2008.01673.x.

Z. Feng, J. Uddling, H. Tang, J. Zhu, K. Kobayashi, Comparison of crop yield sensitivity to ozone between open-top chamber and free-air experiments, Glob. Chang. Biol. 24 (2018b) 2231–2238, https://doi.org/10.1111/gcb.14077.

Z. Feng, Y. Xu, K. Kobayashi, L. Dai, T. Zhang, E. Agathokleous, V. Calatayud, E. Paoletti, A. Mukherjee, M. Agrawal, R.J. Park, Y.J. Oak, X. Yue, Ozone pollution threatens the production of major staple crops in East Asia, Nat. Food 3 (2022b) 47–56, https://doi.org/10.1038/s43016-021-00422-6.

M.D. Flowers, E.L. Fiscus, K.O. Burkey, F.L. Booker, J.-J.B. Dubois, Photosynthesis, chlorophyll fluorescence, and yield of snap bean (Phaseolus vulgaris L.) genotypes differing in sensitivity to ozone, Environ. Exp. Bot. 61 (2007) 190–198, https://doi.org/10.1016/j.envexpbot.2007.05.009.

J. Fuhrer, B. Lehnherr, P. Moeri, W. Tschannen, H. Shariat-Madari, Effects of ozone on the grain composition of spring wheat grown in open-top field chambers, Environ. Pollut. 65 (1990) 181–192, https://doi.org/10.1016/0269-7491(90)90183-D.

S. Gan, R.M. Amasino, Inhibition of leaf senescence by autoregulated production of cytokinin, Science 270 (1995) 1986–1988, https://doi.org/10.1126/science.270.5244.1986.

J. Gelang, H. Pleijel, E. Sild, H. Danielsson, S. Younis, G. Selldén, Rate and duration of grain filling in relation to flag leaf senescence and grain yield in spring wheat (Triticum aestivum) exposed to different concentrations of ozone, Physiol. Plant. 110 (2000) 366–375, https://doi.org/10.1111/j.1399-3054.2000.1100311.x.

A. Ghosh, M. Agrawal, S.B. Agrawal, Effect of water deficit stress on an Indian wheat cultivar (Triticum aestivum L. HD 2967) under ambient and elevated level of ozone, Sci. Total Environ. 714 (2020), 136837, https://doi.org/10.1016/j.scitotenv.2020.136837.

A. Grandjean, J. Fuhrer, Growth and leaf senescence in spring wheat (Triticum aestivum) grown at different ozone concentrations in open-top field chambers, Physiol. Plant. 77 (1989) 389–394, https://doi.org/10.1111/j.1399-3054.1989.tb05658.x.

D.A. Grantz, J.F. Farrar, Acute exposure to ozone inhibits rapid carbon translocation from source leaves of Pima cotton, J. Exp. Bot. 50 (1999) 1253–1262, https://doi.org/DOI 10.1093/jexbot/50.336.1253.

D.A. Grantz, J.F. Farrar, Ozone inhibits phloem loading from a transport pool: compartmental efflux analysis in Pima cotton, Funct. Plant Biol. 27 (2000) 859–868, https://doi.org/10.1071/PP99169.

X. Gu, T. Wang, C. Li, Elevated ozone decreases the multifunctionality of belowground ecosystems, Glob. Chang. Biol. 29 (2023) 890–908, https://doi.org/10.1111/gcb.16507.

H. Han, J. Liu, L. Shu, T. Wang, H. Yuan, Local and synoptic meteorological influences on daily variability in summertime surface ozone in eastern China, Atmos. Chem. Phys. 20 (2020) 203–222, https://doi.org/10.5194/acp-20-203-2020.

X. Lu, J. Hong, L. Zhang, O.R. Cooper, M.G. Schultz, X. Xu, T. Wang, M. Gao, Y. Zhao, Y. Zhang, Severe surface ozone pollution in China: a global perspective, Environ. Sci. Technol. Lett. 5 (2018) 487–494, https://doi.org/10.1021/acs.estlett.8b00366.

X. Luo, C. Ma, Y. Yue, K. Hu, Y. Li, Z. Duan, M. Wu, J. Tu, J. Shen, B. Yi, T. Fu, Unravelling the complex trait of harvest index in rapeseed (Brassica napus L.) with association mapping, BMC Genom. 16 (2015), 379, https://doi.org/10.1186/s12864-015-1607-0.

X. Lv, Y. Zhang, Y. Zhang, S. Fan, L. Kong, Source-sink modifications affect leaf senescence and grain mass in wheat as revealed by proteomic analysis, BMC Plant Biol. 20 (2020), 257, https://doi.org/10.1186/s12870-020-02447-8.

A. Maillard, S. Diquelou, V. Billard, P. Laine, M. Garnica, M. Prudent, J.M. Garcia-Mina, J.C. Yvin, A. Ourry, Leaf mineral nutrient remobilization during leaf senescence and modulation by nutrient deficiency, Front. Plant Sci. 6 (2015) 317, https://doi.org/10.3389/fpls.2015.00317.

R.A. Martinez-Feria, M.J. Castellano, R.N. Dietzel, M.J. Helmers, M. Liebman, I. Huber, S. V. Archontoulis, Linking crop- and soil-based approaches to evaluate system nitrogen-use efficiency and tradeoffs, Agric. Ecosyst. Environ. 256 (2018) 131–143, https://doi.org/10.1016/j.agee.2018.01.002.

U. Meyer, B. Kollner, J. Willenbrink, G.H.M. Krause, Physiological changes on agricultural crops induced by different ambient ozone exposure regimes: I. Effects on photosynthesis and assimilate allocation in spring wheat, N. Phytol. 136 (1997) 645–652, https://doi.org/10.1046/j.1469-8137.1997.00777.x.

G. Mills, A. Buse, B. Gimeno, V. Bermejo, M. Holland, L. Emberson, H. Pleijel, A synthesis of AOT40-based response functions and critical levels of ozone for agricultural and horticultural crops, Atmos. Environ. 41 (2007) 2630–2643, https://doi.org/10.1016/j.atmosenv.2006.11.016.

G. Mills, K. Sharps, D. Simpson, H. Pleijel, M. Frei, K. Burkey, L. Emberson, J. Uddling, M. Broberg, Z. Feng, K. Kobayashi, M. Agrawal, Closing the global ozone yield gap: quantification and cobenefits for multistress tolerance, Glob. Chang. Biol. 24 (2018) 4869–4893, https://doi.org/10.1111/gcb.14381.

P.S. Monks, A.T. Archibald, A. Colette, O. Cooper, M. Coyle, R. Derwent, D. Fowler, C. Granier, K.S. Law, G.E. Mills, D.S. Stevenson, O. Tarasova, V. Thouret, E. von Schneidemesser, R. Sommariva, O. Wild, M.L. Williams, Tropospheric ozone and its precursors from the urban to the global scale from air quality to short-lived climate forcer, Atmos. Chem. Phys. 15 (2015) 8889–8973, https://doi.org/10.5194/acp-15-8889-2015.

P.B. Morgan, E.A. Ainsworth, S.P. Long, How does elevated ozone impact soybean? A meta-analysis of photosynthesis, growth and yield, Plant Cell Environ. 26 (2003) 1317–1328, https://doi.org/10.1046/j.0016-8025.2003.01056.x.

A.S. Nehe, S. Misra, E.H. Murchie, K. Chinnathambi, B. Singh Tyagi, M.J. Foulkes, Nitrogen partitioning and remobilization in relation to leaf senescence, grain yield and protein concentration in Indian wheat cultivars, Field Crops Res 251 (2020), 107778, https://doi.org/10.1016/j.fcr.2020.107778.

J. Peng, Y. Xu, B. Shang, E. Agathokleous, Z. Feng, Effects of elevated ozone on maize under varying soil nitrogen levels: biomass, nitrogen and carbon, and their allocation to kernel, Sci. Total Environ. 765 (2021), 144332, https://doi.org/10.1016/j.scitotenv.2020.144332.

J. Peng, Y. Xu, B. Shang, L. Qu, Z. Feng, Impact of ozone pollution on nitrogen fertilization management during maize (Zea mays L.) production, Environ. Pollut. 266 (2020), 115158, https://doi.org/10.1016/j.envpol.2020.115158.

H. Pleijel, M.C. Broberg, J. Uddling, G. Mills, Current surface ozone concentrations significantly decrease wheat growth, yield and quality, Sci. Total Environ. 613–614 (2018) 687–692, https://doi.org/10.1016/j.scitotenv.2017.09.111.

H. Pleijel, H. Danielsson, J. Gelang, E. Sild, G. Selldén, Growth stage dependence of the grain yield response to ozone in spring wheat (Triticum aestivum L.), Agric. Ecosyst. Environ. 70 (1998) 61–68, https://doi.org/10.1016/S0167-8809(97)00167-9.

H. Pleijel, H. Danielsson, D. Simpson, G. Mills, Have ozone effects on carbon sequestration been overestimated? A new biomass response function for wheat, Biogeosciences 11 (2014) 4521–4528, https://doi.org/10.5194/bg-11-4521-2014.

H. Pleijel, K. Ojanperä, L. Mortensen, Effects of tropospheric ozone on the yield and grain protein content of spring wheat(Triticum aestivumL.) in the Nordic countries, Acta Agric. Scand. B Soil Plant Sci. 47 (1997) 20–25, https://doi.org/10.1080/09064719709362434.

H. Pleijel, J. Uddling, Yield vs. quality trade-offs for wheat in response to carbon dioxide and ozone, Glob. Chang. Biol. 18 (2012) 596–605, https://doi.org/10.1111/j.1365-2486.2011.2489.x.

N. Salim, A. Raza, Nutrient use efficiency (NUE) for sustainable wheat production: a review, J. Plant Nutr. 43 (2019) 297–315, https://doi.org/10.1080/01904167.2019.1676907.

B. Shang, Z. Feng, P. Li, X. Yuan, Y. Xu, V. Calatayud, Ozone exposure- and flux-based response relationships with photosynthesis, leaf morphology and biomass in two poplar clones, Sci. Total Environ. 603–604 (2017) 185–195, https://doi.org/10.1016/j.scitotenv.2017.06.083.

P. Sicard, A. Anav, A. De Marco, E. Paoletti, Projected global ground-level ozone impacts on vegetation under different emission and climate scenarios, Atmos. Chem. Phys. 17 (2017) 12177–12196, https://doi.org/10.5194/acp-17-12177-2017.

D. Simpson, A. Arneth, G. Mills, S. Solberg, J. Uddling, Ozone — the persistent menace: interactions with the N cycle and climate change, Curr. Opin. Environ. Sustain. 9–10 (2014) 9–19, https://doi.org/10.1016/j.cosust.2014.07.008.

Sterner, R.W., Elser, J.J., 2003. Ecological stoichiometry: the biology of elements from molecules to the biosphere. Princeton university press.

M.A. Topa, D.J. McDermitt, S.C. Yun, P.S. King, Do elevated ozone and variable light alter carbon transport to roots in sugar maple? N. Phytol. 162 (2004) 173–186, https://doi.org/10.1111/j.1469-8137.2004.01014.x.

R Core Team. A language and environment for statistical computing, R Foundation for Statistical Computing, Vienna, Austria, 2018.

R. Rai, M. Agrawal, Impact of tropospheric ozone on crop plants, Proc. Natl. Acad. Sci. India Sect. B Biol. Sci. 82 (2012) 241–257, https://doi.org/10.1007/s40011-012-0032-2.

A. Rivas-Ubach, J. Sardans, M. Perez-Trujillo, M. Estiarte, J. Penuelas, Strong relationship between elemental stoichiometry and metabolome in plants, Proc. Natl. Acad. Sci. USA 109 (2012) 4181–4186, https://doi.org/10.1073/pnas.1116092109.

E. Triboi, A.-M. Triboi-Blondel, Productivity and grain or seed composition: a new approach to an old problem, Eur. J. Agron. 16 (2002) 163–186, https://doi.org/10.1016/S1161-0301(01)00146-0.

W. Wang, D.D. Parrish, S. Wang, F. Bao, R. Ni, X. Li, S. Yang, H. Wang, Y. Cheng, H. Su, Long-term trend of ozone pollution in China during 2014–2020: distinct seasonal and spatial characteristics and ozone sensitivity, Atmos. Chem. Phys. 22 (2022) 8935–8949, https://doi.org/10.5194/acp-22-8935-2022.

Y. Wang, M. Frei, Stressed food – the impact of abiotic environmental stresses on crop quality, Agric. Ecosyst. Environ. 141 (2011) 271–286, https://doi.org/10.1016/j.agee.2011.03.017.

J. Wei, Z. Li, K. Li, R.R. Dickerson, R.T. Pinker, J. Wang, X. Liu, L. Sun, W. Xue, M. Cribb, Full-coverage mapping and spatiotemporal variations of ground-level ozone (O3) pollution from 2013 to 2020 across China, Remote Sens. Environ. 270 (2022), 112775, https://doi.org/10.1016/j.rse.2021.112775.

S. Wilkinson, G. Mills, R. Illidge, W.J. Davies, How is ozone pollution reducing our food supply? J. Exp. Bot. 63 (2012) 527–536, https://doi.org/10.1093/jxb/err317.

Z.Y. Yuan, H.Y.H. Chen, Decoupling of nitrogen and phosphorus in terrestrial plants associated with global changes, Nat. Clim. Change 5 (2015) 465–469, https://doi.org/10.1038/nclimate2549.

W. Zhang, G. Wang, X. Liu, Z. Feng, Effects of elevated O3 exposure on seed yield, N concentration and photosynthesis of nine soybean cultivars (Glycine max (L.) Merr.) in Northeast China, Plant Sci. 226 (2014) 172–181, https://doi.org/10.1016/j.plantsci.2014.04.020.

F. Zheng, X. Wang, W. Zhang, P. Hou, F. Lu, K. Du, Z. Sun, Effects of elevated O(3) exposure on nutrient elements and quality of winter wheat and rice grain in Yangtze River Delta, China, Environ. Pollut. 179 (2013) 19–26, https://doi.org/10.1016/j.envpol.2013.03.051.

Chapter 4: Characterization of candidate genes for ozone tolerance in winter wheat (*Triticum aestivum* L.) and associated physiological mechanisms

Manuscript published in Environmental and Experimental Botany 2023 Vol 211, 105368

Environmental and Experimental Botany 211 (2023) 105368

Contents lists available at ScienceDirect

Environmental and Experimental Botany

journal homepage: www.elsevier.com/locate/envexpbot

Characterization of candidate genes for ozone tolerance in winter wheat (*Triticum aestivum* L.) and associated physiological mechanisms

Yanru Feng [a,b], Lin-Bo Wu [a], Sawitree Autarmat [c], Muhammad Shahedul Alam [a], Michael Frei [a,*]

[a] Department of Agronomy and Crop Physiology, Institute of Agronomy and Plant Breeding I, Justus Liebig University Giessen, 35390 Giessen, Germany
[b] Institute of Crop Science and Resource Conservation (INRES), Crop Science, University of Bonn, 53115 Bonn, Germany
[c] School of Bioresources and Technology, King Mongkut's University of Technology Thonburi, Bangkok 10150, Thailand

ARTICLE INFO

Keywords:
Air pollution
Cereals
Food security
Global change
Crop breeding

ABSTRACT

Rising tropospheric ozone causes global yield reduction in wheat and therefore necessitates the breeding of ozone-resistant wheat varieties. The aim of this study was to explore contrasting physiological responses and characterize candidate genes for ozone tolerance in wheat identified in a genome-wide association study. Four wheat genotypes were grouped into tolerant and sensitive haplotypes according to their genetic backgrounds at ozone tolerant loci, and were investigated under season-long ozone fumigation in open-top chambers. Only sensitive haplotypes showed a significant decrease in net photosynthetic rate and a significant increase in lipid peroxidation indicating oxidative stress. Moreover, tolerant and sensitive haplotypes of wheat showed consistently contrasting antioxidant responses to ozone in terms of apoplastic ascorbate, ascorbate peroxidase and peroxidase activity. Candidate genes located within an ozone tolerant locus on chromosome 5A 592.04–593.33 Mb were analyzed through gene expression. The gene TraesCS5A01G400500 putatively involved in peroxidase activity was only upregulated in tolerant haplotypes. The differential regulation was consistent with sequence polymorphisms in the promoter region, where the cis-elements, EVENINGAT and PREATPRODH were only present in tolerant haplotypes. Based on the consistency of differential expression and sequence polymorphisms between tolerant and sensitive haplotypes, TraesCS5A01G400500 might explain contrasting physiological responses after ozone fumigation. This study demonstrated consistent transcriptional regulation, sequence polymorphisms in a candidate gene and physiological responses to ozone in different haplotypes, which represents a step forward in the understanding of the molecular mechanism underlying ozone tolerance in wheat.

1. Introduction

As a damaging environmental pollutant, tropospheric ozone (O_3) forms a major threat to global crop production and food security (Ainsworth, 2017; Ainsworth et al., 2012; Tai et al., 2014). It is produced by photochemical reactions involving sunlight and ozone precursor gases including nitrous oxides (NOx), volatile organic compounds (VOCs), carbon monoxide (CO) and methane (CH_4) (The Royal Society, 2008). While ozone precursor emissions are declining in Europe and North America, the trend is increasing in many Asian countries such as India and Bangladesh in the coming decades due to insufficient environmental legislation, rapid economic development and industrialization (Emberson et al., 2009; Granier et al., 2011; Mills et al., 2018b; Wild et al., 2012). As a powerful oxidant, ozone is absorbed into leaves via stomatal pores and degrades into reactive oxygen species (ROS), which subsequently trigger defense mechanisms and ultimately result in damage to crop productivity (Ainsworth, 2017). The detrimental effects of ozone exposure have been estimated to cause total global agricultural losses of $34 – $45 billion annually based on a modeling projection (Sampedro et al., 2020). In China, relative yield losses for wheat, rice, and corn reached 33 %, 23 %, and 9 %, respectively, making adaptation measures to cope with increased ozone levels urgent. (Feng et al., 2022b).

Wheat is a staple crop and contributes approximately 20 % of human dietary protein and calorie intake worldwide (Shiferaw et al., 2013). Tropospheric ozone causes multiple types of damage to wheat, such as foliar necrotic symptoms, limited carbon dioxide uptake by inducing partial stomatal closure or less efficient stomatal control, reduced photosynthesis capacity, loss of the activity of Calvin cycle enzymes such as Rubisco, and premature leaf senescence (Feng et al., 2008; Nie et al.,

* Corresponding author.
E-mail address: michael.frei@agrar.uni-giessen.de (M. Frei).

https://doi.org/10.1016/j.envexpbot.2023.105368
Received 17 February 2023; Received in revised form 18 April 2023; Accepted 5 May 2023
Available online 8 May 2023

1993). In addition, ozone exposure causes oxidative stress and impacts enzymatic and non-enzymatic antioxidant metabolism in wheat foliar tissues, including ascorbic acid, and peroxidase activity (Feng et al., 2016; Yadav et al., 2019). Consequently, those effects lead to wheat yield losses and changes in grain quality (Broberg et al., 2015; Pleijel et al., 2018; Pleijel et al., 1997). Over 2010–2012, wheat production was greatly reduced by a mean of 9.9 % in the Northern Hemisphere and 6.2 % in the Southern Hemisphere (Mills et al., 2018a). In China, yield losses in wheat were particularly high ranging between 28 % and 37 % from 2017 to 2019 leading to substantial economic losses, which will be exacerbated in the near future due to further increases in ozone levels (Ainsworth et al., 2008; Feng et al., 2022b). By 2030, the global losses of wheat production may reach 25.8 %, particularly in South and East Asia, at 44.4 % and 25.7 % respectively (Avnery et al., 2011). With the growing demand for food imposed by continuing population growth (Godfray et al., 2010), it is essential to explore ozone tolerance and breeding options in wheat to safeguard food supply and security on a global scale.

Previous research with different wheat varieties reported large genetic variations in wheat responses to ozone exposure. For instance, a comparative study demonstrated that modern wheat varieties with high yield tend to be more sensitive to ozone than primitive cultivated wheat, largely due to higher stomatal conductance (Biswas et al., 2008a). Two winter wheat varieties grown under fully open-air field conditions showed differential responses in physiological traits such as gas exchange rates, chlorophyll a fluorescence, lipid oxidation and ascorbate in the apoplast and leaf tissue (Feng et al., 2011; Feng et al., 2010). In addition, antioxidant enzymes such as superoxide dismutase (SOD), peroxidase (POX), glutathione reductase (GR) and guaiacol peroxidase were associated with varying levels of sensitivity against elevated ozone in different wheat cultivars (Fatima et al., 2018). A recent study identified large genotypic variation in average yield loss ranging from 2.7 % to 44.6 % among 18 contrasting wheat cultivars under ozone treatment (Feng et al., 2022a). Those extensive genetic variations in response to elevated ozone provide breeding potential for tolerant wheat varieties. However, in contrast to the advances in molecular breeding for ozone tolerance in rice (Chen et al., 2011; Frei et al., 2010; Frei et al., 2008; Ueda et al., 2015a; Ueda et al., 2015b), only a few studies have attempted to dissect and exploit the genetic variability for breeding ozone tolerance in wheat. Chromosome 7A was previously identified as a major contributor to tolerance to ozone injury in 'Chinese Spring' based on monosomic lines (Mashaheet et al., 2019). We previously conducted a genome-wide association study (GWAS) using a diverse panel of 150 wheat accessions genotyped by 13,006 single nucleotide polymorphism (SNP) markers and dissected the adaptive genetic architecture of ozone tolerance using ozone-responsive traits. Significant marker—trait associations were identified for the leaf bronzing score (LBS) on chromosome 5A and for vegetation indices (NDVI and Lic2) on chromosomes 6B and 6D. Genetic markers located within the identified genomic region were used to form haplotypes representing groups of genotypes within the population that differed significantly in ozone tolerance. Among the observed traits, LBS showed the highest heritability. Within the locus associated with LBS formation under ozone stress, eleven candidate genes were identified to be involved in the redox biology of plants and could underline symptom formation at elevated ozone (Begum et al., 2020). However, the effective use of such candidate genes in the breeding of ozone-tolerant wheat requires further characterization of sequence polymorphisms, transcriptional or translational regulation, and their physiological role in ozone tolerance.

This study represents an in-depth investigation aimed at understanding the molecular and physiological mechanisms based on the different responses to elevated ozone in contrasting haplotypes for gene markers associated with LBS (two ozone-sensitive genotypes and two ozone-tolerant genotypes). Two specific hypotheses were investigated: (1) Different genotypes representing either tolerant or sensitive haplotypes of wheat will show consistent physiological responses to ozone that are linked to their genetic constitution. (2) Among the candidate genes located within a previously identified locus on chromosome 5A, genes showing consistent differential expression and/or sequence polymorphisms between tolerant and sensitive haplotypes may confer ozone tolerance in wheat. This will be an important next step in identifying target genes for the improvement of ozone tolerance in wheat.

2. Materials and methods

2.1. Plant materials and ozone treatment

Four different wheat genotypes were selected from a population of 150 diverse wheat accessions that had previously been screened for ozone tolerance in a GWAS (Begum et al., 2020). They represented two different haplotypes with respect to SNP markers located within a locus significantly associated with LBS. This locus was located on chromosome 5A (592.04–593.33 Mb) and defined by ten SNP markers forming a linkage disequilibrium (LD) block. Two contrasting haplotypes, i.e., ATAGCACCTC (tolerant) and GGGATGTTCA (sensitive), showed significantly different LBS in ozone treatment (Begum et al., 2020). For the current study, we selected two genotypes Cubus (T1) and Jenga (T2) representing the tolerant haplotype ATAGCACCTC, and Solstice (S1) and Highbury (S2) representing the sensitive haplotype GGGATGTTCA (Supplementary Table S1).

In both experiments, seeds were germinated in quickpots for one week in the greenhouse. After five-weeks of vernalization at 4 °C, seedlings were evenly transplanted into eight open-top chambers (OTCs). These chambers were randomly assigned to control and ozone treatments with four replicates. A minimum photosynthetically active radiation (PAR) of 400 μmol m^{-2} s^{-1} for 12 h daytime (8.00 h − 20.00 h) was ensured by natural and artificial light.

Ozone was generated by custom-made ozone generators (UB 01; Gemke Technik GmbH, Ennepetal, Germany) using dried air passing silica desiccant. The generated ozone was percolated through water to remove nitrogen oxides and then blown through a fan connected with a central pipe into perforated plastic pipes above each open top chamber. The ozone output was regulated in real time by an ozone monitor (K 100 W; Dr. A. Kuntze GmbH, Meerbusch, Germany) with an ozone sensor (GE 760 O3; Dr. A. Kuntze GmbH) placed inside the fumigation chambers. In addition, the ozone concentration in different chambers was detected and recorded independently by handheld ozone monitors (series 500; Aeroqual Ltd, Auckland, New Zealand) at 5-min intervals, and downloaded once a week. The target ozone concentration was set to 70 ppb for 7 h (9.00–16.00 h) every day to induce chronic stress, which is comparable to the ambient levels in many Asian countries (Frei, 2015; Ashrafuzzaman et al., 2017). Acute fumigation aimed at 150 ppb was also applied at intervals during the fumigation period to simulate peak ozone episodes. It has been reported that the co-occurrence of high precursor emissions and meteorological conditions favoring ozone formation can lead to peak ozone episodes between 100 and 200 ppb temporarily (The Royal Society, 2008). In each experiment there were four chambers for the ozone treatment and four identical control chambers without ozone.

2.1.1. Experiment 1

Experiment 1 was conducted from December 2019 to July 2020 at the University of Bonn, Germany, and employed season-long ozone exposure. For each cultivar, a total of 40 seedlings were transplanted into pots (Dimensions 25 cm × 25 cm × 25 cm) with five plants inside, and they were randomly assigned to eight chambers (length 2.6 m, width 2.1 m, height 1.7 m). The measured average ozone concentration in the ozone chambers was 70.3 ppb ± 21.0 SD (standard deviation) whereas the average concentration in the control chambers was 27.8 ppb ± 6.1 SD. In addition, acute fumigation was applied at week 8, 10 and 13 after transplanting with an average concentration of 151.4 ppb ± 27.4 SD. The average temperature of the greenhouse was 23.7/17.0 °C

(day/night), and the average relative humidity was 46.7 %. Gene expression analysis and biochemical analyses except for apoplastic ascorbic acid (AsA) were conducted in this experiment. The second youngest fully expanded leaves were harvested at DAT35 (35 days after transplanting) and DAT110. Plant materials were flash frozen in liquid nitrogen and then stored at − 80 °C until analysis. LBS data for four fully expanded leaves on DAT99 were derived from Feng et al. (2022a).

2.1.2. Experiment 2

Experiment 2 was conducted from March to August 2022 at the University of Giessen, Germany. Seedlings were transferred into a greenhouse after vernalization in a climate chamber and single seedlings were transplanted into pots (Dimensions 13 cm × 13 cm × 13 cm). Eight plants were placed in each chamber (length 1.0 m, width 1.0 m, height 1.25 m) with two replicates for each genotype. The average ozone concentration was 74.7 ppb ± 22.0 SD for the ozone chambers and 30.2 ppb ± 10.8 SD for the control chambers. Acute ozone stress at a concentration of 148.5 ppb ± 31.3 SD was applied at weeks 3, 5, 7 and 11 after transplanting. The temperature of the greenhouse was set to 15/10 °C (day/night), and the average relative humidity was 52.8 %. Determination of apoplastic AsA, gas exchange and chlorophyll fluorescence measurements were conducted in this experiment.

2.2. Gas exchange and chlorophyll fluorescence measurement

Gas exchange and chlorophyll fluorescence were measured on the second youngest fully expanded leaf on each plant at DAT77. Net carbon assimilation rate (A), stomatal conductance (g_s), intercellular CO_2 concentration (Ci) and transpiration (E) were measured with an LI-6800 portable photosynthetic system (LI-COR, Inc., Lincoln, Nebraska, USA). The leaves were measured under a constant PPFD of 400 µmol photons m^{-2} s^{-1}, CO_2 reference value of 400 ppm, leaf temperature of 23 °C, relative humidity of 60 % and flow rate at 300 µmol/s. The quantum efficiency of photosystem II (PhiPS2) was measured using an LI-600 Porometer (LI-COR, Inc., Lincoln, Nebraska, USA), and was calculated as PhiPS2 = (Fm' - Fs)/Fm' where Fm' is the maximal fluorescence under actinic light and Fs is the steady-state terminal fluorescence.

2.3. Gene expression and sequence analysis

Total RNA of leaves at DAT110 was extracted by using the PeqGOLD Plant RNA Kit (Peqlab, Erlangen, Germany) and subsequently treated with RQ1 RNase-Free DNase (Promega, Manheim, Germany) to remove genomic DNA. The integrity of RNA was checked by denaturing formaldehyde agarose gel electrophoresis, and the concentration of RNA was determined by a NanoDrop OneC (Thermo Fisher Scientific, Braunschweig, Germany). Five hundred nanograms of total RNA was reverse transcribed with GoScriptTM Reverse Transcriptase (Promega). Quantitative real-time PCR (qRT—PCR) was conducted with GoTaq qPCR Master Mix (Promega) by using the delta-delta CT quantification method, which was performed with a StepOnePlus real-time PCR system (Applied Biosystems, Foster City, CA, USA). The reaction mixture consisted of 5 µL of GoTaq qPCR Master Mix, 0.2 µL of each gene-specific primer (10 µM; Supplementary Table S2), 3.6 µL of nuclease-free water and 1 µLof cDNA sample. The reaction conditions were set up as follows: an initial denaturation step (10 min, 95 °C) followed by 40 cycles of denaturation (15 s, 95 °C) and annealing/extension (1 min, 60 °C). The amplification efficiency of all primers in this study was tested with serial dilutions of cDNA templates and was always > 80 %.

Genomic DNA was isolated by a DNeasy Plant Mini Kit (QIAGEN, Hilden, Germany). Gene TraesCS5A01G400500 was PCR-cloned using Q5® High-Fidelity 2X Master Mix (NEB, Frankfurt am Main, Germany) following the manufacturers' instructions: initial denaturation (98 °C, 30 s), 35 cycles of reaction (98 °C, 10 s; 66 °C 20 s; 72 °C, 2 min 15 s) and final extension (72 °C, 2 min). PCR amplicons were purified using NucleoSpin Gel and PCR Clean-up kits (Macherey-Nagel, Düren, Germany). The zero Blunt™ TOPO™ PCR Cloning Kit (Invitrogen, Carlsbad, CA, USA) was used for gene sequencing. Chromatograms were analyzed with SnapGene Viewer (CSL Biotech LLC, San Diego, CA, USA). Protein motifs were searched through the Interpro database (http://www.ebi.ac.uk/interpro/).

2.4. Biochemical analyses

2.4.1. Malondialdehyde assay

Malondialdehyde (MDA) was determined at DAT35 and DAT110 as described previously (Höller et al., 2014; Alam et al., 2022). Approximately 100 mg of ground tissues was extracted with 1.5 mL of 0.1 % (w/v) trichloroacetic acid (TCA) and then centrifuged at 14,000 *g* and 4 °C for 15 min. One aliquot from the supernatants was mixed with a reaction solution of 0.01 % (w/v) 2,6-di-tert-butyl-4-methylphenol (BHT) dissolved in 20 % (w/v) TCA, and another aliquot contained 0.65 % 2-thiobarbituric acid (TBA). The mixture was incubated at 95 °C for 30 min and then centrifuged at 8000 g for 10 min at 4 °C. Blank samples were also prepared with 0.1 % (w/v) TCA solution substituted for the sample supernatant. Absorbance was measured at 440, 532 and 600 nm with an Infinite M Plex microplate reader (TECAN, Männerdorf, Switzerland).

2.4.2. Proline assay

The proline concentration was determined in lyophilized leaf tissues at DAT35 and DAT110 following Bates et al. (1973) with slight modification. Approximately 50 mg samples were immersed in 1.5 mL 3 % sulphosalicyclic acid, and after vortexing vigorously, the mixture was centrifuged at 12,000 g for 10 min at 4 °C. The test tubes included 500 µL supernatant extract, 500 µL acetic acid and 500 µL ninhydrin reagent were incubated at 100 °C for 60 min before the reaction was terminated on ice. Then 1.5 mL toluene was added into each test tube with mix, and the solution was kept at room temperature for 30 min until the chromophore was separated. The absorbance of the toluene phase was measured at 520 nm, and proline concentrations of leaf tissues were calculated based on a standard proline curve.

2.4.3. Ascorbic acid measurement

Reduced and oxidized AsA from the apoplast and leaf tissue were extracted at DAT35 and DAT110, DAT44 and DAT77, respectively, and quantified by a spectrophotometric method described previously (Gillespie and Ainsworth, 2007; Wu et al., 2017). The absorption of reduced AsA decreased at 265 nm after the addition of 0.1 U ascorbate oxidase (AO) dissolved in 0.1 M potassium phosphate buffer (pH 7.0) to a mixture consisting of of 10 µL of extract and 90 µL of 0.1 M potassium phosphate buffer (pH 7.0). For the measurement of oxidized AsA, the absorption was increased at 265 nm after adding 10 µL of 4 mM dithiothreitol (DTT) to a mixture of 10 µL of sample extract and 0.1 M potassium phosphate buffer (pH 7.8). Absorbance was read using an Infinite M Plex microplate reader in UV-transparent 96-well microplates (UV-Star, Greiner-Bio One, Germany) until the reactions were completed. An extinction coefficient of 14.3 mM^{-1} cm^{-1} for reduced AsA at 265 nm was used for calculation of AsA content. Total AsA was calculated as the sum of reduced and oxidized AsA. The redox state of AsA was calculated as the percentage of reduced AsA in total AsA.

2.4.4. Enzyme activity assays

Ascorbate peroxidase (APX) activity and monodehydroascorbate reductase (MDHAR) activity were measured at DAT35 and DAT110, using the same sample extract treated with 50 mM K-phosphate buffer (pH 7.8) containing 1 mM EDTA and 1 mM AsA (Wu et al., 2021). Approximately 100 mg of ground leaf material was dissolved in 1 mL of extracting buffer and the mixture was centrifuged at 10,000 g for 30 mins at 4 °C. The reaction mixture for APX activity contained 80 µL of 100 mM potassium phosphate buffer (pH 6.8) with 0.6 mM AsA, 10 µL of

0.03 % H_2O_2 and 10 μL of sample extract, which was monitored at 290 nm for 30 s (ε = 2.8 mM^{-1} cm^{-1}). For determination of MDHAR activity, the reaction mixture consisted of 50 mM Tris–HCl buffer (pH 7.6), 0.1 mM nicotinamide adenine dinucleotide (NADH), 2.5 mM AsA, 0.1 U of AO and 10 μL of plant extract. MDHAR activity was determined by monitoring the oxidation of NADH at 340 nm for 3 min (ε = 6.2 mM^{-1} cm^{-1}).

Peroxidase activity was measured at DAT35 and DAT110 according to Lin and Kao (1999). Approximately 100 mg sample was immersed in 1.5 mL of 50 mM phosphate buffer (pH 7.0) and centrifuged at 15,000 g for 15 min at 4 °C. The reaction mixture was 50 mM phosphate buffer (pH 7.0) containing 4 mM guaiacol and 10 mM H_2O_2. Peroxidase activity was determined at 470 nm immediately for 3 min.

Ascorbate oxidase (AO) activity was determined according to Wu et al. (2021). Approximately 80 mg of leaf sample was mixed with 1 mL of 100 mM sodium phosphate buffer (pH 6.5) and then centrifuged at 10,000 g for 20 min at 4 °C. The assay mixture consisted of 80 μL of 100 mM sodium phosphate buffer (pH 5.6), 10 μL of sample extract and 10 μL of 2 mM reduced AsA. The kinetics were measured at a wavelength of 265 nm for 15 min (ε = 14.3 mM^{-1} cm^{-1}). The ionically bound AO activities were determined by mixing 1 mL of 100 mM sodium phosphate buffer (pH 6.5) with 1 M NaCl.

Dehydroascorbate reductase (DHAR) activity was measured at DAT35 and DAT110, according to Wu et al. (2021). Around 100 mg samples were immersed in 1 mL of 50 mM Tris-HCl buffer (pH 7.4) containing 100 mM NaCl, 2 mM EDTA and 1 mM $MgCl_2$. The mixture was centrifuged at 13,000 g for 10 min at 4 °C. The assay mixture contained 70 μL of 50 mM potassium phosphate buffer (pH 6.5), 10 μL of sample extracts, 10 μL of 5 mM dehydroascorbic acid (DHA) and 50 mM reduced glutathione (GSH). The kinetics was at 265 nm for 10 min (ε = 14.3 mM^{-1} cm^{-1}). For all enzyme activity determinations, the protein concentrations of the extracts were measured with Bradford reagent at 595 nm (Bradford, 1976). All biochemical analysis were conducted when plants were in the booting/ear emergence stage and ripening stage.

2.5. Statistical analysis

Analysis of variance (ANOVA) was performed in a mixed linear model with chambers as a random effect, and treatment, cultivar and sampling date as fixed effects by the packages "nlme" and "emmeans" in R (R Core Team, 2018). Pairwise comparisons were conducted to evaluate the responses of individual genotypes to ozone stress. Relative values (ratio of value for plants grown under ozone treatment relative to control condition) were calculated for photosynthetic parameters and biochemical analyses for all genotypes.

3. Results

3.1. Leaf bronzing score and malondialdehyde assay

After long-term ozone fumigation, visible symptoms were scored on four fully expanded leaves based on previous studies (Begum et al., 2020). Sensitive haplotypes S1 and S2 showed significantly higher LBS than T1 and T2 at DAT99, confirming their susceptibility to ozone (Fig. 1A; Table 1). MDA is considered an indicator of oxidative stress preceding symptom formation (Höller et al., 2014). In this study, a significant haplotype, treatment and DAT interaction effect was observed in the MDA content (Table 1). The MDA content in the ozone treatment increased among all genotypes at DAT110, but statistically significant increases were observed only in the sensitive genotypes S1 and S2 after long-term ozone treatment, and the MDA content at DAT110 increased by 39.0 % and 48.9 %, respectively, while T1 and T2 did not respond significantly to ozone on either sampling date (Fig. 1B).

3.2. Gas exchange and chlorophyll fluorescence measurement

The impact of ozone on photosynthesis was studied by gas exchange and chlorophyll fluorescence analysis. Stomatal conductance, intercellular CO_2 and transpiration in both haplotypes were strongly inhibited by ozone treatment, but there was no significant difference between tolerant and sensitive haplotypes (Figs. 2B, 2C; Table 1). In this study, a significant haplotype and treatment interaction effect was observed, and the net photosynthetic rate in tolerant haplotypes under ozone stress was higher than that in sensitive haplotypes after long-term ozone fumigation. Both sensitive genotypes significantly declined compared with the control condition at DAT77, and decreased by 18.9 % and 17.4 %, respectively (Fig. 2A; Table 1). In addition, the photosystem II efficiency was significantly reduced by ozone treatment only in sensitive haplotypes compared to control conditions and decreased by an average of 10.8 % and 10.0 %, respectively (Fig. 2D; Table 1). In summary, S1 and S2 showed more sensitivity to ozone stress than T1 and T2 in terms of photosynthetic activities.

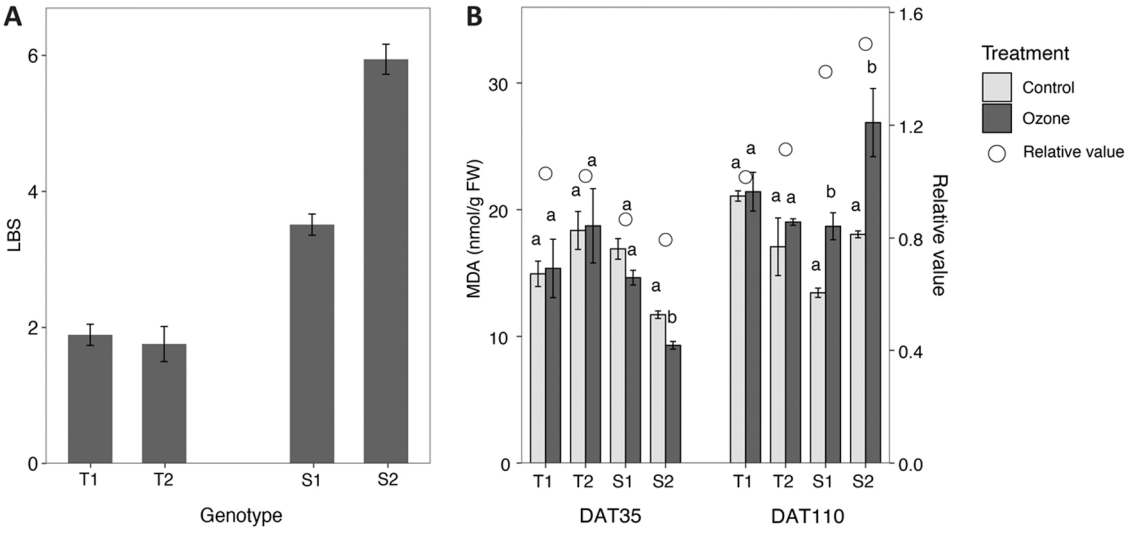

Fig. 1. Leaf bronzing score at 99 days after transplanting and MDA (Malondialdehyde) at 35 and 110 days after transplanting. Bars indicate mean values and standard errors (n = 4). A, LBS B, MDA. Bars not sharing the same superscript letters are significantly different at P < 0.05 within the genotypes (Student's *t* test).

Table 1
Descriptive statistics and ANOVA results of physiological and biochemical analyses from different wheat haplotypes exposed to control and ozone conditions.

Trait	Date	Mean (SE)				ANOVA						
		Control		Ozone		O	H	DAT	O×H	O×DAT	H×DAT	O×H×DAT
		T	S	T	S							
LBS	DAT99	0.00	0.00	1.69 (0.13)	4.38 (0.11)	<0.0001	<0.0001		<0.0001			
MDA (nmol/g FW)	DAT35	17.22 (1.22)	14.68 (1.14)	17.05 (1.83)	11.08 (1.15)	0.1245	0.0537	0.0001	0.3934	0.0034	0.0504	0.0278
	DAT110	18.79 (1.47)	15.75 (0.90)	20.22 (0.85)	22.78 (2.05)							
A (μmol m-2 s-1)	DAT77	13.44 (0.34)	13.54 (0.22)	12.85 (0.43)	11.12 (0.40)	0.0061	0.0299		0.0202			
gs (mmol m-2 s-1)	DAT77	273.93 (14.17)	288.75 (17.67)	134 (15.03)	118.05 (12.55)	<0.0001	0.9407		0.3168			
Ci (μmol mol-1)	DAT77	365.18 (1.54)	363.69 (1.71)	334.18 (4.53)	338.46 (4.46)	0.0007	0.7529		0.3419			
E (mmol m-2 s-1)	DAT77	3.88 (0.17)	3.45 (0.42)	2.04 (0.21)	1.93 (0.20)	0.0017	0.2851		0.5314			
PhiPS2	DAT77	0.67 (0.02)	0.70 (0.01)	0.64 (0.02)	0.63 (0.01)	0.0450	0.4346		0.1393			
Proline content (μg/g FW)	DAT35	45.72 (5.55)	44.96 (4.50)	45.62 (6.456)	47.51 (4.14)	0.0349	0.4384	<0.0001	0.0033	0.0149	0.7622	0.0059
	DAT110	202.78 (28.32)	124.23 (28.51)	74.13 (8.61)	136.62 (24.72)							
Apoplastic reduced AsA (nmol/g FW)	DAT42	28.60 (3.84)	38.96 (1.54)	41.06 (5.90)	22.34 (4.62)	0.7622	0.0055	0.0001	0.0001	0.6520	0.1762	0.1061
	DAT77	23.15 (1.12)	20.41 (2.86)	31.14 (1.03)	14.39 (2.37)							
Apoplastic total AsA (nmol/g FW)	DAT42	37.27 (5.03)	69.50 (5.30)	62.00 (8.20)	49.27 (12.73)	0.1543	0.6537	<0.0001	0.0062	0.5796	0.0406	0.0346
	DAT77	29.83 (1.91)	27.13 (2.45)	41.60 (2.83)	30.35 (4.47)							
Apoplastic AsA redox state (%)	DAT42	77.13 (3.46)	56.55 (2.22)	66.04 (2.57)	49.68 (7.30)	0.0083	<0.0001	0.0417	0.0791	0.4031	0.6254	0.0316
	DAT77	78.31 (3.25)	74.37 (5.72)	75.53 (2.50)	47.36 (5.41)							
Reduced AsA (μmol/g FW)	DAT35	3.29 (0.24)	3.89 (0.22)	3.6 (0.14)	3.41 (0.23)	0.5763	0.9670	<0.0001	0.5709	0.5891	0.1156	0.0125
	DAT110	2.99 (0.14)	2.51 (0.09)	2.74 (0.11)	2.78 (0.15)							
Total AsA (μmol/g FW)	DAT35	3.67 (0.28)	4.34 (0.21)	4.09 (0.14)	3.70 (0.24)	0.4645	0.6909	<0.0001	0.3366	0.5911	0.1654	0.0052
	DAT110	3.28 (0.16)	2.71 (0.08)	3.00 (0.10)	3.00 (0.18)							
AsA redox state (%)	DAT35	89.82 (0.37)	89.63 (1.36)	87.98 (2.73)	92.28 (1.87)	0.4908	0.1072	0.1408	0.1553	0.9773	0.6402	0.4334
	DAT110	91.06 (1.22)	91.55 (0.96)	90.91 (0.85)	92.8 (1.25)							
APX activity (μmol//min/mg protein)	DAT35	690.23 (48.71)	632.98 (81.04)	580.38 (36.14)	717.67 (69.53)	0.4253	0.0004	0.5371	0.0100	0.0637	0.0235	0.8760
	DAT110	543.27 (24.98)	647.48 (42.27)	553.65 (55.93)	901.41 (78.91)							
Peroxidase activity (nmol/min/mg protein)	DAT35	367.46 (16.83)	489.35 (23.76)	332.51 (30.27)	408.26 (21.48)	0.1265	<0.0001	<0.0001	0.3537	0.8277	0.8675	0.0685
	DAT110	606.94 (9.34)	661.39 (44.72)	480.97 (20.16)	656.58 (45.64)							
AO activity (nmol/min/mg protein)	DAT35	1.59 (0.05)	1.23 (0.21)	1.58 (0.09)	1.62 (0.27)	0.0254	0.1488	<0.0001	0.0281	0.495	0.0048	0.6971
	DAT110	2.16 (0.19)	2.45 (0.04)	2.18 (0.01)	3.06 (0.23)							
DHAR activity (nmol/min/mg protein)	DAT35	141.48 (6.91)	164.65 (4.52)	139.4 (11.24)	149.16 (7.05)	0.1463	0.6081	<0.0001	0.4746	0.3195	0.0783	0.6932
	DAT110	197.48 (13.13)	192.11 (8.79)	177.88 (10.42)	169.54 (7.88)							
MDHAR activity (nmol/min/mg protein)	DAT35	126.19 (13.99)	128.03 (4.14)	97.62 (7.10)	125.22 (16.04)	0.9414	0.0558	0.0009	0.1509	0.0686	0.8467	0.7550
	DAT110	135.16 (7.26)	138.58 (9.86)	138.01 (7.91)	155.53 (8.65)							

Note: Mean values of different haplotypes are shown.
Abbreviations: DAT: days after transplanting; H: haplotype; O: treatment.

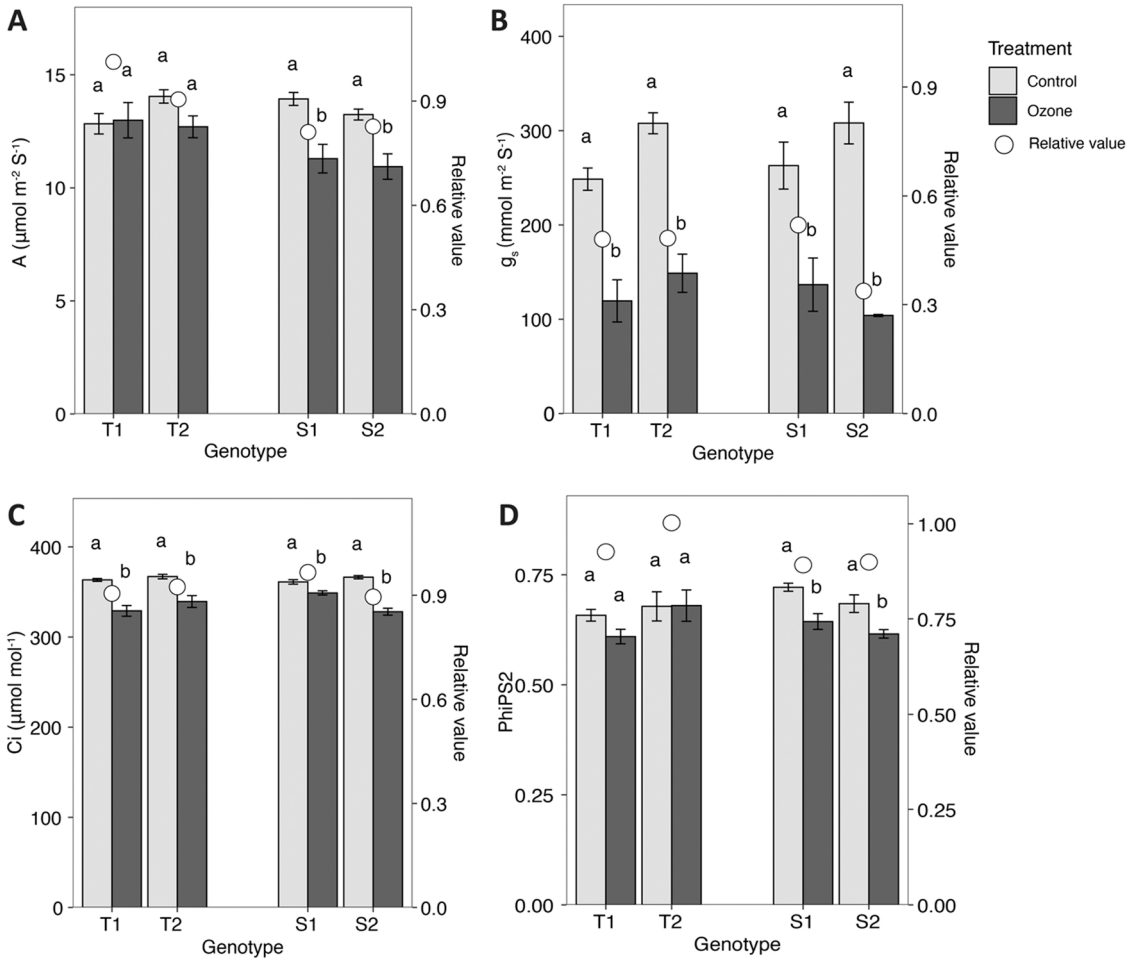

Fig. 2. Photosynthetic parameters of four wheat genotypes at 77 days after transplanting under control and ozone conditions. Bars indicate mean values and standard errors (n = 4). A, Net CO_2 assimilation; B, Stomatal conductance; C, Intercellular CO_2 concentration; D, Photosystem II efficiency were measured on the second fully expanded leaf. Bars not sharing the same superscript letters are significantly different at $P < 0.05$ within the genotypes (Student's *t* test).

3.3. Gene expression and sequence analysis

We analyzed the mRNA levels of eleven candidate genes located within the locus on chromosome 5A (592.04–593.33 Mb) significantly associated with symptom formation in ozone stress. All genes were involved in biological oxidation processes, oxidoreductases and peroxidases according to their annotations (Begum et al., 2020). In this study, quantitative RT-PCR was conducted under both control and ozone conditions (Supplementary Table S2). While most of the genes did not show differential expression between the contrasting haplotypes, a significant difference occurred in TraesCS5A01G400500 (Fig. 3). It was significantly upregulated by ozone treatment at DAT77 in both T1 and T2, but not in the sensitive haplotypes. To investigate whether these differences in expression were associated with sequence polymorphisms we determined the genomic sequence including its promoter region in all four genotypes. This analysis revealed consistent polymorphisms between tolerant and sensitive haplotypes (Fig. 4A; Supplementary Fig. S1). In the promoter region, the cis-elements, EVENINGAT (evening element) and PREATPRODH (pro- or hypoosmolarity–responsive element) were only present in tolerant haplotypes (Fig. 4B; Supplementary Table S3). In addition, two haplotypes showed differential sequences in the domain "secretory peroxidase" (IPR033905) of the protein (Supplementary Fig. S2).

3.4. Proline and ascorbic acid content

Proline contributes to stabilizing subcellular structures, scavenging ROS and buffering cellular redox potential under stress conditions (Ashraf, Foolad, 2007). Averaged over both haplotypes and all sampling days, the proline content in leaf tissues showed a significant interaction effect between the treatment, haplotype and DAT (Table 1). There was no significant ozone impact on the proline content across all genotypes at DAT35. However, after long-term ozone fumigation, both T1 and T2 had significantly decreased proline content in contrast to the control condition at DAT110 (Fig. 5 A).

In the apoplast, reduced AsA and total AsA content were increased significantly in tolerant haplotypes in the ozone treatment compared to the control condition at DAT77, but there was no significant impact on sensitive genotypes regarding both contents (Figs. 5B, 5C). Among both haplotypes and all sampling days, apoplastic total AsA showed significant interaction effects of the treatment, haplotype and DAT (Table 1). The AsA redox state in all genotypes was reduced by ozone fumigation. Although only the most sensitive genotype, S2, exhibited a significant decrease, both sensitive genotypes showed significantly lower redox states than T1 and T2 in the ozone treatment on both sampling dates (Fig. 5D). Moreover, significant effects of the treatment, haplotypes, DAT and interaction effects were observed in the apoplastic AsA redox state (Table 1). Regarding ascorbic acid in leaves, significant interaction effects occurred for treatment, haplotype and DAT in reduced AsA and total AsA among all haplotypes and sampling dates (Table 1). However,

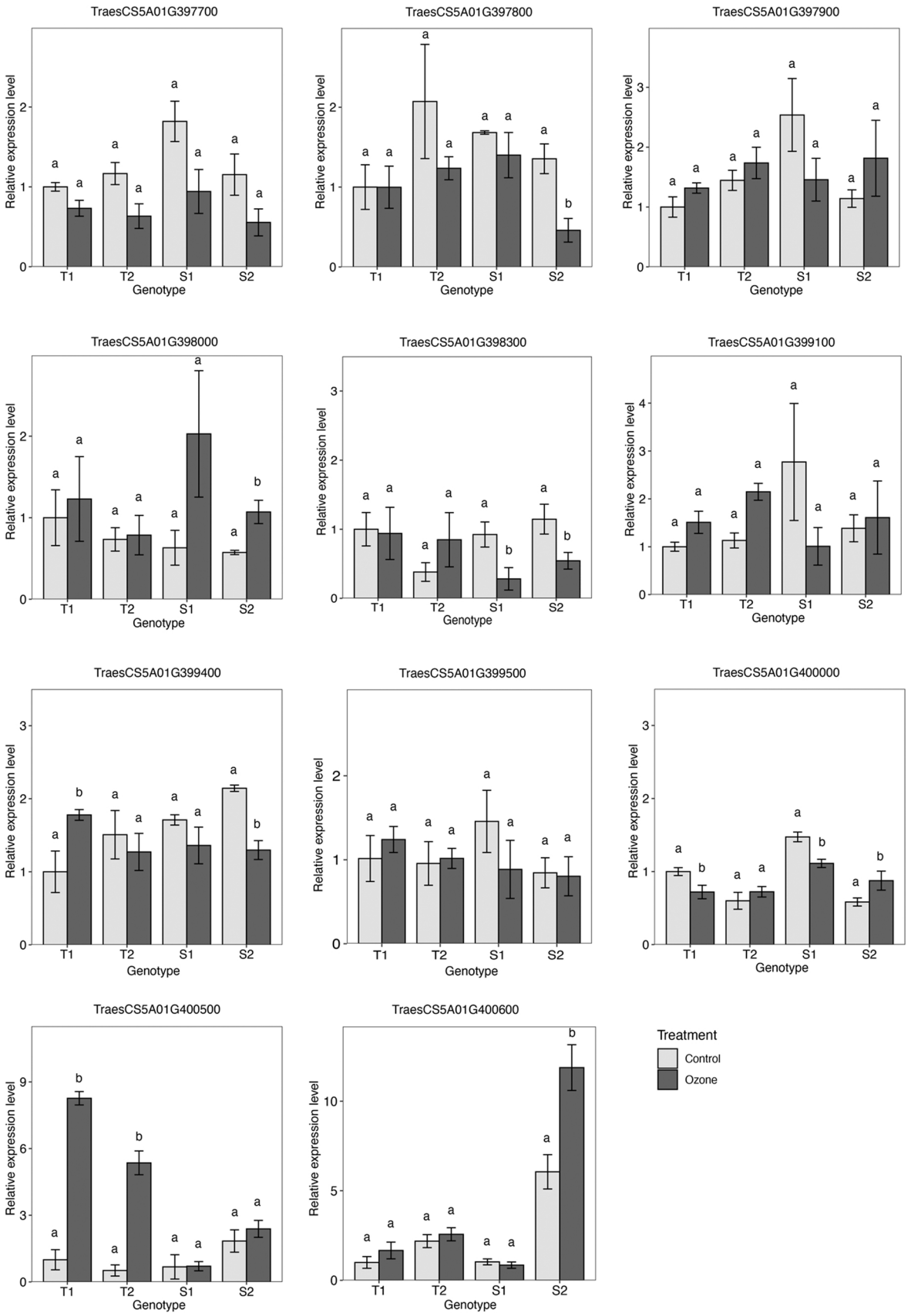

Fig. 3. Quantitative RT—PCR expression analyses of eleven genes of wheat leaves at 110 days after transplanting under control and ozone treatments. Bars indicate mean values and standard errors (n = 4). Bars not sharing the same superscript letters are significantly different at $P < 0.05$ within the genotypes (Student's *t* test).

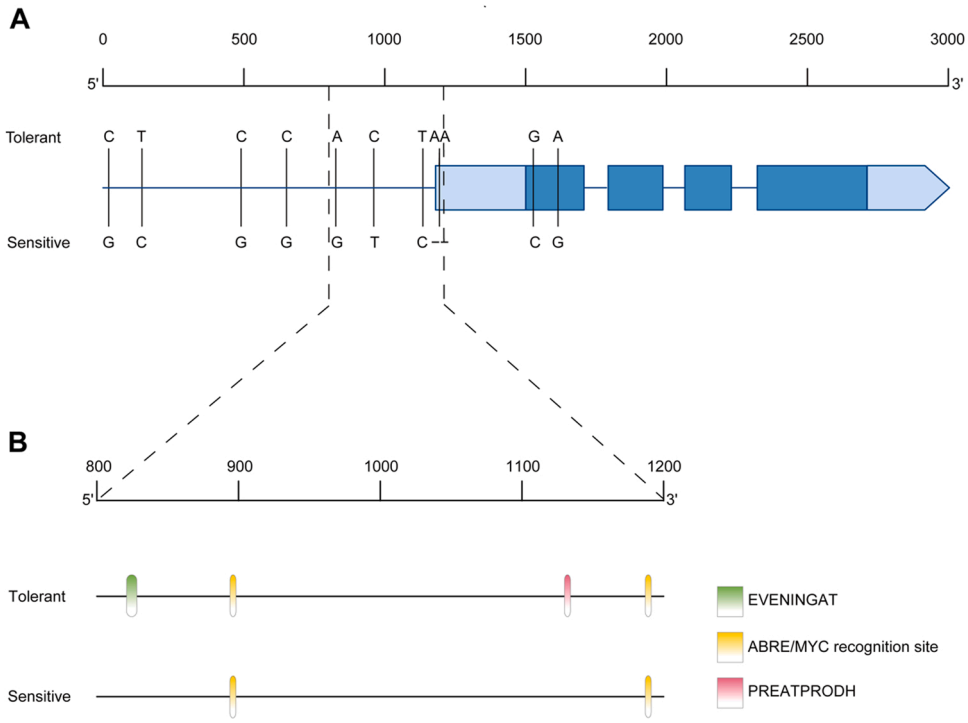

Fig. 4. Sequence and cis-element analyses of TraesCS5A01G400500 of tolerant and sensitive haplotypes. A. Upstream 1500 bp and TraesCS5A01G400500 sequence. B. Cis-elements between 800 and 1200 bp in the promoter of tolerant and sensitive haplotypes. The untranslated regions (UTR), exons, and intron are also shown.

only the most tolerant genotype T2 had significantly higher reduced and total AsA after ozone treatment at DAT35. Contrasting haplotypes did not differ significantly in foliar AsA concentration. There was no significance among all genotypes and all sampling dates in the redox state (Supplementary Fig. S3; Table 1).

3.5. Enzyme activity

APX activity was significantly induced in S1 and S2 by ozone treatment by 34.2 % and 43.0 % at DAT110, respectively, while no responses were observed in tolerant genotypes (Fig. 5E). Moreover, a significant interaction effect occurred between treatment and haplotype for APX activity (Table 1). After long-term ozone fumigation, peroxidase activity in T1 and T2 was significantly decreased under ozone stress compared to the control condition. S1 and S2 had higher peroxidase activity than the tolerant genotypes at elevated ozone on both sampling dates (Fig. 5F). AO activity was significantly induced by ozone among all genotypes and all sampling dates, with a significant interaction effect between treatment and haplotype (Table 1). Only S2 showed significant increases at both sampling dates (Supplementary Fig. S3D), but the relative values of sensitive genotypes were higher than of those tolerant genotypes. DHAR activity and MDHAR activity were not responsive to different treatments or haplotypes (Table 1; Supplementary Fig. S3E, S3F). Based on the sequence polymorphisms in TraesCS5A01G400500 and physiological analyses, we concluded that contrasting haplotypes differed in antioxidant responses and, more specifically, in peroxidases under ozone stress.

4. Discussion

The current concentration of ground-level ozone poses a threat to global food security due to its deleterious effects on crop production (Mills et al., 2018b). As wheat is sensitive to ozone stress, it is urgent to take actions in breeding programs to mitigate ozone impacts on wheat yield (Mills et al., 2018a; Pleijel et al., 2018). A previous GWAS demonstrated significant marker—trait associations for LBSs on chromosome 5A, which laid the foundation for the molecular breeding of tolerant wheat varieties (Begum et al., 2020). This study expanded on these previous findings to identify and characterize specific candidate genes within the tolerant locus. To this aim, we used four genotypes, two of which represented the tolerant haplotype and the other two represented the sensitive haplotype at the concerned locus as defined by 10 SNP markers (Begum et al., 2020). T1 and T2, representing the tolerant haplotype, and S1 and S2, representing the sensitive haplotype, differed significantly in LBS (Fig. 1A). Our reasoning was that any consistent transcriptional and physiological responses to ozone observed in both genotypes representing one haplotype are unlikely to be coincidental, but rather linked to genetically determined ozone tolerance.

Both acute and chronic ozone exposure lead to oxidative damage to membrane lipids, accelerating foliar senescence in plants (Pleijel et al., 2006). As an important indicator of membrane lipid peroxidation, MDA is correlated with the degree of ozone exposure to plants (Biswas et al., 2008b; Feng et al., 2011; Frei, 2015). Consistent with the LBS in this study, higher MDA was observed in the second youngest fully expanded leaves of the sensitive haplotype compared to the tolerant haplotype at DAT110 (Fig. 1B), confirming the different tolerance of distinct haplotypes to ozone.

Regarding photosynthetic capacity, both lines of the sensitive haplotype showed decreased net CO_2 assimilation rate and photosystem II efficiency at DAT77 in the ozone treatment. Stomata form the first line of defense to protect plants from ozone, and various experiments have demonstrated that wheat responds to elevated ozone with reduced stomatal conductance (Biswas et al., 2008b; Biswas et al., 2009). In this study, both tolerant and sensitive haplotypes showed a significant decline in stomatal conductance, suggesting that stomatal conductance did not contribute to the significant difference among haplotypes in response to elevated ozone. A significant interaction effect between haplotype and treatment only occurred in net CO_2 assimilation, indicating that net CO_2 assimilation was an important factor determining ozone sensitivity to ozone stress in different haplotypes, rather than stomatal conductance. Ozone-induced reduction in the photosynthetic rate is caused by nonstomatal factors in wheat (Akhtar et al., 2010; Feng et al., 2016). Although ozone-induced stomatal closure has been

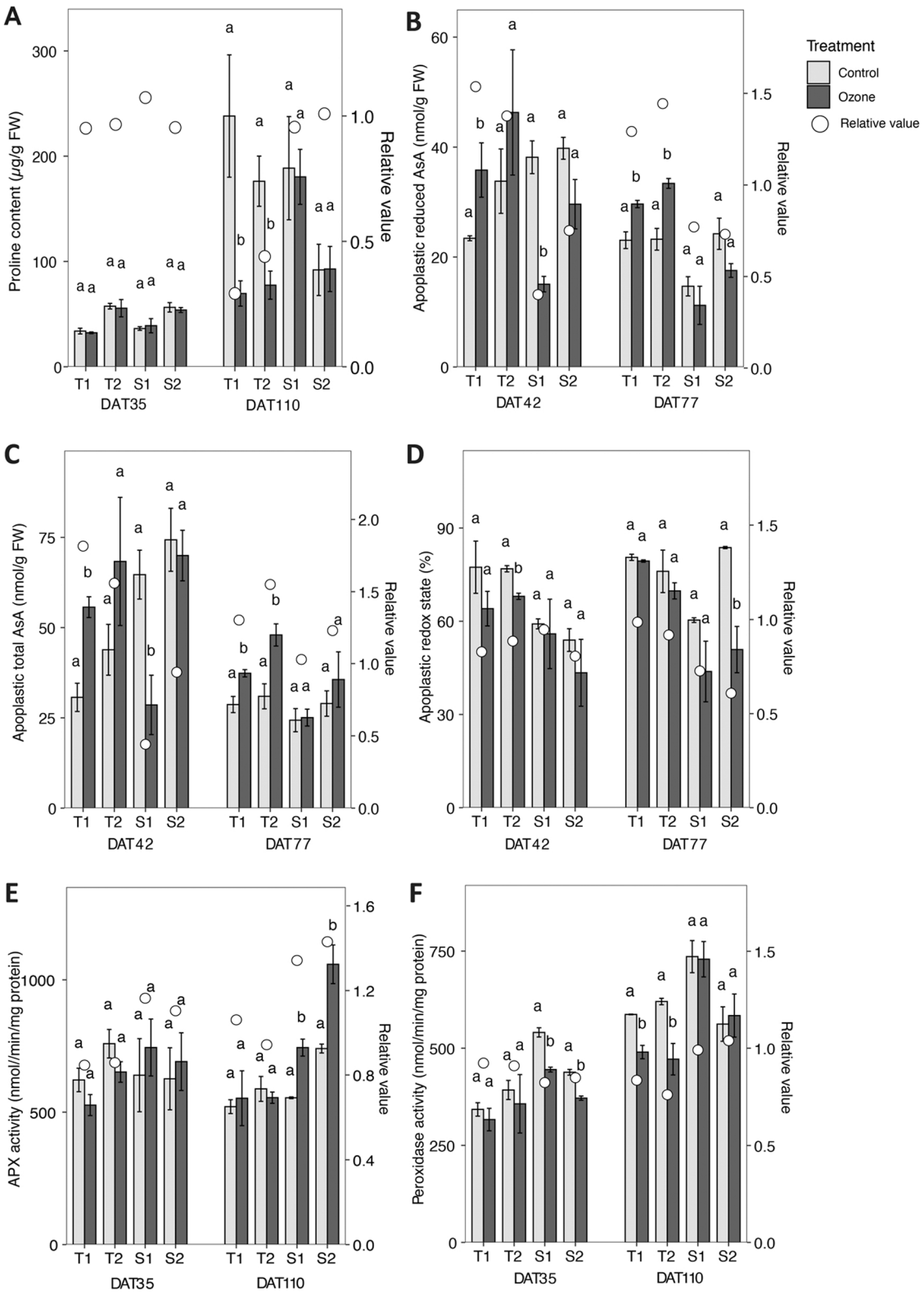

Fig. 5. Proline, apoplastic AsA and enzyme activities of four wheat genotypes under control and ozone conditions. Bars indicate mean values and standard errors (n = 4). A, Proline; B, Reduced AsA; C, Total AsA; D, Redox state E, APX activity; F, Peroxidase activity. All measurements were taken on the second fully expanded leaves. A, E and F were measured at 35 and 100 days after transplanting under control and ozone conditions; B, C and D were determined at 42 days and 77 days after transplanting under control and ozone conditions. Bars not sharing the same superscript letters are significantly different at $P < 0.05$ within the genotypes (Student's *t* test).

implicated in reducing carbon availability, it is not the main factor in the ozone-induced reduction in grain yield. Instead, yield and net photosynthesis had a strong correlation according to a previous study (Feng et al., 2022a). Our results suggested that net photosynthesis is an important physiological indicator of ozone tolerance and showed consistency in both wheat haplotypes.

Furthermore, responses to ozone were also assessed by the gene expression level of eleven putative candidate genes identified in our previous study (Begum et al., 2020). These genes have been proposed due to (1) their locations within a locus significantly associated with foliar symptom formation under ozone stress, and (2) their putative functions in cellular redox homeostasis. Among these genes, only TraesCS5A01G400500 showed significantly different regulation between contrasting haplotypes. It is involved in heme binding and peroxidase activity, which is consistent with the physiological differences between tolerant and sensitive haplotypes observed in this study. It must be noted that peroxidase activity data (Table 1) were not consistent with the expression data of TraesCS5A01G400500, which can be explained by the fact that the enzymatic assay measured the combined activity of multiple peroxidases present in the wheat genome. On the other hand, the paralogous gene Os03g0762300 in rice of TraesCS5A01G400500 was reported to maintain the function of peroxidase, preventing a toxic environment that could induce cell death (Persson et al., 2009). In the cis-element analyses, EVENINGAT and PREATPRODH were found only in the tolerant haplotypes (Fig. 4), which might explain the differential expression of TraesCS5A01G400500. EVENINGAT is an evening element motif that confers circadian rhythmicity on gene expression, and mutation of full-length EVENINGAT resulted in reduced rhythmicity in *Arabidopsis* (Harmer et al., 2000). In addition, PREATPRODH was required for efficient expression of proline dehydrogenase in response to $_{L}$-Pro and hypo-osmolarity (Satoh et al., 2002). Proline is an essential metabolite in response to environmental stress with multiple functions, such as triggering specific gene expression, modulating mitochondrial functions, and influencing cell death (Szabados and Savoure, 2010). In pomegranate, proline content was increased 41 % in biochemical adjustments to protect cells against the negative impact of elevated ozone when compared to ambient ozone concentration (Calzone et al., 2019). Recent studies have suggested a role for proline in the plant response to ozone stress, although it is uncertain whether it is a major determinant of ozone tolerance (Boublin et al., 2022; Ueno et al., 2021). Most recently, proline accumulation induced by ozone was observed only in the most ozone-sensitive ecotypes in Arabidopsis, suggesting that the effect of ozone on proline accumulation might depend on the genotypic variation (Boublin et al., 2022). Compared to the chamber with charcoal filtered air, a significant increase in proline content was detected in non-filtered ambient air in wheat cultivar HUW 234 (Rai et al., 2007). Ethylenediurea (EDU) was used to access protection against ambient ozone under field conditions for five cultivars of tropical wheat, and EDU-treated plants showed a significant increase in proline accumulation (Singh et al., 2009). In this study with different genotypes and experimental conditions, only tolerant haplotypes had significantly decreased proline content after long-term ozone fumigation, and TraesCS5A01G400500 might be a putative L-Pro-inducible gene regulated by proline accumulation under ozone exposure.

Ozone exposure leads to oxidative stress, thus challenging the antioxidant system involved in the scavenging of ROS in plants (Gest et al., 2013). Many studies have indicated that ozone tolerance is related to the detoxification of ozone or ozone-derived ROS, which depends on the antioxidative capacity determined by antioxidants and antioxidant enzymes (Feng et al., 2016; Inada et al., 2012). Ascorbate can neutralize ROS and repair oxidized organic molecules, which has been proposed to play a crucial role in ozone defense (Baier et al., 2005; Smirnoff, 2000). Indeed, both aplopastic and leaf ascorbate contributed to ozone tolerance in wheat (Feng et al., 2010). In our study haplotypes did not differ in whole leaf AsA, while differences in apoplastic AsA were observed between tolerant and sensitive haplotypes (Table 1). The tolerant haplotype had significantly higher concentrations of reduced AsA and total AsA in the aploplast than the sensitive haplotype (Fig. 5). Apoplastic ascorbate has been proposed as the first line of defense against ozone damage in plants (Conklin and Barth, 2004). Apoplastic reduced AsA and its replenishment from the cytoplasmic pool determine the effectiveness of reduced AsA against oxidative damage (Kollist et al., 2000). No significant difference in reduced AsA in the leaf tissues indicated a similar “reservoir” between tolerant and sensitive haplotypes of replenishment apoplastic reduced AsA. Wang et al. (2015) reported that ascorbate in leaf tissues had little response to ozone but was more reductive, facilitating the transport of reduced AsA between the cytoplasm and apoplast for detoxification. Our results suggest that the distribution of AsA in the apoplast forms an important factor contributing to ozone tolerance in T1 and T2.

Antioxidant metabolism in leaf tissues has the function of replenishing antioxidants oxidized by ozone in the apoplast (Feng et al., 2016). Therefore, antioxidative enzymes were analyzed among the two haplotypes to explore the different responses to elevated ozone. Among them, AO, DHAR and MDHAR did not respond to ozone stress, whereas haplotype differences in the response to elevated ozone occurred in APX and peroxidase activity. Peroxidases have a prominent role in controlling the ROS level and redox homeostasis under ozone exposure to mitigate damage to biomolecules (Apel and Hirt, 2004). It was reported that the transcripts for APX and guaiacol peroxidases were increased by ozone through northern blotting and gene expression in Arabidopsis (Ludwikow and Sadowski, 2008; Mahalingam et al., 2006). In this study, the higher APX and peroxidase activity in the sensitive haplotype after ozone fumigation compared to the tolerant haplotype suggest that peroxidases were instrumental in the metabolic regulation of the ozone response and tolerance.

5. Conclusions

Our results suggest that contrasting haplotypes of wheat showed distinct responses to ozone regarding net photosynthetic rate, the antioxidative pool of apoplastic AsA and activity of the enzymes APX and peroxidase. One of eleven previously nominated candidate genes, TraesCS5A01G400500 showed consistent differences in mRNA abundance and sequence polymorphisms between contrasting haplotypes. It is, therefore, a promising candidate gene for ozone tolerance breeding putatively involved in peroxidase regulation. The converging results presented here warrant further efforts to characterize the gene function and its involvment in ozone tolerance through additional approaches, such as reverse genetics and analyses of recombinant proteins derived from TraesCS5A01G400500. This could eventually facilitate its use in adaptive ozone tolerance breeding.

CRediT authorship contribution statement

Yanru Feng: Conceptualization, Investigation, Data curation, Writing – original draft. **Lin-Bo Wu:** Methodology, Software, Writing – review & editing. **Sawitree Autarmat:** Investigation, Writing – review & editing. **Muhammad Shahedul Alam:** Methodology, Writing – review & editing. **Michael Frei:** Supervision, Conceptualization, Methodology, Writing – review & editing.

Declaration of Competing Interest

The authors declare that they have no known competing financial interests or personal relationships that could have appeared to influence the work reported in this paper.

Data availability

Data will be made available on request.

Acknowledgements

We thank Prof. Dr. Rod Snowdon and Dr. Christian Obermeier (University of Giessen) for sharing experimental facilities and technical support (qPCR). The work was financially supported by the China Scholarship Council with a PhD scholarship to Yanru Feng (No. CSC201906300077), and the Thailand Research Fund for financially supporting Sawitree Autarmat through the Royal Gold Jubilee Ph.D. Program (Grant no. PHD/0204/2560).

Appendix A. Supporting information

Supplementary data associated with this article can be found in the online version at doi:10.1016/j.envexpbot.2023.105368.

References

Ainsworth, E.A., 2017. Understanding and improving global crop response to ozone pollution. Plant J. 90, 886–897. https://doi.org/10.1111/tpj.13298.

Ainsworth, E.A., Beier, C., Calfapietra, C., Ceulemans, R., Durand-Tardif, M., Farquhar, G.D., Godbold, D.L., Hendrey, G.R., Hickler, T., Kaduk, J., Karnosky, D.F., Kimball, B.A., Korner, C., Koornneef, M., Lafarge, T., Leakey, A.D., Lewin, K.F., Long, S.P., Manderscheid, R., McNeil, D.L., Mies, T.A., Miglietta, F., Morgan, J.A., Nagy, J., Norby, R.J., Norton, R.M., Percy, K.E., Rogers, A., Soussana, J.F., Stitt, M., Weigel, H.J., White, J.W., 2008. Next generation of elevated [CO_2] experiments with crops: a critical investment for feeding the future world. Plant Cell Environ. 3, 1317–1324. https://doi.org/10.1111/j.1365-3040.2008.01841.x.

Ainsworth, E.A., Yendrek, C.R., Sitch, S., Collins, W.J., Emberson, L.D., 2012. The effects of tropospheric ozone on net primary productivity and implications for climate change. Annu Rev. Plant Biol. 63, 637–661. https://doi.org/10.1146/annurev-arplant-042110-103829.

Akhtar, N., Yamaguchi, M., Inada, H., Hoshino, D., Kondo, T., Izuta, T., 2010. Effects of ozone on growth, yield and leaf gas exchange rates of two Bangladeshi cultivars of wheat (Triticum aestivum L.). Environ. Pollut. 158, 1763–1767. https://doi.org/10.1016/j.envpol.2009.11.011.

Alam, M.S., Maina, A.W., Feng, Y., Wu, L.B., Frei, M., 2022. Interactive effects of tropospheric ozone and blast disease (Magnaporthe oryzae) on different rice genotypes. Environ. Sci. Pollut. Res. 29, 48893–48907. https://doi.org/10.1007/s11356-022-19282-z.

Apel, K., Hirt, H., 2004. Reactive oxygen species: metabolism, oxidative stress, and signaling transduction. Annu Rev. Plant Biol. 55, 373. https://doi.org/10.1146/annurev.arplant.55.031903.141701.

Ashraf, M.F.M.R., Foolad, M.R., 2007. Roles of glycine betaine and proline in improving plant abiotic stress resistance. Environ. Exp. Bot. 59, 206–216. https://doi.org/10.1016/j.envexpbot.2005.12.006.

Ashrafuzzaman, M., Lubna, F.A., Holtkamp, F., Manning, W.J., Kraska, T., Frei, M., 2017. Diagnosing ozone stress and differential tolerance in rice (Oryza sativa L.) with ethylenediurea (EDU). Environ. Pollut. 230. https://doi.org/10.1016/j.envpol.2017.06.055.

Avnery, S., Mauzerall, D.L., Liu, J., Horowitz, L.W., 2011. Global crop yield reductions due to surface ozone exposure: 2. Year 2030 potential crop production losses and economic damage under two scenarios of O3 pollution. Atmos. Environ. 45, 2297–2309. https://doi.org/10.1016/j.atmosenv.2011.01.002.

Baier, M., Kandlbinder, A., Golldack, D., Dietz, K.-J., 2005. Oxidative stress and ozone: perception, signalling and response. Plant Cell Environ. 28, 1012–1020. https://doi.org/10.1111/j.1365-3040.2005.01326.x.

Bates, L.S., Waldren, R.A., Teare, I.D., 1973. Rapid determination of free proline for water-stress studies. Plant Soil 39, 205–207. https://doi.org/10.1007/BF00018060.

Begum, H., Alam, M.S., Feng, Y., Koua, P., Ashrafuzzaman, M., Shrestha, A., Kamruzzaman, M., Dadshani, S., Ballvora, A., Naz, A.A., Frei, M., 2020. Genetic dissection of bread wheat diversity and identification of adaptive loci in response to elevated tropospheric ozone. Plant Cell Environ. 43, 2650–2665. https://doi.org/10.1111/pce.13864.

Biswas, D.K., Xu, H., Li, Y.G., Liu, M.Z., Chen, Y.H., Sun, J.Z., Jiang, G.M., 2008a. Assessing the genetic relatedness of higher ozone sensitivity of modern wheat to its wild and cultivated progenitors/relatives. J. Exp. Bot. 59, 951–963. https://doi.org/10.1093/jxb/ern022.

Biswas, D.K., Xu, H., Li, Y.G., Sun, J.Z., Wang, X.Z., Han, X.G., Jiang, G.M., 2008b. Genotypic differences in leaf biochemical, physiological and growth responses to ozone in 20 winter wheat cultivars released over the past 60 years. Glob. Change Biol. 14, 46–59. https://doi.org/10.1111/j.1365-2486.2007.01477.x.

Biswas, D.K., Xu, H., Yang, J.C., Li, Y.G., Chen, S.B., Jiang, C.D., Li, W.D., Ma, K.P., Adhikary, S.K., Wang, X.Z., Jiang, G.M., 2009. Impacts of methods and sites of plant breeding on ozone sensitivity in winter wheat cultivars. Agric. Ecosyst. Environ. 134, 168–177. https://doi.org/10.1016/j.agee.2009.06.009.

Boublin, F., Cabassa-Hourton, C., Leymarie, J., Leitao, L., 2022. Potential involvement of proline and flavonols in plant responses to ozone. Environ. Res. 207, 112214 https://doi.org/10.1016/j.envres.2021.112214.

Bradford, M.M., 1976. A rapid and sensitive method for the quantitation of microgram quantities of protein utilizing the principle of protein-dye binding. Anal. Biochem. 72, 248–254. https://doi.org/10.1016/0003-2697(76)90527-3.

Broberg, M.C., Feng, Z., Xin, Y., Pleijel, H., 2015. Ozone effects on wheat grain quality - a summary. Environ. Pollut. 197, 203–213. https://doi.org/10.1016/j.envpol.2014.12.009.

Calzone, A., Podda, A., Lorenzini, G., Maserti, B.E., Carrari, E., Deleanu, E., Hoshika, Y., Haworth, M., Nali, C., Badea, O., Pellegrini, E., Fares, S., Paoletti, E., 2019. Cross-talk between physiological and biochemical adjustments by Punica granatum cv. Dente di cavallo mitigates the effects of salinity and ozone stress. Sci. Total Environ. 656, 589–597. https://doi.org/10.1016/j.scitotenv.2018.11.402.

Chen, C.P., Frei, M., Wissuwa, M., 2011. The OzT8 locus in rice protects leaf carbon assimilation rate and photosynthetic capacity under ozone stress. Plant Cell Environ. 34, 1141–1149. https://doi.org/10.1111/j.1365-3040.2011.02312.x.

Conklin, P.L., Barth, C., 2004. Ascorbic acid, a familiar small molecule intertwined in the response of plants to ozone, pathogens, and the onset of senescence. Plant Cell Environ. 27, 959–970. https://doi.org/10.1111/j.1365-3040.2004.01203.x.

Emberson, L.D., Büker, P., Ashmore, M.R., Mills, G., Jackson, L.S., Agrawal, M., Atikuzzaman, M.D., Cinderby, S., Engardt, M., Jamir, C., Kobayashi, K., Oanh, N.T. K., Quadir, Q.F., Wahid, A., 2009. A comparison of North American and Asian exposure–response data for ozone effects on crop yields. Atmos. Environ. 43, 1945–1953. https://doi.org/10.1016/j.atmosenv.2009.01.005.

Fatima, A., Singh, A.A., Mukherjee, A., Agrawal, M., Agrawal, S.B., 2018. Variability in defence mechanism operating in three wheat cultivars having different levels of sensitivity against elevated ozone. Environ. Exp. Bot. 155, 66–78. https://doi.org/10.1016/j.envexpbot.2018.06.015.

Feng, Y., Nguyen, T.H., Alam, M.S., Emberson, L., Gaiser, T., Ewert, F., Frei, M., 2022b. Identifying and modelling key physiological traits that confer tolerance or sensitivity to ozone in winter wheat. Environ. Pollut. 304. https://doi.org/10.1016/j.envpol.2022.119251.

Feng, Z., Kobayashi, K., Ainsworth, E.A., 2008. Impact of elevated ozone concentration on growth, physiology, and yield of wheat (Triticum aestivum L.): a meta-analysis. Glob. Change Biol. 14, 2696–2708. https://doi.org/10.1111/j.1365-2486.2008.01673.x.

Feng, Z., Pang, J., Kobayashi, K., Zhu, J., Ort, D.R., 2011. Differential responses in two varieties of winter wheat to elevated ozone concentration under fully open-air field conditions. Glob. Change Biol. 17, 580–591. https://doi.org/10.1111/j.1365-2486.2010.02184.x.

Feng, Z., Pang, J., Nouchi, I., Kobayashi, K., Yamakawa, T., Zhu, J., 2010. Apoplastic ascorbate contributes to the differential ozone sensitivity in two varieties of winter wheat under fully open-air field conditions. Environ. Pollut. 158, 3539–3545. https://doi.org/10.1016/j.envpol.2010.08.019.

Feng, Z., Wang, L., Pleijel, H., Zhu, J., Kobayashi, K., 2016. Differential effects of ozone on photosynthesis of winter wheat among cultivars depend on antioxidative enzymes rather than stomatal conductance. Sci. Total Environ. 572, 404–411. https://doi.org/10.1016/j.scitotenv.2016.08.083.

Feng, Z., Xu, Y., Kobayashi, K., Dai, L., Zhang, T., Agathokleous, E., Calatayud, V., Paoletti, E., Mukherjee, A., Agrawal, M., Park, R.J., Oak, Y.J., Yue, X., 2022a. Ozone pollution threatens the production of major staple crops in East Asia. Nat. Food 3, 47–56. https://doi.org/10.1038/s43016-021-00422-6.

Frei, M., 2015. Breeding of ozone resistant rice: relevance, approaches and challenges. Environ. Pollut. 197, 144–155. https://doi.org/10.1016/j.envpol.2014.12.011.

Frei, M., Tanaka, J.P., Chen, C.P., Wissuwa, M., 2010. Mechanisms of ozone tolerance in rice: characterization of two QTLs affecting leaf bronzing by gene expression profiling and biochemical analyses. J. Exp. Bot. 61, 1405–1417. https://doi.org/10.1093/jxb/erq007.

Frei, M., Tanaka, J.P., Wissuwa, M., 2008. Genotypic variation in tolerance to elevated ozone in rice: dissection of distinct genetic factors linked to tolerance mechanisms. J. Exp. Bot. 59, 3741–3752. https://doi.org/10.1093/jxb/ern222.

Gest, N., Gautier, H., Stevens, R., 2013. Ascorbate as seen through plant evolution: the rise of a successful molecule? J. Exp. Bot. 64, 33–53. https://doi.org/10.1093/jxb/errs321937.

Gillespie, K.M., Ainsworth, E.A., 2007. Measurement of reduced, oxidized and total ascorbate content in plants. Nat. Protoc. 2, 871–874. https://doi.org/10.1038/nprot.2007.101.

Godfray, H.C.J., Beddington, J.R., Crute, I.R., Haddad, L., Lawrence, D., Muir, J.F., Pretty, J., Robinson, S., Thomas, S.M., Toulmin, C., 2010. Food security: the challenge of feeding 9 billion people. Science 327, 812–818. https://doi.org/10.1126/science.1185383.

Granier, C., Bessagnet, B., Bond, T., D'Angiola, A., Denier van der Gon, H., Frost, G.J., Heil, A., Kaiser, J.W., Kinne, S., Klimont, Z., Kloster, S., Lamarque, J.-F., Liousse, C., Masui, T., Meleux, F., Mieville, A., Ohara, T., Raut, J.-C., Riahi, K., Schultz, M.G., Smith, S.J., Thompson, A., van Aardenne, J., van der Werf, G.R., van Vuuren, D.P., 2011. Evolution of anthropogenic and biomass burning emissions of air pollutants at global and regional scales during the 1980–2010 period. In: Climatic Change, 109, pp. 163–190. https://doi.org/10.1007/s10584-011-0154-1.

Harmer, S.L., Hogenesch, J.B., Straume, M., Chang, H.-S., Han, B., Zhu, T., Wang, X., Kreps, J.A., Kay, S.A., 2000. Orchestrated transcription of key pathways in Arabidopsis by the circadian clock. Science 290, 2110–2113. https://doi.org/10.1126/science.290.5499.2110.

Höller, S., Meyer, A., Frei, M., 2014. Zinc deficiency differentially affects redox homeostasis of rice genotypes contrasting in ascorbate level. J. Plant Physiol. 171, 1748–1756. https://doi.org/10.1016/j.jplph.2014.08.012.

Inada, H., Kondo, T., Akhtar, N., Hoshino, D., Yamaguchi, M., Izuta, T., 2012. Relationship between cultivar difference in the sensitivity of net photosynthesis to ozone and reactive oxygen species scavenging system in Japanese winter wheat (Triticum aestivum). Physiol. Plant 146, 217–227. https://doi.org/10.1111/j.1399-3054.2012.01618.x.

Kollist, H., Moldau, H., Mortensen, L., Rasmussen, S.K., Jørgensen, L.B., 2000. Ozone flux to plasmalemma in barley and wheat is controlled by stomata rather than by direct reaction of ozone with cell wall ascorbate. J. Plant Physiol. 156, 645–651. https://doi.org/10.1016/s0176-1617(00)80226-6.

Lin, C.C., Kao, C.H., 1999. NaCl induced changes in ionically bound peroxidase activity in roots of rice seedlings. Plant Soil 216, 147–153. https://doi.org/10.1023/A:1004714506156.

Ludwikow, A., Sadowski, J., 2008. Gene networks in plant ozone stress response and tolerance. J. Integr. Plant Biol. 50, 1256–1267. https://doi.org/10.1111/j.1744-7909.2008.00738.x.

Mahalingam, R., Jambunathan, N., Gunjan, S.K., Faustin, E., Weng, H., Ayoubi, P., 2006. Analysis of oxidative signalling induced by ozone in Arabidopsis thaliana. Plant Cell Environ. 29, 1357–1371. https://doi.org/10.1111/j.1365-3040.2006.01516.x.

Mashaheet, A.M., Burkey, K.O., Marshall, D.S., 2019. Chromosome location contributing to ozone tolerance in wheat. Plants 8. https://doi.org/10.3390/plants8080261.

Mills, G., Sharps, K., Simpson, D., Pleijel, H., Broberg, M., Uddling, J., Jaramillo, F., Davies, W.J., Dentener, F., Van den Berg, M., Agrawal, M., Agrawal, S.B., Ainsworth, E.A., Buker, P., Emberson, L., Feng, Z., Harmens, H., Hayes, F., Kobayashi, K., Paoletti, E., Van Dingenen, R., 2018b. Ozone pollution will compromise efforts to increase global wheat production. Glob. Change Biol. 24, 3560–3574. https://doi.org/10.1111/gcb.14157.

Mills, G., Sharps, K., Simpson, D., Pleijel, H., Frei, M., Burkey, K., Emberson, L., Uddling, J., Broberg, M., Feng, Z., Kobayashi, K., Agrawal, M., 2018a. Closing the global ozone yield gap: quantification and cobenefits for multistress tolerance. Glob. Change Biol. 24, 4869–4893. https://doi.org/10.1111/gcb.14381.

Nie, G.Y., Tomasevic, M., Baker, N.R., 1993. Effects of ozone on the photosynthetic apparatus and leaf proteins during leaf development in wheat. Plant Cell Environ. 16, 643–651. https://doi.org/10.1111/j.1365-3040.1993.tb00482.x.

Persson, M., Falk, A., Dixelius, C., 2009. Studies on the mechanism of resistance to Bipolaris sorokiniana in the barley lesion mimic mutant bst1. Mol. Plant Pathol. 10, 587–598. https://doi.org/10.1111/j.1364-3703.2009.00555.x.

Pleijel, H., Broberg, M.C., Uddling, J., Mills, G., 2018. Current surface ozone concentrations significantly decrease wheat growth, yield and quality. Sci. Total Environ. 613–614, 687–692. https://doi.org/10.1016/j.scitotenv.2017.09.111.

Pleijel, H., Eriksen, A.B., Danielsson, H., Bondesson, N., Selldén, G., 2006. Differential ozone sensitivity in an old and a modern Swedish wheat cultivar—grain yield and quality, leaf chlorophyll and stomatal conductance. Environ. Exp. Bot. 56, 63–71. https://doi.org/10.1016/j.envexpbot.2005.01.004.

Pleijel, H., Ojanperä, K., Mortensen, L., 1997. Effects of tropospheric ozone on the yield and grain protein content of spring wheat (Triticum aestivumL.) in the Nordic countries. Acta Agric. Scand. Sect. B Soil Plant Sci. 47, 20–25. https://doi.org/10.1080/09064719709362434.

R Core Team, 2018. R: a Language and Environment for Statistical Computing, R Foundation for Statistical Computing, Vienna. ⟨https://www.R-project.org⟩.

Rai, R., Agrawal, M., Agrawal, S.B., 2007. Assessment of yield losses in tropical wheat using open top chambers. Atmos. Environ. 41, 9543–9554. https://doi.org/10.1016/j.atmosenv.2007.08.038.

Sampedro, J., Waldhoff, S.T., Van de Ven, D.-J., Pardo, G., Van Dingenen, R., Arto, I., del Prado, A., Sanz, M.J., 2020. Future impacts of ozone driven damages on agricultural systems. Atmos. Environ. 231. https://doi.org/10.1016/j.atmosenv.2020.117538.

Satoh, R., Nakashima, K., Seki, M., Shinozaki, K., Yamaguchi-Shinozaki, K., 2002. ACTCAT, a novel cis-acting element for proline- and hypoosmolarity-responsive expression of the ProDH gene encoding proline dehydrogenase in Arabidopsis. Plant Physiol. 130, 709–719. https://doi.org/10.1104/pp.009993.

Shiferaw, B., Smale, M., Braun, H.-J., Duveiller, E., Reynolds, M., Muricho, G., 2013. Crops that feed the world 10. Past successes and future challenges to the role played by wheat in global food security. Food Secur 5, 291–317. https://doi.org/10.1007/s12571-013-0263-y.

Singh, S., Agrawal, S.B., Agrawal, M., 2009. Differential protection of ethylenediurea (EDU) against ambient ozone for five cultivars of tropical wheat. Environ. Pollut. 157, 2359–2367. https://doi.org/10.1016/j.envpol.2009.03.029.

Smirnoff, N., 2000. Ascorbic acid: metabolism and functions of a multi-facetted molecule. Curr. Opin. Plant Biol. 3, 229–235. https://doi.org/10.1016/S1369-5266(00)80070-9.

Szabados, L., Savoure, A., 2010. Proline: a multifunctional amino acid. Trends Plant Sci. 15, 89–97. https://doi.org/10.1016/j.tplants.2009.11.009.

Tai, A.P.K., Martin, M.V., Heald, C.L., 2014. Threat to future global food security from climate change and ozone air pollution. Nat. Clim. Change 4, 817–821. https://doi.org/10.1038/nclimate2317.

The Royal Society, 2008 Ground-level Ozone in the 21st Century: FuturE Trends, Impacts and Policy Implications.

Ueda, Y., Frimpong, F., Qi, Y., Matthus, E., Wu, L., Holler, S., Kraska, T., Frei, M., 2015a. Genetic dissection of ozone tolerance in rice (Oryza sativa L.) by a genome-wide association study. J. Exp. Bot. 66, 293–306. https://doi.org/10.1093/jxb/eru419.

Ueda, Y., Siddique, S., Frei, M., 2015b. A novel gene, OZONE-RESPONSIVE APOPLASTIC PROTEIN1, enhances cell death in ozone stress in rice. Plant Physiol. 169, 873–889. https://doi.org/10.1104/pp.15.00956.

Ueno, A.C., Gundel, P.E., Molina-Montenegro, M.A., Ramos, P., Ghersa, C.M., Martinez-Ghersa, M.A., 2021. Getting ready for the ozone battle: vertically transmitted fungal endophytes have transgenerational positive effects in plants. Plant Cell Environ. 44, 2716–2728. https://doi.org/10.1111/pce.14047.

Wang, L., Pang, J., Feng, Z., Zhu, J., Kobayashi, K., 2015. Diurnal variation of apoplastic ascorbate in winter wheat leaves in relation to ozone detoxification. Environ. Pollut. 207, 413–419. https://doi.org/10.1016/j.envpol.2015.09.040.

Wild, O., Fiore, A.M., Shindell, D.T., Doherty, R.M., Collins, W.J., Dentener, F.J., Schultz, M.G., Gong, S., MacKenzie, I.A., Zeng, G., Hess, P., Duncan, B.N., Bergmann, D.J., Szopa, S., Jonson, J.E., Keating, T.J., Zuber, A., 2012. Modelling future changes in surface ozone: a parameterized approach. Atmos. Chem. Phys. 12, 2037–2054. https://doi.org/10.5194/acp-12-2037-2012.

Wu, L.B., Feng, Y., Zeibig, F., Alam, M.S., Frei, M., 2021. High throughput analyses of ascorbate-turnover enzyme activities in rice (Oryza sativa L.) Seedlings. Bio Protoc. 11, e4190 https://doi.org/10.21769/BioProtoc.4190.

Wu, L.B., Ueda, Y., Lai, S.K., Frei, M., 2017. Shoot tolerance mechanisms to iron toxicity in rice (Oryza sativa L.). Plant Cell Environ. 40, 570–584. https://doi.org/10.1111/pce.12733.

Yadav, D.S., Rai, R., Mishra, A.K., Chaudhary, N., Mukherjee, A., Agrawal, S.B., Agrawal, M., 2019. ROS production and its detoxification in early and late sown cultivars of wheat under future O(3) concentration. Sci. Total Environ. 659, 200–210. https://doi.org/10.1016/j.scitotenv.2018.12.352.

Chapter 5: General Discussion

5.1 Identification and modelling of key physiological traits

In this study, eighteen distinct genotypes were selected from a diverse panel of 150 wheat genotypes based on LBS and grain yield (Begum et al., 2020). Different physiological parameters and grain yield were explored, including spectral reflectance, photosynthetic capacity, growth traits and C and N allocation. In Chapter 2, spectral reflectance, gas exchange and biomass analyses were carried out repeatedly during the growth season. Generally, elevated ozone accelerated plant maturity compared to control condition. Those physiological parameters showed significant treatment effects towards the late growth stages. Among them, NDVI and Lic2 were considered suitable traits for the non-invasive diagnosing of ozone stress in wheat, and significant maker-trait associations were identified for them on chromosomes 6B and 6D (Begum et al., 2020). Especially NDVI representing chlorophyll is an effective tool to facilitate the screening of genotypes (Naser et al., 2020) and to provide rapid assessment of large numbers of individual plots across multiple environments in field trials (Hassan et al., 2019). Higher NDVI is associated with higher biomass accumulation during the vegetative stage, and a longer grain filling period by delaying leaf senescence thereby increasing yield (Babar et al., 2006). This study also confirmed that NDVI was also positively correlated with grain yield under ozone stress. Naser et al. (2020) demonstrated that the proximal sensor-based NDVI readings can differentiate the yield of winter wheat genotypes under dryland and irrigated conditions. Compared to the handheld spectroradiometer, remote sensing (RS) could be a more efficient method to monitor the phenological characteristics including NDVI, and to predict the ecological responses to environmental changes (Jiang et al., 2021; Pettorelli et al., 2005). RS provides large capacity to quantify sensitive and robust information of vegetation responses to abiotic change in the cropland, e.g., sun-induced chlorophyll fluorescence and vegetation indices (VIs) (Damm et al., 2022). Those extensive airborne dataset would offer real-time dynamic images of important phenological characteristics and assess the impacts of abiotic stress on crops, including elevated ozone.

Ozone uptake mainly occurs through leaf stomata, and some studies have shown that sensitivity of plants to ozone is linked to g_s, as higher g_s implies a higher ozone flux that may increase leaf injury (Fiscus et al., 2005). For example, stomatal regulation is an important factor determining ozone sensitivity in *Arabidopsis thaliana* and the most sensitive accession, Cvi-0, had constitutively high stomatal conductance (Brosché et al., 2010). However, our results confirmed that ozone-induced reduction in C assimilation would be largely attributed to non-

stomatal factors in wheat (Feng et al., 2016). Similar findings have been reported in poplar (Shang et al., 2020), *Cinnamomum camphora* (Niu et al., 2014) and different broadleaved woody species (Zhang et al., 2012). Based on a comparative study of the ozone responses in 20 winter wheat cultivars, ozone-induced loss in light-saturated net photosynthetic rate (A_{sat}) might be attributed mainly to impaired activity of mesophyll cells, other than stomatal limitation (Biswas et al., 2008).

Biochemical and photochemical processes are also important constraints of photosynthesis (Feng et al., 2011). Rubisco is bifunctional enzyme catalyzing two competing reactions, that is, photosynthetic CO_2 assimilation and photorespiratory carbon oxidation (Leitao et al., 2003). In this study, different photosynthetic parameters were significantly reduced after long-term ozone fumigation. The decrease in V_{cmax} and J_{max} indicated ozone has adverse impacts on Rubisco carboxylation capacity and the Calvin cycle, and their simultaneous decreases possibly reflect an inability to generate RuBP from the lower pools of Calvin cycle following ozone treatment. Previous studies demonstrated that the close relationships between V_{cmax} and J_{max} imply a close functional balance in the resources allocation of within the photosynthetic apparatus to optimize the utilization of available resources, particularly N (Wullschleger, 1993). For instance, the proportion of leaf N in Rubisco and chlorophyll were important determinants of carboxylation- and RuBP-regeneration-limited rates of assimilation, respectively (Farquhar et al., 1980). In addition, Rubisco exits as a hexadecamer made up of eight large subunits (LSUs) encoded by chloroplast *rbcL* genes, and eight small subunits (SSUs) encoded by nuclear *rbcS* gene family (Kellogg and Juliano, 1997; Spreitzer, 1993). In lettuce, ozone exposure enhances an age associated decline in the abundance of the photosynthetic enzymes Rubisco and Rubisco activase (RCA) (Goumenaki et al., 2010). The ozone-induced decline in carboxylation efficiency was linked to a decrease in the amount of Rubisco LSUs and SSUs, which was also observed in beans (Leitao et al., 2008). This decline partly attributes to a decrease in transcript abundance of *rbcS1* and *rbcL* probably via altered signaling processes (Goumenaki et al., 2010). Besides, RCA is an ATP-dependent enzyme regulating the Rubisco activity by releasing the tight-binding sugar phosphates from the active site of Rubisco, and *rca* mRNA quantities also decreased after three months of ozone exposure in Aleppo pine (Pelloux et al., 2001). In wheat, some studies reported that RCA isoforms and *rca* gene expression was modulated by heat stress (Degen et al., 2021; Kumar et al., 2016; Ristic et al., 2009), while lack of investigations under ozone stress urges us further investigation.

The yield loss depends on the ozone sensitivity of the wheat cultivar as well as environmental interactions (Feng et al., 2010). Based on a previous meta-analysis collecting 53 reported

studies, the yield reduction was 24.4% at an average ozone concentration of 69 ppb. This experiment was conducted under chronic fumigation at a mean concentration of 70 ppb and three episodes of acute ozone exposure at a concentration of around 150 ppb, while less yield reduction (18.7%) may be due to different experimental systems and genotypes. All yield-related traits showed genotypic variation of wheat responses to ozone, especially, there was large variation for yield losses ranging from 2.7% to 44.6%, providing the foundation of ozone tolerance breeding and also warranting to improve the accuracy of modelling among wheat cultivars with distinct responses to ozone stress. Crop simulation models have the function of quantitative analysis of crop growth and cropping systems, and models that consider ozone impacts on wheat growth and production could assist to mitigate future yield loss in wheat (Guarin et al., 2019). LINTULCC2 crop shoot growth model has highly detailed calculations of leaf energy balances and the coupling of photosynthesis with stomatal conductance, which was previously validated and compared with different crop models under elevated CO_2 (Rodriguez et al., 2001). In this study, LINTULLCC2, was able to capture naturally occurring variation in ozone responses, following a well-tested approach for spring wheat in AFRCWHEAT2-O3 (Ewert and Porter, 2000). More specific ozone parameters, γ3 and γ4, were optimized for model fine-tuning to capture sensitivity or tolerance of wheat to ozone based on various physiological traits, which emphasized the importance of chlorophyll content represented by NDVI, A_{sat} and V_{cmax} at the late growth period. Accelerated senescence is consider the dominant ozone effect influencing yield in most agricultural environments (Osborne et al., 2019). Our results suggest that ozone induced accelerated senescence is more pronounced and important than direct effects on instantaneous photosynthesis during acute ozone episodes. Rubisco-limited rate of photosynthesis in senescing leaves (f_{LS}) and accumulative effects on leaf senescence (f_{LA}) were more important in contrast to instantaneous effect on photosynthesis rate (f_{O3t}). By considering genotypic differences in ozone response models, this study improved the accuracy of simulation studies, and identified physiological traits for the breeding of ozone tolerant wheat varieties. In addition, root: shoot models coupled LINTULCC2 with other models, including the root growth model SLIMROOT, Couvreur's root water uptake model (RWU), the HILLFLOW soil water balance model, were conducted in simulating CO_2 and H_2O fluxes and growth of wheat and maize (Nguyen et al., 2022; Nguyen et al., 2020). Previous studies reported that elevated ozone concentration inhibits the biomass allocation below ground and decreases root or whole-plant hydraulic conductance and disturbs water use regulation (Grantz et al., 2006; Grantz and Yang, 2000; Zhang et al., 2018). Future modelling growth simulation should be coupled with root model including the dynamic

parameterization of normalized root system conductance and/or more accurate assimilation of allocation to the roots, which would improve simulation of ozone responses, such as yield loss of crops.

5.2 Fertilizer efficiency and nutrient allocation under elevated ozone

N fertilizer played an extremely important role in agriculture, and in developing countries, the application of synthetic N fertilizer contributed to more than 55% of the increase in crop production (Li et al., 2009). As an established metric to benchmark N management, NUE can accurately reflects the complexities of N cycling and provides biological meaning (Congreves et al., 2021). In Chapter 3, compared to control condition, different NUE indicators were significantly decreased by elevated ozone apart from NUtE among all genotypes. Based on a large number of OTC field experiments, ozone exposure reduces grain yield return for a certain investment in N fertilizer and the translocation of accumulated N from straw and leaves to grains is significantly inhibited by ozone (Broberg et al., 2017). In this study, the availability of N was abundant to satisfy the N demand of plant. In addition to economic losses, excess N fertilizer usage and/or the lower NUE have the implication for agro-ecosystems and environmental problems associated with increased N losses at the farm-scale (Langholtz et al., 2021). Compared to control condition, less fraction of the added nutrient was acquired by the plants under ozone stress. The accumulation of nitrate (NO_3^-) in the soil profile that coincides with or is followed by high drainage, would result in NO_3^- leaching losses and adversely affect the aquatic ecosystems, especially for the downstream water (Di and Cameron, 2002). Approximately 30% of N inputs in agriculture were lost by N leaching and runoff, which is the largest component of the indirect N_2O budget (Syakila and Kroeze, 2011; Well et al., 2007). Besides, biological nitrification and denitrification also contribute to nitrous oxide (N_2O) emissions (Ambus, 1998), accounting for 1.3% of global greenhouse gas (GHG) emissions (Jensen et al., 2011).

N fertilizer has limited capacity to improve crop yield. The N application rate (N_{rate}) above the optimum N application rate (N_{opt}) would not result in additional grain yield, along with low NUE and high N surplus (Peng et al., 2020). In China, when compared with knowledge-based N_{opt} with 30-60% N savings, the actual agricultural N practices annually do not significantly increase crop yields but do lead to about 2 times larger N losses to the environment (Ju et al., 2009). Efficient use of N fertilizer has raised concerns and is important for maximizing returns while simultaneously protecting the environment (Dhital and Raun, 2016; Song et al., 2018). N availability or N_{rate} can influence the response of plants to ozone stress (Bielenberg et al.,

2001). The interaction between ozone and N on crops should be explored in order to improve the certainty in the estimation and projection of ozone risk on crop production with consideration of N (Peng et al., 2020). Compared to the recommended N (120 kg N ha^{-1}), the higher N treatment (180 kg N ha^{-1}) benefits the up-regulation of the antioxidant defense system under ozone stress in wheat (Pandey et al., 2018). A recent study found that extra N fertilizer applied at anthesis can mitigate the ozone impacts on N content and translocation (Brewster et al., 2024). More in-depth studies have been carried out in maize, relative to NF (non-filtered ambient air), NF60 significantly increased the N_{opt} by 68.7% and 122.6% in grain yield and plant biomass, respectively, but not potentials of them (Peng et al., 2020). The N_{opt} is dependent on crop species, inter-annual and geographic variability, and there is less information available on the responses of wheat to the interactive effects of ozone and N fertilizer. In this study, the genotypic difference at certain N fertilizer application, manifested as large variation of different NUE indicators under ozone exposure, provided a basis for selecting genotype with higher NUE. The influence of ozone on the benefits from N fertilization managements would be more serious with the raising ozone concentration in some regions, urging us to investigate the impact of ozone on N fertilization management, and optimize the time, frequency, dose and type of fertilization to improve the N uptake capacity and antioxidant capacity of plant to cope with ozone stress (Agathokleous et al., 2023).

Moreover, the reduction in NUE under ozone exposure depends not only on the amount of N accumulated, but also on the N distribution within the plant during grain filling (Broberg et al., 2017). In C3 plant species, the strong linearity between maximum rates of CO_2 assimilation and leaf N emphasised the importance of N, and its allocation, in optimizing CO_2 exchange processes (Farquhar et al., 1980). Our results revealed there was no significant differences of N concentrations in straw between control and ozone conditions, while straw C:N ratios were significantly increased after anthesis and by 12.20% at harvest among all genotypes, relative to control condition. Ozone causes opposite changes in C:N ratios in straw and grain, implying the impacts of ozone on nutrient remobilization. Post-anthesis N remobilization from vegetative organs affects the N accumulation in grain (Chen et al., 2015), while elevated ozone accelerates leaf senescence and shortens grain filling in wheat (Gelang et al., 2000). In soybean, the dynamics of leaf N in elevated ozone mirrored those in ambient air (Dermody et al., 2006), which is different from the results in hybrid poplar that ozone-induced accelerated senescence triggered the N remobilization from the older leaves to young leaves (Bielenberg et al., 2002). Besides the environmental factors, N remobilization from the vegetative organs to the grains also depends on genotypes in wheat (Barbottin et al., 2005). N remobilization efficiency (NRE)

can be estimated as the proportion of N remobilized in total N at anthesis in vegetative organs (Bogard et al., 2010). Chronic ozone reduced the NRE and both N pools of leaf and stem (Broberg et al., 2021). Net gain of elements in grains is the result of both remobilization from vegetative tissues and direct uptake by roots under ozone stress. Since element uptake and remobilization are highly variable for both nutrients including N and non-essential elements, further exploration of ozone impacts on different wheat genotypes, combined with the ^{15}N tracer experiment would contribute to solve how N uptake and remobilization change could affect wheat tolerance to elevated ozone.

Ozone has a strong potential to affect a wide range of quality traits in crops (Wang and Frei, 2011). Our results is consistent to previous observations of positive effects on protein concentration, and reductions on protein yield of grain under ozone exposure in wheat (Broberg et al., 2020). Ozone exposure adversely affects the biomass allocation and growth rate of the whole-plant, because the diversion of biomass to shoot growth is required to facilitate plant defense against ROS and ozone-derived ROS and ultimately to enable repair of ozone-induced foliar wounding (Farrar, 1989; Grantz et al., 2006). In addition, ozone-induced allometric shift in carbohydrate allocation is not mediated by photosynthetic inhibition nor by alteration of development age, while by direct effects on phloem loading (Grantz and Yang, 2000), resulting in inhibition of translocation to other organs including grains. A meta-analysis demonstrated that starch concentration was negatively affected with the exception of spring wheat (Broberg et al., 2015). Based on the structure of starch, the total of starch can be classified into amylose and amylopectin. In rice, the amylose concentration and the ratio of amylose to amylopectin was significantly affected by ozone stress (Wang et al., 2014a). In baking properties of wheat, dry and wet gluten contents were positively influenced by ozone stress. Moreover, the increase in Zeleny values was observed with elevated ozone, indicating the trend of better protein quality (Fuhrer et al., 1992). Ozone exposure also increased the Hagberg falling number, indicating lower α-amylase activity in the endosperm (Piikki et al., 2008). Grain chalkiness is a key factor determining the appearance quality of rice, influencing the acceptance of consumers. Ozone significantly increased the chalkiness area and degree (Wang et al., 2014a), which might be associated with ozone-induced reductions in C and N levels during grain filling (Jing et al., 2016). In addition, the effects of ozone on other minerals in wheat were reported in different experiments, and macronutrient concentrations including P, K, Mg and Ca, were also increased by ozone (Broberg et al., 2015).

Different element HI were analyzed previously, including nutrients and nonessential elements

in wheat in order to investigate the efficiency of nutrient remobilization and transport from vegetative to reproductive tissue during grain filling (Lv et al., 2020). The highest among 13 element HI was found for N and P, and both of them are important macronutrients limiting plant growth (Broberg et al., 2021; Elser et al., 2007). Our study revealed there was a strong positive correlation between HI and NHI, while long-term ozone fumigation led to significant reduction in the regression slope between HI and NHI, indicating that ozone treatment significantly affects the coupling relationship of biomass and the N-related nutrition allocation to grain in wheat. Ecological stoichiometry is aim to assess the balance of multiple chemical elements in ecological interactions (Elser et al., 2000). Since elements operate mostly as parts of molecular compounds, shifts in the elemental stoichiometry to changing environmental conditions, such as ozone, should be related to metabolomic changes (Rivas-Ubach et al., 2012). Some studies have focused on the effects of ozone on C and N allocation and their ecological stoichiometry of plants such as in maize (Peng et al., 2021). P is a critical element in the production of phosphorus-rich ribosomes and rRNA to support the synthesis of N-rich proteins (Ågren, 2008), and was also included in a similar study in which NF60 has negative impacts on C:P ratios in all organs of poplar (Shang et al., 2018). Future assessment of ozone effects on wheat would include C, N and P of the different organs to investigate the nutrient allocation and ecological stoichiometry.

5.3 Molecular breeding of ozone-tolerant crops

In Chapter 4, two haplotypes had 10 SNP markers located within a locus significantly associated with LBS and had significantly different LBS in ozone treatment, that is, tolerant haplotype (ATAGCACCTC) and sensitive haplotype (GGGATGTTCA) (Figure 5.1). Both sensitive genotypes showed significant effects of ozone on net CO_2 assimilation a. The factor causing reduction in net photosynthetic rate can be grouped into stomatal and non-stomatal factors (Akhtar et al., 2010). Environmental stress results in a reduction in net photosynthetic rate through acting on chloroplasts directly, becoming a non-stomatal factor in restricting net photosynthetic rate (Zheng et al., 2000). Non-stomatal factors mainly include following aspects: (1) the increase in diffusive resistance to CO_2 in mesophyll; (2) the decrease in activities of photosystem II, photophosphorylation and Rubisco, (3) the decrease in chlorophyll content and inhibition of electron transport. Besides, leaf metabolism reacts not only via the CO_2: O_2 partitioning of Rubisco kinetics an activation, but also through “ancillary” metabolisms that may have direct and indirect effects on observed CO_2 assimilation rate. N assimilation, amino acid and protein synthesis, lipid production and secondary metabolism represent significant C

and electron sinks, potentially inhibiting sucrose synthesis or RuBP regeneration, and affecting relationships between photosynthesis and photorespiration and thus net CO_2 assimilation (Tcherkez and Limami, 2019).

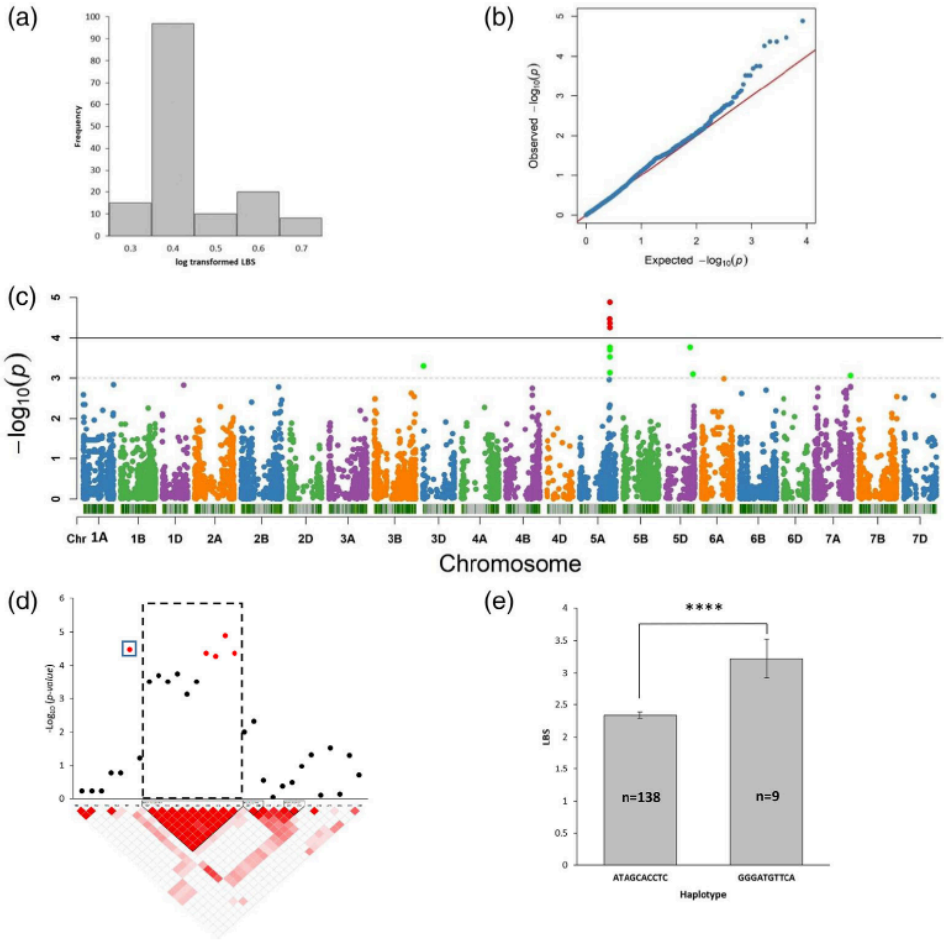

Figure 5.1 Analysis of marker-trait associations for leaf bronzing score (LBS). (a) Frequency distribution of log10 transformed LBS data. (b) qq-Plot illustrating the correlation between expected and observed –log10(p) values. (c) Manhattan plots displaying the significance of marker-trait associations; the vertical line indicates the false discovery rate (FDR) threshold; the green-colored SNPs above the dotted black line represent significant SNPs which did not reach the FDR level. (d) Local linkage disequilibrium (LD) analysis of the peak area on chromosome 5A; in the LD matrix darker red indicates higher pairwise LD between two markers, and the dashed line indicates an LD block. (e) Comparison of phenotypic values between haplotype groups formed for the markers included in the LD block shown in panel (d); mean values and standard errors are plotted; n indicates the number of lines representing each of the haplotypes; ****$p < 0.0001$. This figure was adapted from Begum et al. (2020).

PREATPRODH in the cis-elements of TraesCS5A01G400500 was found only in the tolerant haplotypes, which is involved in expression of proline dehydrogenase (ProDH) in responses to L-Pro and hypo-osmolarity (Satoh et al., 2002). Proline is essential for plant recovery from stress and was discussed herein additionally. In proline metabolism, dehydration can activate

its biosynthesis and catabolism, whereas rehydration triggers the opposite regulation (Verbruggen et al., 1996). While the correlation between proline accumulation and abiotic stress tolerance in plants were obscure, most studies concluded that ability of proline to scavenge ROS and to inhibit ROS-mediated apoptosis can be an important function in response to cellular stress. Increased accumulation of proline was correlated with improved tolerance to various abiotic stresses (Gill and Tuteja, 2010). For example, salt-induced proline accumulation results from the reciprocal action of activated biosynthesis and inhibited proline degradation in *Brassica napus*, while salt-hypersensitive mutants of *Arabidopsis thaliana* had higher proline content than wild type (Liu and Zhu, 1997; Verbruggen and Hermans, 2008). Plants with mutations at the *eskimo1* (*esk1*) locus accumulated high levels of proline, did not exhibit constitutively increased gene expression involved in freezing tolerance (Xin and Browse, 1998). However, overexpression of the *GmDREB6* gene improved salt tolerance accompanied with higher proline accumulation in soybean (Nguyen et al., 2019). As for the involvement of proline in plant responses to ozone, the proline content in blackgram also increased under ozone stress (Dhevagi et al., 2022). Ozone stress only induce accumulation of proline in the most ozone-sensitive ecotypes in Arabidopsis (Boublin et al., 2022). In oak, seedlings of three species had different responses of proline under ozone stress, suggesting that the effect of ozone on proline accumulation might depend on the genotypic variation (Cotrozzi et al., 2016). In wheat, elevated ozone induced accumulation of proline due to the up-regulation of pyrroline-5-carboxylate synthetase (*P5CS*) at transcript level, while the leaf samples were collected after 20 days of fumigation for proline assay (Li et al., 2016). There were less studies related to proline metabolism of wheat under ozone stress, and further research is needed to investigate its involvement in the regulation of the ozone response.

Our previous GWAS revealed large genetic diversity of the ozone response in wheat, which is a key resource for genetic research and trait improvement in plants (Begum et al., 2020). Eleven candidate genes underlie symptom formation in ozone stress, including cytochrome P450 proteins, peroxidases and oxidoreductase, and their identification and elucidation of physiological mechanisms is awaited in the future. In addition to gene expression analyses, followed sequencing analyses is required between haplotypes, and further characterization of gene functions is needed to explore the regulation of ozone tolerance. Bioinformatic analyses and subcellular localization can provide basic information of genes, such as unrooted phylogenetic tree. Generation of transgenic plants or knockout lines should be followed by phenotype observation and quantification of antioxidant enzyme activity. Analyses of

recombinant proteins are helpful for protein characteristics, such as peroxidases type. Those experiments would contribute to the breeding of ozone-tolerant wheat cultivar in the future.

Compared to conventional plant breeding, maker-assisted breeding improved the efficiency and precision, and was suggested to be the most promising breeding approach for ozone-tolerant crops (Agathokleous et al., 2023). QTLs and candidate genes are the prerequisite for marker-assisted selection (MAS) in molecular breeding (Frei, 2015; Mills et al., 2018). QTLs related in ozone tolerance also have been identified in maize and rice. Based on B73-Mo17 nearly isogenic lines (NIL) of maize, a significant leaf damage QTL was identified at 161Mb on chromosome 2 of Mo17 NILs (Sorgini et al., 2019). There were more advances on the breeding of ozone-tolerant rice. Two experiments of QTL mapping were conducted on different recombinant inbred lines (RILs) under acute and chronic ozone exposure, respectively (Frei et al., 2008; Kim et al., 2004). In the latter, three QTLs were identified: OzT3 and OzT9 for LBS, and OzT8 for relative biomass, after confirmation by chromosome segment lines (CSSL) (Frei et al., 2010). The developed OzT8/OzT9 breeding lines showed less reduction in the total biomass, spikelet number per panicle after long-term ozone fumigation (Wang et al., 2014b). Those results suggest that the improvement of crops using marker-based approach is possible and it would contribute to the future food security under climate change. Compared to bi-parental populations, GWAS can dissect large natural populations for important traits and takes advantage of the numerous genetic recombination (Brachi et al., 2011). It has been conducted for ozone tolerance in rice and wheat (Begum et al., 2020; Ueda et al., 2015), and the verification of candidate loci and genes is required for further marker-assisted breeding. However, those approaches remain constraints, such as linkage drag. Transferring large chromosomal fragments in the breeding process might introduce genes with negative effects.

Transgenic approaches would introduce novel ozone tolerance genes from other species into targeted crop, while have the problem of environmental concerns and consumer acceptance. In contrast, the clustered regularly interspaced short palindromic repeat (CRISPR)-associated protein 9 (Cas9) genome editing system is the most powerful gene editing tool available, which are most commonly used to induce the generation of out-frame mutations in interest genes (Mao et al., 2019). Recently, CRISPR/Cas-based gene editing was suggested to fix desirable allelic variants, generate novel alleles, break deleterious genetic linkages, support pre-breeding and for introgression of favorable loci into elite lines (Lyzenga et al., 2021). With the increasing of ozone concentration, it is urgent to improve ozone tolerance of crops in the future, especially for food security.

5.4 Summary

Our experimental results investigated the large variation of ozone responses in wheat among eighteen different genotypes from multi-perspectives, including photosynthesis, phenotype, yield, nutrient allocation and physiological traits. In Chapter 2, experimental data of different tolerant or sensitive varieties, respectively, was used to parametrize the LINTULCC2 crop model expanded with an ozone response routine. The specified parameters representing the distinct physiological responses of contrasting genotypes improved the accuracy of simulation studies. Considering the differences between controlled open-top chamber and field-based FACE-experiments (Feng et al., 2018), further experimental studies under field conditions will be helpful to validate and fine-tune the current model in wheat. In Chapter 3, ozone exposure significantly affected the relationship of N and biomass allocation into wheat grain based on the relationship between HI and NHI. The investigation of interaction between soil nitrogen level and ozone stress in wheat would be helpful to accurately estimate ozone impacts on wheat with consideration of N. Further C and N allocation and their ecological stoichiometric responses in different organs of wheat would contribute to verifying N_{opt} model considering ozone pollution in the future. In Chapter 4, the gene TraesCS5A01G400500 putatively involved in peroxidase activity was only upregulated in tolerant haplotypes, which might explain contrasting physiological responses after ozone fumigation and warrant further studies. Cloning the candidate gene and analyses of recombinant protein would further confirm the gene function. Plant transformation with overexpression gene or mutants would validate the gene function and related-regulation of ozone tolerance, such as comparison of peroxidase activity between different lines. Further studies are warranted to explore the tolerance mechanism under ozone stress in wheat.

References

Agathokleous, E., Frei, M., Knopf, O.M., Muller, O., Xu, Y., Nguyen, T.H., Gaiser, T., Liu, X., Liu, B., Saitanis, C.J., Shang, B., Alam, M.S., Feng, Y., Ewert, F., Feng, Z., 2023. Adapting crop production to climate change and air pollution at different scales. Nat. Food.

Ågren, G.I., 2008. Stoichiometry and Nutrition of Plant Growth in Natural Communities. Annu. Rev. Ecol. Evol. Syst. 39, 153-170.

Akhtar, N., Yamaguchi, M., Inada, H., Hoshino, D., Kondo, T., Izuta, T., 2010. Effects of ozone on growth, yield and leaf gas exchange rates of two Bangladeshi cultivars of

wheat (*Triticum aestivum* L.). Environ. Pollut. 158, 1763-1767.

Ambus, P., 1998. Nitrous oxide production by denitrification and nitrification in temperate forest, grassland and agricultural soils. Eur. J. Soil Sci. 49, 495-502.

Babar, M.A., Reynolds, M.P., van Ginkel, M., Klatt, A.R., Raun, W.R., Stone, M.L., 2006. Spectral Reflectance Indices as a Potential Indirect Selection Criteria for Wheat Yield under Irrigation. Crop Sci. 46, 578-588.

Barbottin, A., Lecomte, C., Bouchard, C., Jeuffroy, M.-H., 2005. Nitrogen Remobilization during Grain Filling in Wheat: Genotypic and Environmental Effects. Crop Sci. 45, 1141-1150.

Begum, H., Alam, M.S., Feng, Y., Koua, P., Ashrafuzzaman, M., Shrestha, A., Kamruzzaman, M., Dadshani, S., Ballvora, A., Naz, A.A., Frei, M., 2020. Genetic dissection of bread wheat diversity and identification of adaptive loci in response to elevated tropospheric ozone. Plant Cell Environ. 43, 2650-2665.

Bielenberg, D.G., Lynch, J.P., Pell, E.J., 2001. A decline in nitrogen availability affects plant responses to ozone. New Phytol. 151, 413-425.

Bielenberg, D.G., Lynch, J.P., Pell, E.J., 2002. Nitrogen dynamics during O_3-induced accelerated senescence in hybrid poplar. Plant Cell Environ. 25, 501-512.

Biswas, D.K., Xu, H., Li, Y.G., Sun, J.Z., Wang, X.Z., Han, X.G., Jiang, G.M., 2008. Genotypic differences in leaf biochemical, physiological and growth responses to ozone in 20 winter wheat cultivars released over the past 60 years. Glob. Chang. Biol. 14, 46-59.

Bogard, M., Allard, V., Brancourt-Hulmel, M., Heumez, E., Machet, J.M., Jeuffroy, M.H., Gate, P., Martre, P., Le Gouis, J., 2010. Deviation from the grain protein concentration-grain yield negative relationship is highly correlated to post-anthesis N uptake in winter wheat. J. Exp. Bot. 61, 4303-4312.

Boublin, F., Cabassa-Hourton, C., Leymarie, J., Leitao, L., 2022. Potential involvement of proline and flavonols in plant responses to ozone. Environ. Res. 207, 112214.

Brachi, B., Morris, G.P., Borevitz, J.O., 2011. Genome-wide association studies in plants: the missing heritability is in the field. Genome Biol.

Brewster, C., Fenner, N., Hayes, F., 2024. Chronic ozone exposure affects nitrogen remobilization in wheat at key growth stages. Sci. Total Environ. 908, 168288.

Broberg, M., Daun, S., Pleijel, H., 2020. Ozone Induced Loss of Seed Protein Accumulation Is Larger in Soybean than in Wheat and Rice. Agronomy 10.

Broberg, M.C., Feng, Z., Xin, Y., Pleijel, H., 2015. Ozone effects on wheat grain quality - a

summary. Environ. Pollut. 197, 203-213.

Broberg, M.C., Uddling, J., Mills, G., Pleijel, H., 2017. Fertilizer efficiency in wheat is reduced by ozone pollution. Sci. Total Environ. 607-608, 876-880.

Broberg, M.C., Xu, Y., Feng, Z., Pleijel, H., 2021. Harvest index and remobilization of 13 elements during wheat grain filling: Experiences from ozone experiments in China and Sweden. Field Crops Res. 271.

Brosché, M., Merilo, E., Mayer, F., Pechter, P., Puzõrjova, I., Brader, G., Kangasjärvi, J., Kollist, H., 2010. Natural variation in ozone sensitivity among Arabidopsis thaliana accessions and its relation to stomatal conductance. Plant Cell Environ. 33, 914-925.

Chen, Y., Xiao, C., Wu, D., Xia, T., Chen, Q., Chen, F., Yuan, L., Mi, G., 2015. Effects of nitrogen application rate on grain yield and grain nitrogen concentration in two maize hybrids with contrasting nitrogen remobilization efficiency. Eur. J. Agron. 62, 79-89.

Congreves, K.A., Otchere, O., Ferland, D., Farzadfar, S., Williams, S., Arcand, M.M., 2021. Nitrogen Use Efficiency Definitions of Today and Tomorrow. Front. Plant Sci. 12, 637108.

Cotrozzi, L., Remorini, D., Pellegrini, E., Landi, M., Massai, R., Nali, C., Guidi, L., Lorenzini, G., 2016. Variations in physiological and biochemical traits of oak seedlings grown under drought and ozone stress. Physiol. Plant 157, 69-84.

Damm, A., Cogliati, S., Colombo, R., Fritsche, L., Genangeli, A., Genesio, L., Hanus, J., Peressotti, A., Rademske, P., Rascher, U., Schuettemeyer, D., Siegmann, B., Sturm, J., Miglietta, F., 2022. Response times of remote sensing measured sun-induced chlorophyll fluorescence, surface temperature and vegetation indices to evolving soil water limitation in a crop canopy. Remote Sens. Environ. 273.

Degen, G.E., Orr, D.J., Carmo-Silva, E., 2021. Heat-induced changes in the abundance of wheat Rubisco activase isoforms. New Phytol. 229, 1298-1311.

Dermody, O., Long, S.P., DeLucia, E.H., 2006. How does elevated CO_2 or ozone affect the leaf-area index of soybean when applied independently? New Phytol. 169, 145-155.

Dhevagi, P., Ramya, A., Poornima, R., Priyatharshini, S., 2022. Response of blackgram cultivars to elevated tropospheric ozone. Madras Agric. J. 108, 1.

Dhital, S., Raun, W.R., 2016. Variability in Optimum Nitrogen Rates for Maize. Agron. J. 108, 2165-2173.

Di, H., Cameron, K., 2002. Nitrate leaching in temperate agroecosystems: sources, factors and mitigating strategies. Nutr. Cycling Agroecosyst. 64, 237-256.

Elser, J.J., Bracken, M.E., Cleland, E.E., Gruner, D.S., Harpole, W.S., Hillebrand, H., Ngai,

J.T., Seabloom, E.W., Shurin, J.B., Smith, J.E., 2007. Global analysis of nitrogen and phosphorus limitation of primary producers in freshwater, marine and terrestrial ecosystems. Ecol. Lett. 10, 1135-1142.

Elser, J.J., Sterner, R.W., Gorokhova, E., Fagan, W.F., Markow, T.A., Cotner, J.B., Harrison, J.F., Hobbie, S.E., Odell, G.M., Weider, L.W., 2000. Biological stoichiometry from genes to ecosystems. Ecol. Lett. 3, 540-550.

Ewert, F., Porter, J.R., 2000. Ozone effects on wheat in relation to CO_2: modelling short-term and long-term responses of leaf photosynthesis and leaf duration. Glob. Chang. Biol. 735-750, 1354-1013.

Farquhar, G.D., von Caemmerer, S., Berry, J.A., 1980. A biochemical model of photosynthetic CO_2 assimilation in leaves of C3 species. Planta 149, 78-90.

Farrar, J., 1989. The carbon balance of fast-growing and slow-growing species. Causes and consequences of variation in growth rate and productivity of higher plants, 241-256.

Feng, Z., Pang, J., Kobayashi, K., Zhu, J., Ort, D.R., 2011. Differential responses in two varieties of winter wheat to elevated ozone concentration under fully open-air field conditions. Glob. Chang. Biol. 17, 580-591.

Feng, Z., Pang, J., Nouchi, I., Kobayashi, K., Yamakawa, T., Zhu, J., 2010. Apoplastic ascorbate contributes to the differential ozone sensitivity in two varieties of winter wheat under fully open-air field conditions. Environ. Pollut. 158, 3539-3545.

Feng, Z., Uddling, J., Tang, H., Zhu, J., Kobayashi, K., 2018. Comparison of crop yield sensitivity to ozone between open-top chamber and free-air experiments. Glob. Chang. Biol. 24, 2231-2238.

Feng, Z., Wang, L., Pleijel, H., Zhu, J., Kobayashi, K., 2016. Differential effects of ozone on photosynthesis of winter wheat among cultivars depend on antioxidative enzymes rather than stomatal conductance. Sci. Total Environ. 572, 404-411.

Fiscus, E.L., Booker, F.L., Burkey, K.O., 2005. Crop responses to ozone: uptake, modes of action, carbon assimilation and partitioning. Plant Cell Environ. 28, 997-1011.

Frei, M., 2015. Breeding of ozone resistant rice: relevance, approaches and challenges. Environ. Pollut. 197, 144-155.

Frei, M., Tanaka, J.P., Chen, C.P., Wissuwa, M., 2010. Mechanisms of ozone tolerance in rice: characterization of two QTLs affecting leaf bronzing by gene expression profiling and biochemical analyses. J. Exp. Bot. 61, 1405-1417.

Frei, M., Tanaka, J.P., Wissuwa, M., 2008. Genotypic variation in tolerance to elevated ozone in rice: dissection of distinct genetic factors linked to tolerance mechanisms. J. Exp.

Bot. 59, 3741-3752.

Fuhrer, J., Grimm, A.G., Tschannen, W., Shariat-Madari, H., 1992. The response of spring wheat (Triticum aestivum L.) to ozone at higher elevations. II. Changes in yield, yield components and grain quality in response to ozone flux. New Phytol. 121, 211-219.

Gelang, J., Pleijel, H., Sild, E., Danielsson, H., Younis, S., Selldén, G., 2000. Rate and duration of grain filling in relation to flag leaf senescence and grain yield in spring wheat (Triticum aestivum) exposed to different concentrations of ozone. Physiol. Plant. 110, 366-375.

Gill, S.S., Tuteja, N., 2010. Reactive oxygen species and antioxidant machinery in abiotic stress tolerance in crop plants. Plant Physiol. Biochem. 48, 909-930.

Goumenaki, E., Taybi, T., Borland, A., Barnes, J., 2010. Mechanisms underlying the impacts of ozone on photosynthetic performance. Environ. Exp. Bot. 69, 259-266.

Grantz, D.A., Gunn, S., Vu, H.B., 2006. O_3 impacts on plant development: a meta-analysis of root/shoot allocation and growth. Plant Cell Environ. 29, 1193-1209.

Grantz, D.A., Yang, S., 2000. Ozone impacts on allometry and root hydraulic conductance are not mediated by source limitation nor developmental age. J. Exp. Bot. 51, 919-927.

Guarin, J.R., Kassie, B., Mashaheet, A.M., Burkey, K., Asseng, S., 2019. Modeling the effects of tropospheric ozone on wheat growth and yield. Eur. J. Agron. 105, 13-23.

Hassan, M.A., Yang, M., Rasheed, A., Yang, G., Reynolds, M., Xia, X., Xiao, Y., He, Z., 2019. A rapid monitoring of NDVI across the wheat growth cycle for grain yield prediction using a multi-spectral UAV platform. Plant Sci. 282, 95-103.

Jensen, L.S., Schjoerring, J.K., van Der Hoek, K.W., Damgaard-Poulsen, H., Zevenbergen, J.F., Pallière, C., Lammel, J., Brentrup, F., Jongbloed, A.W., Willems, J., 2011. Benefits of nitrogen for food, fibre and industrial production.

Jiang, L., Liu, Y., Wu, S., Yang, C., 2021. Analyzing ecological environment change and associated driving factors in China based on NDVI time series data. Ecol. Indic. 129.

Jing, L., Dombinov, V., Shen, S., Wu, Y., Yang, L., Wang, Y., Frei, M., 2016. Physiological and genotype-specific factors associated with grain quality changes in rice exposed to high ozone. Environ. Pollut. 210, 397-408.

Ju, X.T., Xing, G.X., Chen, X.P., Zhang, S.L., Zhang, L.J., Liu, X.J., Cui, Z.L., Yin, B., Christie, P., Zhu, Z.L., Zhang, F.S., 2009. Reducing environmental risk by improving N management in intensive Chinese agricultural systems. Proc. Natl. Acad. Sci. U S A 106, 3041-3046.

Kellogg, E.A., Juliano, N.D., 1997. The structure and function of RuBisCO and their

Implications for Systematic Studies. Am. J. Bot. 84, 413-428.

Kim, K.-M., Kwon, Y.-S., Lee, J.-J., Eun, M.-Y., Sohn, J.-K., 2004. QTL mapping and molecular marker analysis for the resistance of rice to ozone. Mol. Cells (Springer Science & Business Media BV) 17.

Kumar, R.R., Goswami, S., Singh, K., Dubey, K., Singh, S., Sharma, R., Verma, N., Kala, Y.K., Rai, G.K., Grover, M., Mishra, D.C., Singh, B., Pathak, H., Chinnusamy, V., Rai, A., Praveen, S., 2016. Identification of Putative RuBisCo Activase (TaRca1)-The Catalytic Chaperone Regulating Carbon Assimilatory Pathway in Wheat (Triticum aestivum) under the Heat Stress. Front. Plant Sci. 7, 986.

Langholtz, M., Davison, B.H., Jager, H.I., Eaton, L., Baskaran, L.M., Davis, M., Brandt, C.C., 2021. Increased nitrogen use efficiency in crop production can provide economic and environmental benefits. Sci. Total Environ. 758, 143602.

Leitao, L., Dizengremel, P., Biolley, J.P., 2008. Foliar CO_2 fixation in bean (Phaseolus vulgaris L.) submitted to elevated ozone: distinct changes in Rubisco and PEPc activities in relation to pigment content. Ecotoxicol. Environ. Saf. 69, 531-540.

Leitao, L., Goulas, P., Biolley, J.-P., 2003. Time-course of Rubisco oxidation in beans (Phaseolus vulgaris L.) subjected to a long-term ozone stress. Plant Sci. 165, 613-620.

Li, C., Meng, J., Guo, L., Jiang, G., 2016. Effects of ozone pollution on yield and quality of winter wheat under flixweed competition. Environ. Exp. Bot. 129, 77-84.

Li, S.X., Wang, Z.H., Hu, T.T., Gao, Y.J., Stewart, B.A., 2009. Chapter 3 Nitrogen in Dryland Soils of China and Its Management, pp. 123-181.

Liu, J., Zhu, J.-K., 1997. Proline accumulation and salt-stress-induced gene expression in a salt-hypersensitive mutant of Arabidopsis. Plant Physiol. 114, 591-596.

Lv, X., Zhang, Y., Zhang, Y., Fan, S., Kong, L., 2020. Source-sink modifications affect leaf senescence and grain mass in wheat as revealed by proteomic analysis. BMC Plant Biol. 20, 257.

Lyzenga, W.J., Pozniak, C.J., Kagale, S., 2021. Advanced domestication: harnessing the precision of gene editing in crop breeding. Plant Biotechnol. J. 19, 660-670.

Mao, Y., Botella, J.R., Liu, Y., Zhu, J.K., 2019. Gene editing in plants: progress and challenges. Natl. Sci. Rev. 6, 421-437.

Mills, G., Sharps, K., Simpson, D., Pleijel, H., Frei, M., Burkey, K., Emberson, L., Uddling, J., Broberg, M., Feng, Z., Kobayashi, K., Agrawal, M., 2018. Closing the global ozone yield gap: Quantification and cobenefits for multistress tolerance. Glob. Chang. Biol. 24, 4869-4893.

Naser, M., Khosla, R., Longchamps, L., Dahal, S., 2020. Using NDVI to Differentiate Wheat Genotypes Productivity Under Dryland and Irrigated Conditions. Remote Sens. 12.

Nguyen, Q.H., Vu, L.T.K., Nguyen, L.T.N., Pham, N.T.T., Nguyen, Y.T.H., Le, S.V., Chu, M.H., 2019. Overexpression of the GmDREB6 gene enhances proline accumulation and salt tolerance in genetically modified soybean plants. Sci. Rep. 9, 19663.

Nguyen, T.H., Langensiepen, M., Hueging, H., Gaiser, T., Seidel, S.J., Ewert, F., 2022. Expansion and evaluation of two coupled root–shoot models in simulating CO_2 and H_2O fluxes and growth of maize. Vadose Zone Journal 21.

Nguyen, T.H., Langensiepen, M., Vanderborght, J., Hüging, H., Mboh, C.M., Ewert, F., 2020. Comparison of root water uptake models in simulating CO_2 and H_2O fluxes and growth of wheat. Hydro. Earth Syst. Sci. 24, 4943-4969.

Niu, J., Feng, Z., Zhang, W., Zhao, P., Wang, X., 2014. Non-stomatal limitation to photosynthesis in Cinnamomum camphora seedings exposed to elevated O_3. PLoS One 9, e98572.

Osborne, S., Pandey, D., Mills, G., Hayes, F., Harmens, H., Gillies, D., Buker, P., Emberson, L., 2019. New Insights into Leaf Physiological Responses to Ozone for Use in Crop Modelling. Plants (Basel) 8.

Pandey, A.K., Ghosh, A., Agrawal, M., Agrawal, S.B., 2018. Effect of elevated ozone and varying levels of soil nitrogen in two wheat (Triticum aestivum L.) cultivars: Growth, gas-exchange, antioxidant status, grain yield and quality. Ecotoxicol. Environ. Saf. 158, 59-68.

Pelloux, J., Jolivet, Y., Fontaine, V., Banvoy, J., Dizengremel, P., 2001. Changes in Rubisco and Rubisco activase gene expression and polypeptide content in Pinus halepensis M. subjected to ozone and drought. Plant Cell Environ. 24, 123-131.

Peng, J., Xu, Y., Shang, B., Agathokleous, E., Feng, Z., 2021. Effects of elevated ozone on maize under varying soil nitrogen levels: Biomass, nitrogen and carbon, and their allocation to kernel. Sci. Total Environ. 765, 144332.

Peng, J., Xu, Y., Shang, B., Qu, L., Feng, Z., 2020. Impact of ozone pollution on nitrogen fertilization management during maize (Zea mays L.) production. Environ. Pollut. 266, 115158.

Pettorelli, N., Vik, J.O., Mysterud, A., Gaillard, J.M., Tucker, C.J., Stenseth, N.C., 2005. Using the satellite-derived NDVI to assess ecological responses to environmental change. Trends Ecol. Evol. 20, 503-510.

Piikki, K., De Temmerman, L., Ojanperä, K., Danielsson, H., Pleijel, H., 2008. The grain

quality of spring wheat (Triticum aestivum L.) in relation to elevated ozone uptake and carbon dioxide exposure. Eur. J. Agron. 28, 245-254.

Ristic, Z., Momcilovic, I., Bukovnik, U., Prasad, P.V., Fu, J., Deridder, B.P., Elthon, T.E., Mladenov, N., 2009. Rubisco activase and wheat productivity under heat-stress conditions. J. Exp. Bot. 60, 4003-4014.

Rivas-Ubach, A., Sardans, J., Perez-Trujillo, M., Estiarte, M., Penuelas, J., 2012. Strong relationship between elemental stoichiometry and metabolome in plants. Proc. Natl. Acad. Sci. U S A 109, 4181-4186.

Rodriguez, D., Ewert, F., Goudriaan, J.M., R. Burkart, S., Weigel, H.J., 2001. Modelling the response of wheat canopy assimilation to atmospheric CO_2 concentrations. New Phytol. 150, 337-346.

Satoh, R., Nakashima, K., Seki, M., Shinozaki, K., Yamaguchi-Shinozaki, K., 2002. ACTCAT, a novel cis-acting element for proline- and hypoosmolarity-responsive expression of the ProDH gene encoding proline dehydrogenase in Arabidopsis. Plant Physiol. 130, 709-719.

Shang, B., Feng, Z., Gao, F., Calatayud, V., 2020. The ozone sensitivity of five poplar clones is not related to stomatal conductance, constitutive antioxidant levels and morphology of leaves. Sci. Total Environ. 699, 134402.

Shang, B., Feng, Z., Li, P., Calatayud, V., 2018. Elevated ozone affects C, N and P ecological stoichiometry and nutrient resorption of two poplar clones. Environ. Pollut. 234, 136-144.

Song, X., Liu, M., Ju, X., Gao, B., Su, F., Chen, X., Rees, R.M., 2018. Nitrous Oxide Emissions Increase Exponentially When Optimum Nitrogen Fertilizer Rates Are Exceeded in the North China Plain. Environ. Sci. Technol. 52, 12504-12513.

Sorgini, C.A., Barrios-Perez, I., Brown, P.J., Ainsworth, E.A., 2019. Examining Genetic Variation in Maize Inbreds and Mapping Oxidative Stress Response QTL in B73-Mo17 Nearly Isogenic Lines. Front. Sustain. Food Syst. 3.

Spreitzer, R.J., 1993. Genetic dissection of Rubisco structure and function. Annu. Rev. Plant Biol. 44, 411-434.

Syakila, A., Kroeze, C., 2011. The global nitrous oxide budget revisited. Greenh. Gas Meas. Manag. 1, 17-26.

Tcherkez, G., Limami, A.M., 2019. Net photosynthetic CO_2 assimilaiton: more than just CO_2 and O2 reduction cycles. New Phytol. 223, 520-529.

Ueda, Y., Frimpong, F., Qi, Y., Matthus, E., Wu, L., Holler, S., Kraska, T., Frei, M., 2015.

Genetic dissection of ozone tolerance in rice (Oryza sativa L.) by a genome-wide association study. J. Exp. Bot. 66, 293-306.

Verbruggen, N., Hermans, C., 2008. Proline accumulation in plants: a review. Amino Acids 35, 753-759.

Verbruggen, N., Hua, X.-J., May, M., Van Montagu, M., 1996. Environmental and developmental signals modulate proline homeostasis: evidence for a negative transcriptional regulator. Proc. Natl. Acad. Sci. 93, 8787-8791.

Wang, Y., Frei, M., 2011. Stressed food – The impact of abiotic environmental stresses on crop quality. Agric. Ecosyst. Environ. 141, 271-286.

Wang, Y., Song, Q., Frei, M., Shao, Z., Yang, L., 2014a. Effects of elevated ozone, carbon dioxide, and the combination of both on the grain quality of Chinese hybrid rice. Environ. Pollut. 189, 9-17.

Wang, Y., Yang, L., Höller, M., Zaisheng, S., Pariasca-Tanaka, J., Wissuwa, M., Frei, M., 2014b. Pyramiding of ozone tolerance QTLs *OzT8* and *OzT9* confers improved tolerance to season-long ozone exposure in rice. Environ. Exp. Bot. 104, 26-33.

Well, R., Weymann, D., Flessa, H., 2007. Recent research progress on the significance of aquatic systems for indirect agricultural N_2O emissions. Environ. Sci. 2, 143-151.

Wullschleger, S.D., 1993. Biochemical limitations to carbon assimilation in C3 plants—a retrospective analysis of the *A/Ci* curves from 109 species. J. Exp. Bot. 44, 907-920.

Xin, Z., Browse, J., 1998. Eskimo1 mutants of Arabidopsis are constitutively freezing-tolerant. Proc. Natl. Acad. Sci. 95, 7799-7804.

Zhang, W., Feng, Z., Wang, X., Niu, J., 2012. Responses of native broadleaved woody species to elevated ozone in subtropical China. Environ. Pollut. 163, 149-157.

Zhang, W.W., Wang, M., Wang, A.Y., Yin, X.H., Feng, Z.Z., Hao, G.Y., 2018. Elevated ozone concentration decreases whole-plant hydraulic conductance and disturbs water use regulation in soybean plants. Physiol. Plant 163, 183-195.

Zheng, Y., Lyons, T., Ollerenshaw, J.H., Barnes, J.D., 2000. Ascorbate in the leaf apoplast is a factor mediating ozone resistance in Plantago major. Plant Physiol. Biochem. 38, 403-411.

Appendices

Chapter 2

Title: Identifying and modelling key physiological traits that confer tolerance or sensitivity to ozone in winter wheat

Supplementary materials

Table A. 1 List of the wheat accessions used in this study

No	Cultivar	Origin	Year of Release
1	Memory	Germany	2013
2	KWS Santiago	England	2011
3	Durin	France	Unknown
4	Solstice	England	2001
5	Capone	Germany	2012
6	Cubus	Germany	2002
7	Edward	Germany	2013
8	Jenga	Germany	2007
9	Transit	Germany	1994
10	Gaucho	United States	1993
11	Skalmeje	Germany	2006
12	Enorm	Germany	2002
13	Sponsor	France, Ireland	1994
14	Sperber	Germany	1982
15	Apache	Czech Republic	1997
16	Isengrain	France/Slovenia/Spain	1996
17	Highbury	United Kingdom	1968
18	NS 46/90	Serbia	Unknown

Table A. 2 List of model variables and parameters

Variables	Explanation	Unit
V_{cmax}	Maximum carboxylation rate of Rubisco at leaf temperature	μM m^{-2} s^{-1}
J	Conversion energy from radiation to mole photon	mole photons MJ^{-1}
Ca	Atmospheric CO_2 concentration	μM mol^{-1}
Ci	Intercellular CO_2 concentration	μM mol^{-1}
O2	Atmospheric O_2 concentration	mM mol^{-1}
g_{st}	Stomatal conductance	mol m^{-2} s^{-1}
g_0	Residual stomatal conductance when irradiance approaches zero	mol m^{-2} s^{-1}
DS	Leaf to air vapor pressure deficit (VPD)	kPa
D_0	Parameters reflect the sensitivity of stomatal conductance to VPD	kPa
I^*	CO_2 compensation point in the absence of day respiration	μM mol^{-1}
a_1	Empirical coefficient relates photosynthesis and stomatal conductance	[-]
KMC	Michaelis-Menten constant for CO_2	μM mol^{-1}
KMO	Michaelis-Menten constant for O_2	mM mol^{-1}
EAVCMX	Energy activation for maximum carboxylation rate	J mol^{-1}
$FGR_{l,t}$	Leaf assimilation rate	μM m^{-2} s^{-1}
$AMAX_{l,t}$	Saturated photosynthesis rate	μM m^{-2} s^{-1}
$EFF_{l,t}$	Quantum yield	μM CO_2 MJ^{-1}
$I_{l,t}$	The absorbed irradiance	μM m^{-2} s^{-1}
DIFFO	Ratio of O_3/CO_2 diffusion coefficient	[-]
$OZIF_t$	Instantaneous ozone flux through stomata	nmol m^{-2} s^{-1}
OZH_t	Hourly O_3 concentration	nmol mol^{-1}
γ_1	Ozone instantaneous damage coefficient	[-]
γ_2	Ozone instantaneousdamage coefficient	(nmol m^{-2} s^{-1})$^{-1}$
γ_3	Ozone accumulative damage coefficient on leaf senescence	(nmol m^{-2} s^{-1})$^{-1}$
γ_4	Ozone accumulative damage coefficient on photosynthesis	(nmol m^{-2} s^{-1})$^{-1}$
$C_{LAO3,min}$	Cumulative ozone flux at onset of leaf senescence	nmol m^{-2}
$C_{LSO3,min}$	Cumulative ozone flux at onset of leaf senescence and effect on photosynthesis	nmol m^{-2}
MaxO3Se	Maximum rate of leaf area loss due to ozone	d^{-1}
C_{O3}	Cumulative ozone flux at certain period	nmol m^{-2}
f_{O3t}	Instantaneous damage of photosynthesis	[-]
f_{LS}	Effects of leaf senescence induced reduction of photosynthesis	[-]
f_{LA}	Ozone effects on leaf senescence	[-]
t	Subscript for time step, hour of day	
l	Subscript for sunlit and shaded leaves	
$gsO3_t$	Stomatal conductance for ozone	m s^{-1}
$G_{cuticule}$	Cuticle conductance	m s^{-1}
$rO3_t$	Leaf surface resistance to ozone	s m^{-1}

Note: The italicized and non-italicized indicate modeling variables and constants, respectively.

Table A. 3 Descriptive statistics and ANOVA results of vegetation indices collected from different wheat genotypes exposed to control and ozone conditions

		Control		Ozone		ANOVA						
Trait	**Date**	**Mean**	**SD**	**Mean**	**SD**	**T**	**G**	**DAT**	**G×T**	**DAT×T**	**DAT×G**	**DAT×G×T**
NDVI	DAT36	0.59[a]	0.02	0.59[a]	0.02	0.0865	<0.0001	<0.0001	0.0050	<0.0001	<0.0001	<0.0001
	DAT53	0.66[a]	0.02	0.66[a]	0.02							
	DAT77	0.59[a]	0.04	0.57[a]	0.05							
	DAT92	0.66[a]	0.06	0.65[a]	0.08							
	DAT106	0.67[a]	0.06	0.66[a]	0.09							
	DAT120	0.41[a]	0.21	0.33[b]	0.21							
SR	DAT36	3.9[a]	0.28	3.9[a]	0.28	0.0598	<0.0001	<0.0001	0.0270	<0.0001	<0.0001	0.0015
	DAT53	4.95[a]	0.37	4.97[a]	0.37							
	DAT77	3.97[a]	0.45	3.73[b]	0.49							
	DAT92	5.06[a]	0.93	4.98[a]	1.11							
	DAT106	5.26[a]	0.85	5.15[a]	1.07							
	DAT120	2.91[a]	1.48	2.38[b]	1.35							
MCARI	DAT36	0.14[a]	0.03	0.14[a]	0.03	0.7934	<0.0001	<0.0001	0.0001	0.0268	<0.0001	<0.0001
	DAT53	0.09[a]	0.02	0.09[a]	0.02							
	DAT77	0.06[a]	0.02	0.06[a]	0.02							
	DAT92	0.05[a]	0.02	0.06[a]	0.02							
	DAT106	0.08[a]	0.04	0.09[a]	0.07							
	DAT120	0.15[a]	0.11	0.14[a]	0.13							
SPRI	DAT36	0.97[a]	0.04	0.96[a]	0.05	0.0905	<0.0001	<0.0001	<0.0001	<0.0001	<0.0001	<0.0001
	DAT53	1.02[a]	0.04	1.01[a]	0.04							
	DAT77	1.02[a]	0.11	1.03[a]	0.11							
	DAT92	1.05[a]	0.10	1.06[a]	0.13							
	DAT106	1.12[a]	0.10	1.09[a]	0.12							
	DAT120	0.77[a]	0.30	0.68[b]	0.30							
Ctr1	DAT36	1.41[a]	0.10	1.44[a]	0.10	0.3080	<0.0001	<0.0001	0.0035	<0.0001	<0.0001	<0.0001
	DAT53	1.24[a]	0.08	1.23[a]	0.08							
	DAT77	1.16[a]	0.15	1.14[a]	0.18							
	DAT92	1.12[a]	0.22	1.14[a]	0.32							
	DAT106	1.09[a]	0.17	1.16[a]	0.35							
	DAT120	2.10[a]	0.97	2.33[b]	0.86							
Lic2	DAT36	0.86[a]	0.04	0.84[a]	0.04	0.1616	<0.0001	<0.0001	0.0020	<0.0001	<0.0001	<0.0001
	DAT53	0.94[a]	0.04	0.93[a]	0.04							
	DAT77	0.97[a]	0.11	0.99[a]	0.12							
	DAT92	1.00[a]	0.11	1.01[a]	0.14							
	DAT106	1.06[a]	0.11	1.02[a]	0.13							
	DAT120	0.70[a]	0.28	0.61[b]	0.26							
GM2	DAT36	2.52[a]	0.18	2.51[a]	0.19	0.0587	<0.0001	<0.0001	0.0264	<0.0001	<0.0001	0.0004
	DAT53	3.27[a]	0.30	3.33[a]	0.30							
	DAT77	2.95[a]	0.24	2.86[a]	0.29							
	DAT92	3.67[a]	0.51	3.61[a]	0.67							
	DAT106	3.72[a]	0.61	3.66[a]	0.79							
	DAT120	2.09[a]	1.00	1.73[b]	0.87							
ARI1	DAT36	0.13[a]	0.10	0.16[a]	0.13	0.7710	<0.0001	<0.0001	0.0001	<0.0001	<0.0001	<0.0001
	DAT53	0.18[a]	0.12	0.18[a]	0.12							
	DAT77	0.09[a]	0.23	0.01[a]	0.21							
	DAT92	-0.21[a]	0.30	-0.27[a]	0.38							
	DAT106	-0.4[a]	0.26	-0.37[a]	0.31							
	DAT120	0.53[a]	0.75	0.68[b]	0.64							
CRI2	DAT36	2.55[a]	0.33	2.69[a]	0.41	0.3951	<0.0001	<0.0001	0.2770	<0.0001	<0.0001	0.0209
	DAT53	2.57[a]	0.32	2.45[a]	0.35							
	DAT77	1.41[a]	0.69	1.10[b]	0.63							
	DAT92	2.02[a]	1.12	1.94[a]	1.12							
	DAT106	1.90[a]	0.58	1.87[a]	0.65							
	DAT120	2.00[a]	0.75	1.93[a]	0.76							

Note: Mean values per individual plant of all genotypes are shown.

Abbreviations: different superscript letters following mean values within one row indicate significant differences at $p < 0.05$ by Tukey's HSD test. ARI1, anthocyanin reflectance index 1; CRI2, carotenoid reflectance index 2; Ctr1, Carter index 1; DAT, days after transplanting; GM2, Gitelson and Merzlyak index 2; Lic2, Lichtenthaler index 2; MCARI, modified chlorophyll absorption in reflectance index; NDVI, normalized difference vegetation index; SD, standard deviation; G, genotype; SR, simple ratio

index; SRPI, simple ratio pigment index; T, treatment.

Table A. 4 Descriptive statistics and ANOVA results of photosynthesis collected from different wheat genotypes exposed to control and ozone conditions

		Control		Ozone		ANOVA						
Trait	**Date**	**Mean**	**SD**	**Mean**	**SD**	**T**	**G**	**DAT**	**G×T**	**DAT×T**	**DAT×G**	**DAT×G×T**
Net CO_2 assimilation ($\mu mol\ m^{-2}\ s^{-1}$)	DAT41	20.42[a]	3.49	21.05[a]	3.96	0.0354	0.0336	<0.0001	0.0024	<0.0001	<0.0001	0.0006
	DAT73	15.61[a]	2.76	15.19[a]	3.79							
	DAT111	11.47[a]	4.04	7.56[b]	2.17							
Stomatal conductance ($mmol\ m^{-2}\ s^{-1}$)	DAT41	379.07[a]	118.32	402.93[a]	119.49	0.1588	<0.0001	<0.0001	0.0001	0.0082	<0.0001	<0.0001
	DAT73	217.41[a]	70.39	199.22[a]	67.64							
	DAT111	267.08[a]	150.92	211.63[b]	97.94							
Intercellular CO_2 ($\mu mol\ mol^{-1}$)	DAT41	252.63[a]	27.10	264.14[b]	25.15	0.2377	<0.0001	<0.0001	0.2514	0.0001	<0.0001	0.0193
	DAT73	239.91[a]	19.52	230.60[a]	17.46							
	DAT111	294.17[a]	22.18	308.55[b]	25.77							
Transpiration ($mmol\ m^{-2}\ s^{-1}$)	DAT41	4.01[a]	0.82	4.21[a]	0.73	0.0407	0.0001	<0.0001	0.0028	0.0008	0.0004	<0.0001
	DAT73	2.73[a]	0.62	2.38[a]	0.60							
	DAT111	2.60[a]	0.90	2.10[b]	0.76							
V_{cmax} ($\mu mol\ m^{-2}\ s^{-1}$)	DAT41	67.44[a]	9.41	65.53[a]	8.24	0.0275	0.0435	<0.0001	0.5412	0.0736	0.0035	0.1644
	DAT73	72.62[a]	9.48	68.52[a]	10.27							
	DAT111	51.23[a]	7.35	41.59[b]	10.36							
J_{max} ($\mu mol\ m^{-2}\ s^{-1}$)	DAT41	161.96[a]	11.94	163.90[a]	15.92	0.0106	0.2114	<0.0001	0.8914	0.0035	0.0269	0.5601
	DAT73	199.81[a]	28.03	175.16[b]	20.80							
	DAT111	151.70[a]	21.81	121.70[b]	33.59							

Note: Mean values per individual plant of all genotypes are shown.

Abbreviations: DAT, days after transplanting; J_{max}: the maximum electron transport rate; SD, standard deviation; T, treatment; V_{cmax}: the maximum carboxylation rate of Rubisco.

Table A. 5 Descriptive statistics and ANOVA results of biomass and yield components collected from different wheat genotypes exposed to control and ozone condition.

Trait	Date	Control		Ozone		ANOVA						
		Mean	SD	Mean	SD	T	G	DAT	G×T	DAT×T	DAT×G	DAT×G×T
Total dry biomass	DAT34	0.73[a]	0.23	0.77[a]	0.25	0.0003	<0.0001	<0.0001	0.9947	<0.0001	<0.0001	0.0338
(g plant^{-1})	DAT61	4.39[a]	1.41	4.26[a]	1.20							
	DAT84	10.30[a]	2.83	9.91[a]	3.05							
	DAT106	17.03[a]	5.61	15.79[a]	5.57							
	DAT126	19.42[a]	7.23	15.02[b]	6.57							
	Harvest	11.09[a]	6.91	9.48[b]	5.76							
Stem dry weight	DAT34	0.22[a]	0.11	0.23[a]	0.12	0.0018	<0.0001	<0.0001	0.9880	0.0003	<0.0001	0.1030
(g plant^{-1})	DAT61	1.80[a]	0.78	1.74[a]	0.56							
	DAT84	3.73[a]	1.10	3.32[a]	1.05							
	DAT106	5.20[a]	1.73	4.75[a]	1.60							
	DAT126	5.15[a]	1.83	4.03[b]	1.85							
	Harvest	3.23[a]	1.52	2.59[b]	1.08							
Green leaf dry weight	DAT34	0.52[a]	0.14	0.54[a]	0.16	0.0429	<0.0001	<0.0001	0.6515	<0.0001	<0.0001	0.1855
(g plant^{-1})	DAT61	2.28[a]	0.75	2.12[a]	0.67							
	DAT84	3.10[a]	1.42	2.80[a]	1.40							
	DAT106	3.46[a]	1.43	3.11[a]	1.25							
	DAT126	2.03[a]	1.02	1.07[b]	1.22							
Brown leaf dry weight	DAT61	0.00[a]	0.00	0.01[a]	0.00	0.3371	<0.0001	<0.0001	0.3466	<0.0001	0.0182	0.9131
(g plant^{-1})	DAT84	0.13[a]	0.10	0.20[a]	0.17							
	DAT106	0.33[a]	0.24	0.35[a]	0.25							
	DAT126	1.41[a]	1.05	1.69[a]	1.02							
	Harvest	2.17[a]	1.17	1.72[b]	0.92							
Brown/ total leaf dry weight	DAT61	0.11[a]	0.15	0.27[a]	0.22	0.0013	<0.0001	<0.0001	<0.0001	<0.0001	<0.0001	<0.0001
(%)	DAT84	4.45[a]	3.82	7.25[a]	6.42							
	DAT106	10.18[a]	11.65	11.71[a]	11.25							
	DAT126	41.67[a]	21.31	68.54[b]	24.26							
Spike dry weight	DAT61	0.31[a]	0.42	0.40[a]	0.45	0.0109	<0.0001	<0.0001	0.6652	<0.0001	<0.0001	0.0001
(g plant^{-1})	DAT84	3.34[a]	2.03	3.60[a]	2.26							
	DAT106	8.04[a]	3.64	7.58[a]	3.69							
	DAT126	10.82[a]	4.39	8.22[b]	3.77							
	Harvest	6.21[a]	2.66	5.10[b]	2.31							
Spike number	DAT61	0.76[a]	0.91	0.96[a]	0.97	0.2585	<0.0001	<0.0001	0.3040	0.0302	<0.0001	0.0309
	DAT84	3.06[a]	1.14	2.99[a]	0.86							
	DAT106	4.64[a]	1.65	4.51[a]	1.48							
	DAT126	5.76[a]	2.08	5.11[b]	2.09							
	Harvest	3.06[a]	2.09	2.86[a]	1.87							
Tiller number	DAT34	3.07[a]	0.78	3.03[a]	0.96	0.0158	<0.0001	<0.0001	0.8803	0.1392	<0.0001	0.8559
	DAT61	5.14[a]	1.75	4.88[a]	1.64							
	DAT84	4.78[a]	1.90	5.03[a]	2.01							
	DAT106	6.11[a]	2.20	5.83[a]	1.98							
	DAT126	6.43[a]	2.35	5.72[b]	2.47							
	Harvest	4.83[a]	2.06	4.53[b]	1.89							
GLAI	DAT34	1.33[a]	0.39	1.37[a]	0.50	0.0986	<0.0001	<0.0001	0.6635	<0.0001	<0.0001	0.7585
	DAT61	4.32[a]	1.56	3.73[a]	1.34							
	DAT84	4.72[a]	2.72	4.50[a]	2.36							
	DAT106	5.02[a]	2.46	4.51[a]	1.92							
	DAT126	2.25[a]	1.15	1.10[b]	1.27							
BLAI	DAT61	0.00[a]	0.01	0.00[a]	0.00	0.3933	<0.0001	<0.0001	0.1826	<0.0001	0.1792	0.9352
	DAT84	0.12[a]	0.09	0.19[a]	0.17							
	DAT106	0.32[a]	0.25	0.31[a]	0.24							
	DAT126	0.97[a]	0.54	1.16[a]	0.57							
	Harvest	1.37[a]	0.73	1.06[b]	0.56							
LAI	DAT34	1.33[a]	0.39	1.37[a]	0.50	0.1343	<0.0001	<0.0001	0.6512	0.0038	<0.0001	0.3728
	DAT61	4.32[a]	1.56	3.73[a]	1.35							
	DAT84	4.84[a]	2.76	4.69[a]	2.43							
	DAT106	5.34[a]	2.51	4.82[a]	1.94							
	DAT126	3.22[a]	1.27	2.26[b]	1.44							
	Harvest	1.37[a]	0.73	1.06[b]	0.56							
BLAI/LAI	DAT61	0.07[a]	0.15	0.12[a]	0.13	0.0004	<0.0001	<0.0001	<0.0001	<0.0001	<0.0001	<0.0001
(%)	DAT84	2.94[a]	2.61	4.76[a]	5.61							
	DAT106	7.60[a]	0.11	8.10[a]	0.10							
	DAT126	33.49[a]	20.47	62.92[b]	27.19							
Specific leaf area	DAT34	322.70[a]	31.18	320.83[a]	45.16	0.4323	0.7613	<0.0001	0.1525	0.9257	0.1338	0.1651
(cm^2 g^{-1})	DAT61	236.39[a]	38.65	216.94[b]	36.86							
	DAT84	181.15[a]	43.99	194.48[b]	30.19							
	DAT106	172.55[a]	32.47	172.05[a]	22.12							
	DAT126	121.14[a]	21.54	102.11[b]	22.31							

	Harvest	81.34[a]	18.96	78.83[a]	14.67							
Spike dry matter content	DAT61	10.38[a]	10.78	13.36[a]	10.94	0.1366	<0.0001	<0.0001	0.4833	<0.0001	<0.0001	<0.0001
(%)	DAT84	32.32[a]	12.50	35.63[a]	14.87							
	DAT106	46.15[a]	14.26	46.70[a]	15.91							
	DAT126	67.96[a]	10.77	75.77[b]	11.90							
	Harvest	91.25[a]	2.26	91.46[a]	5.10							
Straw dry matter content	DAT34	13.16[a]	1.45	13.44[a]	1.78	0.0488	<0.0001	<0.0001	<0.0001	<0.0001	<0.0001	<0.0001
(%)	DAT61	17.07[a]	3.12	18.24[a]	2.19							
	DAT84	22.44[a]	3.41	22.10[a]	3.47							
	DAT106	25.15[a]	3.99	24.67[a]	3.79							
	DAT126	34.14[a]	6.90	46.65[b]	16.69							
	Harvest	93.61[a]	2.08	94.28[a]	2.32							
Days to flowering		130.79[a]	7.82	128.64[a]	7.92	0.0726	<0.0001		0.0004			
Maturity time		170.93[a]	5.85	168.54[b]	6.10	0.0003	<0.0001		<0.0001			
Plant height (cm)	Harvest	76.22[a]	10.13	70.20[a]	9.48	0.1761	<0.0001		0.2513			
Spike length (cm)	Harvest	11.32[a]	1.78	10.90[a]	1.82	0.2495	<0.0001		0.1067			
Grain yield (g plant^{-1})	Harvest	4.66[a]	2.04	3.78[b]	1.84	0.0009	0.0003		0.6511			
Filled grain number (plant^{-1})	Harvest	139.19[a]	60.46	119.43[b]	53.68	0.0026	<0.0001		0.2917			
Thousand kernel weight (g)	Harvest	34.10[a]	6.56	31.51[b]	7.35	0.0037	<0.0001		0.1357			
Straw biomass (g plant^{-1})	Harvest	5.40[a]	2.16	4.66[a]	1.84	0.1332	<0.0001		0.9864			
Harvest index	Harvest	0.40[a]	0.07	0.38[a]	0.09	0.3052	<0.0001		0.0007			
LBS	DAT99	0.00	0.00	3.00	0.96	<0.0001	NA		NA			

Note: Mean values per individual plant of all genotypes are shown. Treatment and genotype × treatment interaction effects were not analysed for leaf bronzing score (LBS) as there were no leaf damage symptoms on plants grown under control conditions.

Abbreviations: DAT, days after transplanting; LBS, leaf bronzing score; SD, standard deviation; T, treatment.

Table A. 6 Descriptive statistics and ANOVA results of fresh biomass collected from different wheat genotypes exposed to control and ozone condition.

Trait	Date	Control		Ozone		ANOVA						
		Mean	SD	Mean	SD	T	G	DAT	G×T	DAT×T	DAT×G	DAT×G×T
Total fresh biomass	DAT34	5.60[a]	1.70	5.75[a]	1.83	0.0018	<0.0001	<0.0001	0.9935	<0.0001	<0.0001	0.0666
(g plant^{-1})	DAT61	25.94[a]	8.05	23.28[a]	6.61							
	DAT84	42.20[a]	14.27	39.35[a]	13.35							
	DAT106	55.16[a]	19.60	51.22[b]	18.42							
	DAT126	42.19[a]	15.29	28.63[b]	15.72							
	Harvest	12.53[a]	5.29	10.16[a]	4.71							
Stem fresh weight	DAT34	1.96[a]	0.99	1.97[a]	0.99	0.0023	<0.0001	<0.0001	0.9685	<0.0001	<0.0001	0.0628
(g plant^{-1})	DAT61	12.44[a]	4.31	11.13[a]	3.33							
	DAT84	18.73[a]	6.59	16.84[b]	6.07							
	DAT106	22.45[a]	8.10	20.82[a]	6.80							
	DAT126	16.94[a]	6.24	11.56[b]	7.22							
	Harvest	3.44[a]	1.61	2.75[a]	1.15							
Green leaf fresh weight	DAT34	3.63[a]	1.07	3.78[a]	1.04	0.0954	<0.0001	<0.0001	0.7739	0.0008	<0.0001	0.7302
(g plant^{-1})	DAT61	12.04[a]	4.59	10.37[a]	3.98							
	DAT84	13.52[a]	7.47	12.67[a]	7.12							
	DAT106	14.32[a]	6.98	12.98[a]	5.84							
	DAT126	7.29[a]	3.76	3.68[b]	4.22							
Brown leaf fresh weight	DAT61	0.00[a]	0.00	0.01[a]	0.00	0.3710	<0.0001	<0.0001	0.0580	<0.0001	<0.0001	0.4038
(g plant^{-1})	DAT84	0.19[a]	0.13	0.29[a]	0.29							
	DAT106	0.48[a]	0.36	0.51[a]	0.44							
	DAT126	1.93[a]	1.33	2.18[a]	1.28							
	Harvest	2.32[a]	1.23	1.83[b]	0.98							
Brown/ total leaf fresh weight	DAT61	0.04[a]	0.04	0.09[a]	0.06	0.0004	<0.0001	<0.0001	<0.0001	<0.0001	<0.0001	<0.0001
(%)	DAT84	1.64[a]	1.65	2.74[a]	3.92							
	DAT106	4.71[a]	9.20	5.19[a]	7.14							
	DAT126	25.13[a]	20.09	53..62[b]	29.33							
Spike fresh weight	DAT61	1.46[a]	1.84	1.77[a]	1.82	0.0588	<0.0001	<0.0001	0.9294	<0.0001	<0.0001	0.0057
(g plant^{-1})	DAT84	9.76[a]	4.38	9.55[a]	4.29							
	DAT106	17.91[a]	7.56	16.91[a]	7.65							
	DAT126	16.04[a]	5.95	11.21[b]	5.49							
	Harvest	6.77[a]	2.97	5.58[a]	3.02							

Note: Mean values per individual plant of all genotypes are shown.

Abbreviations: DAT, days after transplanting; SD, standard deviation; T, treatment.

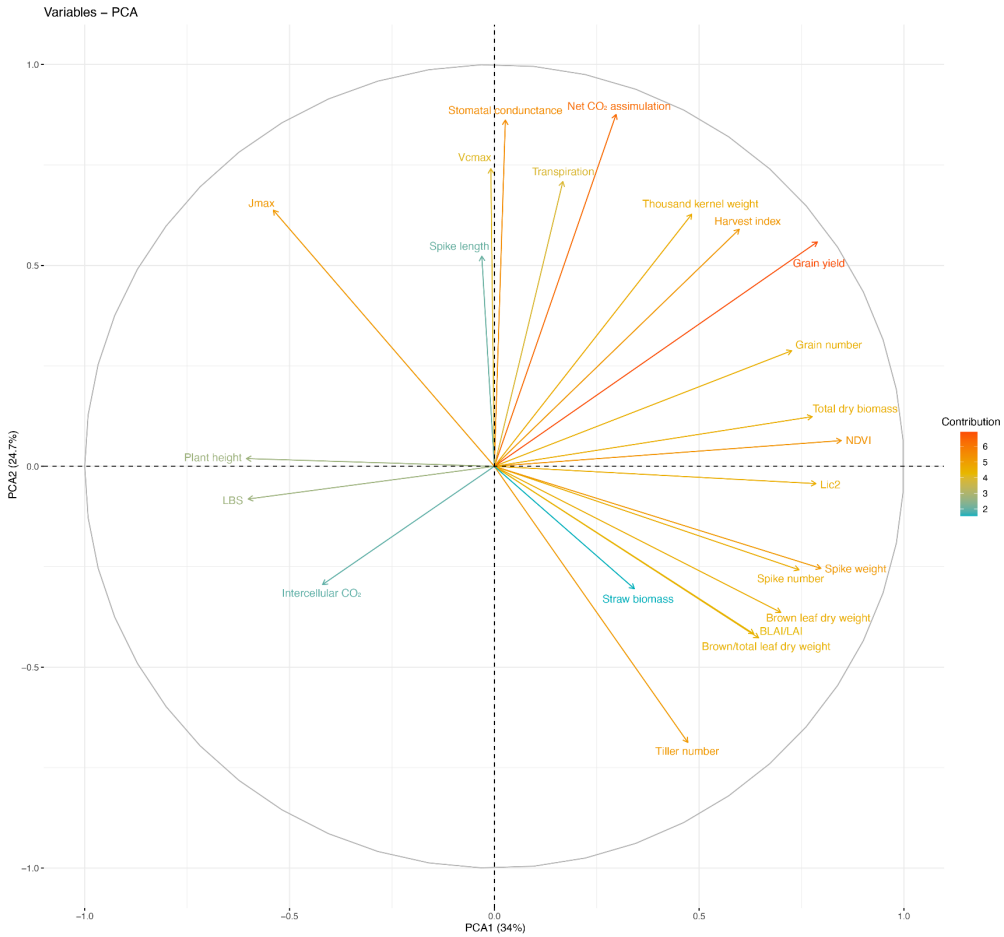

Figure A. 1 Principal component analysis of phenotypic traits and yield components of ten contrasting wheat genotypes exposed to ozone concentration and control conditions.

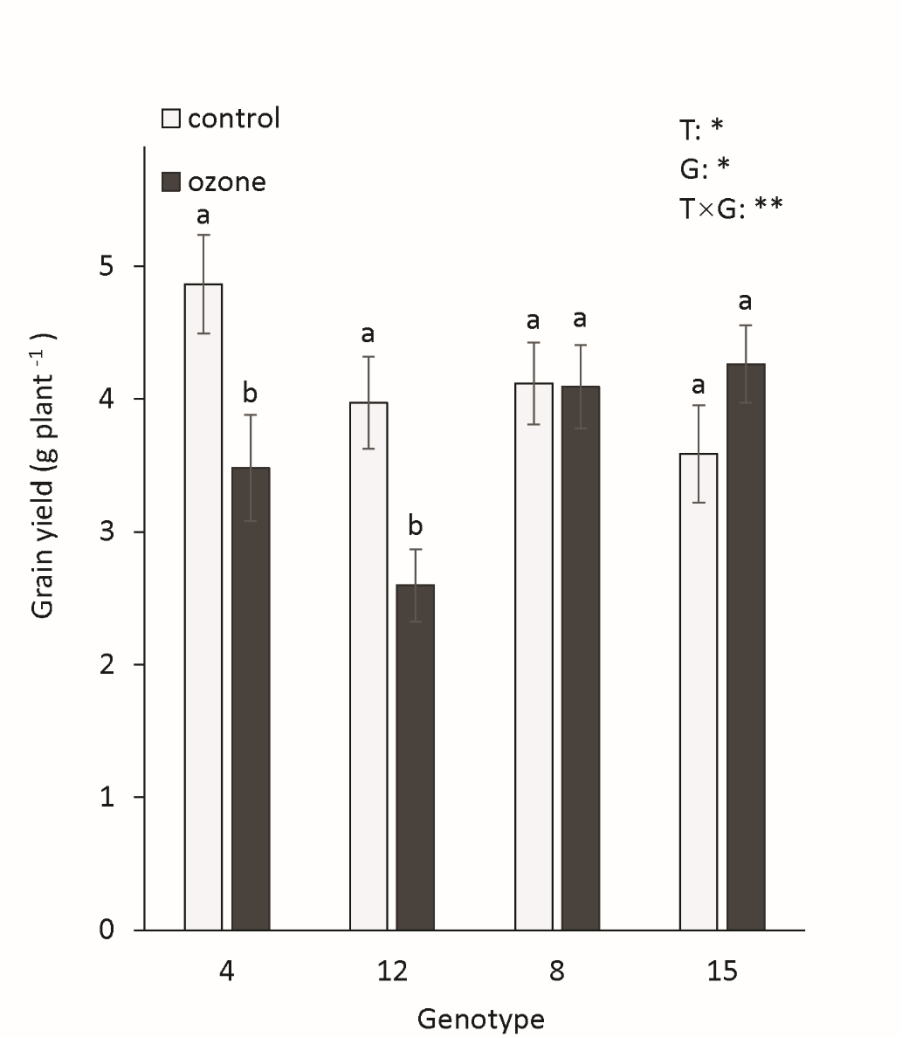

Figure A. 2 Grain yield of four different genotypes selected for model parametrization as an average of two independent fumigation experiments. Data were taken from this current study an from a previous experiment (Begum et al., 2020). Data were analyzed by mixed model analsysis with treatment, genotype and their interactions as fixed effects and experiment and fumigation chamber as random effects. Bars indicate mean values and standard errors (n=30). Bars not sharing the same superscript letters are significantly different at $P < 0.05$ within the genotypes. T: treatment; G: genotype; T × G: treatment by genotype interaction; * $P < 0.05$; ** $P < 0.01$.

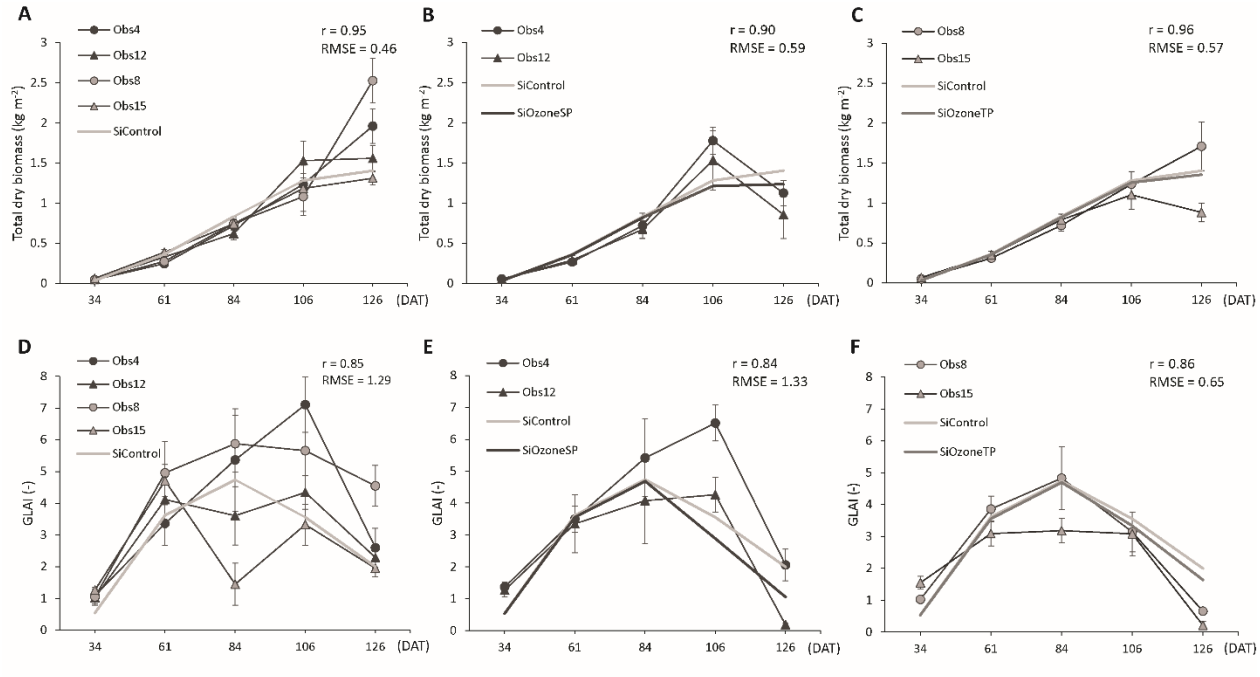

Figure A. 3 Comparison of observed and simulated dry biomass (upper panel) and green LAI (lower panel) using different cultivars and treatments. A & D, all cultivars in control condition. B & E, sensitive cultivars 4 (black dots) and 12 (black triangles) under ozone treatment. C & F, tolerant cultivars 8 (grey dots) and 15 (grey triangles) under ozone treatment. The simulated control values (grey lines) in B, C, E, and F are the same as the grey line with no symbol in A and D, while the black lines with no symbols represent the simulated values in the ozone treatment with sensitive parameters (SP) or tolerant parameters (TP). The measurements are at days 34, 61, 84, 106, and 125 after transplanting. The error bars indicate the standard deviation of four measured replicates. The units of RMSEs of dry biomass and green LAI are kg m^{-2} and (-), respectively.

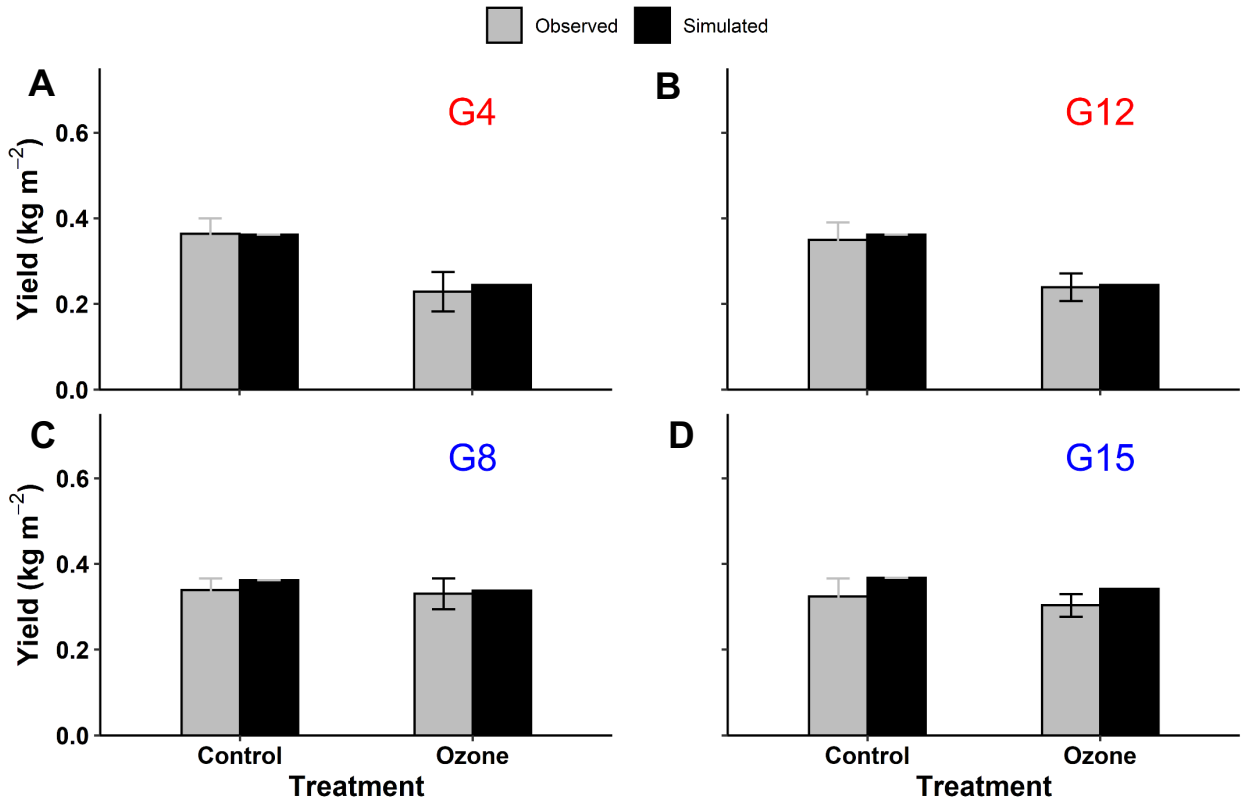

Figure A. 4 Comparison of observed and simulated grain yield in different cultivars. (A) cultivar 4, (B) cultivar 12, (C) cultivar 8, and (D) cultivar 15. The error bars indicate the standard deviation of four measured replicates.

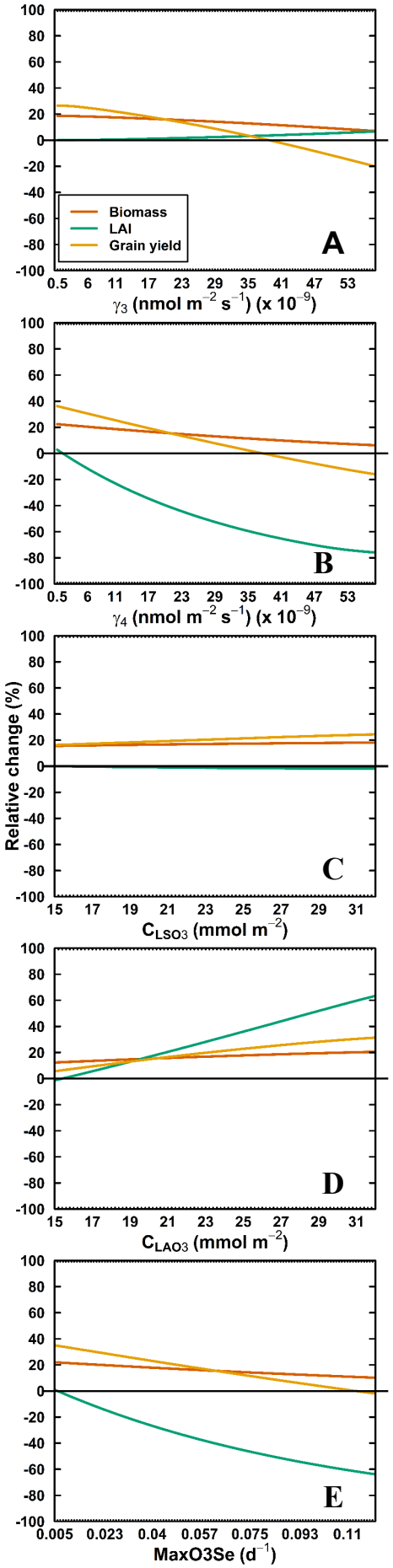

Figure A. 5 Sensitivity analysis of total aboveground dry biomass, *LAI*, and grain yield at harvest under ozone treatment to the changes of (A) γ_3, (B) γ_4, (C) C_{LSO3}, (D) C_{LAO3}, and (E) MaxO3Se while the remaining parameters were kept. The initial values are γ_3 = 0.012 x 10^{-6} nmol m^{-2} s^{-1}, γ_4 = 0.015 x 10^{-6} nmol m^{-2} s^{-1}, C_{LSO3} = 24 mmol m^{-2}, (D) C_{LAO3} = 25 mmol m^{-2}, and (E) MaxO3Se = 0.045 d^{-1}. The γ_3 and γ_4 were in step-wise changes (by 0.005 x 10^{-6} nmol m^{-2} s^{-1} from 0.005 x 10^{-6} nmol m^{-2} s^{-1} to 0.058 x 10^{-6} nmol m^{-2} s^{-1}. The C_{LSO3} and C_{LAO3} were in step-wise changes by 0.2 mmol m^{-2} from 15 mmol m^{-2} to 32 mmol m^{-2}. The MaxO3Se was changed from 0.005 d^{-1} to 0.12 d^{-1} with the incremental step of 0.001 d^{-1}. The simulated values of biomass (orange lines) and grain yield (yellow lines) were compared to the average of observed biomass and grain yield of all four cultivars at harvest under ozone treatment, respectively. Because the observed *LAI* at harvest was zero, the simulated *LAI* (cyan lines) from the change of each parameter was compared to the simulated *LAI* from the simulation with the lowest value in the range of that parameter.

SUPPLEMENTAL METHODS

A. 1 Coupled photosynthesis and stomatal conductance model

The CO_2 diffuses from atmospheric to the leaf stomata follows the Fick's law:

$$Ci = Ca - \left(\frac{FGR_{l,t}}{gs_{l,t}}\right) \quad \text{(B1)}$$

Stomatal conductance was simulated based on the Leuning approach (Leuning, 1995) with consideration of the effect of leaf to air vapor pressure deficit ($1 + DS/D_0$), intercellular CO_2 concentration (C_i), Γ^* is CO_2 compensation point in the absence of day respiration (see the variables and explanation in Table A. 2).

$$gs_{l,t} = g_0 + \frac{a_1 FGR_{l,t}}{(Ci - \Gamma^*)(1 + \frac{DS}{D_0})} \quad \text{(B2)}$$

Following the approach from Farquhar et al. (1980) and von Caemmerer (2000), the light saturated photosynthesis rate ($AMAX_{l,t}$) is given as follows:

$$AMAX_{l,t} = \frac{Vcmax\,(Ci-\Gamma^*)}{Ci+KMC\left(1+\frac{O2}{KMO}\right)} \min(f_{O3t}, f_{LS}) \quad \text{(B3)}$$

Where C_i and O_2 are the intercellular CO_2 and O_2 concentration, respectively; V_{cmax} is the maximum catalytic activity of Rubisco at leaf temperature; Γ^* is CO_2 compensation point at the absence of leaf respiration; *KMC* and *KMO* are Michaelis-Menten kinetics for CO_2 and O_2 (Table A. 2).

$$EFF_{l,t} = \frac{J}{2.1} \frac{Ci - \Gamma^*}{4.5(Ci + 2\Gamma^*)} \quad \text{(B4)}$$

Where C_i is the intercellular CO_2 concentration. J is conversion energy from radiation to mole photon (mole photons MJ^{-1}). The leaf photosynthesis rate ($FGR_{l,t}$) is the function of both $AMAX_{l,t}$ and $EFF_{l,t}$ where $EFF_{l,t}$ is quantum yield [μM CO_2 MJ^{-1}].

$$FGR_{l,t} = AMAX_{l,t}\left(1 - e^{-I_{l,t}\frac{EFF_{l,t}}{AMAX_{l,t}}}\right) \quad \text{(B5)}$$

A. 2 Ozone flux calculation

Ozone concentration might be different at top and within the crop canopy and vegetation height (Emberson et al., 2018). In our model, we estimated ozone flux from the top of canopy (sunlit leaves). The ozone conductance $gsO3_t$ [m s^{-1}] of the sunlit leaves was calculated from sunlit leaves' stomatal conductance for CO_2 [mol m^{-2} s^{-1}] using Equation C1 based on diffusive ratio between CO_2 and O_3 (DIFFO = 0.93) (Ewert and Porter, 2000) (see the variables and

explanation in Table A. 2).

$$gsO3_t = gs_t * \text{DIFFO} * 1000/41000 \quad \text{(C1)}$$

Leaf surface resistance ($rO3_t$ – s m^{-1}) to ozone was calculated based on the cuticle ($G_{cuticle}$ - m s^{-1}) and stomatal conductance $gsO3_t$ through Equation C2 where the $G_{cuticle}$ was assumed the same for sunlit leaf as 1/2500 [m s^{-1}] (Mills et al., 2017).

$$rO3_t = 1/(\mathrm{G_{cuticle}} + gsO3_t) \quad \text{(C2)}$$

The ozone concentration at the canopy height was converted from ppb to nmol m^{-3} using multiplication with 41.56. Ozone flux to the leaf stomata ($OZIF_t$ – nmol m^{-2} leaf area s^{-1}) was the function of hourly ozone concentration ($OZIH_t$) and the resistance of leaf surface to ozone ($rO3_t$) and boundary layer resistance (r_b – s m^{-1}).

$$OZIF_t = OZIH_t * gsO3_t * \frac{rO3_t}{\mathrm{r_b} + rO3_t} \quad \text{(C3)}$$

The r_b depends on wind speed (u – m s^{-1}) at given measured height and leaf width (L - m). Since the leaf width will be changed during growing season, for the sake of simplification, r_b was assumed constant at 7 [s m^{-1}].

A. 3 List of model variables and parameters used in calculation of radiation partitioning

Variables	Explanation	Unit
PAR	Photosynthetically active radiation	J m^{-2} s^{-1}
I_{b0}	Incident direct-beam above the canopy	J m^{-2} s^{-1}
I_{d0}	Incident diffuse radiation above the canopy	J m^{-2} s^{-1}
f_b	Fraction of the direct-beam component of incoming radiation	(-)
f_a	Fraction of diffuse radiation	(-)
ρ_{cb}	Canopy reflection coefficient of direct beam radiation	(-)
ρ_{cd}	Canopy reflection coefficient of diffuse radiation	(-)
k'_b	Extinction coefficient for scattered beam radiation	(-)
k'_d	Extinction coefficient for diffuse radiation	(-)
σ	Leaf scattering coefficient	(-)
L	Leaf area index	m^2 m^{-2}
τ	Atmospheric transmissivity	(-)
$I_{c,sun}$	Absorbed radiation by sunlit leaves	J m^{-2} s^{-1}
$I_{c,sha}$	Absorbed radiation by shaded leaves	J m^{-2} s^{-1}
I_c	Total absorbed radiation by the canopy	J m^{-2} s^{-1}

A. 4 Partitioning of sunlit and shaded leave in LINTULCC2 crop model

This supplemental methods explain the estimation of the absorbed radiance ($I_{l,t}$) for sunlit and shaded leave (Table A. 2) which used for calculation of photosynthesis of sunlit and shaded leaves in the equation B5. The LINTULCC2 crop model (Rodriguez et al., 2001) used a concept of two-leaf model which was introduced by De Pury and Farquhar (1997), Wang and Leuning (1998), later Yin and van Laar (2005), in which the canopy was divided into sunlit and shaded fractions. Each fraction was modelled separately with a single-layer leaf model.

Radiation absorbed by the canopy, I_c was determined as:

$$\boldsymbol{I_c = (1-\rho_{cb})I_{b0}\left(1-e^{-k'_b L}\right) + (1-\rho_{cd})I_{d0}\left(1-e^{-k'_d L}\right)} \quad \text{(E4.1)}$$

Where L is leaf area index. I_{b0} and I_{d0} are incident direct-beam and diffuse radiation above the canopy. The ρ_{cb} and ρ_{cd} are canopy reflection coefficients for the direct-beam and diffuse radiation, respectively. The k_b' is the extinction coefficient for beam and scattered-beam radiation and k_d' is the extinction coefficient for diffuse and scattered-diffuse radiation.

The I_{b0} and I_{d0} was calculated based on photosynthetically active radiation (PAR) and the fraction of the direct-beam component of incoming radiation (f_b) and the fraction of diffuse radiation (f_d), where $f_b = 1 - f_d$. The f_d was estimated by the empirical algorithm from Goudrian and van Laar (1994):

$$\boldsymbol{f_d = \begin{cases} 1 & \tau \le 0.22 \\ 1-6.4(\tau-0.22)^2 & 0.22 < \tau < 0.35 \\ 1.47-1.66\tau & \tau \ge 0.35 \end{cases}} \quad \text{(E4.2)}$$

Where τ is the atmospheric transmissivity which depends on the direct radiation on a horizontal

plane at the earth's surface, solar constant, solar elevation, and the instantaneous global radiation (assumed as two times of PAR) at a particular time of the day.

Radiation absorbed by the sunlit leaf fraction of the canopy $I_{c,sun}$ followed by De Pury and Farquhar (1997) and Yin and van Laar (2005), was given as the sum of direct-beam, diffuse and scattered-beam components.

$$I_{c,sun} = (1-\sigma)I_{b0}\left(1-e^{-k_b L}\right) + (1-\rho_{cd})I_{d0}\frac{k'_d\left[1-e^{-(k'_d+k_b)L}\right]}{k'_d+k_b} \quad \text{(E4.3)}$$

$$+ I_{b0}\{(1-\rho_{cb})\frac{k'_b\left[1-e^{-(k'_b+k_b)L}\right]}{k'_b+k_b} - (1-\sigma)\frac{1-e^{-2k_b L}}{2}\}$$

Where σ is the leaf scattering coefficient and k_b is the direct-beam radiation extinction coefficient.

Radiation absorbed the shaded fraction of the canopy $I_{c,\ sha}$ can be calculated as the sum of incoming diffuse and scattered direct-beam radiation absorbed by these leaves. For the sake of simplification, $I_{c,\ sha}$ is computed as the difference between total radiation absorbed by the canopy (I_c) and the radiation observed by the sunlit fraction ($I_{c,sun}$). Estimation of all extinction and reflection coefficients ($\sigma, \rho_{cb}, \rho_{cd}, k_b', k_b,$ and k_d') was described in Yin and van Laar (2005).

References

Begum H, Alam MS, Feng Y, Koua P, Ashrafuzzama M, Shrestha A, Kamruzzaman M, Dadshani S, Ballvora A, Naz AA, Frei M (2020) Genetic dissection of bread wheat diversity and identification of adaptive loci in response to elevated tropospheric ozone. Plant Cell Environ 43: 2650-2665. https://doi.org/10.1111/pce.13864

De Pury DGG, Farquhar GD (1997) Simple scaling of photosynthesis from leaves to canopies without the errors of big-leaf models. Plant Cell Environ 20: 537–557. https://doi.org/10.1111/j.1365-3040.1997.00094.x

Emberson LD, Pleijel H, Ainsworth EA., van den Berg M, Ren W, Osborne S, Mills G, Pandey D, Dentener F, Büker P, Ewert F, Koeble R, Van Dingenen R (2018) Ozone effects on crops and consideration in crop models. Eur J Agron 100: 19-34 https://doi.org/10.1016/j.eja.2018.06.002

Ewert F,Porter JR (2000) Ozone effects on wheat in relation to CO2: modelling short-term and long-term responses of leaf photosynthesis and leaf duration. Glob Chang Biol 6: 735-750 https://doi.org/10.1046/j.1365-2486.2000.00351.x

Farquhar GD, von Caemmerer S, Berry JA (1980) A biochemical model of photosynthetic CO2 assimilation in leaves of C3 species. Planta 149: 78-90 https://doi.org/10.1007/BF00386231

Leuning R (1995) A critical appraisal of a combined stomatal-photosynthesis model for C3 plants. Plant Cell Environ 18: 339-355 https://doi.org/10.1111/j.1365-3040.1995.tb00370.x

Mills G, Harmens H, Hayes F, Pleijel H, Buker P, González-Fernández I (2017) Chapter 3: Mapping critical levels for vegetation. https://icpvegetation.ceh.ac.uk/chapter-3-mapping-critical-levels-vegetation

von Caemmerer S (2000) Biochemical Models of Leaf Photosynthesis. CSIRO Publishing, Collingwood

Wang YP, Leuning R (1998) A two-leaf model for canopy conductance, photosynthesis and partitioning of available energy I: Model description and comparison with a multi-layered model. Agric For Meteorol 91: 89–111. https://doi.org/10.1016/S0168-1923(98)00061-6

Yin X, van Laar HH (2005) Crop Systems Dyanamics: An ecophysiological simulation model for genotype-by-environment interactions, 1st ed. Wageningen Academic Publishers.

Chapter 3

Title: Alteration of carbon and nitrogen allocation in winter wheat under elevated ozone

Supplementary materials

Table A1. List of the wheat accessions used in this study

No	Cultivar	Origin	Year of Release	Type
1	Memory	Germany	2013	Tolerant
2	KWS Santiago	England	2011	Tolerant
3	Durin	France	Unknown	Tolerant
4	Solstice	England	2001	Sensitive
5	Capone	Germany	2012	Sensitive
6	Cubus	Germany	2002	Tolerant
7	Edward	Germany	2013	Tolerant
8	Jenga	Germany	2007	Tolerant
9	Transit	Germany	1994	Tolerant
10	Gaucho	United States	1993	Tolerant
11	Skalmeje	Germany	2006	Sensitive
12	Enorm	Germany	2002	Sensitive
13	Sponsor	France, Ireland	1994	Sensitive
14	Sperber	Germany	1982	Sensitive
15	Apache	Czech Republic	1997	Tolerant
16	Isengrain	France/Slovenia/Spain	1996	Tolerant
17	Highbury	United Kingdom	1968	Sensitive
18	NS 46/90	Serbia	Unknown	Sensitive

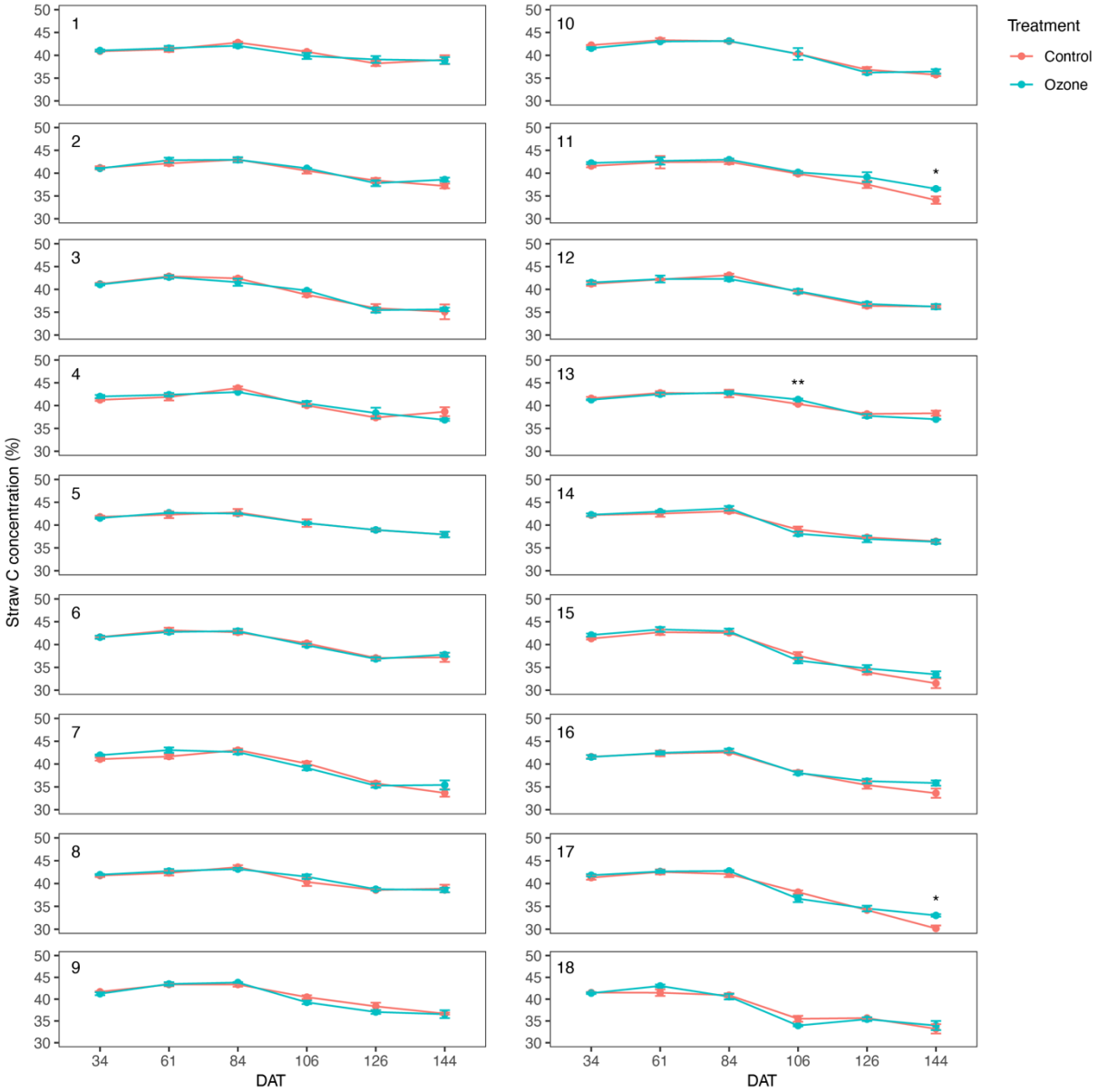

Fig. A1. Straw C concentration of different wheat genotypes during the growth season under control and ozone conditions. Within the growth stage, an asterisk (*) indicates a significant treatment difference at $P < 0.05$, and a double asterisk (**) indicates a significant treatment difference at $P < 0.01$ (n = 4) by Student's *t* test.

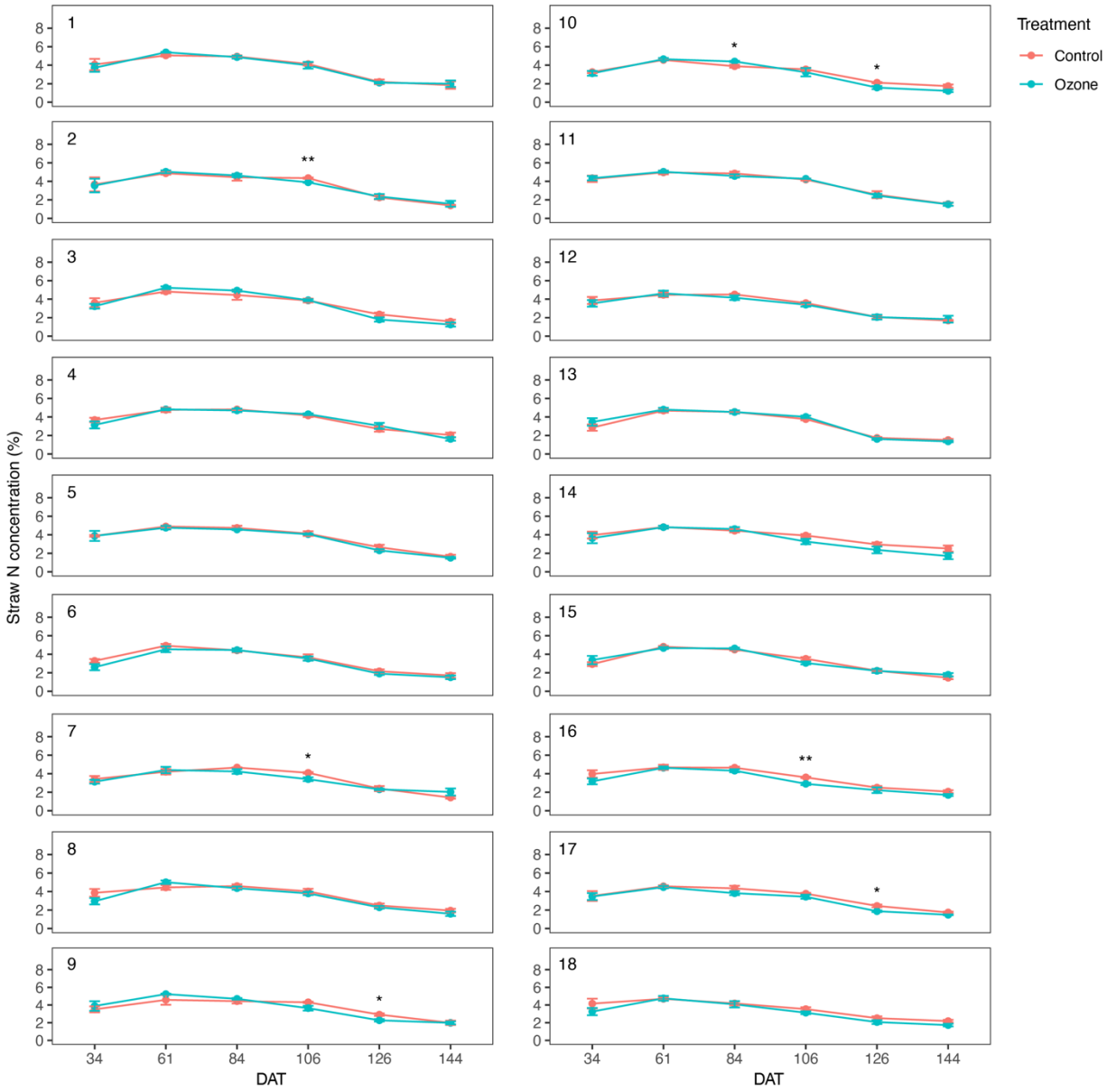

Fig. A2. Straw N concentration of different wheat genotypes during the growth season under control and ozone conditions. Within the growth stage, an asterisk (*) indicates a significant treatment difference at $P < 0.05$, and a double asterisk (**) indicates a significant treatment difference at $P < 0.01$ (n = 4) by Student's *t* test.

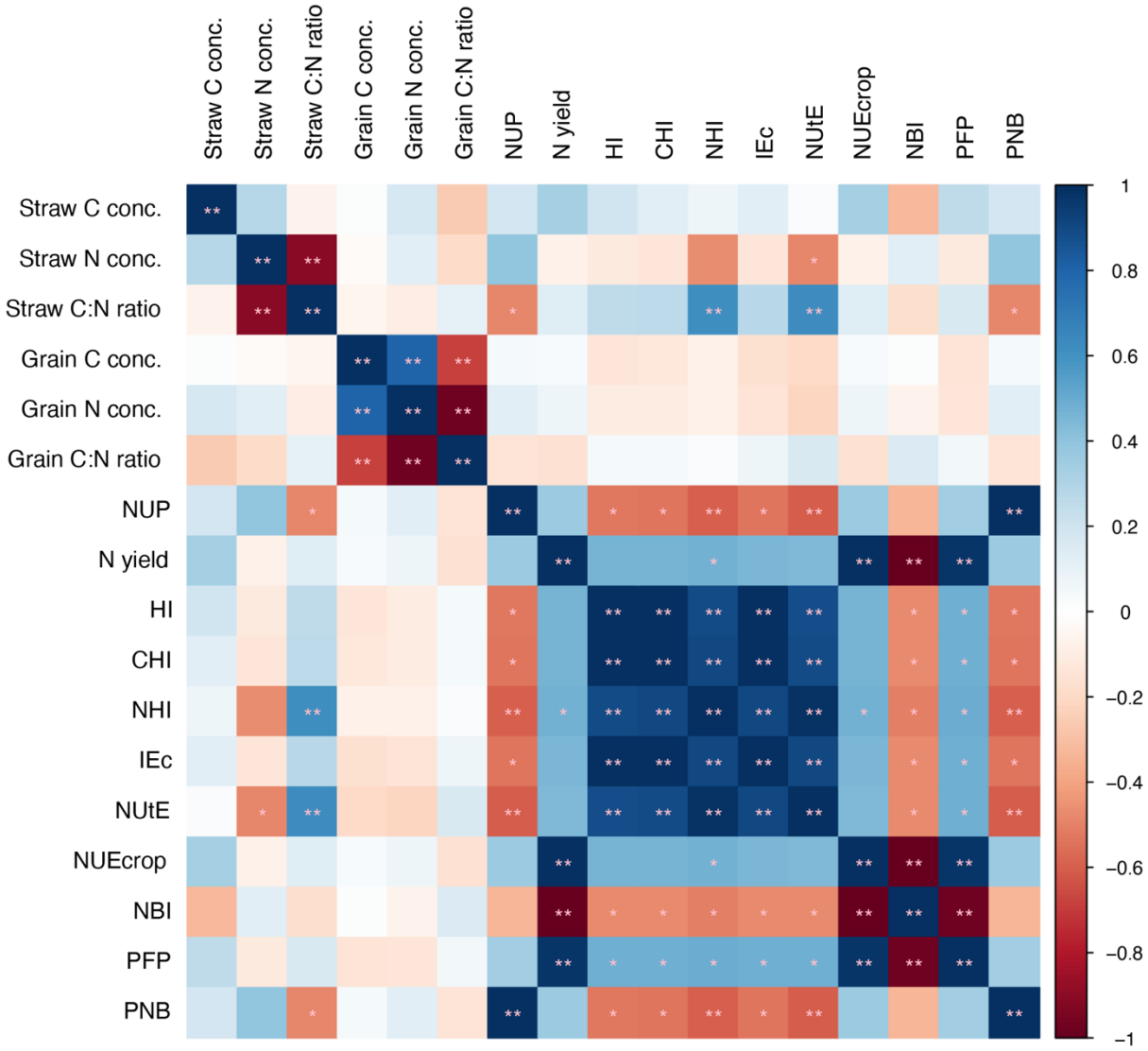

Fig. A3. Pearson correlation matrix for relative values (ozone/control) of C- and N-related parameters and NUE indicators of eighteen wheat genotypes exposed to ozone (* $P < 0.05$; ** $P < 0.01$; n = 18).

Chapter 4

Title: Characterization of candidate genes for ozone tolerance in winter wheat (*Triticum aestivum* L.) and associated physiological mechanisms

Supplementary materials

Supplementary Table S1. List of the wheat accessions used in this study

Haplotype	No	Cultivar	Origin	Year of Release
ATAGCACCTC	T1	Cubus	Germany	2002
	T2	Jenga	Germany	2007
GGGATGTTCA	S1	Solstice	England	2001
	S2	Highbury	United Kingdom	1968

Supplementary Table S2. Primers used for gene expression and sequencing in this study

Gene ID	5‘-Forward perimer-3‘	5‘-Reverse primer-3‘
TraesCS5A01G397700 (qRT–PCR)	GACAGAGACCACGGCGAC	CATCTCGGCCTGCGCTTTC
TraesCS5A01G397800 (qRT–PCR)	TCATTGCTCTGTGTGCGAATATG	CGGGAGGTCCCGATGGAC
TraesCS5A01G397900 (qRT–PCR)	TGCTGCGTCTCATCGACAAC	CCGGCCCCAAATAAATTCGC
TraesCS5A01G398000 (qRT–PCR)	ACACCGATACTATGATCACG	TCTCGCTCACGATGCACT
TraesCS5A01G398300 (qRT–PCR)	AAAGCCACTTGATGAGGACAC	CGTCATCTTTATCCGATACCTCC
TraesCS5A01G399100 (qRT–PCR)	CCAGATTTCACGGTTCTGC	CTTGTATATGGACGCTAGCTC
TraesCS5A01G399400 (qRT–PCR)	GCTCGCCAACACTGACCAC	AAATAAACACAACAGGCACACCA
TraesCS5A01G399500 (qRT–PCR)	TACAAGAGATACCCGTGCCC	GGAGCTGTCGTTGTAGAGGT
TraesCS5A01G400000 (qRT–PCR)	CCTCCTCTTCACCCAGGATC	GGTTGCCAGCTCAAAATCTGG
TraesCS5A01G400500 (qRT–PCR)	ACGGCAACATACGCAAGCA	ACTAATTCAGCCAGCGTGGTA
TraesCS5A01G400600 (qRT–PCR)	GAAGCGGGAGAACAAGATGC	ACGCAACAATGGCAGATCAA
TaEF1(housekeeping gene)	CAGATTGGCAACGGCTACG	CGGACAGCAAAACGACCAAG
TraesCS5A01G400500 (sequencing)	GTGTGGGGCGTTTGTATCTC	TAACCCGCACGTTCGAAATC

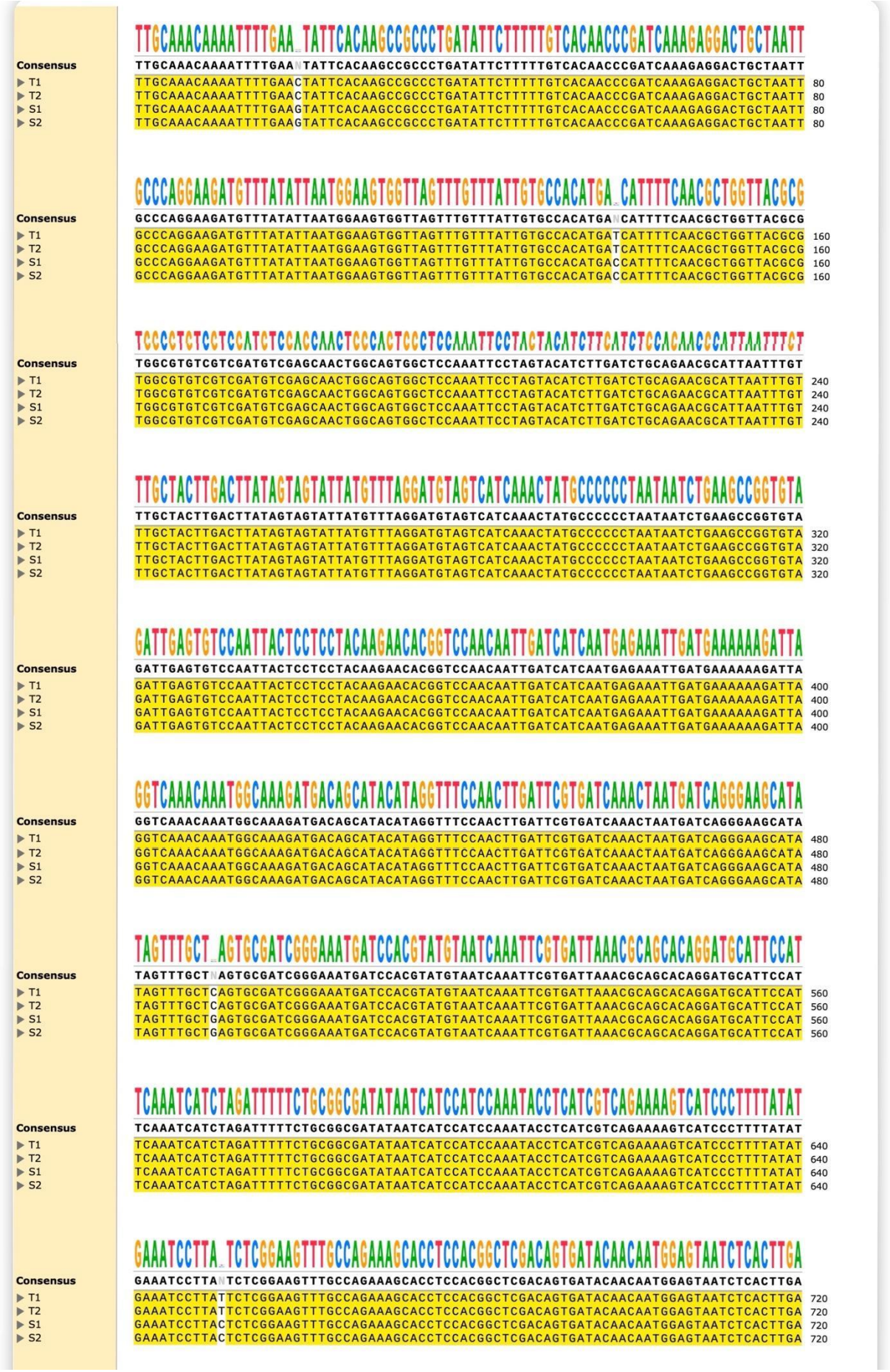
Consensus
TTGCAAACAAAATTTTGAANTATTCACAAGCCGCCCTGATATTCTTTTTGTCACAACCCGATCAAAGAGGACTGCTAATT
T1 TTGCAAACAAAATTTTGAACTATTCACAAGCCGCCCTGATATTCTTTTTGTCACAACCCGATCAAAGAGGACTGCTAATT 80
T2 TTGCAAACAAAATTTTGAACTATTCACAAGCCGCCCTGATATTCTTTTTGTCACAACCCGATCAAAGAGGACTGCTAATT 80
S1 TTGCAAACAAAATTTTGAAGTATTCACAAGCCGCCCTGATATTCTTTTTGTCACAACCCGATCAAAGAGGACTGCTAATT 80
S2 TTGCAAACAAAATTTTGAAGTATTCACAAGCCGCCCTGATATTCTTTTTGTCACAACCCGATCAAAGAGGACTGCTAATT 80
Consensus
GCCCAGGAAGATGTTTATATTAATGGAAGTGGTTAGTTTGTTTATTGTGCCACATGANCATTTTCAACGCTGGTTACGCG
T1 GCCCAGGAAGATGTTTATATTAATGGAAGTGGTTAGTTTGTTTATTGTGCCACATGATCATTTTCAACGCTGGTTACGCG 160
T2 GCCCAGGAAGATGTTTATATTAATGGAAGTGGTTAGTTTGTTTATTGTGCCACATGATCATTTTCAACGCTGGTTACGCG 160
S1 GCCCAGGAAGATGTTTATATTAATGGAAGTGGTTAGTTTGTTTATTGTGCCACATGACCATTTTCAACGCTGGTTACGCG 160
S2 GCCCAGGAAGATGTTTATATTAATGGAAGTGGTTAGTTTGTTTATTGTGCCACATGACCATTTTCAACGCTGGTTACGCG 160
Consensus
TGGCGTGTCGTCGATGTCGAGCAACTGGCAGTGGCTCCAAATTCCTAGTACATCTTGATCTGCAGAACGCATTAATTTGT
T1 TGGCGTGTCGTCGATGTCGAGCAACTGGCAGTGGCTCCAAATTCCTAGTACATCTTGATCTGCAGAACGCATTAATTTGT 240
T2 TGGCGTGTCGTCGATGTCGAGCAACTGGCAGTGGCTCCAAATTCCTAGTACATCTTGATCTGCAGAACGCATTAATTTGT 240
S1 TGGCGTGTCGTCGATGTCGAGCAACTGGCAGTGGCTCCAAATTCCTAGTACATCTTGATCTGCAGAACGCATTAATTTGT 240
S2 TGGCGTGTCGTCGATGTCGAGCAACTGGCAGTGGCTCCAAATTCCTAGTACATCTTGATCTGCAGAACGCATTAATTTGT 240
Consensus
TTGCTACTTGACTTATAGTAGTATTATGTTTAGGATGTAGTCATCAAACTATGCCCCCCTAATAATCTGAAGCCGGTGTA
T1 TTGCTACTTGACTTATAGTAGTATTATGTTTAGGATGTAGTCATCAAACTATGCCCCCCTAATAATCTGAAGCCGGTGTA 320
T2 TTGCTACTTGACTTATAGTAGTATTATGTTTAGGATGTAGTCATCAAACTATGCCCCCCTAATAATCTGAAGCCGGTGTA 320
S1 TTGCTACTTGACTTATAGTAGTATTATGTTTAGGATGTAGTCATCAAACTATGCCCCCCTAATAATCTGAAGCCGGTGTA 320
S2 TTGCTACTTGACTTATAGTAGTATTATGTTTAGGATGTAGTCATCAAACTATGCCCCCCTAATAATCTGAAGCCGGTGTA 320
Consensus
GATTGAGTGTCCAATTACTCCTCCTACAAGAACACGGTCCAACAATTGATCATCAATGAGAAATTGATGAAAAAAGATTA
T1 GATTGAGTGTCCAATTACTCCTCCTACAAGAACACGGTCCAACAATTGATCATCAATGAGAAATTGATGAAAAAAGATTA 400
T2 GATTGAGTGTCCAATTACTCCTCCTACAAGAACACGGTCCAACAATTGATCATCAATGAGAAATTGATGAAAAAAGATTA 400
S1 GATTGAGTGTCCAATTACTCCTCCTACAAGAACACGGTCCAACAATTGATCATCAATGAGAAATTGATGAAAAAAGATTA 400
S2 GATTGAGTGTCCAATTACTCCTCCTACAAGAACACGGTCCAACAATTGATCATCAATGAGAAATTGATGAAAAAAGATTA 400
Consensus
GGTCAAACAAATGGCAAAGATGACAGCATACATAGGTTTCCAACTTGATTCGTGATCAAACTAATGATCAGGGAAGCATA
T1 GGTCAAACAAATGGCAAAGATGACAGCATACATAGGTTTCCAACTTGATTCGTGATCAAACTAATGATCAGGGAAGCATA 480
T2 GGTCAAACAAATGGCAAAGATGACAGCATACATAGGTTTCCAACTTGATTCGTGATCAAACTAATGATCAGGGAAGCATA 480
S1 GGTCAAACAAATGGCAAAGATGACAGCATACATAGGTTTCCAACTTGATTCGTGATCAAACTAATGATCAGGGAAGCATA 480
S2 GGTCAAACAAATGGCAAAGATGACAGCATACATAGGTTTCCAACTTGATTCGTGATCAAACTAATGATCAGGGAAGCATA 480
Consensus
TAGTTTGCTNAGTGCGATCGGGAAATGATCCACGTATGTAATCAAATTCGTGATTAAACGCAGCACAGGATGCATTCCAT
T1 TAGTTTGCTCAGTGCGATCGGGAAATGATCCACGTATGTAATCAAATTCGTGATTAAACGCAGCACAGGATGCATTCCAT 560
T2 TAGTTTGCTCAGTGCGATCGGGAAATGATCCACGTATGTAATCAAATTCGTGATTAAACGCAGCACAGGATGCATTCCAT 560
S1 TAGTTTGCTGAGTGCGATCGGGAAATGATCCACGTATGTAATCAAATTCGTGATTAAACGCAGCACAGGATGCATTCCAT 560
S2 TAGTTTGCTGAGTGCGATCGGGAAATGATCCACGTATGTAATCAAATTCGTGATTAAACGCAGCACAGGATGCATTCCAT 560
Consensus
TCAAATCATCTAGATTTTTCTGCGGCGATATAATCATCCATCCAAATACCTCATCGTCAGAAAAGTCATCCCTTTTATAT
T1 TCAAATCATCTAGATTTTTCTGCGGCGATATAATCATCCATCCAAATACCTCATCGTCAGAAAAGTCATCCCTTTTATAT 640
T2 TCAAATCATCTAGATTTTTCTGCGGCGATATAATCATCCATCCAAATACCTCATCGTCAGAAAAGTCATCCCTTTTATAT 640
S1 TCAAATCATCTAGATTTTTCTGCGGCGATATAATCATCCATCCAAATACCTCATCGTCAGAAAAGTCATCCCTTTTATAT 640
S2 TCAAATCATCTAGATTTTTCTGCGGCGATATAATCATCCATCCAAATACCTCATCGTCAGAAAAGTCATCCCTTTTATAT 640
Consensus
GAAATCCTTANTCTCGGAAGTTTGCCAGAAAGCACCTCCACGGCTCGACAGTGATACAACAATGGAGTAATCTCACTTGA
T1 GAAATCCTTATTCTCGGAAGTTTGCCAGAAAGCACCTCCACGGCTCGACAGTGATACAACAATGGAGTAATCTCACTTGA 720
T2 GAAATCCTTATTCTCGGAAGTTTGCCAGAAAGCACCTCCACGGCTCGACAGTGATACAACAATGGAGTAATCTCACTTGA 720
S1 GAAATCCTTACTCTCGGAAGTTTGCCAGAAAGCACCTCCACGGCTCGACAGTGATACAACAATGGAGTAATCTCACTTGA 720
S2 GAAATCCTTACTCTCGGAAGTTTGCCAGAAAGCACCTCCACGGCTCGACAGTGATACAACAATGGAGTAATCTCACTTGA 720

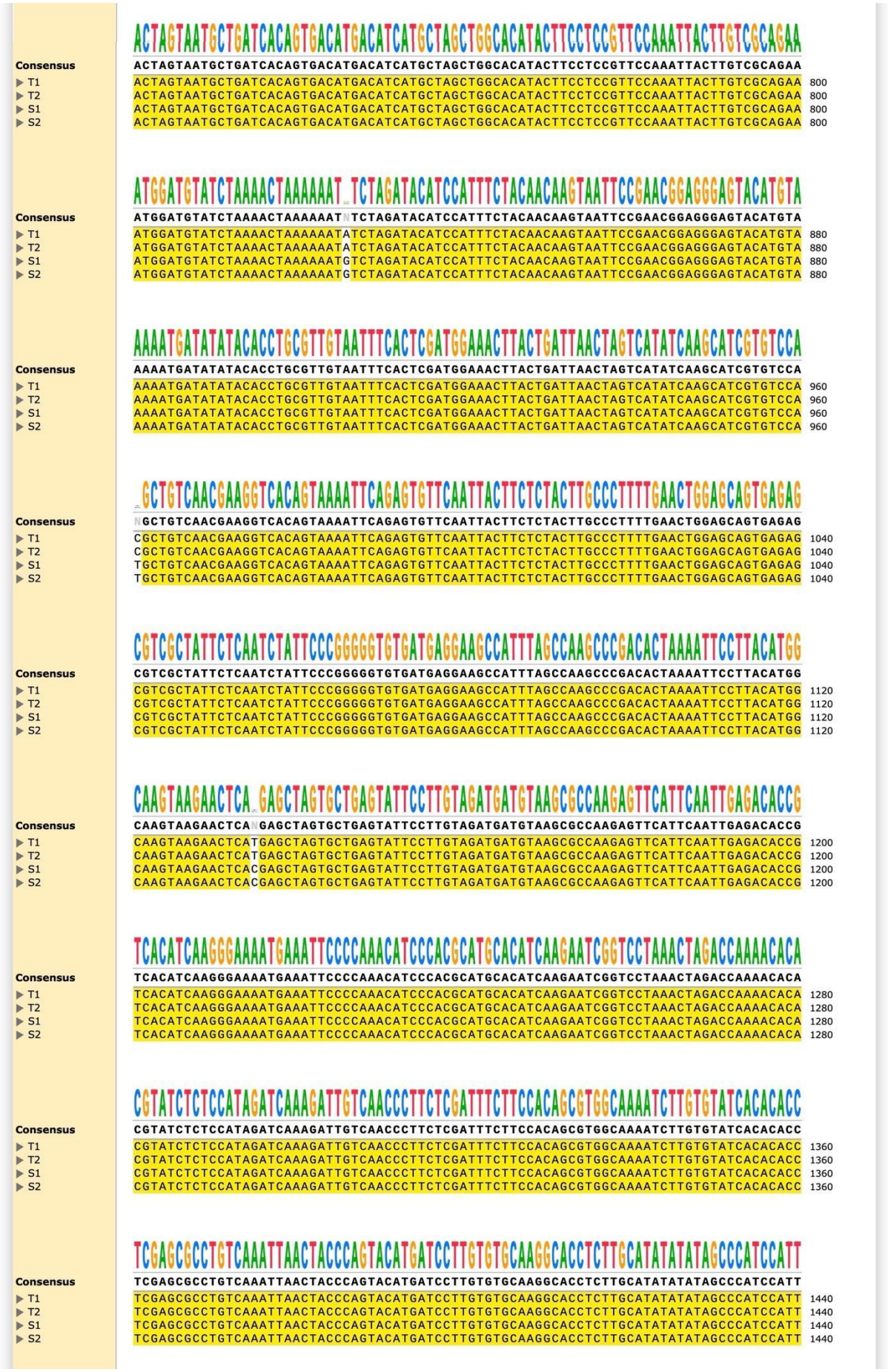
Consensus
ACTAGTAATGCTGATCACAGTGACATGACATCATGCTAGCTGGCACATACTTCCTCCGTTCCAAATTACTTGTCGCAGAA
T1 ACTAGTAATGCTGATCACAGTGACATGACATCATGCTAGCTGGCACATACTTCCTCCGTTCCAAATTACTTGTCGCAGAA 800
T2 ACTAGTAATGCTGATCACAGTGACATGACATCATGCTAGCTGGCACATACTTCCTCCGTTCCAAATTACTTGTCGCAGAA 800
S1 ACTAGTAATGCTGATCACAGTGACATGACATCATGCTAGCTGGCACATACTTCCTCCGTTCCAAATTACTTGTCGCAGAA 800
S2 ACTAGTAATGCTGATCACAGTGACATGACATCATGCTAGCTGGCACATACTTCCTCCGTTCCAAATTACTTGTCGCAGAA 800
Consensus
ATGGATGTATCTAAAACTAAAAAAT_TCTAGATACATCCATTTCTACAACAAGTAATTCCGAACGGAGGGAGTACATGTA
Consensus
ATGGATGTATCTAAAACTAAAAAATNTCTAGATACATCCATTTCTACAACAAGTAATTCCGAACGGAGGGAGTACATGTA
T1 ATGGATGTATCTAAAACTAAAAAATATCTAGATACATCCATTTCTACAACAAGTAATTCCGAACGGAGGGAGTACATGTA 880
T2 ATGGATGTATCTAAAACTAAAAAATATCTAGATACATCCATTTCTACAACAAGTAATTCCGAACGGAGGGAGTACATGTA 880
S1 ATGGATGTATCTAAAACTAAAAAATGTCTAGATACATCCATTTCTACAACAAGTAATTCCGAACGGAGGGAGTACATGTA 880
S2 ATGGATGTATCTAAAACTAAAAAATGTCTAGATACATCCATTTCTACAACAAGTAATTCCGAACGGAGGGAGTACATGTA 880
Consensus
AAAATGATATATACACCTGCGTTGTAATTTCACTCGATGGAAACTTACTGATTAACTAGTCATATCAAGCATCGTGTCCA
Consensus
AAAATGATATATACACCTGCGTTGTAATTTCACTCGATGGAAACTTACTGATTAACTAGTCATATCAAGCATCGTGTCCA
T1 AAAATGATATATACACCTGCGTTGTAATTTCACTCGATGGAAACTTACTGATTAACTAGTCATATCAAGCATCGTGTCCA 960
T2 AAAATGATATATACACCTGCGTTGTAATTTCACTCGATGGAAACTTACTGATTAACTAGTCATATCAAGCATCGTGTCCA 960
S1 AAAATGATATATACACCTGCGTTGTAATTTCACTCGATGGAAACTTACTGATTAACTAGTCATATCAAGCATCGTGTCCA 960
S2 AAAATGATATATACACCTGCGTTGTAATTTCACTCGATGGAAACTTACTGATTAACTAGTCATATCAAGCATCGTGTCCA 960
Consensus
_GCTGTCAACGAAGGTCACAGTAAAATTCAGAGTGTTCAATTACTTCTCTACTTGCCCTTTTGAACTGGAGCAGTGAGAG
Consensus
NGCTGTCAACGAAGGTCACAGTAAAATTCAGAGTGTTCAATTACTTCTCTACTTGCCCTTTTGAACTGGAGCAGTGAGAG
T1 CGCTGTCAACGAAGGTCACAGTAAAATTCAGAGTGTTCAATTACTTCTCTACTTGCCCTTTTGAACTGGAGCAGTGAGAG 1040
T2 CGCTGTCAACGAAGGTCACAGTAAAATTCAGAGTGTTCAATTACTTCTCTACTTGCCCTTTTGAACTGGAGCAGTGAGAG 1040
S1 TGCTGTCAACGAAGGTCACAGTAAAATTCAGAGTGTTCAATTACTTCTCTACTTGCCCTTTTGAACTGGAGCAGTGAGAG 1040
S2 TGCTGTCAACGAAGGTCACAGTAAAATTCAGAGTGTTCAATTACTTCTCTACTTGCCCTTTTGAACTGGAGCAGTGAGAG 1040
Consensus
CGTCGCTATTCTCAATCTATTCCCGGGGGGTGTGATGAGGAAGCCATTTAGCCAAGCCCGACACTAAAATTCCTTACATGG
Consensus
CGTCGCTATTCTCAATCTATTCCCGGGGGGTGTGATGAGGAAGCCATTTAGCCAAGCCCGACACTAAAATTCCTTACATGG
T1 CGTCGCTATTCTCAATCTATTCCCGGGGGGTGTGATGAGGAAGCCATTTAGCCAAGCCCGACACTAAAATTCCTTACATGG 1120
T2 CGTCGCTATTCTCAATCTATTCCCGGGGGGTGTGATGAGGAAGCCATTTAGCCAAGCCCGACACTAAAATTCCTTACATGG 1120
S1 CGTCGCTATTCTCAATCTATTCCCGGGGGGTGTGATGAGGAAGCCATTTAGCCAAGCCCGACACTAAAATTCCTTACATGG 1120
S2 CGTCGCTATTCTCAATCTATTCCCGGGGGGTGTGATGAGGAAGCCATTTAGCCAAGCCCGACACTAAAATTCCTTACATGG 1120
Consensus
CAAGTAAGAACTCA_GAGCTAGTGCTGAGTATTCCTTGTAGATGATGTAAGCGCCAAGAGTTCATTCAATTGAGACACCG
Consensus
CAAGTAAGAACTCANGAGCTAGTGCTGAGTATTCCTTGTAGATGATGTAAGCGCCAAGAGTTCATTCAATTGAGACACCG
T1 CAAGTAAGAACTCATGAGCTAGTGCTGAGTATTCCTTGTAGATGATGTAAGCGCCAAGAGTTCATTCAATTGAGACACCG 1200
T2 CAAGTAAGAACTCATGAGCTAGTGCTGAGTATTCCTTGTAGATGATGTAAGCGCCAAGAGTTCATTCAATTGAGACACCG 1200
S1 CAAGTAAGAACTCACGAGCTAGTGCTGAGTATTCCTTGTAGATGATGTAAGCGCCAAGAGTTCATTCAATTGAGACACCG 1200
S2 CAAGTAAGAACTCACGAGCTAGTGCTGAGTATTCCTTGTAGATGATGTAAGCGCCAAGAGTTCATTCAATTGAGACACCG 1200
Consensus
TCACATCAAGGGAAAATGAAATTCCCCAAACATCCCACGCATGCACATCAAGAATCGGTCCTAAACTAGACCAAAACACA
Consensus
TCACATCAAGGGAAAATGAAATTCCCCAAACATCCCACGCATGCACATCAAGAATCGGTCCTAAACTAGACCAAAACACA
T1 TCACATCAAGGGAAAATGAAATTCCCCAAACATCCCACGCATGCACATCAAGAATCGGTCCTAAACTAGACCAAAACACA 1280
T2 TCACATCAAGGGAAAATGAAATTCCCCAAACATCCCACGCATGCACATCAAGAATCGGTCCTAAACTAGACCAAAACACA 1280
S1 TCACATCAAGGGAAAATGAAATTCCCCAAACATCCCACGCATGCACATCAAGAATCGGTCCTAAACTAGACCAAAACACA 1280
S2 TCACATCAAGGGAAAATGAAATTCCCCAAACATCCCACGCATGCACATCAAGAATCGGTCCTAAACTAGACCAAAACACA 1280
Consensus
CGTATCTCTCCATAGATCAAAGATTGTCAACCCTTCTCGATTTCTTCCACAGCGTGGCAAAATCTTGTGTATCACACACC
Consensus
CGTATCTCTCCATAGATCAAAGATTGTCAACCCTTCTCGATTTCTTCCACAGCGTGGCAAAATCTTGTGTATCACACACC
T1 CGTATCTCTCCATAGATCAAAGATTGTCAACCCTTCTCGATTTCTTCCACAGCGTGGCAAAATCTTGTGTATCACACACC 1360
T2 CGTATCTCTCCATAGATCAAAGATTGTCAACCCTTCTCGATTTCTTCCACAGCGTGGCAAAATCTTGTGTATCACACACC 1360
S1 CGTATCTCTCCATAGATCAAAGATTGTCAACCCTTCTCGATTTCTTCCACAGCGTGGCAAAATCTTGTGTATCACACACC 1360
S2 CGTATCTCTCCATAGATCAAAGATTGTCAACCCTTCTCGATTTCTTCCACAGCGTGGCAAAATCTTGTGTATCACACACC 1360
Consensus
TCGAGCGCCTGTCAAATTAACTACCCAGTACATGATCCTTGTGTGCAAGGCACCTCTTGCATATATATAGCCCATCCATT
Consensus
TCGAGCGCCTGTCAAATTAACTACCCAGTACATGATCCTTGTGTGCAAGGCACCTCTTGCATATATATAGCCCATCCATT
T1 TCGAGCGCCTGTCAAATTAACTACCCAGTACATGATCCTTGTGTGCAAGGCACCTCTTGCATATATATAGCCCATCCATT 1440
T2 TCGAGCGCCTGTCAAATTAACTACCCAGTACATGATCCTTGTGTGCAAGGCACCTCTTGCATATATATAGCCCATCCATT 1440
S1 TCGAGCGCCTGTCAAATTAACTACCCAGTACATGATCCTTGTGTGCAAGGCACCTCTTGCATATATATAGCCCATCCATT 1440
S2 TCGAGCGCCTGTCAAATTAACTACCCAGTACATGATCCTTGTGTGCAAGGCACCTCTTGCATATATATAGCCCATCCATT 1440

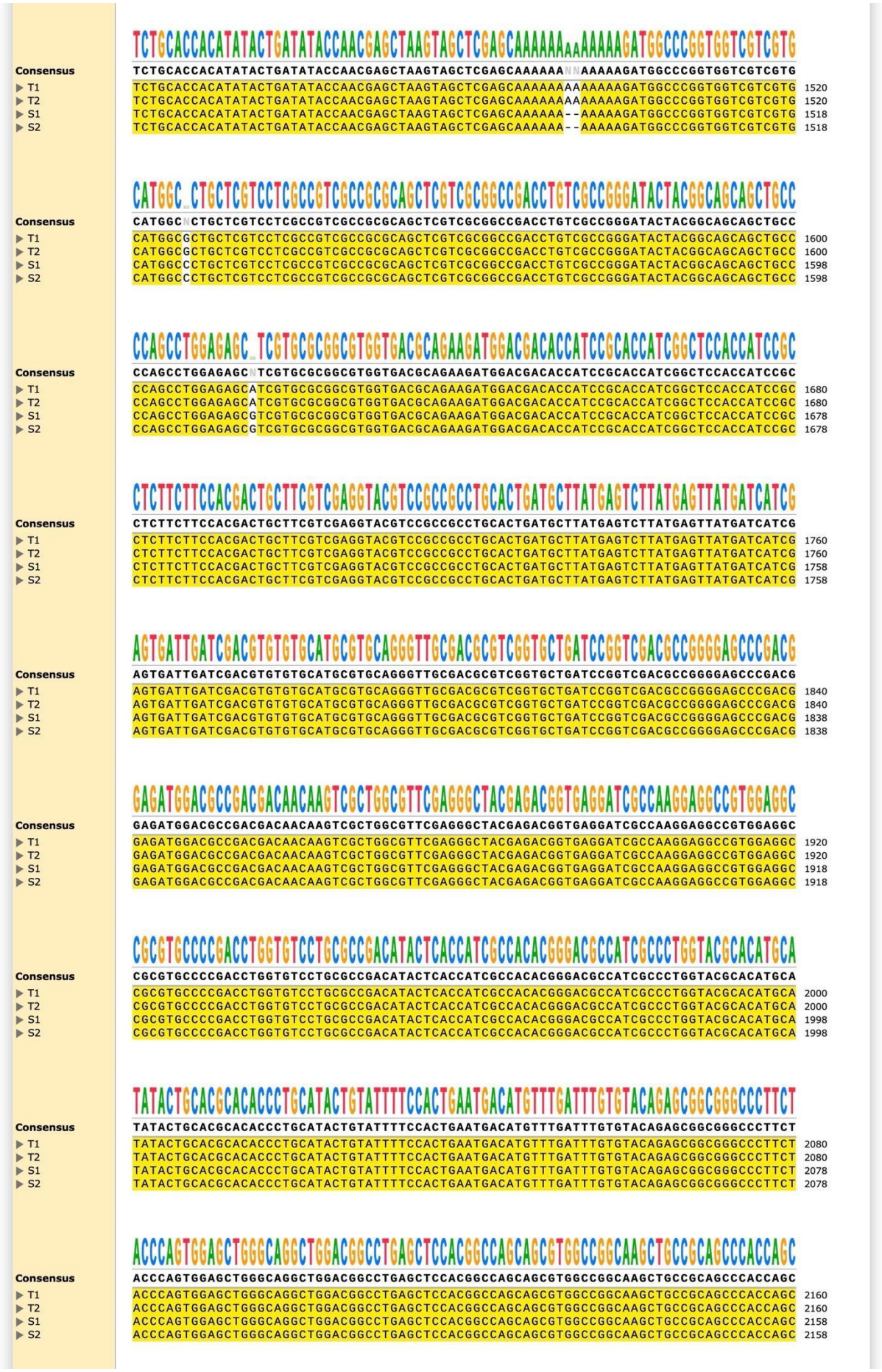
Consensus
TCTGCACCACATATACTGATATACCAACGAGCTAAGTAGCTCGAGCAAAAAANNAAAAAGATGGCCCGGTGGTCGTCGTG
T1 TCTGCACCACATATACTGATATACCAACGAGCTAAGTAGCTCGAGCAAAAAAAAAAAAAGATGGCCCGGTGGTCGTCGTG 1520
T2 TCTGCACCACATATACTGATATACCAACGAGCTAAGTAGCTCGAGCAAAAAAAAAAAAAGATGGCCCGGTGGTCGTCGTG 1520
S1 TCTGCACCACATATACTGATATACCAACGAGCTAAGTAGCTCGAGCAAAAAA--AAAAAGATGGCCCGGTGGTCGTCGTG 1518
S2 TCTGCACCACATATACTGATATACCAACGAGCTAAGTAGCTCGAGCAAAAAA--AAAAAGATGGCCCGGTGGTCGTCGTG 1518
Consensus
CATGGCNCTGCTCGTCCTCGCCGTCGCCGCGCAGCTCGTCGCGGCCGACCTGTCGCCGGGATACTACGGCAGCAGCTGCC
T1 CATGGCGCTGCTCGTCCTCGCCGTCGCCGCGCAGCTCGTCGCGGCCGACCTGTCGCCGGGATACTACGGCAGCAGCTGCC 1600
T2 CATGGCGCTGCTCGTCCTCGCCGTCGCCGCGCAGCTCGTCGCGGCCGACCTGTCGCCGGGATACTACGGCAGCAGCTGCC 1600
S1 CATGGCCCTGCTCGTCCTCGCCGTCGCCGCGCAGCTCGTCGCGGCCGACCTGTCGCCGGGATACTACGGCAGCAGCTGCC 1598
S2 CATGGCCCTGCTCGTCCTCGCCGTCGCCGCGCAGCTCGTCGCGGCCGACCTGTCGCCGGGATACTACGGCAGCAGCTGCC 1598
Consensus
CCAGCCTGGAGAGCNTCGTGCGCGGCGTGGTGACGCAGAAGATGGACGACACCATCCGCACCATCGGCTCCACCATCCGC
T1 CCAGCCTGGAGAGCATCGTGCGCGGCGTGGTGACGCAGAAGATGGACGACACCATCCGCACCATCGGCTCCACCATCCGC 1680
T2 CCAGCCTGGAGAGCATCGTGCGCGGCGTGGTGACGCAGAAGATGGACGACACCATCCGCACCATCGGCTCCACCATCCGC 1680
S1 CCAGCCTGGAGAGCGTCGTGCGCGGCGTGGTGACGCAGAAGATGGACGACACCATCCGCACCATCGGCTCCACCATCCGC 1678
S2 CCAGCCTGGAGAGCGTCGTGCGCGGCGTGGTGACGCAGAAGATGGACGACACCATCCGCACCATCGGCTCCACCATCCGC 1678
Consensus
CTCTTCTTCCACGACTGCTTCGTCGAGGTACGTCCGCCGCCTGCACTGATGCTTATGAGTCTTATGAGTTATGATCATCG
T1 CTCTTCTTCCACGACTGCTTCGTCGAGGTACGTCCGCCGCCTGCACTGATGCTTATGAGTCTTATGAGTTATGATCATCG 1760
T2 CTCTTCTTCCACGACTGCTTCGTCGAGGTACGTCCGCCGCCTGCACTGATGCTTATGAGTCTTATGAGTTATGATCATCG 1760
S1 CTCTTCTTCCACGACTGCTTCGTCGAGGTACGTCCGCCGCCTGCACTGATGCTTATGAGTCTTATGAGTTATGATCATCG 1758
S2 CTCTTCTTCCACGACTGCTTCGTCGAGGTACGTCCGCCGCCTGCACTGATGCTTATGAGTCTTATGAGTTATGATCATCG 1758
Consensus
AGTGATTGATCGACGTGTGTGCATGCGTGCAGGGTTGCGACGCGTCGGTGCTGATCCGGTCGACGCCGGGGAGCCCGACG
T1 AGTGATTGATCGACGTGTGTGCATGCGTGCAGGGTTGCGACGCGTCGGTGCTGATCCGGTCGACGCCGGGGAGCCCGACG 1840
T2 AGTGATTGATCGACGTGTGTGCATGCGTGCAGGGTTGCGACGCGTCGGTGCTGATCCGGTCGACGCCGGGGAGCCCGACG 1840
S1 AGTGATTGATCGACGTGTGTGCATGCGTGCAGGGTTGCGACGCGTCGGTGCTGATCCGGTCGACGCCGGGGAGCCCGACG 1838
S2 AGTGATTGATCGACGTGTGTGCATGCGTGCAGGGTTGCGACGCGTCGGTGCTGATCCGGTCGACGCCGGGGAGCCCGACG 1838
Consensus
GAGATGGACGCCGACGACAACAAGTCGCTGGCGTTCGAGGGCTACGAGACGGTGAGGATCGCCAAGGAGGCCGTGGAGGC
T1 GAGATGGACGCCGACGACAACAAGTCGCTGGCGTTCGAGGGCTACGAGACGGTGAGGATCGCCAAGGAGGCCGTGGAGGC 1920
T2 GAGATGGACGCCGACGACAACAAGTCGCTGGCGTTCGAGGGCTACGAGACGGTGAGGATCGCCAAGGAGGCCGTGGAGGC 1920
S1 GAGATGGACGCCGACGACAACAAGTCGCTGGCGTTCGAGGGCTACGAGACGGTGAGGATCGCCAAGGAGGCCGTGGAGGC 1918
S2 GAGATGGACGCCGACGACAACAAGTCGCTGGCGTTCGAGGGCTACGAGACGGTGAGGATCGCCAAGGAGGCCGTGGAGGC 1918
Consensus
CGCGTGCCCCGACCTGGTGTCCTGCGCCGACATACTCACCATCGCCACACGGGACGCCATCGCCCTGGTACGCACATGCA
T1 CGCGTGCCCCGACCTGGTGTCCTGCGCCGACATACTCACCATCGCCACACGGGACGCCATCGCCCTGGTACGCACATGCA 2000
T2 CGCGTGCCCCGACCTGGTGTCCTGCGCCGACATACTCACCATCGCCACACGGGACGCCATCGCCCTGGTACGCACATGCA 2000
S1 CGCGTGCCCCGACCTGGTGTCCTGCGCCGACATACTCACCATCGCCACACGGGACGCCATCGCCCTGGTACGCACATGCA 1998
S2 CGCGTGCCCCGACCTGGTGTCCTGCGCCGACATACTCACCATCGCCACACGGGACGCCATCGCCCTGGTACGCACATGCA 1998
Consensus
TATACTGCACGCACACCCTGCATACTGTATTTTCCACTGAATGACATGTTTGATTTGTGTACAGAGCGGCGGGCCCTTCT
T1 TATACTGCACGCACACCCTGCATACTGTATTTTCCACTGAATGACATGTTTGATTTGTGTACAGAGCGGCGGGCCCTTCT 2080
T2 TATACTGCACGCACACCCTGCATACTGTATTTTCCACTGAATGACATGTTTGATTTGTGTACAGAGCGGCGGGCCCTTCT 2080
S1 TATACTGCACGCACACCCTGCATACTGTATTTTCCACTGAATGACATGTTTGATTTGTGTACAGAGCGGCGGGCCCTTCT 2078
S2 TATACTGCACGCACACCCTGCATACTGTATTTTCCACTGAATGACATGTTTGATTTGTGTACAGAGCGGCGGGCCCTTCT 2078
Consensus
ACCCAGTGGAGCTGGGCAGGCTGGACGGCCTGAGCTCCACGGCCAGCAGCGTGGCCGGCAAGCTGCCGCAGCCCACCAGC
T1 ACCCAGTGGAGCTGGGCAGGCTGGACGGCCTGAGCTCCACGGCCAGCAGCGTGGCCGGCAAGCTGCCGCAGCCCACCAGC 2160
T2 ACCCAGTGGAGCTGGGCAGGCTGGACGGCCTGAGCTCCACGGCCAGCAGCGTGGCCGGCAAGCTGCCGCAGCCCACCAGC 2160
S1 ACCCAGTGGAGCTGGGCAGGCTGGACGGCCTGAGCTCCACGGCCAGCAGCGTGGCCGGCAAGCTGCCGCAGCCCACCAGC 2158
S2 ACCCAGTGGAGCTGGGCAGGCTGGACGGCCTGAGCTCCACGGCCAGCAGCGTGGCCGGCAAGCTGCCGCAGCCCACCAGC 2158

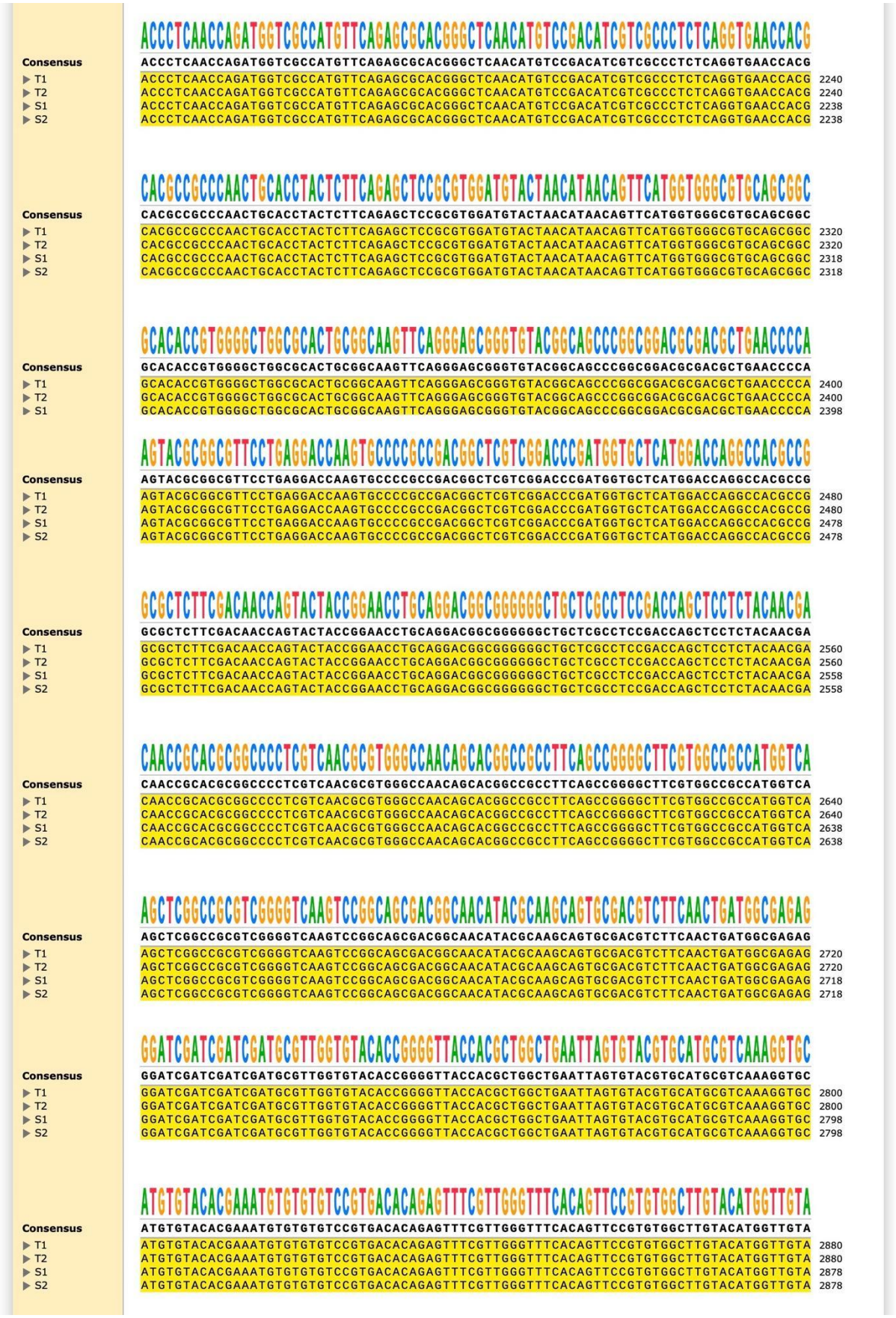
Consensus
ACCCTCAACCAGATGGTCGCCATGTTCAGAGCGCACGGGCTCAACATGTCCGACATCGTCGCCCTCTCAGGTGAACCACG
T1 ACCCTCAACCAGATGGTCGCCATGTTCAGAGCGCACGGGCTCAACATGTCCGACATCGTCGCCCTCTCAGGTGAACCACG 2240
T2 ACCCTCAACCAGATGGTCGCCATGTTCAGAGCGCACGGGCTCAACATGTCCGACATCGTCGCCCTCTCAGGTGAACCACG 2240
S1 ACCCTCAACCAGATGGTCGCCATGTTCAGAGCGCACGGGCTCAACATGTCCGACATCGTCGCCCTCTCAGGTGAACCACG 2238
S2 ACCCTCAACCAGATGGTCGCCATGTTCAGAGCGCACGGGCTCAACATGTCCGACATCGTCGCCCTCTCAGGTGAACCACG 2238
Consensus
CACGCCGCCCAACTGCACCTACTCTTCAGAGCTCCGCGTGGATGTACTAACATAACAGTTCATGGTGGGCGTGCAGCGGC
T1 CACGCCGCCCAACTGCACCTACTCTTCAGAGCTCCGCGTGGATGTACTAACATAACAGTTCATGGTGGGCGTGCAGCGGC 2320
T2 CACGCCGCCCAACTGCACCTACTCTTCAGAGCTCCGCGTGGATGTACTAACATAACAGTTCATGGTGGGCGTGCAGCGGC 2320
S1 CACGCCGCCCAACTGCACCTACTCTTCAGAGCTCCGCGTGGATGTACTAACATAACAGTTCATGGTGGGCGTGCAGCGGC 2318
S2 CACGCCGCCCAACTGCACCTACTCTTCAGAGCTCCGCGTGGATGTACTAACATAACAGTTCATGGTGGGCGTGCAGCGGC 2318
Consensus
GCACACCGTGGGGCTGGCGCACTGCGGCAAGTTCAGGGAGCGGGTGTACGGCAGCCCGGCGGACGCGACGCTGAACCCCA
T1 GCACACCGTGGGGCTGGCGCACTGCGGCAAGTTCAGGGAGCGGGTGTACGGCAGCCCGGCGGACGCGACGCTGAACCCCA 2400
T2 GCACACCGTGGGGCTGGCGCACTGCGGCAAGTTCAGGGAGCGGGTGTACGGCAGCCCGGCGGACGCGACGCTGAACCCCA 2400
S1 GCACACCGTGGGGCTGGCGCACTGCGGCAAGTTCAGGGAGCGGGTGTACGGCAGCCCGGCGGACGCGACGCTGAACCCCA 2398
Consensus
AGTACGCGGCGTTCCTGAGGACCAAGTGCCCCGCCGACGGCTCGTCGGACCCGATGGTGCTCATGGACCAGGCCACGCCG
T1 AGTACGCGGCGTTCCTGAGGACCAAGTGCCCCGCCGACGGCTCGTCGGACCCGATGGTGCTCATGGACCAGGCCACGCCG 2480
T2 AGTACGCGGCGTTCCTGAGGACCAAGTGCCCCGCCGACGGCTCGTCGGACCCGATGGTGCTCATGGACCAGGCCACGCCG 2480
S1 AGTACGCGGCGTTCCTGAGGACCAAGTGCCCCGCCGACGGCTCGTCGGACCCGATGGTGCTCATGGACCAGGCCACGCCG 2478
S2 AGTACGCGGCGTTCCTGAGGACCAAGTGCCCCGCCGACGGCTCGTCGGACCCGATGGTGCTCATGGACCAGGCCACGCCG 2478
Consensus
GCGCTCTTCGACAACCAGTACTACCGGAACCTGCAGGACGGCGGGGGGCTGCTCGCCTCCGACCAGCTCCTCTACAACGA
T1 GCGCTCTTCGACAACCAGTACTACCGGAACCTGCAGGACGGCGGGGGGCTGCTCGCCTCCGACCAGCTCCTCTACAACGA 2560
T2 GCGCTCTTCGACAACCAGTACTACCGGAACCTGCAGGACGGCGGGGGGCTGCTCGCCTCCGACCAGCTCCTCTACAACGA 2560
S1 GCGCTCTTCGACAACCAGTACTACCGGAACCTGCAGGACGGCGGGGGGCTGCTCGCCTCCGACCAGCTCCTCTACAACGA 2558
S2 GCGCTCTTCGACAACCAGTACTACCGGAACCTGCAGGACGGCGGGGGGCTGCTCGCCTCCGACCAGCTCCTCTACAACGA 2558
Consensus
CAACCGCACGCGGCCCCTCGTCAACGCGTGGGCCAACAGCACGGCCGCCTTCAGCCGGGGCTTCGTGGCCGCCATGGTCA
T1 CAACCGCACGCGGCCCCTCGTCAACGCGTGGGCCAACAGCACGGCCGCCTTCAGCCGGGGCTTCGTGGCCGCCATGGTCA 2640
T2 CAACCGCACGCGGCCCCTCGTCAACGCGTGGGCCAACAGCACGGCCGCCTTCAGCCGGGGCTTCGTGGCCGCCATGGTCA 2640
S1 CAACCGCACGCGGCCCCTCGTCAACGCGTGGGCCAACAGCACGGCCGCCTTCAGCCGGGGCTTCGTGGCCGCCATGGTCA 2638
S2 CAACCGCACGCGGCCCCTCGTCAACGCGTGGGCCAACAGCACGGCCGCCTTCAGCCGGGGCTTCGTGGCCGCCATGGTCA 2638
Consensus
AGCTCGGCCGCGTCGGGGTCAAGTCCGGCAGCGACGGCAACATACGCAAGCAGTGCGACGTCTTCAACTGATGGCGAGAG
T1 AGCTCGGCCGCGTCGGGGTCAAGTCCGGCAGCGACGGCAACATACGCAAGCAGTGCGACGTCTTCAACTGATGGCGAGAG 2720
T2 AGCTCGGCCGCGTCGGGGTCAAGTCCGGCAGCGACGGCAACATACGCAAGCAGTGCGACGTCTTCAACTGATGGCGAGAG 2720
S1 AGCTCGGCCGCGTCGGGGTCAAGTCCGGCAGCGACGGCAACATACGCAAGCAGTGCGACGTCTTCAACTGATGGCGAGAG 2718
S2 AGCTCGGCCGCGTCGGGGTCAAGTCCGGCAGCGACGGCAACATACGCAAGCAGTGCGACGTCTTCAACTGATGGCGAGAG 2718
Consensus
GGATCGATCGATCGATGCGTTGGTGTACACCGGGGTTACCACGCTGGCTGAATTAGTGTACGTGCATGCGTCAAAGGTGC
T1 GGATCGATCGATCGATGCGTTGGTGTACACCGGGGTTACCACGCTGGCTGAATTAGTGTACGTGCATGCGTCAAAGGTGC 2800
T2 GGATCGATCGATCGATGCGTTGGTGTACACCGGGGTTACCACGCTGGCTGAATTAGTGTACGTGCATGCGTCAAAGGTGC 2800
S1 GGATCGATCGATCGATGCGTTGGTGTACACCGGGGTTACCACGCTGGCTGAATTAGTGTACGTGCATGCGTCAAAGGTGC 2798
S2 GGATCGATCGATCGATGCGTTGGTGTACACCGGGGTTACCACGCTGGCTGAATTAGTGTACGTGCATGCGTCAAAGGTGC 2798
Consensus
ATGTGTACACGAAATGTGTGTGTCCGTGACACAGAGTTTCGTTGGGTTTCACAGTTCCGTGTGGCTTGTACATGGTTGTA
T1 ATGTGTACACGAAATGTGTGTGTCCGTGACACAGAGTTTCGTTGGGTTTCACAGTTCCGTGTGGCTTGTACATGGTTGTA 2880
T2 ATGTGTACACGAAATGTGTGTGTCCGTGACACAGAGTTTCGTTGGGTTTCACAGTTCCGTGTGGCTTGTACATGGTTGTA 2880
S1 ATGTGTACACGAAATGTGTGTGTCCGTGACACAGAGTTTCGTTGGGTTTCACAGTTCCGTGTGGCTTGTACATGGTTGTA 2878
S2 ATGTGTACACGAAATGTGTGTGTCCGTGACACAGAGTTTCGTTGGGTTTCACAGTTCCGTGTGGCTTGTACATGGTTGTA 2878

Supplementary Figure S1. Sequencing alignment of TraesCS5A01G400500 from genotypes T1, T2, S1 and S2. Upstream 1,500 bp and TraesCS5A01G400500 region were obtained and aligned by Clustal Omega (https://www.ebi.ac.uk/Tools/msa/).

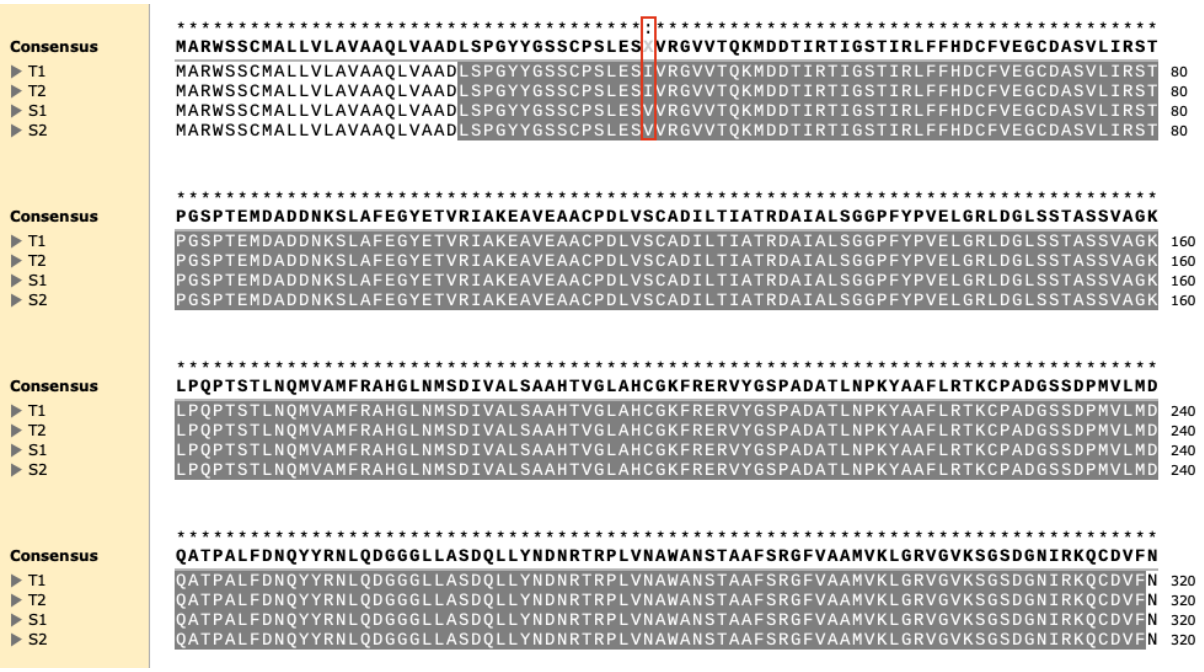

Supplementary Figure S2. Protein alignment of TraesCS5A01G400500 from genotypes T1, T2, S1 and S2. The sites in gray color represented domain "secretory peroxidase" (IPR033905), and the squared position showed different sequence. Multiple alignments were generated by Clustal Omega (https://www.ebi.ac.uk/Tools/msa/).

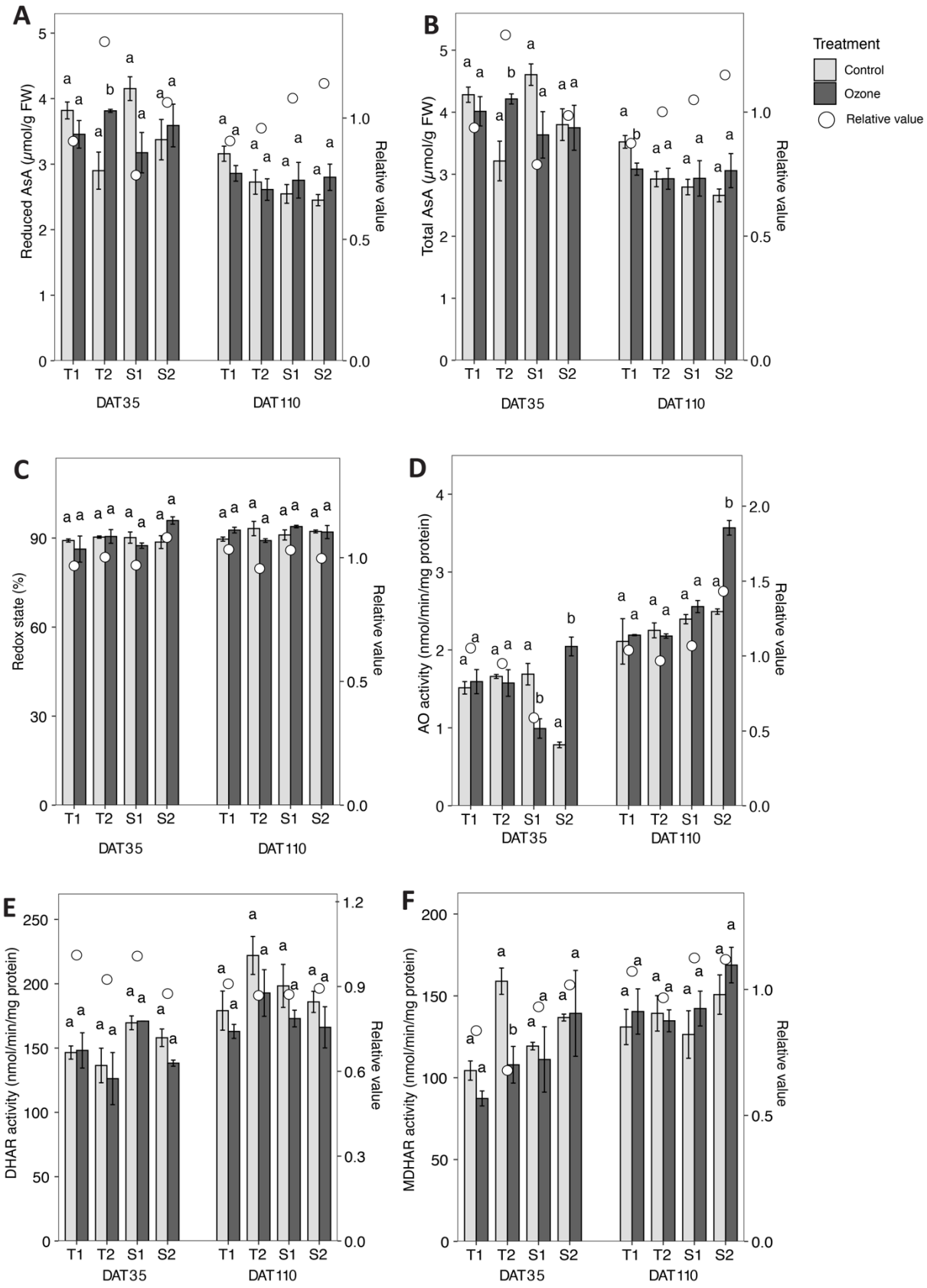

Supplementary Figure S3. Ascorbate acid and enzyme activities in leaves of four wheat genotypes under control and ozone conditions at 35 and 110 days after transplanting. Bars indicate mean values

and standard errors (n=4). A, Reduced AsA; B, Total AsA; C, Redox state； D, Ascorbate oxidase activity; E, Dehydroascorbate reductase activity; F monodehydroascorbate reductase activity. All measurements were determined on the second fully expanded leaves at 35 days and 110 days after transplanting. Bars not sharing the same superscript letters are significantly different at $P < 0.05$ within the genotypes (Student's *t* test).

Supplementary Table S3. Cis-elements in promoter found only in tolerant genotypes.

Name	Sequence	PLACE ID	Description
EVENINGAT	AAAATATCT	S000385	"Evening element" found 46 times in the promoters of 31 cycling genes in Arabidopsis thaliana (Harmer et al. 2000); Required for circadian control of gene expression; "EE (evening element) motif"; Also found in the promoter of the Solanum melongena gene encoding cysteine protease, and identified as cis-element for its circadian regulation (Rawat et al. 2005)
PREATPRODH	ACTCAT	S000450	"PRE (Pro- or hypoosmolarity-responsive element) found in the promoter region of proline dehydrogenase (ProDH) gene in Arabidopsis; Core of 9-bp sequence ACTCATCCT which is necessary for the efficient expression of ProDH in response to L-Pro and hypoosmolarity (Satoh et al., 2002); ATB2-binding site; Similar to GCN4 motif (ATGA(C/G)TCAT); ATB2 subgroup of bZIP transcription factors function as transcriptional activator for hypoosmolarity-inducible ProDH (Satoh et al., 2004)

Upstream 1,500 bp from the transcript initiation site of different wheat genotypes was subjected to cis-element search through New PLACE database (https://www.dna.affrc.go.jp/PLACE/?action=newplace) using default settings. The cis-elements which appear to shown with name, ID and description.

Supplementary Table S4. Cis-elements in promoter found in all genotypes.

Name	Sequence	PLACE ID	Description
ANAERO1CONSENSUS	AAACAAA	S000477	One of 16 motifs found in silico in promoters of 13 anaerobic genes involved in the fermentative pathway (anaerobic set 1) (Mohanty et al., 2005); Arbitrary named ANAERO1CONSENSUS by the PLACEdb curator; See also S000478, S000479, S000480, S000481
CACTFTPPCA1	YACT	S000449	Tetranucleotide (CACT) is a key component of Mem1 (mesophyll expression module 1) found in the cis-regulatory element in the distal region of the phosphoenolpyruvate carboxylase (ppcA1) of the C4 dicot F. trinervia
GTGANTG10	GTGA	S000378	"GTGA motif" found in the promoter of the tobacco (N.t.) late pollen gene g10 which shows homology to pectate lyase and is the putative homologue of the tomato gene lat56; Located between96 and -93
AGCBOXNPGLB	AGCCGCC	S000232	"AGC box" repeated twice in a 61 bp enhancer element in tobacco (N.p.) class I beta-1,3-glucanase (GLB) gene; See S000036, S000089; "GCC-box"; Binding sequence of Arabidopsis AtERFs; AtERF1,2 and 5 functioned as activators of GCC box-dependent transcription; AtERF3 and 4 acted as repressors; AtERF proteins are stress signal-response factors; EREBP2 binding site; Conserved in most PR-protein genes; Rice MAPK (BWMK1) phosphorylates OS EREBP1, which enhance DNA-binding activity of the factor to the GCC box
GCCCORE	GCCGCC	S000430	Core of GCC-box found in many pathogen-responsive genes such as PDF1.2, Thi2.1, and PR4; Has been shown to function as ethylene-responsive element; See S000036, S000232, S000332; Appears to play important roles in regulating jasmonate-responsive gene expression; Tomato Pti4 (ERF) regulates defence-related gene expression via GCC box and non-GCC box cis elements (Myb1 (GTTAGTT) and G-box(CACGTG))
GATABOX	GATA	S000039	"GATA box"; GATA motif in CaMV 35S promoter; Binding with ASF-2; Three GATA box repeats were found in the promoter of Petunia (P.h.) chlorophyll a/b binding protein, Cab22 gene; Required for high level, light regulated, and tissue specific expression; Conserved in the promoter of all LHCII type I Cab genes
ROOTMOTIFTAPOX1	ATATT	S000098	Motif found both in promoters of rolD
-10PEHVPSBD	TATTCT	S000392	"-10 promoter element" found in the barley (H.v.) chloroplast psbD gene promoter; Involved in the expression of the plastid gene psbD which encodes a photosystem II reaction center chlorophyll-binding protein that is activated by blue, white or UV-A light

Supplementary Table S4 (continued)

Name	Sequence	PLACE ID	Description
DOFCOREZM	AAAG	S000265	Core site required for binding of Dof proteins in maize (Z.m.); Dof proteins are DNA binding proteins, with presumably only one zinc finger, and are unique to plants; Four cDNAs encoding Dof proteins, Dof1, Dof2, Dof3 and PBF, have been isolated from maize; PBF is an endosperm specific Dof protein that binds to prolamin box; Maize Dof1 enhances transcription from the promoters of both cytosolic orthophosphate kinase (CyPPDK) and a non-photosynthetic PEPC gene; Maize Dof2 supressed the C4PEPC promoter
SEBFCONSSTPR10A	YTGTCWC	S000391	Binding site of the potato silencing element binding factor (SEBF) gene found in promoter of pathogenesis-related gene (PR-10a); Located between -45 and -39; Similar to the auxin response element
TGTCACACMCUCUMISIN	TGTCACA	S000422	"TGTCACA motif" found in the region (from -254 to -215) of cucumisin (a subtilisin-like serine protease) in the fruit of melon (Cucumis melo L.); A novel enhancer element necessary for fruit-specific expression of the cucumisin gene
BIHD1OS	TGTCA	S000498	Binding site of OsBIHD1, a rice BELL homeodomain transcription factor
RKY71OS	TGAC	S000447	"A core of TGAC-containing W-box" of, e.g., Amy32b promoter; Binding site of rice WRKY71, a transcriptional repressor of the gibberellin signaling pathway; Parsley WRKY proteins bind specifically to TGAC-containing W box elements within the Pathogenesis-Related Class10 (PR-10) genes (Eulgem et al., 1999)
CIACADIANLELHC	CAANNNNATC	S000252	Region necessary for circadian expression of tomato (L.e.) Lhc gene
MYBCOREATCYCB1	AACGG	S000502	"Myb core" in the 18 bp sequence which is able to activate reporter gene without leading to M-phase-specific expression, found in the promoter of Arabidopsis thaliana cyclin B1:1 gene; the 18 bp sequence share homology with a sequence found in the N. sylvestris cyclin B1 promoter (Trehin et al., 1999; see S000283)
OSE2ROOTNODULE	CTCTT	S000468	One of the consensus sequence motifs of organ-specific elements (OSE) characteristic of the promoters activated in infected cells of root nodules; See also S000467
WUSATAg	TTAATGG	S000433	Target sequence of WUS in the intron of AGAMOUS gene in Arabidopsis; See Lohmann et al. Cell 105:793-803 (2003)
NODCON2GM	CTCTT	S000462	One of two putative nodulin consensus sequences (NODCON1GM);
EBOXBNNAPA	CANNTG	S000144	E-box of napA storage-protein gene of Brassica napus (B.n.); See S000042 (CACGTGMOTIF); see S000407 (Myc consensus: CANNTG); This sequence is also known as RRE (R response element) (Hartmann et al., 2005)

Supplementary Table S4 (continued)

Name	Sequence	PLACE ID	Description
PRECONSCRHSP70A	SCGAYNRNN NNNNNNNNN NNNNHD	S000506	Consensus sequence of PRE (plastid response element) in the promoters of HSP70A in Chlamydomonas; Involved in induction of HSP70A gene by both MgProto and light
SV40COREENHAN	GTGGWWHG	S000123	"SV40 core enhancer"; Similar sequences found in rbcS genes
MYBATRD22	CTAACCA	S000175	Binding site for MYB (ATMYB2) in dehydration-responsive gene, rd22; MYB binding site in rd22 gene of Arabidopsis thaliana; ABA-induction; Located at ca. -141 of rd22 gene; Also MYC at ca. -200 of rd22 gene; See S000174 (MYCATRD22); See S000355
MYB1AT	WAACCA	S000408	MYB recognition site found in the promoters of the dehydration-responsive gene rd22 and many other genes in Arabidopsis
MYB1LEPR	GTTAGTT	S000443	Tomato Pti4(ERF) regulates defence-related gene expression via GCC box and non-GCC box cis elements (Myb1(GTTAGTT), G box (CACGTG))
AACACOREOSGLUB1	AACAAAC	S000353	Core of AACA motifs found in rice (O.s.) glutelin genes, involved in controlling the endosperm-specific expression; AACA is also closely associated with the GCN4 motif in all rice glutelin genes and together have been shown to confer endosperm-specific enhancement to the truncated -90 CaMV 35S promoter; See also S000045, S000181, S000276
MARABOX1	AATAAAYAAA	S000063	"A-box" found in SAR(scaffold attachment region; or matrix attachment region, MAR)
NODCON1GM	AAAGAT	S000461	One of two putative nodulin consensus sequences; See also S000462 (NODCON2GM)
POLASIG1	AATAAA	S000080	"PolyA signal"; poly A signal found in legA gene of pea, rice alpha-amylase; -10 to -30 in the case of animal genes. Near upstream elements (NUE) in Arabidopsis (Loke et al. 2005)
MYCATERD1	CATGTG	S000413	MYC recognition sequence (from -466 to -461) necessary for expression of erd1 (early responsive to dehydration) in dehydrated Arabidopsis; NAC protein bound specifically to the CATGTG motif (Tran et al., 2004)); NAC protein bound specifically to the CATGTG motif (Tran et al., 2004)
SORLIP1AT	GCCAC	S000482	one of "Sequences Over-Represented in Light-Induced Promoters (SORLIPs) in Arabidopsis; Computationally identified phyA-induced motifs; SORLIP 1 is most over-represented, and most statistically singnificant; See also S000483, S000484, S000485, S000486 (all SORLIPs), and also S000487, S000488, S000489, S000490 (all SORLREPs); Over-represented in light-induced cotyledon and root common genes and root-specific genes (Jiao et al. 2005; see S000486)
TATABOX3	TATTAAT	S000110	"TATA box"; TATA box found in the 5'upstream region of sweet potato sporamin A gene

Supplementary Table S4 (continued)

Name	Sequence	PLACE ID	Description
E2FCONSENSUS	WTTSSCSS	S000476	"E2F consensus sequence" of all different E2F-DP-binding motifs that were experimentally verified in plants (Vandepoele et al., 2005); See also S000417, S000397, S000396, S000367, S000366
MYCCONSENSUSAT	CANNTG	S000407	MYC recognition site found in the promoters of the dehydration-responsive gene rd22 and many other genes in Arabidopsis; Binding site of ATMYC2 (previously known as rd22BP1); see S000144 (E-box; CANNTG), S000174 (MYCATRD22); N=A/T/G/C; MYC recognition sequence in CBF3 promoter; Binding site of ICE1 (inducer of CBF expression 1) that regulates the transcription of CBF/DREB1 genes in the cold in Arabidopsis; ICE1 (Chinnusamy et al., 2004);) This sequence is also known as RRE (R response element)(Hartmann et al., 2005)
SBOXATRBCS	CACCTCCA	S000500	"S-box" conserved in several rbcS promoters in Arabidopsis; ABI4 binding site; "Important for the sugar and ABA responsiveness of CMA5"(Acevedo-Hernandez et al., 2005)
MYCATRD22	CACATG	S000174	Binding site for MYC (rd22BP1) in Arabidopsis (A.t.) dehydration-resposive gene, rd22; MYC binding site in rd22 gene of Arabidopsis thaliana; ABA-induction; Located at ca. -200 of rd22 gene; Also MYB at ca. -141 of rd22 gene; See also S000175 (MYBATRD22)
WBOXNTERF3	TGACY	S000457	"W box" found in the promoter region of a transcriptional repressor ERF3 gene in tobacco; May be involved in activation of ERF3 gene by wounding ;(Nishiuchi et al., 2004) Y=C/T; See S000142, S000390, S000442, S000447
GT1CONSENSUS	GRWAAW	S000198	Consensus GT-1 binding site in many light-regulated genes, e.g., RBCS from many species, PHYA from oat and rice, spinach RCA and PETA, and bean CHS15; R=A/G; W=A/T; For a compilation of related GT elements and factors, see Villain et al. (1996); GT-1 can stabilize the TFIIA-TBP-DNA (TATA box) complex; The activation mechanism of GT-1 may be achieved through direct interaction between TFIIA and GT-1; Binding of GT-1-like factors to the PR-1a promoter influences the level of SA-inducible gene expression
CGCGBOXAT	VCGCGB	S000501	"CGCG box" recognized by AtSR1-6 (Arabidopsis thaliana signal-responsive genes); Multiple CGCG elements are found in promoters of many genes; Ca++/calmodulin binds to all AtSRs
CGACGOSAMY3	CGACG	S000205	"CGACG element" found in the GC-rich regions of the rice (O.s.) Amy3D and Amy3E amylase genes, but not in Amy3E gene; May function as a coupling element for the G box element

Supplementary Table S4 (continued)

Name	Sequence	PLACE ID	Description
ABRERATCAL	MACGYGB	S000507	"ABRE-related sequence" or "Repeated sequence motifs" identified in the upstream regions of 162 Ca(2+)-responsive upregulated genes; see also ABRE
CBFHV	RYCGAC	S000497	Binding site of barley (H.v.) CBF1, and also of barley CBF2; CBF = C-repeat (CRT) binding factors; CBFs are also known as dehydration-responsive element (DRE) binding proteins (DREBs); See also S000411 (SQ=GTCGAC)
MYBCORE	CNGTTR	S000176	Binding site for all animal MYB and at least two plant MYB proteins ATMYB1 and ATMYB2, both isolated from Arabidopsis; ATMYB2 is involved in regulation of genes that are responsive to water stress in Arabidopsis; A petunia MYB protein (MYB.Ph3) is involved in regulation of flavonoid biosynthesis (Solano et al. EMBO J 14:1773 (1995)) ; See S000355
MYB2CONSENSUSAT	YAACKG	S000409	MYB recognition site found in the promoters of the dehydration-responsive gene rd22 and many other genes in Arabidopsis; See S000177 (MYB2), S000175 (MYBATRD22)
CURECORECR	GTAC	S000493	GTAC is the core of a CuRE (copper-response element) found in Cyc6 and Cpx1 genes in Chlamydomonas; Also involved in oxygen-response of these genes; For CuRE, see Quin and Merchant, 1995
WBOXATNPR1	TTGAC	S000390	"W-box" found in promoter of Arabidopsis thaliana (A.t.) NPR1 gene; Located between +70 and +79 in tandem; They were recognized specifically by salicylic acid (SA)-induced WRKY DNA binding proteins; See S000142 (SQ=TTGACC); See S000310 (SQ=TTTGACY); A cluster of WRKY binding sites act as negative regulatory elements for the inducible expression of AtWRKY18 (Chena and Chen, 2002)); See also S000142
POLASIG3	AATAAT	S000088	"Plant polyA signal"; Consensus sequence for plant polyadenylation signal
CPBCSPOR	TATTAG	S000491	The sequence critical for Cytokinin-enhanced Protein Binding in vitro, found in -490 to -340 of the promoter of the cucumber (CS) POR (NADPH-protochlorophyllide reductase) gene
DPBFCOREDCDC3	ACACNNG	S000292	A novel class of bZIP transcription factors, DPBF-1 and 2 (Dc3 promoter-binding factor-1 and 2) binding core sequence; Found in the carrot (D.c.) Dc3 gene promoter; Dc3 expression is normally embryo-specific, and also can be induced by ABA; The Arabidopsis abscisic acid response gene ABI5 encodes a bZIP transcription factor; abi5 mutant have a pleiotropic defects in ABA response; ABI5 regulates a subset of late embryogenesis-abundant genes; GIA1 (growth-insensitivity to ABA) is identical to ABI5

Supplementary Table S4 (continued)

Name	Sequence	PLACE ID	Description
ARR1AT	NGATT	S000454	"ARR1-binding element" found in Arabidopsis; ARR1 is a response regulator; N=G/A/C/T; AGATT is found in the promoter of rice non-symbiotic haemoglobin-2 (NSHB) gene (Ross et al., 2004)
WBOXHVISO1	TGACT	S000442	SUSIBA2 bind to W-box element in barley iso1 (encoding isoamylase1) promoter
INRNTPSADB	YTCANTYY	S000395	"Inr (initiator)" elements found in the tobacco psaDb gene promoter without TATA boxes; Light-responsive transcription of psaDb depends on Inr, but not TATA box
CCAATBOX1	CCAAT	S000030	Common sequence found in the 5'-non-coding regions of eukaryotic genes; "CCAAT box" found in the promoter of heat shock protein genes; Located immediately upstream from the most distal HSE of the promoter; "CCAAT box" act cooperatively with HSEs to increase the hs promoter activity
RAV1AAT	CAACA	S000314	Binding consensus sequence of Arabidopsis (A.t.) transcription factor, RAV1; RAV1 specifically binds to DNA with bipartite sequence motifs of RAV1-A (CAACA) and RAV1-B (CACCTG); RAV1 protein contain AP2-like and B3-like domains; The AP2-like and B3-like domains recognize the CAACA and CACCTG motifs, respectively; The expression level of RAV1 were relatively high in rosette leaves and roots; See S000315(CACCTG)
OSE1ROOTNODULE	AAAGAT	S000467	One of the consensus sequence motifs of organ-specific elements (OSE) characteristic of the promoters activated in infected cells of root nodules; See also S000468
QELEMENTZMZM13	AGGTCA	S000254	"Q(quantitative)-element" in maize (Z.m.) ZM13 gene promoter; Found at -107 to -102; Involved in expression enhancing activity; ZM13 is a maize homolog of tomato LAT52 gene; ZM13 is a pollen-specific maize gene
ACGTATERD1	ACGT	S000415	ACGT sequence (from -155 to -152) required for etiolation-induced expression of erd1 (early responsive to dehydration) in Arabidopsis
POLLEN1LELAT52	AGAAA	S000245	One of two co-dependent regulatory elements responsible for pollen specific activation of tomato (L.e.) lat52 gene; Found at -72 to -68 region; See S000246 (POLLEN2LELAT52); AGAAA and TCCACCATA (S000246) are required for pollen specific expression; Also found in the promoter of tomato endo-beta-mannanase gene (LeMAN5) gene (Filichkin et al. 2004)
GT1GMSCAM4	GAAAAA	S000453	"GT-1 motif" found in the promoter of soybean (Glycine max) CaM isoform, SCaM-4; Plays a role in pathogen- and salt-induced SCaM-4 gene expression; See also S000198 (GT-1 consensus)

Supplementary Table S4 (continued)

Name	Sequence	PLACE ID	Description
ELRECOREPCRP1	TTGACC	S000142	ElRE (Elicitor Responsive Element) core of parsley (P.c.) PR1 genes; consensus sequence of elements W1 and W2 of parsley PR1-1 and PR1-2 promoters; Box W1 and W2 are the binding site of WRKY1 and WRKY2, respectively; ERE; "WA box"; One of the W boxes found in the Parsley (P.c.) WRKY1 gene promoter; Required for elicitor responsiveness; See S000310; "WC box" WB box (S000310) and WC box constitute a palindrome; WRKY1 protein binding site; W-box found in thioredoxin h5 gene in Arabidopsis (Laloi et al.)
WBBOXPCWRKY1	TTTGACY	S000310	"WB box"; WRKY proteins bind specifically to the DNA sequence motif (T)(T)TGAC(C/T), which is known as the W box; Found in amylase gene in sweet potato, alpha-Amy2 genes in wheat, barley, and wild oat, PR1 gene in parsley, and a transcription factor gene in Arabidopsis; The motif was initially registered in PLACEdb as TTGACT, and was corrected to TTGACY on 22 June, 2006
CCA1ATLHCB1	AAMAATCT	S000149	CCA1 binding site; CCA1 protein (myb-related transcription factor) interact with two imperfect repeats of AAMAATCT in Lhcb1*3 gene of Arabidopsis thaliana (A.t.); Related to regulation by phytochrome
CAATBOX1	CAAT	S000028	"CAAT promoter consensus sequence" found in legA gene of pea
PYRIMIDINEBOXOSRAMY1A	CCTTTT	S000259	Pyrimidine box found in rice (O.s.) alpha-amylase (RAmy1A) gene; Gibberellin-respons cis-element of GARE and pyrimidine box are partially involved in sugar repression; Found in the promoter of barley alpha-amylase (Amy2/32b) gene which is induced in the aleurone layers in response to GA; BPBF protein binds specifically to this site; See S000265
ASF1MOTIFCAMV	TGACG	S000024	"ASF-1 binding site" in CaMV 35S promoter; ASF-1 binds to two TGACG motifs; See S000023 (AS1); Found in HBP-1 binding site of wheat histone H3 gene; TGACG motifs are found in many promoters and are involved in transcriptional activation of several genes by auxin and/or salicylic acid; May be relevant to light regulation; Binding site of tobacco TGA1a; TGA1a and b show homology to CREB; TGA6 is a new member of the TGA family; Abiotic and biotic stress differentially stimulate "as-1 element" activity
RHERPATEXPA7	KCACGW	S000512	"Right part of RHEs (Root Hair-specific cis-Elements)" conserved among the Arabidopsis thaliana A7 (AtEXPA7) orthologous (and paralogous) genes from diverse angiosperm species with different hair distribution patterns

Supplementary Table S4 (continued)

Name	Sequence	PLACE ID	Description
ABRELATERD1	ACGTG	S000414	ABRE-like sequence (from -199 to -195) required for etiolation-induced expression of erd1 (early responsive to dehydration) in Arabidopsis
SEF4MOTIFGM7S	RTTTTTR	S000103	"SEF4 binding site"; Soybean (G.m.) consensus sequence found in 5'upstream region (-199) of beta-conglycinin (7S globulin) gene (Gmg17.1); "Binding with SEF4 (soybean embryo factor 4)"
RAV1BAT	CACCTG	S000315	Binding consensus sequence of an Arabidopsis (A.t.) transcription factor, RAV1; RAV1 specifically binds to DNA with bipartite sequence motifs of RAV1-A (CAACA) and RAV1-B (CACCTG); RAV1 protein contain AP2-like and B3-like domains; The AP2-like and B3-like domains recognize the CAACA and CACCTG motifs, respectively; The expression level of RAV1 were relatively high in rosette leaves and roots; See S000314(CAACA)
QELEMENTZMZM13	AGGTCA	S000254	"Q(quantitative)-element" in maize (Z.m.) ZM13 gene promoter; Found at -107 to -102; Involved in expression enhancing activity; ZM13 is a maize homolog of tomato LAT52 gene; ZM13 is a pollen-specific maize gene
LTRECOREATCOR15	CCGAC	S000153	Core of low temperature responsive element (LTRE) of cor15a gene in Arabidopsis (A.t.); A portion of repeat-C (C-repeat), TGGCCGAC, which is repeated twice in cor15a promoter (Baker et al., 1994); ABA responsiveness; Involved in cold induction of BN115 gene from winter Brassica napus; LTRE; See S000157, S000152; Light signaling mediated by phytochrome is necessary for cold- or drought-induced gene expression through the C/DRE in Arabidopsis; See S000152
EECCRCAH1	GANTTNC	S000494	"EEC"; Consensus motif of the two enhancer elements, EE-1 and EE-2, both found in the promoter region of the Chlamydomonas Cah1 (encoding a periplasmic carbonic anhydrase); Binding site of Myb transcription factor LCR1 (see Yoshioka et al, 2004)
RYREPEATLEGUMINBOX	CATGCAY	S000100	"RY repeat (CATGCAY)" or legumin box found in seed-storage protein genes in legume such as soybean (G.m.)
MARTBOX	TTWTWTTWTT	S000067	"T-Box"; Motif found in SAR (scaffold attachment region; or matrix attachment region, MAR)
SORLREP3AT	TGTATATAT	S000488	one of "Sequences Over-Represented in Light-Repressed Promoters (SORLREPs) in Arabidopsis; Computationally identified phyA-repressed motifs; See also S000487, S000489, S000490 (all SORLREPs); and also S000482, S000483, S000484, S000485, S000486 (all SORLIPs);

Supplementary Table S4 (continued)

Name	Sequence	PLACE ID	Description
ARFAT	TGTCTC	S000270	ARF (auxin response factor) binding site found in the promoters of primary/early auxin response genes of Arabidopsis thaliana (A.t.); AuxRE; See S000337; Binding site of Arabidopsis ARF1 (Auxin response factor1); Sequence found in NDE element in Soybean (G.m.) SAUR (Small Auxin-Up RNA) 15A gene promoter; See S000359, S000360; Found in D1 or D4 element in Soybean (G.m.) GH3 promoter; This element was enriched in the 5'-flanking region of genes up-regulated by both IAA and BL (Goda et al., 2004)
RYREPEATBNNAPA	CATGCA	S000264	"RY repeat" found in RY/G box (the complex containing the two RY repeats and the G-box) of napA gene in Brassica napus (B.n.); Found between -78 and -50; Required for seed specific expression; See S000262, S000263; dist B ABRE mediated transactivation by ABI3 adn ABI3-dependent response to ABA; a tetramer of the composite RY/G complex mediated only ABA-independent transactivation by ABI3; B2 domain of ABI3 is necessary for ABA-independent and ABA-dependent activation through the dist B ABRE
ZDNAFORMINGATCAB1	ATACGTGT	S000321	"Z-DNA-forming sequence" found in the Arabidopsis (A.t.) chlorophyll a/b binding protein gene (cab1) promoter; Involved in light-dependent developmental expression of the gene; "Z-box"; Activation of Z-box containing promoters is regulated by downstream regulatory components, COP1 and HY5; phyB and CRY1 photoreceptors act redundantly to induce Z-box containing promoters in white light
SITEIIATCYTC	TGGGCY	S000474	"Site II element" found in the promoter regions of cytochrome genes (Cytc-1, Cytc-2) in Arabidopsis; Located between -147 and -156 from the translational starts sites (Welchen et al., 2005); See also S000308; Overrepresented in the promoters of nuclear genes encoding components of the oxidative phosphorylation (OxPhos) machinery from both Arabidopsis and rice (Welchen and Gonzalez, 2006);)
CARGCW8GAT	CWWWWWWWWG	S000431	A variant of CArG motif (see S000404), with a longer A/T-rich core; Binding site for AGL15 (AGAMOUS-like 15)
ANAERO3CONSENSUS	TCATCAC	S000479	One of 16 motifs found in silico in promoters of 13 anaerobic genes involved in the fermentative pathway (anaerobic set 1)(Mohanty et al., 2005); Arbitrary named ANAERO3CONSENSUS by the PLACEdb curator; See also S000477, S000478, S000480, S000481

Publications

Feng, Y.*, Nguyen, T.H.*, Alam, M.S., Emberson, L., Gaiser, T., Ewert, F., Frei, M., 2022. Identifying and modelling key physiological traits that confer tolerance or sensitivity to ozone in winter wheat. Environmental Pollution 304, 229251. https://doi.org/10.1016/j.envpol.2022.119251 (*: co-first authors)

Feng, Y., Alam, M.S., Yan, F., Frei, M., 2024. Alteration of carbon and nitrogen allocation in winter wheat under elevated ozone. Plant Science 338, 111924. https://doi.org/10.1016/j.plantsci.2023.111924

Feng, Y., Wu, L.-B., Autarmat, S., Alam, M.S., Frei, M., 2023. Characterization of candidate genes for ozone tolerance in winter wheat (Triticum aestivum L.) and associated physiological mechanisms. Environmental and Experimental Botany 211, 105368. https://doi.org/10.1016/j.envexpbot.2023.105368

Begum, H., Alam, M.S., Feng, Y., Koua, P., Ashrafuzzaman, M., Shrestha, A., Kamruzzaman, M., Dadshani, S., Ballvora, A., Naz, A.A., Frei, M., 2020. Genetic dissection of bread wheat diversity and identification of adaptive loci in response to elevated tropospheric ozone. Plant Cell Environ 43, 2650-2665. https://doi.org/10.1111/pce.13864

Wu, L.B., Feng, Y., Zeibig, F., Alam, M.S., Frei, M., 2021. High Throughput Analyses of Ascorbate-turnover Enzyme Activities in Rice (Oryza sativa L.) Seedlings. Bio Protoc 11, e4190. https://doi.org/10.21769/BioProtoc.4190

Alam, M.S., Maina, A.W., Feng, Y., Wu, L.-B., Frei, M., 2022. Interactive effects of tropospheric ozone and blast disease (Magnaporthe oryzae) on different rice genotypes. Environmental Science and Pollution Research 29, 48893-48907. https://doi.org/10.1007/s11356-022-19282-z

Agathokleous, E., Frei, M., Knopf, O.M., Muller, O., Xu, Y., Nguyen, T.H., Gaiser, T., Liu, X., Liu, B., Saitanis, C.J., Shang, B., Alam, M.S., Feng, Y., Ewert, F., Feng, Z., 2023. Adapting crop production to climate change and air pollution at different scales. Nat Food 4(10), 854-865. https://doi.org/10.1038/s43016-023-00858-y

Conference participation

22nd-25th February 2021: ICP Vegetation 34th Task Force Meeting. online.<Oral Presentation>
Feng Y., Alam M.S., Nguyen T.H., Frei M. Genetic variation of wheat tolerance to ozone treatment. Abstract pp. 17.

Acknowledgment

Firstly, I would like to sincerely thank Prof. Dr. Michael Frei for providing me with the great opportunity to work on this interesting topic, and he gave me scientific suggestions throughout the research.

I am also grateful to Prof. Dr. Gabriel Schaaf for being my co-supervisor, and my gratitude also goes to Prof. Dr. Eike Lüdeling for accepting the request to be in the committee, and Prof. Dr. Mathias Becker for his contribution as the chairman.

In addition, I would also like to thank Prof. Dr. Frank Ewert, Prof. Dr. Thomas Gaiser, Dr. Thuy Huu Nguyen and Prof. Dr. Lisa Emberson for the modelling collaboration. Thanks to Prof. Dr. Rod Snowdon and Dr. Christian Obermeier in University of Giessen for sharing experimental facilities and technical support. I am also grateful to Prof. Dr. Zhaozhong Feng for giving the wonderful learning opportunity in Nanjing University of Information Science and Technology (NUIST).

Sincere thanks to the colleges in my group, they supported and encouraged me a lot. Especially, Dr. Feng Yan and Dr. Lin-Bo Wu gave me scientific suggestions, methodology guidance of my experiments as well as critical comments in my thesis. I would also like to express my sincere appreciation to Shahed and his family who always warm me throughout the whole period in Germany. Thanks to Ambika, Frederike, Sumitra, Sawitree, Dr. Andriele Wairich and Dr. Yavar Vaziritabar who kindly shared their experimental technique and knowledge. Thanks to Christine for administrative support and Erika, Denise and Liane for their valued technical support. I am also grateful to the colleges of INRES and EEEC group of NUIST who I did not mention their name here, but they also helped me a lot with my experiments.

Finally, I would like to sincerely appreciate to my best friends. No matter how far apart we are, your companions are always there for me, which saved me in the toughest time and encouraged me to be stronger.